



**Contribution of PPCK-PPC module to phosphate-dependent malate
accumulation and exudation in *Arabidopsis thaliana***

Dissertation

zur Erlangung des Doktorgrades der Naturwissenschaften

(Dr. rer. nat.)

der

Naturwissenschaftlichen Fakultät I

Biowissenschaften

der Martin-Luther-Universität Halle-Wittenberg

vorgelegt von

Herrn M.Sc. Samuel Ngure Kariithi

1. Gutachter: Prof. Dr. Steffen Abel
2. Gutachter: Prof. Dr. Edgar Peiter
3. Gutachter: Prof. Dr. Paul B. Larsen

Tag der öffentlichen Verteidigung: 30.04.2024

TABLE OF CONTENTS

LIST OF FIGURES.....	vii
LIST OF TABLES	viii
LIST OF SUPPLEMENTARY FIGURES.....	viii
LIST OF SUPPLEMENTARY TABLES	ix
ABBREVIATIONS AND SYMBOLS	x
1.0 INTRODUCTION.....	1
1.1 Importance of phosphorus	1
1.2 Phosphorus availability in soil and plants	1
1.3 Symptoms of phosphorus deficiency in plants	2
1.4 Phosphorus sensing and acquisition by plants.....	2
1.4.1 Formation of symbiotic relations with mycorrhiza fungi	2
1.4.2 Change in root system architecture via local Pi sensing.....	3
1.4.3 Adjustment of cellular metabolism via systemic phosphate sensing	4
1.4.4 Exudation of phospho-hydrolases and carboxylic acids.....	6
1.5 Biosynthesis and role of organic acids in plants.....	6
1.5.1 Biosynthesis and role of citrate in plants.....	7
1.5.2 Biosynthesis and role of malate in plants	8
1.6 Phosphoenolpyruvate carboxylases (PPCs) and their role in plants	9
1.7 Regulation of phosphoenolpyruvate carboxylases in plants.....	11
1.8 Phosphoenolpyruvate carboxylase kinases and their role in plants	12
1.9 Regulation of phosphoenolpyruvate carboxylase kinases	13
1.10 Previous work on PPC and PPCK manipulation	13
1.11 Aim of the present study.....	14
1.11.1 Cell-specific expression domains of Arabidopsis plant-type <i>PPCs</i>	15
1.11.2 Overexpression of Arabidopsis plant-type <i>PPCs</i>	15
1.11.3 Loss of function (knockouts) of Arabidopsis <i>PPCKs</i>	15
2.0 RESULTS.....	17
2.1 Differential expression of Arabidopsis <i>PPC</i> genes	17
2.2 Cell type-specific expression of Arabidopsis <i>PPC</i> genes in roots.....	18
2.3 Generation of Arabidopsis <i>PPC</i> overexpression lines.....	20
2.4 Molecular characterization of Arabidopsis <i>PPC</i> overexpression lines.....	21
2.4.1 Analysis of <i>PPC</i> transcript levels.....	21
2.4.2 <i>PPC</i> overexpression increases PPC protein levels in roots	22
2.4.3 <i>PPC</i> overexpression increases PPC activity in crude extracts.....	26
2.4.4 Pi deficiency increases PPC protein phosphorylation in shoots and roots.....	26

2.5	Determination of malate and citrate content in tissues of <i>PPC</i> overexpression lines	28
2.5.1	Overexpression of <i>PPCs</i> increases root but not shoot malate	28
2.5.2	Overexpression of <i>PPCs</i> increases shoot and root citrate content.....	29
2.5.3	Overexpression of <i>PPC2</i> enhances malate and citrate exudation.....	31
2.6	Other metabolite changes in <i>PPC</i> overexpression lines	32
2.6.1	Overexpression of <i>PPCs</i> enhances amino acid content under sufficient Pi	32
2.6.2	Changes in TCA intermediates in <i>PPC</i> overexpression lines.....	34
2.7	Phenotypic characteristics of <i>PPC</i> overexpression lines	36
2.7.1	<i>PPC</i> overexpression increases tissue fresh weight.....	36
2.7.2	<i>PPC</i> overexpression increases gain of root length	38
2.7.3	<i>PPC</i> overexpression reduces seed weight and seed number	39
2.8	<i>PPCK1</i> is predominantly expressed in Arabidopsis shoots and roots	41
2.9	Complementation of <i>ppck1-4</i> mutant reverts <i>PPCK1</i> transcripts to wild type levels.....	42
2.10	Generation of <i>ppck2</i> knockout lines by CRISPR/Cas 9 technology	43
2.10.1	Identification and genotyping of <i>ppck2</i> CRISPR/Cas 9 mutant lines.....	44
2.10.2	Generation of a <i>ppck1ppck2</i> double knockout mutant	45
2.11	Determination of malate and citrate content in tissues of <i>ppck</i> mutant lines.....	46
2.11.1	Loss of <i>PPCK1</i> and <i>PPCK2</i> reduces shoot and root malate content.....	46
2.11.2	Loss of <i>PPCK1</i> increases shoot and root citrate content	47
2.11.3	The <i>ppck1ppck2</i> double knockout mutant has reduced malate and citrate exudation.....	49
2.12	Other metabolites changes in the <i>ppck</i> mutants and <i>ppck1-4</i> complementation lines	50
2.12.1	Loss of <i>PPCK1</i> and <i>PPCK2</i> enhances accumulation of amino acids in tissues	50
2.12.2	TCA intermediates in <i>ppck</i> knockouts and <i>ppck1-4</i> complementation lines	52
2.13	Phenotypic characteristics of <i>ppck</i> mutant lines	53
2.13.1	Loss of <i>PPCK1</i> reduces root and shoot weight	53
2.13.2	The <i>ppck1</i> mutant has higher gain of root length upon Pi starvation.....	55
3.0	DISCUSSION	56
3.1	The different Arabidopsis PPC isoforms have different functions	56
3.1.1	Differential induction of <i>PPC</i> genes during Pi starvation points to different roles	56
3.1.2	Cell-specific expression domains of <i>PPC</i> genes support different role for PPCs	57
3.1.3	<i>PPC</i> overexpression lines have different malate and citrate exudation profiles.....	58
3.1.4	Overexpression of C3 <i>PPCs</i> results in specific phenotypes	59
3.2	Effects of overexpressing C3 <i>PPCs</i> in Arabidopsis	61
3.2.1	Effects of <i>PPC</i> overexpression on PPC crude activity and protein amount	61
3.2.2	Phosphate starvation enhances PPC phosphorylation in the transgenic lines.....	62
3.2.3	Pi starvation increases root malate levels in <i>PPC</i> overexpression lines	63
3.2.4	<i>PPC</i> overexpression increases shoot and root citrate levels in Arabidopsis.....	64

3.2.5	<i>PPC2</i> overexpression induces malate and citrate exudation during Pi starvation	65
3.3	Role of <i>PPCKs</i> during plant development and Pi starvation	67
3.3.1	Effects of <i>ppck</i> knockouts on tissue fresh weight.....	67
3.3.2	Effects of <i>ppck</i> mutants on root length upon Pi starvation	68
3.4	Effects of <i>PPCK</i> loss affects tissue metabolites during Pi starvation	69
3.4.1	Effects of <i>ppck</i> mutants on shoot malate and citrate content during Pi starvation.....	69
3.4.2	Effects of <i>ppck</i> knockouts on root malate and citrate content during Pi starvation	70
3.4.3	Effects of <i>ppck</i> knockout on exuded malate and citrate during Pi starvation	71
4.0	SUMMARY	73
5.0	OUTLOOK.....	74
6.0	MATERIAL AND METHODS.....	75
6.1	Chemicals and reagents	75
6.2	Plant growth and bacterial culture media	75
6.3	Bacterial strains, plasmid vectors, culture and transformation	76
6.3.1	Bacterial strains and plasmid vectors	76
6.3.2	<i>Escherichia coli</i> and <i>Agrobacterium tumefaciens</i> cultivation.....	76
6.3.3	<i>Escherichia coli</i> and <i>Agrobacterium tumefaciens</i> transformation.....	77
6.4	Generation of stably transformed lines and plant growth conditions.....	77
6.4.1	Generation of <i>PPC</i> expression reporter lines	77
6.4.2	Generation of <i>PPC</i> overexpression lines	78
6.4.3	Generation of <i>ppck2</i> CRISPR/Cas 9 knockout line.....	78
6.4.4	Generation of <i>ppck1ppck2</i> double knockout line	79
6.5	Transformation and selection of <i>Arabidopsis</i> transgenic lines	80
6.6	Plant growth conditions.....	80
6.7	Analysis of <i>PPC</i> protein from whole seedlings, shoot and root tissues	80
6.7.1	Protein extraction and quantification.....	80
6.7.2	Sodium dodecyl sulfate polyacrylamide gel electrophoresis (SDS-PAGE)	81
6.7.3	Immunoblotting (Western Blot)	81
6.7.4	<i>PPC</i> enzyme activity	82
6.7.5	<i>PPC</i> phosphorylation status.....	82
6.8	Molecular Biology methods	83
6.8.1	Isolation of genomic DNA	83
6.8.2	Isolation of plasmid DNA from <i>E. coli</i>	83
6.8.3	Standard polymerase chain reaction (PCR).....	83
6.8.4	High fidelity PCR for molecular cloning.....	84
6.8.5	Agarose gel electrophoresis and purification of gel products.....	84
6.8.6	Isolation of RNA with on column dNASE digestion.....	85

6.8.7 cDNA synthesis.....	85
6.9 Analysis of metabolites from plant tissues and exudates.....	86
6.9.1 Preparation of tissue extracts for targeted metabolite profiling.....	86
6.9.2 Analysis of amino acids	86
6.9.3 Analysis of organic acids.....	87
6.9.4 Organic acid exudation experiments	88
6.10 Confocal Laser microscopy.....	88
6.11 Root elongation assay.....	88
6.12 Statistical analysis and data visualization.....	89
7.0 REFERENCES.....	90
8.0 APPENDIX.....	115
ACKNOWLEDGEMENT.....	132
STATUTORY DECLARATION.....	135

LIST OF FIGURES

Figure 1: Schematic diagram representing major players involved in the local Pi deficiency response	4
Figure 2: A model for the action of InsP8 in controlling Pi homeostasis.	5
Figure 3: Phosphoenolpyruvate carboxylase reaction	9
Figure 4: A schematic model for depicting regulation of PPCs by PPCKs and PP2A	12
Figure 5: <i>PPCs</i> transcript levels in wild type shoots and roots	17
Figure 6: Diagram showing the design of transcriptional reporter expression construct.....	18
Figure 7: Root cell type-specific expression domains of Arabidopsis <i>PPC</i> promoters.	19
Figure 8: <i>PPC</i> activity in shoots of Arabidopsis epidermal leaf cells.	20
Figure 9: Diagram showing the design of <i>PPC</i> overexpression constructs.	20
Figure 10: <i>PPC</i> transcript analysis in Arabidopsis seedlings overexpressing plant-type <i>PPCs</i>	21
Figure 11: Detection of total PPCs in <i>PPC</i> overexpression lines by immunoblot analysis.	22
Figure 12: Total PPC protein levels in tissues of transgenic Arabidopsis <i>PPC</i> overexpression lines ...	23
Figure 13: NADH-coupled PPC activity assay in crude protein extract of whole seedlings	26
Figure 14: PPC phosphorylation levels in shoots and roots of <i>PPC</i> overexpression lines	27
Figure 15: Tissue malate content in <i>PPC</i> overexpression lines.....	29
Figure 16: Tissue citrate content in <i>PPC</i> overexpression lines	30
Figure 17: Root malate and citrate exudation in <i>PPC</i> overexpression lines.....	32
Figure 18: Heatmap showing metabolite changes in tissues of <i>PPC</i> overexpression lines	35
Figure 19: Tissue fresh weights of <i>PPC</i> overexpression lines	37
Figure 20: Gain of root length of <i>PPC</i> overexpression lines.....	38
Figure 21: Growth of <i>PPC</i> overexpression lines on soil	39
Figure 22: Phenotypic characteristics of <i>PPC</i> overexpression lines grown on soil.....	40
Figure 23: <i>PPCK</i> transcript levels in wild type shoots and roots.	41
Figure 24: <i>PPCK</i> transcript levels in wild type and <i>ppck</i> mutants.	42
Figure 25: <i>PPCK1</i> transcript levels in <i>ppck1-4</i> mutant and <i>ppck1-4</i> complementation lines.....	43
Figure 26: Generation of <i>ppck2</i> mutants using CRISPR/Cas 9 technology.....	44
Figure 27: Selection of <i>ppck2</i> mutant lines generated using CRISPR/Cas 9 technology	45
Figure 28: Tissue malate content in <i>ppck</i> mutants and <i>ppck1-4</i> complementation lines	47
Figure 29: Tissue citrate content in <i>ppck</i> mutants and <i>ppck1-4</i> complementation lines.....	48
Figure 30: Root OAs exudation profiles of <i>ppck</i> mutants and <i>ppck1-4</i> complementation lines.....	49
Figure 31: Heatmap showing metabolite changes in <i>ppck</i> knockouts and <i>ppck1-4</i> complementation lines	51
Figure 32: Seedling tissue fresh weights in wild type, <i>ppck</i> mutants and <i>ppck1-4</i> complementation lines.	54
Figure 33: Gain of root length in wild type, <i>ppck</i> mutants and <i>ppck1-4</i> complementation lines.....	55

LIST OF TABLES

Table 1: Plant growth and bacterial culture media composition.....	75
Table 2: Plasmid vectors used in generation of PPCs overexpression lines and features.....	76
Table 3: Transgenic lines and knockout mutants used in this study.....	77
Table 4: Sequences for guide RNA used to generate <i>ppck2</i> through CRISPR/Cas 9.....	78
Table 5: Composition of SDS-PAGE Gel	81
Table 6: Components of standard PCR and colony PCR reaction.....	83
Table 7: Thermal profile for DreamTaq PCR.....	84
Table 8: Components of high-fidelity PCR.....	84
Table 9: Thermal profile Phusion High-Fidelity PCR.....	84
Table 10: Components of RT-qPCR reaction.....	86

LIST OF SUPPLEMENTARY FIGURES

Supplementary figure 1: Cell-specific expression domains of <i>PPCs</i> in shoots of <i>Arabidopsis</i>	115
Supplementary figure 2: <i>PPC</i> transcript analysis in wild type and overexpression lines.....	116
Supplementary figure 3: Detection of total <i>PPCs</i> in <i>PPC</i> overexpression lines by immunoblot analysis.	116
Supplementary figure 4: Shoot and root <i>PPC</i> levels in wild type and overexpression lines	117
Supplementary figure 5: Sequencing chromatograms showing deletions in the <i>PPCK2</i> gene.....	117
Supplementary figure 6: <i>PPCK</i> transcript levels in whole seedlings of wild type, <i>ppck</i> mutants and <i>ppck1-4</i> complementation lines.....	118

LIST OF SUPPLEMENTARY TABLES

Supplementary table 1: List of primers used for RT qPCR analysis	118
Supplementary table 2: Primers used for amplification of Arabidopsis plant type <i>PPC</i> promoters. ...	119
Supplementary table 3: Restriction enzymes used to confirm <i>PPC</i> promoter positive clones	119
Supplementary table 4: List of sequencing primers used for confirmation of positive clones for <i>PPC</i> promoters.....	120
Supplementary table 5: Primers used for amplification of open reading frames of <i>PPCs</i> for Directional TOPO cloning	120
Supplementary table 6: List of restriction enzymes used to confirm positive entry and destination clones for <i>PPC</i> overexpression lines	121
Supplementary table 7: Primers used for sequencing of <i>PPC</i> overexpression entry clones	121
Supplementary table 8: Restriction enzymes used in confirmation of <i>ppck2</i> CRISPR/Cas 9 mutant positive clones.....	121
Supplementary table 9: List of primers used to genotype and sequence positive clones for <i>ppck2</i> CRISPR/Cas 9 and <i>ppck1ppck2</i> mutants.....	121
Supplementary table 10: List of primers used for colony PCR in <i>Agrobacterium</i>	122
Supplementary table 11: Mass spectrophotometry (MS) parameters for MRM-transitions of organic acids.	123
Supplementary table 12: Comparison of metabolite in shoots of <i>PPC</i> overexpression lines compared to wild type on sufficient Pi.....	124
Supplementary table 13: Comparison of metabolite in shoots of <i>PPC</i> overexpression lines compared to wild type upon Pi starvation.	125
Supplementary table 14: Comparison of metabolite in roots of <i>PPC</i> overexpression lines compared to wild type grown on sufficient Pi condition.....	126
Supplementary table 15: Comparison of metabolite in roots of <i>PPC</i> overexpression lines compared to wild type upon Pi starvation.	127
Supplementary table 16: Comparison of metabolite in shoots of <i>ppck</i> mutants and <i>ppck1-4</i> complementation lines compared to wild type on sufficient Pi condition.	128
Supplementary table 17: Comparison of metabolite in shoots of <i>ppck</i> mutants and <i>ppck1-4</i> complementation lines compared to wild type upon Pi starvation.....	129
Supplementary table 18: Comparison of metabolite in roots of <i>ppck</i> mutants and <i>ppck1-4</i> complementation lines compared to wild type on sufficient Pi condition.	130
Supplementary table 19: Comparison of metabolite in roots of <i>ppck</i> mutants and <i>ppck1-4</i> complementation lines compared to wild type upon Pi starvation	131

ABBREVIATIONS AND SYMBOLS

ADP	Adenosine diphosphate
Al	Aluminum
AMF	Arbuscular mycorrhizal fungi
ANOVA	Analysis of variance
<i>At</i>	<i>Arabidopsis thaliana</i>
ATP	Adenosine triphosphate
bp	Base pairs
BTPC	Bacterial-type PPC
C3	Cavin cycle (C3 photosynthesis)
C4	Hatch and Slack cycle (C4 photosynthesis)
Ca ²⁺	Calcium (ii) ions
Cas 9	CRISPR associated protein 9
CAM	Crassulacean Acid Metabolism
cDNA	Complementary deoxyribonucleic acid
CDPKs	Ca ²⁺ -dependent protein kinases
Col-0	Columbia-0
CRISPR	Clustered Regularly Interspaced Short Palindromic Repeats
Ct	Cycle threshold
C-terminal	Carboxy-terminal
CTP	Cytidine triphosphate
DAG	Diacylglycerol
DNA	Deoxyribonucleic acid
EDTA	Ethylenediaminetetraacetic acid
EZ	Elongation zone
FADH ₂	Flavine adenine dinucleotide
Fe	Iron
FRD3	Ferric reductase defective 3
GABA	γ-Aminobutyric acid
GFP	Green fluorescent protein
GTP	Guanosine triphosphate
GUS	β-glucuronidase
InsP8	Inositol pyrophosphate 8
kb	Kilo bases
kDa	Kilodaltons
K _M	Michaelis-Menten constant
LPR1	LOW PHOSPHATE RESPONSE 1
LSM	Laser scanning microscope
MATE	MULTIDRUG AND TOXIC COMPOUND
cMDH	Cytosolic malate dehydrogenase
Mg ²⁺	Magnesium (ii) ions
Min	Minute(s)
mM	Milli molar
MRM	Multiple reaction monitoring
mRNA	Messenger ribonucleic acid
NADH	Nicotinamide adenine dinucleotide (NAD) + hydrogen (H).
nmol	Nano molar
N	Nitrogen
NLS	Nuclear localization signal
N-terminal	Amino terminal
OA	Organic acid
OD ₆₀₀	Optical density at 600 nm wavelength
ORF	Open reading frame
P	Phosphorus

p	Probability value
PA	Phosphatidic acid
PDR2	PHOSPHATE DEFICIENCY RESPONSE 2
PEP	Phospho <i>enol</i> pyruvate
pH	Potential of hydrogen
PHL1	PHR1-LIKE
PHR1	PHOSPHATE STARVATION RESPONSE 1
Pi	Inorganic phosphate
PP2A	Protein phosphatase 2A
PPC	Phospho <i>enol</i> pyruvate carboxylase
PPCK	Phospho <i>enol</i> pyruvate carboxylase kinase
PSR	PHOSPHATE STARVATION RESPONSE
PSI	PHOSPHATE STARVATION INDUCED
PTPC	Plant-type PPCs
PUE	Phosphate use efficiency
RAM	Root apical meristem
RNA	Ribonucleic acid
ROS	Reactive oxygen species
rpm	Rotations per minute
RT-PCR	Reverse transcription polymerase chain reaction
RT-qPCR	Reverse transcription quantitative real-time polymerase chain reaction
RUBISCO	Ribulose-1,5- bisphosphate carboxylase/oxygenase
SCN	Stem cell niche
SCR	SCARECROW
SE	Standard error
SDS	Sodium dodecyl sulfate
SDS-PAGE	Sodium dodecyl sulfate polyacrylamide gel electrophoresis
SHR	SHORT-ROOT
STOP1	SENSITIVE TO PROTON RHIZOTOXICITY 1
TCA	Tricarboxylic acid cycle
T-DNA	Transfer deoxyribonucleic acid
UBQ10	UBIQUITIN 10
UTP	Uridine triphosphate
UTR	Untranslated region
v/v	Volume per volume
wPi	Phosphate sufficient
woPi	Phosphate deficient
WOX5	WUSCHEL-RELATED HOMEBOX 5
w/v	Weight per volume
μl	Microliter
μg	Microgram
μM	Micro molar
35S CaMV	<i>Cauliflower Mosaic Virus</i> 35S promoter

1.0 INTRODUCTION

1.1 Importance of phosphorus

Phosphorus (P) is the second most essential macronutrient required for plant growth and development along with nitrogen (N) (Roch et al., 2019). It regulates various physiological and molecular plant processes (Razaq et al., 2017), e.g. phospholipid biosynthesis, and is a structural element of DNA and RNA. Chemical energy stored in adenosine triphosphate (ATP), cytidine triphosphate (CTP), guanosine triphosphate (GTP), uridine triphosphate (UTP), phospho*enol*pyruvate and other phosphorylated compounds drive cellular endergonic processes (Lambers & Plaxton, 2018; Razaq et al., 2017; Stigter & Plaxton, 2015; D. Wang et al., 2017; Zhang et al., 2009). P limitation negatively impacts crop yield and grain quality, and it is estimated that P deficiency reduces crop yields on 30–40% of the world's arable land. This necessitates the use of large amounts of P fertilizers to ameliorate its deficiency since P application and availability stimulates seed germination, is essential for all developmental stages, and increases the N-fixing capacity of leguminous plants (Malhotra et al., 2018). However, the P use efficiency (PUE), estimated to be as low as 15–20% in arable agricultural fields, indicate that most of the soil-applied P is not available to plants and leaches into ground and surface waters leading to eutrophication (Correll, 1998; L. Smith & Monaghan, 2003). Considering the increasing world population set to reach 9 billion by the year 2050, the need to increase food production by up to 70% is necessary to feed the human population (Bechtaoui et al., 2021). This requires a better understanding and efficient utilization of the limited P resource to meet the increased food demand and production.

1.2 Phosphorus availability in soil and plants

Bioavailable P concentration in plants ranges from 0.05% to 0.5% of total plant dry weight, and in the soil P concentration is on average 2000-fold higher than in plants. However, as the only form that can be assimilated by plants from soil, Pi is present at low concentrations in soil solution (usually less than 2 μ M). At low and high soil pH, Pi forms insoluble complexes with aluminum or iron and with calcium or magnesium respectively, which reduces its mobility in soil, leading to an uneven distribution and low Pi availability for plant uptake (Hinsinger, 2001; Raghothama, 1999b; Shen et al., 2011; Tetsuro Mimura, 1999). As a result, Pi availability in the soil is rarely sufficient for optimum plant growth and development. Thus, plants often face the problem of Pi deficiency in agricultural fields. Approximately 60% of applied P fertilizers are produced from non-renewable phosphate rock (Cordell, 2010; Liu et al., 2008; Smit et al., 2009). Due to the high P demand, several studies suggest that the phosphate rock reserves could be depleted within the next 100 years (Cordell, 2010; Haes et al., 2009; Smit et al., 2009; Vaccari, 2009).

1.3 Symptoms of phosphorus deficiency in plants

Diagnosing P deficiency is a tedious task, since crops generally display no visual symptoms at an early growth stage, which is often confused with N deficiency because the veins of young leaves appear red under both deficiencies. P deficiency in plants disturbs the production of chlorophyll, causing leaf chlorosis (Choi et al., 2013; Viégas, Ismael de Jesus Matos et al., 2018), which leads to reduced plant growth because of reduced photosynthetic activity. P-deficient plants additionally have stunted thin stems, which are spindly. Their foliage, rather than being bright green, is often dark, almost bluish-green, and prolonged P deficiency results in the accumulation of anthocyanins, consequently leading to purple discoloration on the leaf surface (Osbourne et al., 2002; Ticconi & Abel, 2004). Delayed maturity, sparse flowering, poor seed quality and even leaf senescence have been reported in very severe cases (Weil & Brady, 2017). However, due to its mobile nature within the plant, Pi is recycled and transferred from older to younger leaves when in short supply; thus, older leaves show P deficiency symptoms first.

1.4 Phosphorus sensing and acquisition by plants

Pi acquisition from soil occurs at the roots due to their contact with the soil interface. Due to its very immobile nature in soils, plant roots preferentially grow towards Pi patches (Aerts, 1999). Plants have evolved various morphological, physiological, and biochemical adaptations to improve Pi acquisition and utilization under Pi-deficient conditions (Abel, 2011; Kopriva & Chu, 2018; van de Wiel et al., 2016). These strategies could be broadly categorized into:

- (i) Formation of symbiotic relations with mycorrhiza fungi.
- (ii) Change in root system architecture via local Pi sensing.
- (iii) Adjustment of cellular metabolism via systemic Pi sensing.
- (iv) Exudation of phospho-hydrolases and carboxylic acids.

1.4.1 Formation of symbiotic relations with mycorrhiza fungi

The nutrient uptake system of crops includes not only their unique transport system on the root epidermis but also a transport system mediated by interaction with specific soil microorganisms. Among these interactions, symbiosis with arbuscular mycorrhizal fungi (AMF) in the roots is an ancient and ubiquitous relationship that began over 400 million years ago (Fonseca & Berbara, 2008) and has been observed in many economically important crops such as soybean, wheat, and corn. AMF hyphae growing outside the roots allow plants to access Pi further away from the root surface and provide an enhanced foraging system that improves the acquisition of nutrients such as Pi and water while the plants provide compounds such as carbohydrates, lipids or organic acids in a mutually beneficial way for both organisms (Smith & Smith, 2011).

1.4.2 Change in root system architecture via local Pi sensing

Root system architecture (RSA) is highly plastic and its developmental response to Pi-deficient conditions in various plants is well studied and documented. Since Pi availability is generally higher in the topsoil layers, plants change their RSA to access this Pi-rich layer in what is termed as the local response. Plants develop shallow root systems to increase the surface area for Pi exploration from the topsoil. In the case of common bean (*Phaseolus vulgaris*) and soybean (*Glycine max.*), the shallow root system arises from repeated branching of the primary root while in rice (*Oryza sativa*) and maize (*Zea mays*), the existing adventitious root system explores the topsoil for Pi absorption (Hochholdinger et al., 2004; Lynch, 1995; Lynch & Brown, 2008; Osmont et al., 2007). Other plant species such as white lupin (*Lupinus albus*), develop cluster roots with dense and determinant lateral roots which are covered by large numbers of root hairs (Lambers et al., 2006; Vance, 2008). In *Arabidopsis thaliana* (*Arabidopsis*), significant low Pi reduces primary root growth accompanied by the emergence of lateral roots and root hairs, which increase Pi exploration, solubilization and absorption (Jain et al., 2007; Lynch & Brown, 2008; Williamson et al., 2001)

The local response in *Arabidopsis* is regulated by external Pi and Fe availability in the soil solution surrounding the rhizosphere and requires direct contact with the root tip (Bates & Lynch, 1996; Müller et al., 2015; Svistoonoff et al., 2007; Ward et al., 2008). During Pi starvation, *Arabidopsis* root tips, including the root stem cell niche (SCN), accumulate Fe in the apoplast, which is thought to trigger the generation of reactive oxygen species (ROS) (Müller et al., 2015). ROS generation leads to callose deposition in the cell walls and plasmodesmata of the root apex (Benitez-Alfonso et al., 2009; Müller et al., 2015; Petricka et al., 2012). This prevents cell-to-cell movement of SHORT ROOT (SHR) and SCARECROW (SCR), which are essential regulators of WUSCHEL-RELATED HOMEODOMAIN 5 (WOX5) (Helariutta et al., 2000; Vatén et al., 2011). Ultimately the SCN and dividing cells are exhausted, resulting in growth inhibition and short roots (Müller et al., 2015). Two modules (Figure 1) have so far been proposed, which further explain the local response, i.e. LOW PHOSPHATE ROOT 1-PHOSPHATE DEFICIENCY RESPONSE 2 (LPR1-PDR2) module and the SENSITIVE TO PROTON RHIZOTOXICITY 1-ALUMINIUM ACTIVATED MALATE TRANSPORTER 1 (STOP1-ALMT1) module (Abel, 2017; Mora-Macías et al., 2017; Müller et al., 2015)

During Pi starvation, the PDR2-LPR1 module mediates Fe accumulation in the SCN and root elongation zone (EZ) triggering accumulation of ROS and callose deposition in cell walls of the SCN and EZ (Hoehenwarter et al., 2016; Müller et al., 2015). *LPR1* encodes a cell wall-resident bacterial-type multicopper ferroxidase, which oxidizes Fe²⁺ to Fe³⁺ in the apoplast of the root apical meristem (RAM), while *PDR2* encodes a P5-type ATPase of unknown specificity residing in the endoplasmic reticulum (Müller et al., 2015; Naumann et al., 2022; Naumann et al., 2019; Sørensen et al., 2015). The *lpr1* mutant is insensitive to low Pi and neither accumulates Fe nor attenuates its primary root growth during

Pi starvation as opposed to the *pdr2* mutant, which is hypersensitive to low Pi, over-accumulates Fe, and its primary growth is strongly inhibited during Pi starvation (Müller et al., 2015; Naumann et al., 2022; Naumann et al., 2019).

The second module implicated in local Pi sensing involves citrate and malate extrusion (Maruyama et al., 2019; Peng et al., 2018; Sawaki et al., 2009). STOP1, which is a zinc finger transcription factor, induces during Pi starvation one of its target genes, *ALMT1*, which encodes a malate transporter (Balzergue et al., 2017; Sawaki et al., 2009). Once induced, *ALMT1* effluxes malate into the apoplast where it liberates Fe bound to Pi, which is then absorbed. Both *stop1* and *almt1* mutants show insensitivity to low Pi as evidenced by their long roots compared to the wild type (Mora-Macías et al., 2017).

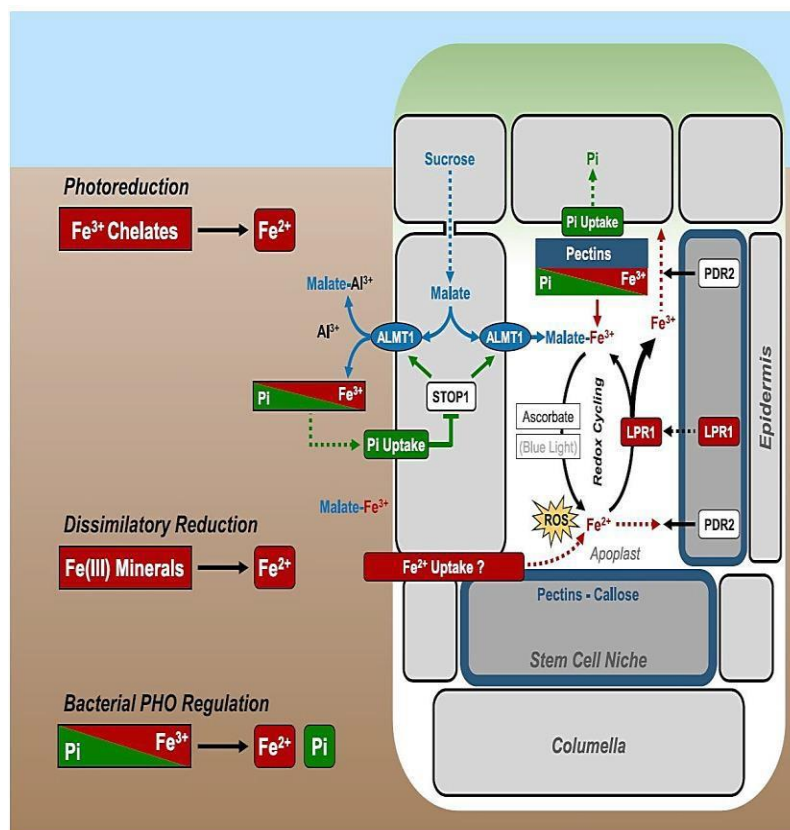


Figure 1: Schematic diagram representing major players involved in the local Pi deficiency response

ALMT1 releases malate into the rhizosphere as well as into the root apoplast, resulting in the remobilization of Pi from Fe-Pi complexes by Fe^{3+} -chelation. Subsequent reduction of Fe^{3+} -malate promotes reactive oxygen species (ROS) formation, while LPR1 dependent Fe^{2+} oxidation ameliorates ROS production and possibly mediates ROS signaling in the SCN. PDR2 counteracts LPR1 function by maintaining Fe homeostasis in root tips. Adapted from Naumann et al., (2022).

1.4.3 Adjustment of cellular metabolism via systemic phosphate sensing

Systemic or long-distance responses depend on the internal Pi concentration and participate in the overall enhancement of Pi uptake, reallocation and recycling to ensure the metabolic balance of P at the

whole-plant level (Thibaud et al., 2010). Systemic signals are conveyed by internal Pi, sugars, hormones and RNAs (Lin et al., 2014). These signals are generated at one site and due to their mobile nature move in the vasculature to elicit their function at a distance. During Pi starvation, hydrolysis of phosphorylated compounds and internal Pi stores increases. For example, phospholipids which are a reserve for internal Pi are hydrolyzed to release Pi and diacylglycerol (DAG), which is then subsequently converted into galactolipids or sulfolipids to compensate for reduced phospholipids (Härtel et al., 2000; Yu et al., 2002). Expression of genes involved in phospholipid turnover (e.g., *PLD ζ 1* and *PLD ζ 2* encoding lipases) and sulfolipid biosynthesis (e.g., *SQD1* and *SQD2*) are highly induced leading to reduced phospholipid content and increased sulfolipids and galactolipids in membranes of plants growing under low Pi (Cruz-Ramírez et al., 2006; Qin et al., 2006; Welte & Wang, 2006). A model that explains the systemic phosphate starvation response (PSR) involves the transcription factor PHOSPHATE STARVATION RESPONSE 1 (PHR1) and the SPX domain proteins which control the transcription of the majority of *PSR* genes (Bustos et al., 2010). The SPX domain named after SYG1 (suppressor of yeast *gpa1*), Pho81 (CDK inhibitor in yeast PHO pathway) and XPR1 (xenotropic and polytropic retrovirus receptor) negatively regulates the systemic PSR. In contrast, transcription factor PHR1 and its close PHR1-like (PHLs) relatives, which are transcription factors, positively regulate the PSR by binding to the promoters of phosphate starvation inducible (PSI) genes (Puga et al., 2014; Zhou et al., 2008). During sufficient Pi conditions, SPX proteins interact with PHR1/PHLs due to high levels of a ‘molecular glue’, inositol pyrophosphate 8 (InsP₈), in the cytosol and nucleus, preventing binding of PHR1/PHLs to the promoters of *PSI* genes (Dong et al., 2019; Ried et al., 2021).

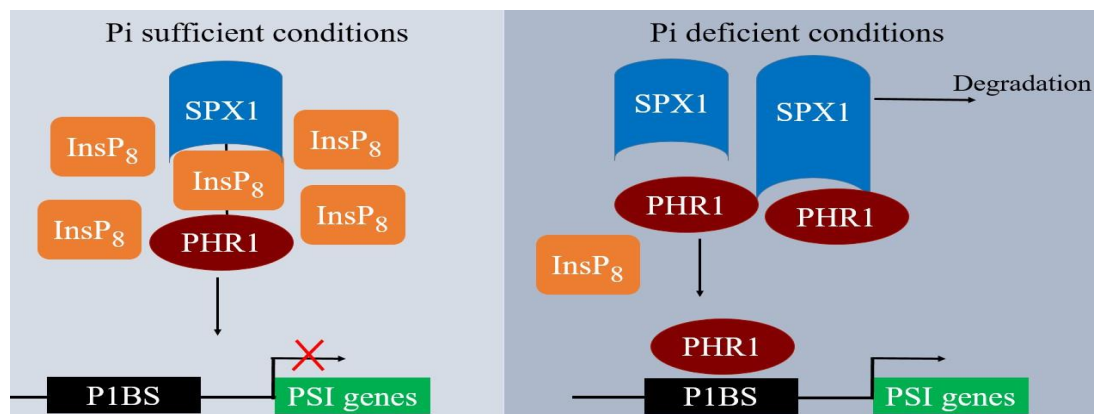


Figure 2: A model for the action of InsP₈ in controlling Pi homeostasis.

Under Pi sufficient conditions, high InsP₈ levels facilitate binding of SPX to PHR1 inhibiting its activation of *PSI* genes, while in the Pi deficient conditions, low levels of InsP₈ favors dissociation of the SPX-PHR1 complex, allowing nuclear localization and binding of PHR1 to P1BS promoter elements, which activates the expression of *PSI* genes. Adapted and modified from Dong et al., (2019).

However, during Pi starvation, low levels of cytosolic InsP₈ result in the dissociation of the SPX-PHR1/PHLs complexes followed by degradation of SPX proteins (Figure 2). This allows the movement

of PHR1/PHLs from the cytosol to the cell nucleus where they activate transcription of *PSI* genes (Zhou et al., 2015).

1.4.4 Exudation of phospho-hydrolases and carboxylic acids

Induction and exudation of P-hydrolases such as phosphatases is another strategy involved in Pi acquisition and plays a role in both local and systemic Pi deficiency response (Tran et al., 2010; Zhang et al., 2014). Once secreted, the extracellular or secreted phosphatases are believed to release Pi groups from organophosphates by hydrolysis of P-esters and P-anhydrides at low pH and thereby increase Pi availability for plants (Schmidt & Laskowski, 1961).

Another Pi acquisition mechanism is the exudation of carboxylic acids. The free organic acids (OAs) and corresponding carboxylate anions constitute the major fraction of root exudates during Pi deficiency. The most common OAs anions found in the rhizosphere are lactate, acetate, oxalate, succinate, fumarate, malate, citrate, isocitrate, and aconitate (Jones & Brassington, 1998). These carboxylates were suggested to improve P availability by remobilizing the sparingly available Pi forms from the soil solution (Jones & Brassington, 1998; Koyama et al., 1988). This occurs by chelation of metals ions like Al, Fe or Ca due to the negative charges of carboxylates, resulting in the displacement of anions, such as Pi, from the soil matrix (Delgado et al., 2013; Jones & Brassington, 1998; Vance et al., 2003). Pi deficiency-induced OAs exudation from roots was first identified in white lupin (*Lupinus albus* L.) (Gardner et al., 1983; Gardner et al., 1981). When grown on P-limited soils, this pioneer crop develops cluster roots as the sites of profuse OAs exudation, which synergistically enhances Pi acquisition from soil (Johnson et al., 1994; Kochian et al., 2004; Larsen & Gunary, 1961; Neumann et al., 1999; Wu et al., 2011). Exudation of OAs in response to metal stress and Pi starvation also occurs in other plant species in a time- and tissue-specific manner. Under Al toxicity, exudation of OAs such as malate, citrate and oxalate is quick and instant while under low Pi induction exudation occurs after a few days of low Pi exposure (Dong et al., 2004; Wang et al., 2007).

1.5 Biosynthesis and role of organic acids in plants

OAs are produced in the mitochondria via the tricarboxylic acid (TCA) cycle and to a lesser extent in the glyoxysome as part of the glyoxylate cycle. As products of the oxidation of photosynthetic assimilates, OAs can either be converted back to carbohydrates or undergo terminal oxidation yielding CO₂ and H₂O (Igamberdiev & Eprintsev, 2016). OAs metabolism is fundamentally important at the cellular level for several biochemical pathways including energy production, formation of precursors for amino acid biosynthesis, and at the whole plant level in modulating adaptation to the environment (López-Bucio et al., 2000). Being negatively charged, OAs play a critical role in balancing excess of positively charged ions and regulating osmotic potential and cellular pH (Xiang et al., 2019).

In addition to their role inside plant cells, OAs are also secreted into the rhizosphere where they act as chemo-attractants by providing carbon and energy sources to microbes, which promotes symbiotic

microbial root associations leading to increased plant mineral uptake (Macias-Benitez et al., 2020; Zhang et al., 2014). Because of their cation chelating potential, OAs play crucial roles during plant responses to various stresses (Panchal et al., 2021). Plants secrete OAs in response to metal stresses, a mechanism which enhances their tolerance to metal toxicities. Binding affinities to metal cations increases with the number of carboxyl groups, making OAs such as citrate and malate very efficient metal chelators, as exemplified by the Al-induced exudation of malate by wheat and Arabidopsis roots (Ryan et al., 2011; Yang et al., 2013), and of citrate by maize, sorghum, barley, and soybean roots (Meyer et al., 2010; Ryan et al., 2011; Wu et al., 2014).

Chelation of metal cations by OAs results in solubilization of Pi from Pi-metal complexes and their exudation plays a pivotal role in Pi acquisition. In transgenic tobacco plants, increased OAs biosynthesis and secretion led to enhanced Pi uptake by dissolving insoluble Pi compounds present in the soil (López-Bucio et al., 2000). In the Proteaceae family, plants bear specialized roots, called proteoid or cluster roots, which secrete OAs in response to Pi deficiency in soil (Dinkelaker et al., 1995; Shahbaz et al., 2006). Due to their negative charges and ability to form complexes with positively charged ions, OAs, especially malate and citrate, provide a great tool with which alleviation of several different plant stresses such as Pi starvation can be studied (Zhang et al., 2018).

1.5.1 Biosynthesis and role of citrate in plants

Citrate belongs to compounds, which plant tissues usually contain in considerable amounts. It is synthesized from the condensation of oxalacetate with the acetyl-CoA in both the TCA and glyoxylate pathways, a reaction which is catalyzed by citrate synthase (Fernie et al., 2004; Popova & Pinheiro de Carvalho, 1998). As an intermediate of the TCA cycle, citrate sustains the regeneration of nicotinamide adenine dinucleotide (NADH) and flavine adenine dinucleotide (FADH₂) molecules resulting in energy production in form of ATP (Icard et al., 2012). It is a key regulator of several catabolic and anabolic pathways such as fatty acid synthesis β -oxidation, Fatty acid synthesis, glycolysis or gluconeogenesis. It is stored in the vacuoles where it maintains cytosolic pH (Etienne et al., 2013; Pracharoenwattana et al., 2005) Citrate is degraded through the GABA shunt which results in succinate synthesis or it is converted back to oxaloacetate and acetyl-CoA (Etienne et al., 2013). Movement of citrate in the plant occurs through channels and transporters and among the well characterized citrate transporters is the multidrug and toxic compound extrusion proteins (MATE) which exports citrate and other small organic molecules (Kuroda & Tsuchiya, 2009).

Facilitation of Fe distribution and transport throughout the plant was shown to be a major role for citrate. In iron deficient conditions, enhanced citrate concentration in the xylem sap and exudation into the rhizosphere has been reported (Durrett et al., 2007; Martínez-Cuenca et al., 2013). Upon exudation into the rhizosphere, citrate acidifies the local environment which facilitates the reduction of the insoluble Fe³⁺ to the more soluble Fe²⁺ which is then taken up by plants (Carvalhais et al., 2011). Once inside

the plant, iron is complexed to citrate secreted by a specialized MATE transporter ferric reductase defective 3 (FRD3), loaded into the xylem and transported to distal tissues (Durrett et al., 2007; Roschztardt et al., 2011).

Other studies have also shown citrate importance in alleviating different stresses such as lead phytotoxicity in castor beans, aluminum phytotoxicity in sorghum, barley, wheat, maize and Arabidopsis, phosphorus in white lupin, soybean and in tobacco and alkaline tolerance in Medicago (Furukawa et al., 2007; Liu et al., 2009; López-Bucio et al., 2000; Magalhaes et al., 2007; Mallhi et al., 2019; Maron et al., 2010; Peng., et al., 2018; Ryan et al., 2009; Tiziani et al., 2020).

1.5.2 Biosynthesis and role of malate in plants

Like citrate, malate is among the most accumulated OAs in many plants. Malate is synthesized in three main compartments in plants i.e. mitochondria, glycosome and the cytoplasm (Wu et al., 2020). In the cytoplasm, phosphoenolpyruvate carboxylases (PPCs) catalyze the reaction of phosphoenolpyruvate (PEP) with hydrogen carbonate ions in the presence of Mg^{2+} to form oxaloacetate which is then reduced to malate by cytosolic malate dehydrogenase (cMDH). Malate participates in the transfer of redox equivalents between cell compartments (Geigenberger & Fernie, 2014; Maurino & Engqvist, 2015). It also plays an important role in carbon metabolism, ionic homeostasis and is the origin of carbon skeletons for amino acid biosynthesis in plants (Cheffings et al., 1997; Schneidereit et al., 2006). Malate also acts as an osmolyte and an anion where it compensates for the positive charge of potassium, which is particularly important in stomatal responses (Meyer et al., 2010). Disruption of malate metabolism has a specific effect on root growth that is independent of alterations in leaf metabolism (van der Merwe et al., 2008).

Malate plays a pivotal role when exuded into the rhizosphere (Schulze et al., 2002). It is the primary substrate for bacteroid respiration that fuels nitrogenase as it is easily taken up via transporters such as the dicarboxylate transporter A (Udvardi & Day, 1997) while the conversion of malate to oxaloacetate by malate dehydrogenases provides carbon skeletons for the assimilation of fixed nitrogen into amino acids (Driscoll & Finan, 1993; Rosendahl et al., 1990). Malate secretion promotes plant adaptation to aluminum toxicity (Dinkelaker et al., 1995; Raghothama, 1999; Skene, 2001) which has been confirmed by identification of a family of aluminum activated malate transporters (ALMT) in various plants such as wheat (Sasaki et al., 2004), barley (Delhaize et al., 2004), rye (Fontecha et al., 2007), rapeseed (Ligaba et al., 2006) and Arabidopsis (Hoekenga et al., 2006). In a study by (Tesfaye et al., 2001) and its follow up (Tesfaye et al., 2003), increased malate levels resulting from overexpressing malate dehydrogenase (MDH) in alfalfa roots enhanced Pi uptake in the transgenic plants compared to the control. In soybean, Pi starvation increased the secretion of organic acid such as malate which enabled plants to survive when insoluble Pi fertilizer was applied (Wei et al., 2013). In Arabidopsis, *AtALMT3* upregulation during Pi deficiency was accompanied by increased malate exudation inferring the

important role of malate exudation and Pi liberation from bound metal complexes (Maruyama et al., 2019).

1.6 Phosphoenolpyruvate carboxylases (PPCs) and their role in plants

Phosphoenolpyruvate carboxylase (PPC) is largely a cytosolic carbon dioxide fixing enzyme that in an irreversible manner and in the presence of Mg^{2+} , converts phosphoenolpyruvate and bicarbonate into oxaloacetate and Pi (Figure 3) (O'Leary et al., 2011). It is widely present in algae, bacteria (including cyanobacteria) and plants but has not been identified in fungi or animals (Durall & Lindblad, 2015; Izui et al., 2004; Mamedov et al., 2005).

Phosphoenolpyruvate carboxylase (PPC) reaction

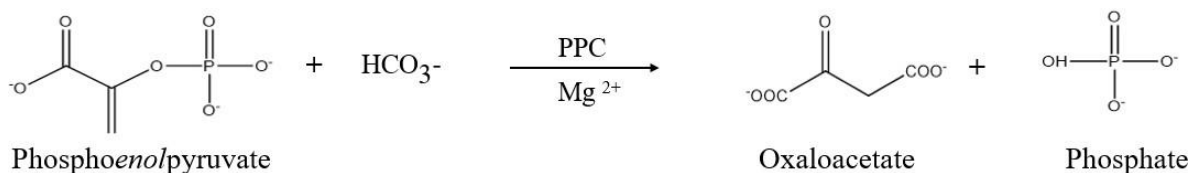


Figure 3: Phosphoenolpyruvate carboxylase reaction.

In the cytoplasm, PPC in the presence of HCO_3^- and Mg^{2+} converts phosphoenolpyruvate to oxaloacetate liberating Pi in the process.

Two distinct classes of PPCs are known to occur in plants and are classified as either bacterial-type (BT PPC) or plant type (PT PPC) enzymes (O'leary et al., 2011; Sánchez & Cejudo, 2003). The *BT PPC* gene encodes a polypeptide of approximately 116-118 kDa that lack the classic N-terminal regulatory phosphorylation site present in PT PPCs but contains a prokaryotic-like R(K)NTG tetrapeptide at the C-terminus (Sánchez & Cejudo, 2003; Sánchez et al., 2006; Sullivan et al., 2004; Yasushi et al., 1999). Interestingly, BT PPCs possess inhibitory phosphorylation sites identified in developing castor oil seed (Uhrig et al., 2008), which is embedded in an intrinsically disordered region absent in PT PPCs (Dalziel et al., 2012; O'leary et al., 2011). BT PPCs exhibit lower affinity for PEP and PPC allosteric activators but also show a higher insensitivity to allosteric inhibitors such as malate and aspartate (O'Leary et al., 2009). PT PPCs and BT PPCs also interact to form larger 900 kDa hetero- octameric proteins (class 2), which have been identified in unicellular green algae, lily, and castor bean (O'leary et al., 2011). Unlike class 1 PPC proteins (homo-tetramers), the class 2 PPC proteins are highly desensitized to allosteric effectors (Blonde & Plaxton, 2003; Gennidakis et al., 2007; Moellering et al., 2007).

On the other hand, plant-type PPCs belong to a small multigene family, whose members encode smaller polypeptides of approximately 100-110k Da, with a conserved N-terminal serine phosphorylation site and a critical C-terminal tetra peptide QNTG (Chollet et al., 1996; Gennidakis et al., 2007; Izui et al., 2004; Sánchez & Cejudo, 2003; Xu et al., 2006). PT PPCs exist as homo-tetramers (class 1) of

approximately 400 kDa composed of identical subunits of approximately 410 kDa (Izui et al., 2004). PTPPCs are further categorized into non-photosynthetic (C3 PPCs) and photosynthetic (C4 and CAM PPCs) isoenzymes (O'Leary et al., 2011). In C3 PPCs, the presence of an arginine residue (Arg884) at the malate binding site provides an additional hydrogen bond which promotes stronger binding to the feedback inhibitor while its substitution with glycine in C4/CAM plants reduces the steric restriction making C4/CAM PPCs more tolerant towards feedback inhibition than the C3 enzyme (Paulus et al., 2013).

The best described function of PPCs is the pre-fixation of CO₂ (in the form of HCO₃⁻ provided by the carbonic anhydrase reaction) during C4 and CAM photosynthesis (Hatch, 1987). In C4 plants, bicarbonate is initially fixed by PPCs to form oxaloacetate in the mesophyll cells before its transport to the bundle sheath cells, where CO₂ is released and concentrated at the site of ribulose-1,5- biphosphate carboxylase/oxygenase (RUBISCO) action. This compartmentalization of CO₂ pre- fixation reduces the oxygenase activity of RUBISCO and resulting photorespiration, making C4 plants photosynthetically more efficient compared to C3 plants (Hatch, 1987).

In C3 plants, PPC functions not only in the anaplerotic replenishment of the TCA cycle intermediates consumed during lipid biosynthesis (Chollet et al., 1996; Podestá & Plaxton, 1994; Sangwan et al., 1992), but also in the nitrogen assimilation which is well demonstrated by reduced amino acid levels in *ppc* mutants (Masumoto et al., 2010; Shi et al., 2015). In *Solanum tuberosum*, plants overexpressing a *Corynebacterium glutamicum* PPC showed increased rate of stomatal opening compared to the controls (Gehlen et al., 1996) while transformation of C4 PPC enhanced drought tolerance and yields in wheat (Qin et al., 2016) and conferred aluminum tolerance in rice (Begum et al., 2009). In Arabidopsis, PPCs have been associated with germination, normal plant growth, seed quality and filling (Feria et al., 2016; Feria et al., 2022). In these two studies, *ppc* mutants showed an impaired or reduced plant size, reduced fresh rosette weight, and had poor seed quality and seed filling.

Plant genomes code for several isoforms of C4 or C3 PPCs. There are ten PPC genes in *Glycine max* (Wang et al., 2016), five each in *Medicago truncatula* and *Solanum lycopersicum* (Wang et al., 2016; Waseem & Ahmad, 2019), three in *Flaveria spp* (Engelmann et al., 2003), two in *Lotus japonicas* (Nakagawa et al., 2003), and six each in *Zea mays*, *Phaseolus vulgaris*, *Oryza sativa* (Wang et al., 2016) and *Sorghum bicolor* (Lepiniec et al., 1993). The *Arabidopsis thaliana* genome encodes four PPCs: three PTPPCs (*AtPPC1*, *AtPPC2*, *AtPPC3*) and one BTPC (*AtPPC4*). The differential expression of Arabidopsis PPCs in different tissues suggests that these PTPPCs could be involved in specialized functions (Sánchez et al., 2006). In our study, PTPPCs will be referred to as PPCs.

1.7 Regulation of phosphoenolpyruvate carboxylases in plants

PPCs regulation is multifaceted and tightly regulated in plants (Jiao & Chollet, 1991). Transcriptional control regulates the amount of PPCs through changes in the abundance of PPC mRNA (Theng et al., 2007). In CAM and C₄ plants, PPC phosphorylation and PPC activity increased in response to light but drastically reduced by dawn while in C₃ plants, PPC expression and PPC activity has been shown to increase in response to abiotic stresses such as salt stress, drought stress, Pi starvation (Doubnerová et al., 2014; Gregory et al., 2009; Sánchez et al., 2006; Taybi et al., 2004; Theng et al., 2007).

PPCs are also tightly regulated allosterically. They are positively activated by hexose phosphates (e.g., G6P), triose phosphates (e.g., PEP) and neutral amino acids such as glycine, serine or alanine (Muñoz-Clares et al., 2020; Schlieper et al., 2014). In contrast, PPCs are inhibited by malate, aspartate and glutamate (Chollet et al., 1996; Izui et al., 2004). In a model that explains PPC activation, binding of the positive effectors at the active site causes a conformation change on the other subunits which then lowers the K_M for the substrate PEP (Rustin et al., 1988; Schlieper et al., 2014; Wong & Davies, 1973). However, in the negative feedback inhibition, the negative effectors malate and aspartate bind to a different site from the active site on the C-terminal end (Kai et al., 1999; Matsumura et al., 2002; Paulus et al., 2013).

Monoubiquitination of PPCs is a posttranslational modification which regulates PPC activity. Monoubiquitination at lysine 624 in sorghum and lysine 628 in castor oil seeds renders PPCs more sensitive to the inhibition by malate and citrate, reduces their activity and additionally targets them for proteasomal degradation (Schulz et al., 1993; Uhrig et al., 2008). Chemical regulation also controls PPC activity. Phosphatidic acid (PA), an anionic phospholipid, binds and inhibits C₄ PPC. The addition of 50 μ M PA decreased PPC activity by 60% compared to the control activity in maize plants (Monreal et al., 2010).

The most investigated and well-studied regulation of PPCs is phosphorylation which also impacts on their control by allosteric effectors (Figure 4). Reversible phosphorylation and dephosphorylation occurs at a single, strictly conserved serine (e.g., Ser11 in AtPPCs) residue near the N-terminus of the protein (Jiao & Chollet, 1991; Vidal & Chollet, 1997). Compared to non-phosphorylated PPCs, phosphorylated PPCs are more active since their affinities to positive effectors increases while the affinity to inhibitors, mainly malate and aspartate, decreases (Buchanan-Bollig & Smith, 1984; Nimmo et al., 1984; Winter, 1982). PPCs are phosphorylated by a specific phosphoenolpyruvate carboxylase kinase (PPCK) and are dephosphorylated by a non-specific phosphatase 2 (PP2A) (Dong et al., 2001). In a study on *Nicotiana tabacum* L. leaves, potato virus Y (PVY) infection led to increased PPC phosphorylation levels and increased activity while the transcript levels remained comparable to the control (Müller et al., 2009).

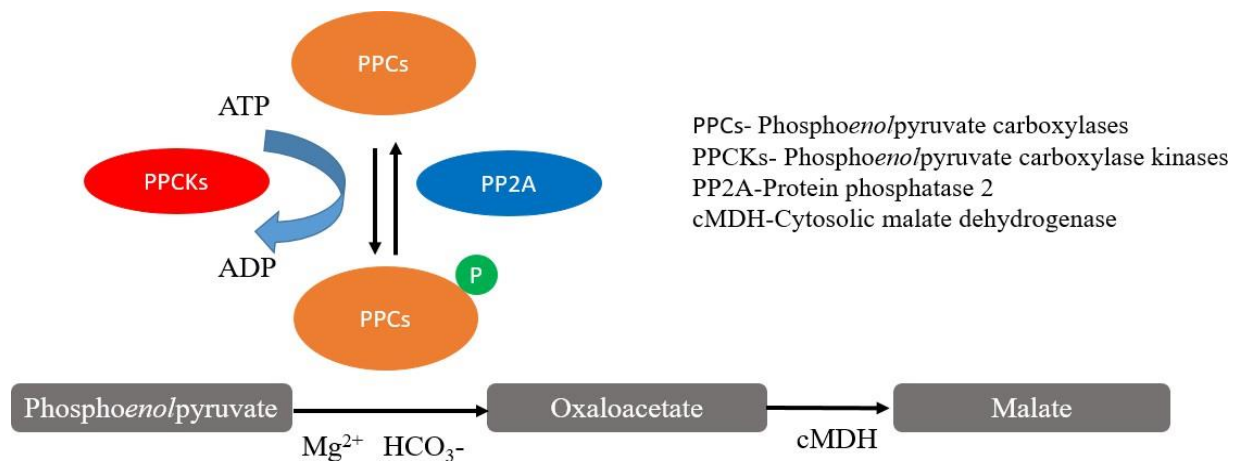


Figure 4: A schematic model for depicting regulation of PPCs by PPCKs and PP2A.

PPCKs phosphorylate PPCs increasing their affinity for allosteric activators such as glucose-6-phosphate, glycine and PEP while PP2A dephosphorylates PPCs, increasing their affinity for allosteric inhibitors such as malate and aspartate. Adapted and modified from Yang et al., (2017).

1.8 Phospho*enol*pyruvate carboxylase kinases and their role in plants

Phospho*enol*pyruvate carboxylase kinases (PPCKs) control the phosphorylation and activity of PPCs in plants (Hartwell et al., 2002; Nimmo et al., 2001). They are grouped in the superfamily of Ca^{2+} /calmodulin-regulated protein kinases (CDPK) although their activity is Ca^{2+} -independent. PPCKs are the smallest known protein kinases (30-39 kDa) (Hartwell. et al., 1999; Nimmo, 2003), because they only contain the catalytic kinase domain but lack the auto-inhibitory region and EF hands of plant *bona fide* CDPKs, which explains their Ca^{2+} independence. PPCKs are localized in the cytoplasm (Chutia, 2019) and are only known to phosphorylate PPCs (Chollet et al., 1996; Nimmo, 2003; Nimmo et al., 2001).

Plant genomes encode several isoforms of C3 or C4/CAM PPCKs, which are encoded by small gene families with at least two isoforms present in most species (Fontaine et al., 2002; Fukayama et al., 2006; Nimmo, 2003; Shenton et al., 2006; Sullivan et al., 2004; Xu et al., 2003). Rice has three isoforms, while Flaveria and soybean have one and at least four *PPCKs* isoforms, respectively (Fukayama et al., 2006; Furumoto et al., 2007; Sullivan et al., 2004; Tsuchida et al., 2001). In tomato, potato and Arabidopsis, two *PPCK* isoforms have so far been described (Fontaine et al., 2002; Marsh et al., 2003). The two PPCK isoforms identified in Arabidopsis show different expression patterns in relation to plant organs and environmental cues (Fontaine et al., 2002; Nimmo, 2003). *AtPPCK1* is expressed primarily in rosette leaves and to a lower extent in flowers and roots whereas *PPCK2* has been detected mainly in roots and flowers, and to a lower extent in cauline leaves (Meimoun et al., 2009).

1.9 Regulation of phosphoenolpyruvate carboxylase kinases

Plant PPCKs are protein kinases known to be regulated mainly at the level of synthesis and degradation (Bakrim et al., 2001; Carter et al., 1991; Jiao & Chollet, 1991; Nimmo, 2003). *PPCK* transcript abundance is controlled by light in C4 plants, and by a circadian oscillator in CAM plants (Hartwell et al., 1999; Nimmo et al., 2001; Nimmo, 2000; Taybi et al., 2000), while in C3 plants, light and nitrogen regulate *PPCK* expression (Duff & Chollet, 1995; Li et al., 1996).

Two less studied PPCK regulatory mechanisms are a possible monoubiquitination and the control by allosteric effectors. The *PPCKs* genes identified so far encode PPCKs of around 30 kDa (Nimmo, 2003). However, the presence of a larger PPCK (37 kDa) in several plants such as maize, ice plants, tobacco and soybean strongly indicate a posttranslational regulation. Since the small ubiquitin molecule is about 8 kDa in size, this large PPCK is thought to result from monoubiquitination on one of its lysine residues (Li & Chollet, 1993; Li et al., 1996; Zhang & Chollet, 1997). In other studies, PPCK activity in crude extracts increased with increasing dilution which led to the speculation that plant tissues contain an unknown protein that inhibits PPCK activity (Nimmo et al., 2001). In an assay by (Borland et al., 1999), increased temperature treatments caused malate efflux from the vacuole which decreased PPCK activity. Transcript analysis in leaves with reduced malate levels revealed an induction of *PPCK* genes, which led to the suggestion that cytosolic malate may act as a possible feedback regulator of *PPCK* expression (Borland et al., 1999).

Abiotic stresses also play a crucial role in regulating *PPCK* expression and PPCK activity. Salt stress in sorghum leaves enhances the activity of PPCKs which was accompanied by increased PPC phosphorylation and activity (Monreal et al., 2007). Nitrogen deficiency in wheat increased PPCK activity, which was attributed to increased phosphorylation (Duff & Chollet, 1995). In Arabidopsis, significant upregulation of both *PPCK1* and *PPCK2* in shoots and roots has been reported during Pi starvation. This has been associated with increased PPC phosphorylation, PPC activity and OAs levels (Chen et al., 2007; Chutia, 2019; Gregory et al., 2009; O'Leary et al., 2011) while in Arabidopsis roots, the induction of *PPCK2* was significantly enhanced under both low Pi and salt stress, indicating its importance during adaptation to salt stress (Feria et al., 2016).

1.10 Previous work on PPC and PPCK manipulation

Thus far, manipulation of the PPCK-PPC module has focused on either the overexpression of different C4 and bacterial PPCs or on the characterization of PPC mutant enzymes showing reduced allosteric inhibition or different allosteric regulation. In addition, introduction of C4 PPCs into C3 plants with the aim to improve their photosynthetic capacity, to enhance growth and to improve yield has been well investigated. However, these attempts have had contradictory results. Expression of maize C4 *PPC* in tobacco increased PPC activity (Hudspeth et al., 1992) but had no effect on the photosynthetic rate, and the transgenic plants had reduced growth (Kogami et al., 1994). Rice plants transformed with C4 *PPC*

from maize had reduced CO₂ assimilation and reduced photosynthetic rate compared to non-transgenic plants (Fukayama et al., 2003). Transformation with a C4 *PPC* from *F. trinervia* or sorghum, or with a bacterial *PPC*, led to diminished plant growth, unaltered photosynthetic rate and accelerated stomatal opening in potato (Beaujean et al., 2001; Gehlen et al., 1996; Rademacher et al., 2002). Interestingly, expression of maize C4 *PPC* in *Arabidopsis* under the CaMV 35S promoter led to improved plant performance with reported higher chlorophyll content, increased *PPC* activity, CO₂ consumption, starch content and plant dry weight in the transgenic plants when compared to the control (Kandoi et al., 2016).

Modulation of *PPC* activity has been performed with respect to stress resilience. Overexpression of CAM-specific *PPCI* from *Agave americana* into tobacco led to enhanced proline biosynthesis resulting in improved salt and drought tolerance in the transgenic plants (Liu et al., 2021). Transgenic rice overexpressing maize C4 *PPC* was found to exude more oxalate in response to Pi deficiency (Begum et al., 2005). In rice transformed with C4 *PPC* from sugarcane, increased *PPC* activity and photosynthetic capacity in transgenic lines did not result in improved grain weight when compared to the control (Lian et al., 2014). Transgenic wheat overexpressing a C4 *PPC* from maize had improved nitrogen absorption which resulted in increased amino acids in transgenic lines compared to the control (Peng et al., 2018).

Studies on the manipulation of *PPCKs* has mostly been in relation to alkali stress response whereby overexpression of *Glycine soja PPCK3* and *PPCK1* in alfalfa (*Medicago sativa*) plants led to increased citric acid, chlorophyll and improved alkali tolerance (Sun et al., 2014; Wei et al., 2013). The role of *PPCKs* in relation to Pi starvation has been studied in the past. Overexpression of *Arabidopsis C3 PPCKs* was found to increase endogenous root malate and malate exudation in transgenic lines compared to the control during Pi starvation (Chutia, 2019).

As mentioned above, the effects of *PPC* overexpression were mainly analyzed with respect to photosynthetic efficiency and stress related phenotypes. Malate and citrate were only occasionally measured, and if so, it was almost exclusively measured in shoots (Agarie et al., 2002; Gehlen et al., 1996; Hudspeth et al., 1992; Kogami et al., 1994). However, endogenous root malate and citrate content and root exudates were not extensively investigated in relation to most stresses and especially Pi starvation and in *PPC* overexpression plants.

1.11 Aim of the present study

This study was designed with the aim of gaining more knowledge on the *Arabidopsis PPCK-PPC* module and how its manipulation would affect the plant response to Pi starvation. We focused on studying the effects of overexpression of C3 plant-type *PPCs* and of knocking out *PPCKs*, which regulate *PPCs* in *Arabidopsis*. In a nutshell, this study was divided into the following subtopics:

- (i) Cell-type specific expression domains of plant-type *PPCs*
- (ii) Consequences of overexpressing plant-type *PPCs* in relation to Pi starvation
- (iii) Consequences of knocking out *PPCKs* in relation to Pi starvation

1.11.1 Cell-specific expression domains of Arabidopsis plant-type *PPCs*

Arabidopsis thaliana codes for three plant-type PPC isoenzymes (AtPPC1, AtPPC2, and AtPPC3), which are known to function in the cytoplasm and are differentially induced upon various stresses. While various strides have been made in understanding their role in plants, their cell type-specific expression domains are still unexplored. Previous attempts to localize PPCs using immunocytochemistry localized PPCs in the cytosol of sorghum (C4 plant) and *Kalanchoe* (CAM plant). Additionally, in leaves of bean (C3 plant), it was distributed between the chloroplast and cytoplasm (Perrot-Rechenmann et al., 1982). These results cemented earlier observations for crucial roles of C4 and CAM PPCs in photosynthetic CO₂ pre-fixation and probably an additional role in nitrogen assimilation. However, from these results, it remains unclear whether plant-type *PPCs* are expressed in the same or different cell types and whether their differential induction might be cell-specific or not. To address this gap, we decided to study the cell-specific expression domains of Arabidopsis plant-type *PPCs* under Pi starvation to understand the disparities described so far for the induction of *PPC* genes in different tissues. The information generated will be used in the future to carry out more precise manipulation of the PPCK-PPC module in the context of plant stress resilience.

1.11.2 Overexpression of Arabidopsis plant-type *PPCs*

Various studies on PPCs have previously focused mainly on improving C3 plant photosynthetic capacity, yield and tolerance to various stresses. This was majorly attempted through the introduction of C4 PPCs into C3 plants with differing results such as reduced plant growth and yield, reduced photosynthetic capacity and at times no changes all reported (Gehlen et al., 1996; Kogami et al., 1994; Rademacher et al., 2002). Since the PPCK-PPC module is tightly regulated, these negative observations led us to speculate that they might have stemmed from an incompatibility between C3 PPCKs and the introduced C4 PPCs. To investigate if this could be the reason, and since no report existed (to the best of our knowledge), we decided to overexpress the three Arabidopsis plant-type *PPCs* in Arabidopsis as a C3 system and to characterize their phenotypes, the malate and citrate tissue content, and the exudation of malate and citrate in relation to Pi starvation.

1.11.3 Loss of function (knockouts) of Arabidopsis *PPCKs*

To have a wholesome view of effects of manipulating the master regulator of PPCs, we decided to investigate loss-of-function *ppck* mutants in relation to tissue OAs production (malate and citrate) and OAs exudation during Pi starvation. Several studies on *PPCK* gene induction had revealed their enhanced expression in various tissues in response to different stress conditions (Chutia, 2019; Feria et

al., 2016; Gregory et al., 2009). However, from these studies, it was still unclear whether PPCKs are redundant, or they have specific roles. Additionally, Feria et al., (2022) observed reduced seed dry weight and seed yield in *Arabidopsis ppck1* mutants compared to the *ppck2* mutant and wild type control (Columbia 0). From this study, effects of *ppck* knockouts on exuded and endogenous malate and citrate level was not studied, leaving unanswered questions which need to be addressed. Furthermore, their study did not investigate effects of *ppck* mutants in relation to any stress condition and the lack of a double *ppck1ppck2* mutant meant they could not make a definitive conclusion on the important role or specificity of the *PPCKs*. To address these gaps, we studied the impacts of *Arabidopsis ppck* mutants on endogenous root malate and citrate content and root exudates in relation to Pi starvation. The above outlined gaps were pursued as part of this research project with the following objectives:

1. Analysis of cell-specific expression of *Arabidopsis* PPC isoforms under their native promoters.
2. Modification of the *PPCK-PPC* module by overexpressing *Arabidopsis* C3 plant-type PPCs in *Arabidopsis thaliana* under control of the CaMV 35S promoter.
3. Characterization of *Arabidopsis ppck* loss-of-function mutants.

2.0 RESULTS

2.1 Differential expression of Arabidopsis *PPC* genes

Previous transcript analysis performed in our group revealed differential *PPC* genes expression in wild type shoots and roots during sufficient and insufficient Pi conditions (Chutia, 2019). This was further confirmed by our analysis of shoots and roots using *PPC* gene specific primers (Supplementary table 1). In shoots of seedlings grown on sufficient Pi, *PPC2* was the predominantly expressed *PPC* gene, followed by *PPC1*, while *PPC3* transcripts were the least abundant (Figure 5A). *PPC2* transcripts in shoots were about 6.0-fold higher than *PPC1* and about 100-fold higher than *PPC3* transcripts while *PPC1* transcripts were about 18-fold those of *PPC3* (Figure 5A). Pi starvation induced all *PPCs* albeit to different magnitudes. *PPC1* transcripts were induced 15-fold, *PPC3* about 10-fold while *PPC2* transcripts were the least induced at about 2.2-fold (Figure 5A). ANOVA analysis revealed stronger significance induction of *PPC3* upon Pi starvation compared to the induction of either *PPC1* or *PPC2* (two-way ANOVA. $p=1.01e^{-05}$ between *PPC1* and *PPC3*, two-way ANOVA: $p=0.04$ between *PPC1* and *PPC3*, and two-way ANOVA: $p=0.01$ between *PPC2* and *PPC3*).

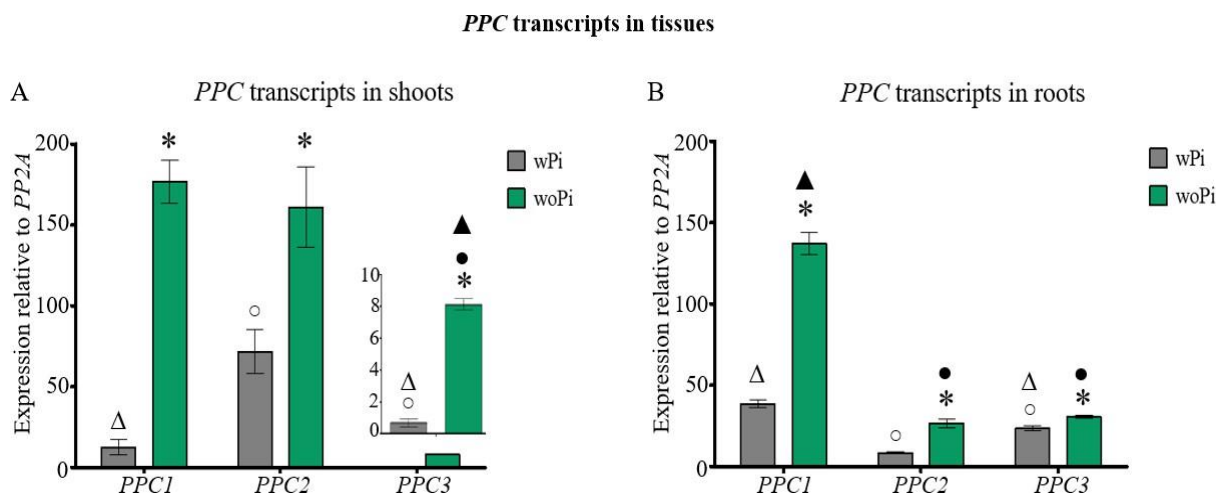


Figure 5: *PPCs* transcript levels in wild type shoots and roots.

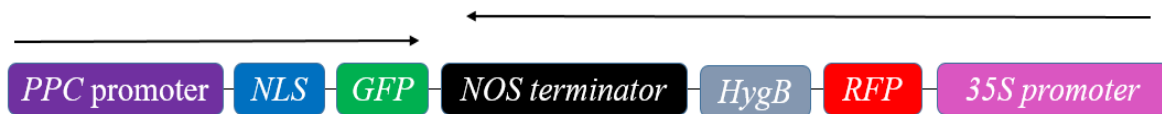
Transcript levels in wild type **A-Shoots** and **B-Roots**. Seedlings were grown for six days on sufficient Pi before transfer to either sufficient or deficient Pi conditions for an additional five days before harvest. Error bars denote \pm SE ($n=3$). Significance analyses were performed by Student's t-test (two-tailed, equal variances): * $p \leq 0.05$ compared to wPi, $\circ p \leq 0.05$ compared to *PPC1* wPi, $\bullet p \leq 0.05$ compared to *PPC1* woPi, $\Delta p \leq 0.05$ compared to *PPC2* wPi, $\blacktriangle p \leq 0.05$ compared to *PPC2* respectively.

Like shoots, root *PPCs* transcripts were differentially expressed on sufficient Pi condition and differentially induced upon Pi starvation (Figure 5B). On sufficient Pi, *PPC1* was the most predominant *PPC* followed by *PPC3* while *PPC2* was the least abundant (Figure 5B). *PPC1* transcripts were about 5-fold of *PPC2* and about 1.6-fold of *PPC3*, while *PPC3* transcripts were about 3-fold those of *PPC2* (Figure 5B). Upon Pi starvation, *PPC1* was induced about 4-fold, *PPC2* about 3-fold while *PPC3* was

the least induced at about 1.3-fold (Figure 5B). As observed in shoots, induction was stronger for *PPC3* (two-way ANOVA. $p=2.38e^{-06}$ between *PPC1* and *PPC3*) followed by induction of *PPC1* (two-way ANOVA. $p=8.15e^{-06}$ between *PPC1* and *PPC2*) while induction of *PPC2* was the weakest (two-way ANOVA. $p=0.01$ between *PPC2* and *PPC3*).

2.2 Cell type-specific expression of Arabidopsis *PPC* genes in roots

From the data results on *PPC* gene expression obtained in previous studies (Chutia, 2019; Feria et al., 2022), it is impossible to discern cell type-specific expression patterns of *PPCs* genes, which is crucial for determining their specific roles. This prompted us to generate transcriptional reporter expression lines driven by the native promoters of Arabidopsis plant-type *PPCs* genes. Promoter regions spanning 2790 bp, 2468 bp and 2433 bp upstream of the start codon were selected for *PPC1*, *PPC2* and *PPC3*, respectively. The promoter regions were then fused to coding GFP sequence. For selection of positively transformed bacterial clones and transgenic plants, a hygromycin antibiotic resistance gene and a fluorescent seed coat marker driven by the CaMV 35S promoter were used, respectively (Figure 6). To enhance the intensity of GFP fluorescence, a nuclear localization signal (NLS) fused to the N-terminus of the GFP sequence was added, which would concentrate the GFP in the nucleus enabling not only clear visualization of the signal but also cells in which the signal was located.



PPC-Phosphoenolpyruvate carboxylase promoter 1/2/3
 NLS-Nuclear localization signal
 GFP-Green fluorescent protein
 NOS-Nopaline synthase terminator
 Hyg-Hygromycin B selective gene
 RFP-Red fluorescent protein
 35S-Cauli mosaic virus constitutive promoter

Figure 6: Diagram showing the design of transcriptional reporter expression construct.

The construct was designed to harbor the *PPC* promoter, a nuclear localization signal (NLS), and green fluorescent protein (GFP) sequences, and two selection markers, i.e. the red seed coat fluorescent marker (RFP) and hygromycin resistance gene under control of the CaMV 35S promoter.

A.thaliana (accession Col-0) plants were transformed using the above construct for either *PPC1*, *PPC2* or *PPC3* and propagated through T1, T2, and T3 generations until two independent homozygous lines for each promoter reporter construct were obtained. The root cell type- specific expression patterns of each *PPC* promoter were then investigated in plants grown in sufficient and insufficient Pi conditions.

Under sufficient Pi conditions, strong *PPC1* expression as evidenced by the GFP signal was observed in the root tip, the epidermis, and the root stele, while a weak signal for *PPC3* was observed, which was restricted to the epidermal cells (Figure 7). *PPC2* expression was hardly visible under sufficient Pi condition. Upon transfer to insufficient Pi conditions, weak signals corresponding to *PPC2* promoter activity were then visible in the epidermal cell layer, the root stele, and the root tip cells. The *PPC1*

promoter activity was strongly induced, and the signal was detectable throughout the root tip (Figure 7). Strong induction of the *PPC3* promoter was also observed under Pi starvation with the signal restricted to the root epidermal cell layer, the stele, and the root cap (Figure 7).

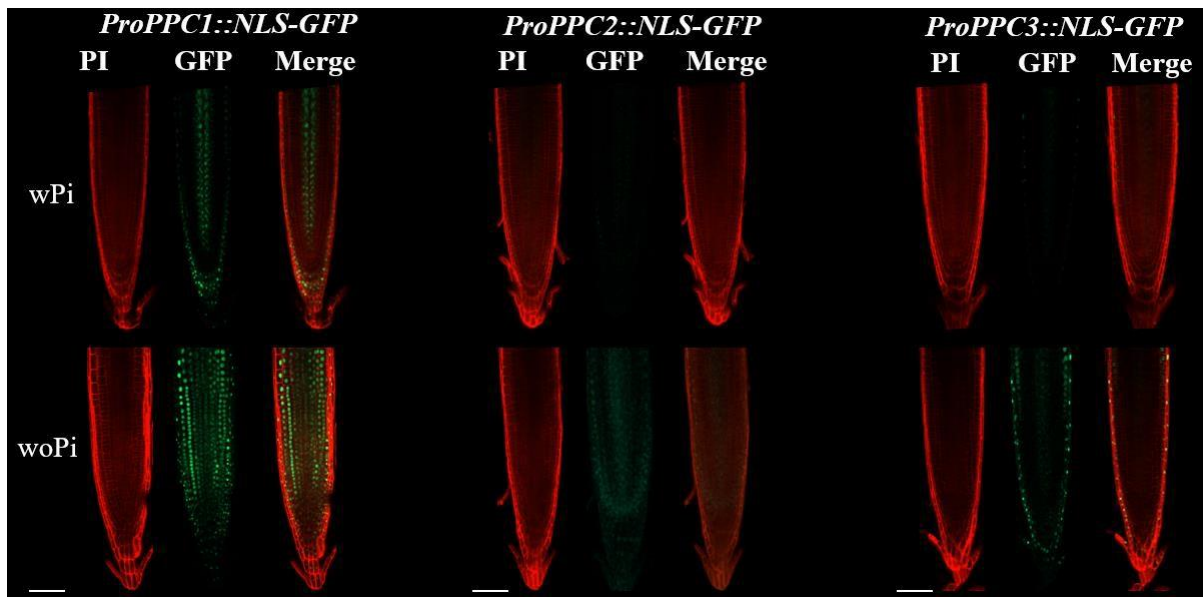


Figure 7: Root cell type-specific expression domains of Arabidopsis *PPC* promoters.

PPC reporters expressing GFP under control of the native *PPC1*, *PPC2*, and *PPC3* promoters fused to a NLS-GFP reporter. Seedlings were grown for six days on sufficient Pi before transfer to either sufficient or deficient Pi conditions for an additional five days before harvest. Scale bars represent 20 μ m. Left picture (red channel): identification of intact cell walls using propidium iodide; center picture (green channel): GFP signal, right picture: merged pictures of GFP fluorescence and propidium iodide staining.

From our analysis, it was astonishing to observe low *PPC2* promoter activity (weak fluorescent signals) in roots since RT qPCR results showed almost similar levels as for *PPC3* transcript levels upon Pi starvation. This prompted us to investigate its expression in shoots to determine whether the *PPC2* reporter construct was functional since *PPC2* transcripts levels were high in shoots (Figure 5A). Images were captured (GFP channel and bright field) and merged (Supplementary figure 1). Presence of visible GFP signal in shoots of *PPC2* promoter reporter line under sufficient Pi and its strong induction on low Pi confirmed a functional construct (Figure 8). Expression of the *PPC1* and *PPC3* in sufficient Pi condition in shoots was also confirmed by presence of strong GFP signals especially in the nucleus for each of the respective construct (Figure 8). While shoot transcript analysis has confirmed induction of *PPC* upon transfer to Pi insufficient conditions, this was not clear in our shoot microscopic images especially for *PPC1* and *PPC3* promoter reporter lines since GFP fluorescent signals under sufficient and insufficient Pi were indistinguishable (Figure 8).

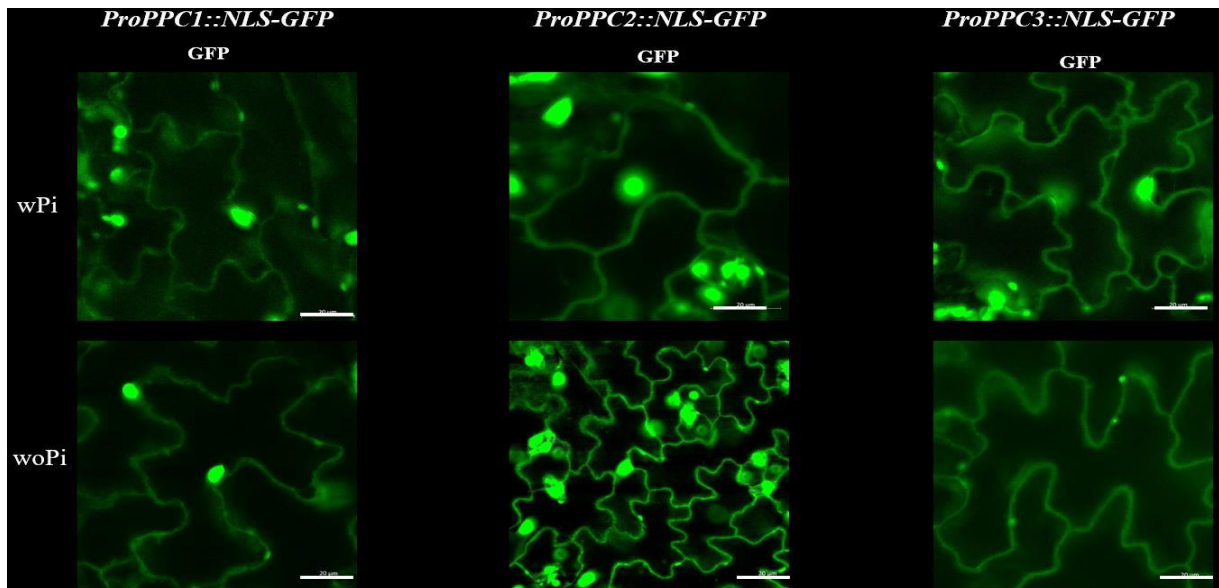


Figure 8: *PPC* activity in shoots of *Arabidopsis* epidermal leaf cells.

Expression of NLS-GFP under control of native *Arabidopsis* *PPC* promoters in transgenic leaves. Seedlings were grown for six days on sufficient Pi before transfer to either sufficient or deficient Pi conditions for an additional five days before harvest. Scale bars represent 20 μm .

2.3 Generation of *Arabidopsis* *PPC* overexpression lines

To study the effects of *PPC* overexpression, three different versions for each *Arabidopsis* plant-type *PPC* were cloned. All constructs contained the *PPC* ORFs (*PPC1*:-2,904 bp, *PPC2*:-2,892 bp and *PPC3*:-2,907 bp) under control of the CaMV 35S promoter as well as the BASTA resistance gene for selection. The three versions encoded *PPC* proteins (i) without a terminal tag or with a (ii) C-terminal or (iii) N-terminal GFP tag, to investigate the subcellular localization of *PPC* proteins (Figure 9). The constructs were transformed into *Arabidopsis* (Col-0) wild type plants and transgenic lines were selected by BASTA spraying in each generation (T1, T2 and T3) until several independent lines for each construct were obtained. Only transgenic lines, which had a 100% survival on BASTA selection plates and a single copy number, were considered homozygous.

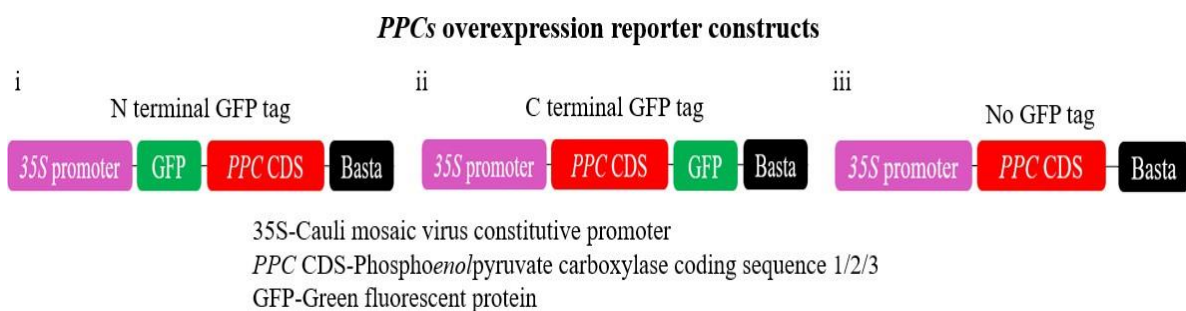


Figure 9: Diagram showing the design of *PPC* overexpression constructs.

Pink boxes represent the constitutive CaMV 35S promoter. Green boxes indicate (i) N-terminal or (ii) C-terminal and (iii) untagged *PPC* fusions with GFP reporter tag. Red boxes indicate the *PPC* ORF (CDS) and the black boxes indicate the BASTA resistance gene.

We first performed PPC enzyme activity assays with the tagged and untagged overexpression lines to determine which constructs were active. Extracts from all lines overexpressing GFP-tagged PPC fusion proteins did not show increased PPC activity compared to wild type extracts, however, only the untagged PPC versions were active. We therefore used the untagged overexpression lines throughout the study. From the untagged overexpression lines, three independent transgenic lines overexpressing *PPC1* (line 3.6, 4.10 and 8.10), two for *PPC2* (line 1.8 and 4.9) and three for *PPC3* (line 5.11, 8.12 and 9.12) showed higher enzyme activities than wild type and were further characterized for their transcript levels, PPC protein amounts and PPC activity as detailed below.

2.4 Molecular characterization of Arabidopsis *PPC* overexpression lines

2.4.1 Analysis of *PPC* transcript levels

Transcript analysis of the three different *PPC* genes in the identified transgenic lines was first carried out on whole seedlings grown on sufficient Pi using gene specific primers (Supplementary table 1). The Ct values of the target *PPC* genes were normalized using the Ct values of *PP2A* as a constitutively expressed gene.

In transgenic lines overexpressing *PPC1*, transcript levels in lines 3.6 and 4.10 were 20-fold and 2.5-fold higher compared to the wild type, respectively while line 8.10 showed transcript levels comparable to wild type (Figure 9A). Similarly, *PPC2* overexpression lines 1.8 and 4.9 showed both about 15-fold increase in transcript levels compared to wild type (Figure 10B). *PPC3* overexpressing lines 5.11 exhibited about 6-fold higher *PPC* mRNA levels compared to wild type, while lines 8.12 and 9.12 both showed about 3-fold increase in *PPC3* transcript abundance (Figure 10C).

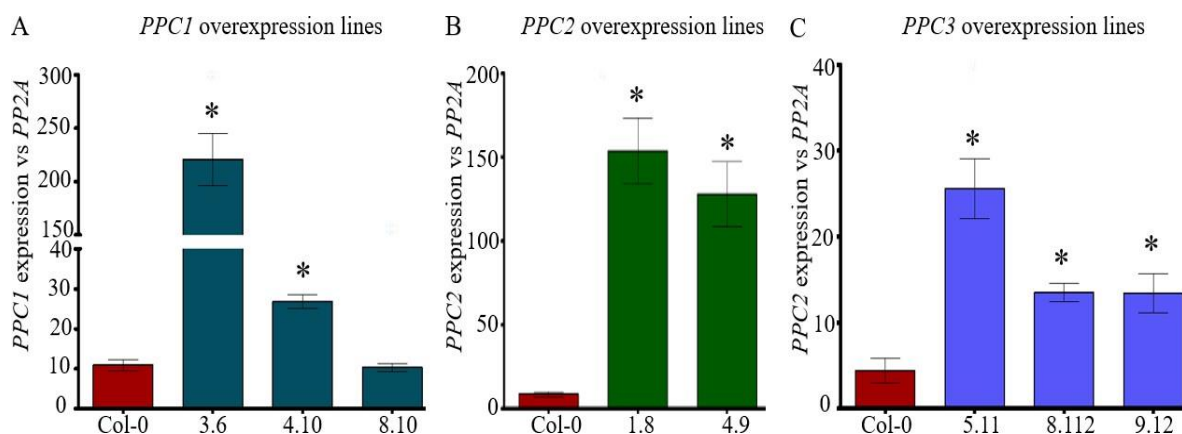


Figure 10: *PPC* transcript analysis in Arabidopsis seedlings overexpressing plant-type *PPCs*.

A-*PPC1* transcript level analysis in *PPC1* overexpression lines, **B-*PPC2*** transcript level analysis in *PPC2* overexpression lines and **C-*PPC3*** transcript level analysis in *PPC3* overexpression. Seedlings were grown for six days on sufficient Pi before harvest and *PP2A* was used as the reference gene. Error bars denote \pm SE (n=4). Significance test was by student t-test (two tailed), * $p \leq 0.05$ compared to wild type Col-0.

Since plant-type *PPCs* show high similarity, we were also interested in whether overexpressing a single *PPC* would influence the transcript levels of the others. We therefore performed transcript analysis of all three Arabidopsis plant-type *PPC* genes in each *PPC* overexpression line and compared them to wild type levels. *PPC1* transcripts in *PPC2* and *PPC3* overexpression lines were comparable to wild type but were higher in the *PPC1* overexpression except for *PPC1* overexpression line 8.10 (Supplementary figure 2A). In contrast, *PPC2* transcript levels were slightly reduced by about almost 0.5-fold in *PPC1* and *PPC3* overexpression lines but were strongly expressed in the *PPC2* overexpression lines (Supplementary figure 2B). Like *PPC1* transcript levels, *PPC3* mRNAs were comparable to wild type levels in lines overexpressing *PPC1* and *PPC2* but were higher in *PPC3* overexpression lines (Supplementary figure 2C). This data revealed that overexpressing a single Arabidopsis plant-type *PPC* has no influence on the mRNA levels of the other two *PPC* genes.

2.4.2 *PPC* overexpression increases *PPC* protein levels in roots

Next, we were interested in whether increased transcript levels resulted in increased protein levels. For that, immunoblot analysis was carried out on 11-day old roots (Figure 11) and shoots (Supplementary figure 3). *PPC* proteins were detected with a polyclonal anti-sorghum C4 PTPPC antibody (Pacquit et al., 1995) which does not discriminate between *PPC* isoforms. To ensure equal loading of protein amounts actin, which was detected with a monoclonal anti-actin antibody (Sigma), was used as a loading control. Bands were subsequently visualized using goat anti-rabbit IgG horseradish peroxidase conjugate or goat anti-mouse IgG horseradish peroxidase conjugate (Thermo Fisher Scientific) for *PPC* and actin respectively.

As judged from the intensities of protein bands around 107 kDa, *PPC* protein level for most of the overexpression lines was higher under both sufficient Pi (Figure 11A) and insufficient Pi conditions (Figure 11B) compared to wild type. However, based on the intensities of the actin bands used as loading control, for *PPC1* overexpression lines 4.10 and 8.10 and for the *PPC3* overexpression lines it was unclear whether they had more *PPC* protein levels.

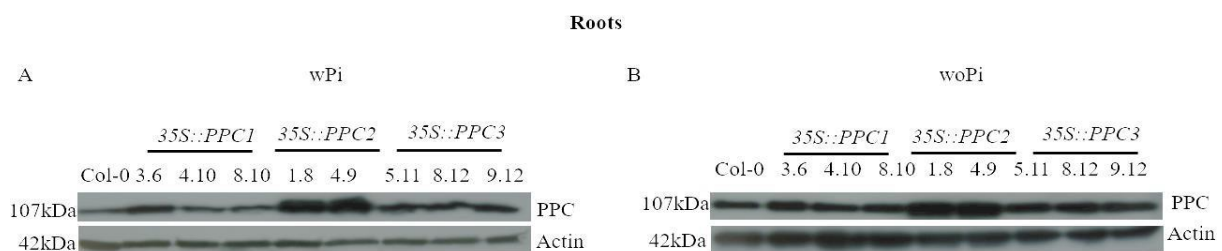


Figure 11: Detection of total PPCs in *PPC* overexpression lines by immunoblot analysis.

PPC protein quantification in **A**-Roots grown in Pi sufficient conditions and **B**-Roots grown in Pi deficient conditions. Seedlings were grown for six days on sufficient Pi before transfer to either sufficient or deficient Pi conditions for an additional five days before harvest. 30 µg of total protein extract was loaded on to the SDS-PAGE gel and after transfer to the membrane was probed with anti-*PPC* or anti-actin antibody. Actin was used as the loading control.

Similarly, in shoots, higher accumulation of PPC protein during sufficient Pi and elevation upon Pi starvation was observed (Supplementary figure 3). Just like in roots, based on weaker actin bands for some samples especially wild type and *PPC1* overexpression line 3.6 under sufficient Pi, it was unclear whether the highly accumulated PPC levels was because of unequal sample loading. To confirm this, we used a targeted proteomics approach and quantified PPC levels in wild type and two independent lines for each *PPC* overexpression line in shoot and root tissues.

30 μg of total protein was resolved by SDS-PAGE and gel regions between the 35-50kDa and 90-130kDa marker bands for actin and PPC respectively were excised and processed under denaturing conditions according to Bassal et al., (2020) (see material and methods). The samples were reduced, alkylated, digested with trypsin and desalted before dissolving in 5% (v/v) acetonitrile in 0.1% trifluoroacetic acid (Bassal et al., 2020). Samples were then injected into an EASY-nLC 1200 liquid chromatography system (Thermo Fisher Scientific) where the spectral counts of eight target peptides of PPC1, PPC2 and PPC3 in their unmodified, oxidized methionine and phosphorylated serine forms were recorded. For quantification, all PPC spectral counts detected in each overexpression line and wild type, were summed up and normalized to the sum of all spectral counts recorded for all actins present in the sample (Figure 12).

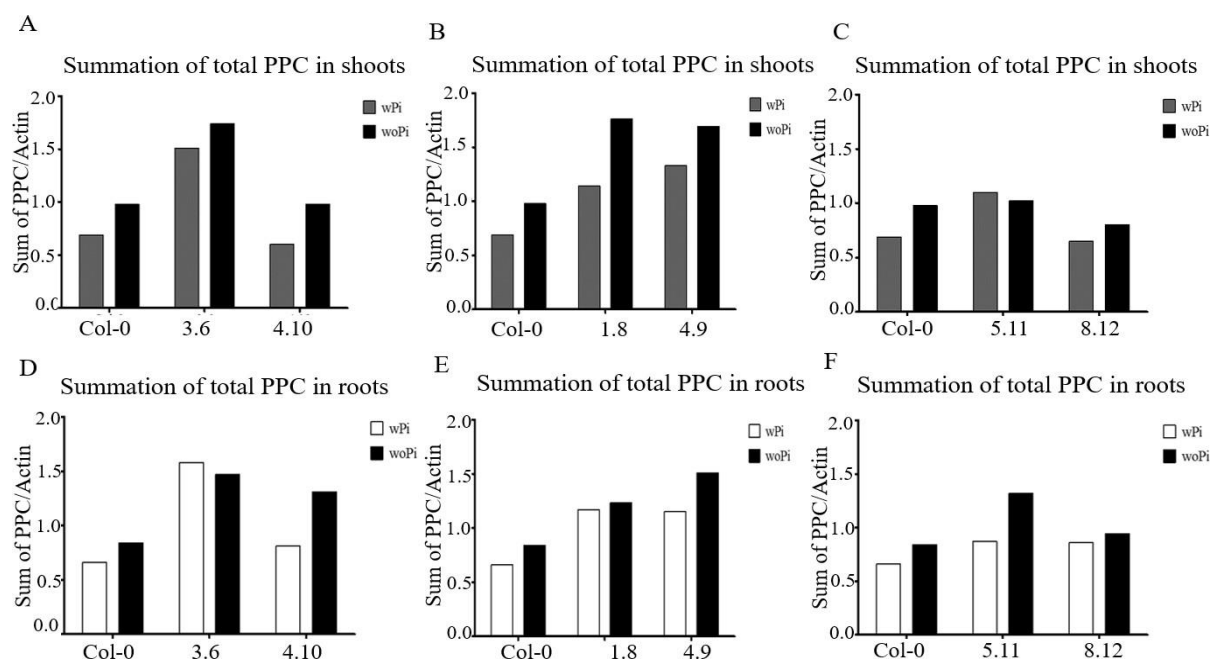


Figure 12: Total PPC protein levels in tissues of transgenic Arabidopsis *PPC* overexpression lines.

Total PPC levels were detected in shoots of **A-*PPC1*** overexpression lines, **B-*PPC2*** overexpression lines and **C-*PPC3*** overexpression lines. Total PPC levels detected in roots of **D-*PPC1*** overexpression lines, **E-*PPC2*** overexpression lines and **F-*PPC3*** overexpression lines. Seedlings were grown for six days on sufficient Pi before transfer to either sufficient or deficient Pi conditions for an additional five days before harvest. 30 μg of total protein extract was loaded on to the SDS-PAGE gel and bands corresponding to PPC and actin excised and processed. Total PPC spectral counts were summed up then normalized to total actin spectral counts detected in the sample. Data shown were collected from one biological sample only.

In shoots, total PPC levels in *PPC1* overexpression lines 3.6 and 4.10 were 2.2-fold and 0.87-fold of the wild type level respectively (Figure 12A) while in both *PPC2* overexpression lines, total PPC levels in shoots was about 1.7-fold higher than wild type levels (Figure 12B). In *PPC3* overexpression line 5.11 total PPC levels were 1.6-fold higher than wild type but were comparable to wild type levels in *PPC3* overexpression line 8.12 (Figure 12C). On transfer to insufficient Pi, PPC levels in line 3.6 were increased by 1.8-fold higher but were comparable to wild type levels in line 4.10 overexpressing *PPC1* (Figure 12A). Similar to PPC levels on sufficient Pi condition, Pi starvation enhanced PPC accumulation by about 1.8-fold compared to levels in wild type under the same growth condition (Figure 12B). In *PPC3* overexpression line 8.12, total PPC levels were lower by about 20% compared to wild type levels but were comparable to wild type levels in *PPC3* overexpression line 5.11 under insufficient Pi (Figure 12C).

Total PPC levels in roots of the overexpression lines were higher than wild type levels in both sufficient and insufficient Pi levels (Figure 12). In *PPC1* overexpression lines PPC fold change ranged between 1.2-2.5 (Figure 12D) of wild type levels under sufficient Pi and was about 1.5-fold and 1.3-fold higher in *PPC2* (Figure 12E) and *PPC3* (Figure 12F) overexpression lines respectively. On transfer to Pi deficient conditions, total PPC levels were about 1.5-fold of wild type levels in *PPC1* (Figure 12D) and *PPC2* overexpression lines (Figure 12E) while in *PPC3* overexpression lines 5.11 and 8.12 PPC levels were 1.5-fold and 1.1-fold higher than wild type levels (Figure 12F).

The proteomics results enabled us to additionally quantify the levels of individual PPCs in the wild type and the overexpression lines. As it was observed for total PPC levels, Pi starvation induced the accumulation of PPC proteins in shoots and roots (Supplementary figure 4). On sufficient Pi, PPC1 was 3.5-fold higher in lines 3.6 overexpressing *PPC1* and about 0.85-fold in line 4.10 compared to wild type (Supplementary figure 4A). In both *PPC2* overexpression lines, PPC1 protein levels were about 1.8-fold higher than wild type (Supplementary figure 4A) while in *PPC3* overexpression lines PPC1 levels were 1.3-fold and 0.84-fold compared to wild type (Supplementary figure 4A). On transfer to insufficient Pi, PPC1 levels were 2.4-fold higher in line 3.6 but were comparable to wild type in line 4.10 overexpressing *PPC1* (Supplementary figure 4A). Likewise, PPC1 levels were higher in *PPC2* overexpression lines by about 1.7-fold but were in contrast lower in *PPC3* overexpression lines by about 20% compared to wild type upon Pi starvation (Supplementary figure 4A).

On sufficient Pi, shoot PPC2 levels was higher in line 3.6 overexpressing *PPC1* by about 1.6-fold and in *PPC2* overexpression lines by about 2.0-fold but were comparable to wild type levels in lines overexpressing *PPC3* (Supplementary figure 4B). In a similar trend, upon Pi starvation, PPC2 levels remained high in *PPC1* overexpression line 3.6 by about 1.4-fold and lines overexpressing *PPC2* by about 2.0-fold but were comparable to wild type in *PPC3* overexpression lines (Supplementary figure 4B).

Unlike the other two plant type PPCs, more inconsistencies were observed for PPC3 levels in shoots. In *PPC1* overexpressing line 3.6, PPC3 protein levels were higher by about 1.9-fold but were lower in line 4.10 while *PPC2* overexpression line 1.8 had PPC3 levels comparable to wild type with line 4.9 accumulating about 1.3-fold more PPC3 than wild type. PPC3 overexpression lines accumulated higher PPC3 levels at about 3.2 and 1.2-fold compared to wild type levels on sufficient Pi (Supplementary figure 4C). Upon Pi starvation, PPC3 levels in *PPC1* overexpression lines were increased by 40% in line 3.6 but were about 14% lower in line 4.10 compared to wild type. *PPC2* overexpression lines accumulated about 20% more PPC3 protein compared to wild type. In contrast to Pi sufficient condition, only one line (5.11) overexpressing *PPC3* accumulated about 60% more PPC3 compared to wild type while line 8.12 had 20% lower PPC3 levels (Supplementary figure 4C).

Unlike in shoots, in roots, all overexpression lines accumulated all three plant-types PPCs to higher levels than wild type under both sufficient and insufficient Pi (Supplementary figure 4). On sufficient Pi, PPC1 levels ranged between 1.4-fold and 3.0-fold higher in the *PPC1* overexpression lines and about 1.5-fold higher than wild type in the *PPC2* overexpression lines but were indistinguishable from wild type in the *PPC3* overexpression lines (Supplementary figure 4A). Upon Pi starvation, PPC1 levels were about 2.0-fold higher in *PPC1* overexpression lines and about 1.5-fold higher in *PPC2* overexpression lines and line 5.11 overexpressing *PPC3* compared to wild type (Supplementary figure 4A).

PPC2 levels in *PPC1* overexpression lines 3.6 and 4.10 were 2.8-fold and 1.2-fold higher than wild type on sufficient Pi and about 3.3-fold in *PPC2* overexpression lines (Supplementary figure 4B). However, lines overexpressing *PPC3* had PPC2 levels comparable to wild type. Upon Pi starvation, *PPC1* overexpression accumulated about 1.8-fold higher PPC2 levels than wild type while in *PPC2* overexpression lines accumulated about 2.3-fold and 3.0-fold higher PPC2 levels in lines 1.8 and 4.9, respectively (Supplementary figure 4B). In *PPC3* overexpression line 5.11 PPC2 levels were 1.5-fold higher but comparable to wild type in line 8.12 (Supplementary figure 4B).

PPC3 levels in *PPC1* and *PPC2* overexpression levels was comparable to wild type except in line 3.6 overexpressing *PPC1* which had 1.5-fold higher PPC3 levels than wild type (Supplementary figure 4C). In contrast, both *PPC3* overexpression accumulated 1.6-fold higher PPC3 levels in roots on sufficient Pi compared to wild type (Supplementary figure 4C). Upon Pi starvation, PPC3 levels in *PPC1* and *PPC2* overexpression lines was about 1.5-fold and 1.3-fold higher than wild type respectively (Supplementary figure 4C). In roots of *PPC3* overexpression lines, PPC3 levels were 1.7-fold and 1.3-fold higher in lines 5.11 and 8.12 than wild type respectively (Supplementary figure 4C).

In general, overexpression of plant-type *AtPPC* genes increased AtPPC1 and AtPPC2 in shoots and roots of both *PPC1* and *PPC2* overexpression lines, while AtPPC3 levels were elevated in roots of *PPC3* overexpression lines compared to wild type.

2.4.3 PPC overexpression increases PPC activity in crude extracts

Finally, we determined PPC activity in crude extracts of whole seedlings to elucidate whether increased transcript and protein levels observed for most overexpression lines also resulted in increased PPC enzyme activity. An increase in PPC activity would be the goal for PPC dependent OAs manipulation since it may result in metabolite changes associated with the PPCK-PPC module so that plants may better adapt to stress. We therefore determined PPC activity with the assumption that the overexpression lines would have higher activity compared to the wild type. PPC activity was measured in an enzyme coupled assay by monitoring the consumption of NADH at 340 nm.

Enzyme activity increased in all overexpression lines apart from line 8.12 overexpressing *PPC3* whose activity was comparable to the wild type (Figure 13). PPC activity increased by upto 200% for line 3.6 overexpressing *PPC1* while the increase in lines 4.10 and 8.10 overexpressing *PPC1* was 30% and 73% more compared to wild type (Figure 13A). In *PPC2* overexpression lines 1.8 and 4.9, enzyme activity increased by 80% and 45 % respectively (Figure 13B) while in *PPC3* overexpression lines 5.11 and 9.12 PPC enzyme activity increased by about 35% except in line 8.12 which had an enzyme activity comparable to the wild type (Figure 13C).

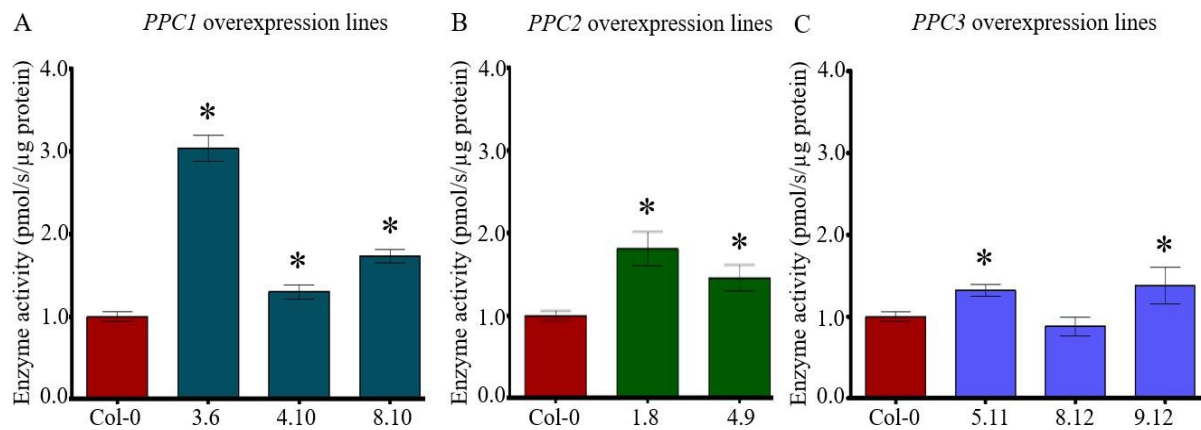


Figure 13: NADH-coupled PPC activity assay in crude protein extract of whole seedlings.

A-PPC activity in *PPC1* overexpression lines crude extract, **B**-PPC activity in *PPC2* overexpression lines crude extract and **C**-PPC activity in *PPC3* overexpression lines crude extract. Seedlings were grown for six days on sufficient Pi before harvest. Data were collected from four biological replicates then normalized to wild type (Col-0). Error bars denote \pm SE (n=9). Significance test was by student t-test (two tailed), * $p \leq 0.05$ compared to wild type Col-0.

2.4.4 Pi deficiency increases PPC protein phosphorylation in shoots and roots

Malate and aspartate reduce via negative feedback inhibition the activity of plant-type PPCs. However, allosteric inhibition of PPCs is reduced by phosphorylation of a single serine residue at the N-terminal end (Ser11 of AtPPCs). PPC phosphorylation additionally increases affinity of PPC to positive effectors such as glucose-6-phosphate and PEP, resulting in increased conversion of PEP to oxaloacetate and

other downstream metabolites. The phosphorylation status of PPCs in the transgenic lines was enhanced under Pi deficient condition for wild type and most overexpression lines in both shoots and roots. Phosphorylation levels in the *PPC* overexpression lines increased upon transfer to insufficient Pi condition (Figure 14).

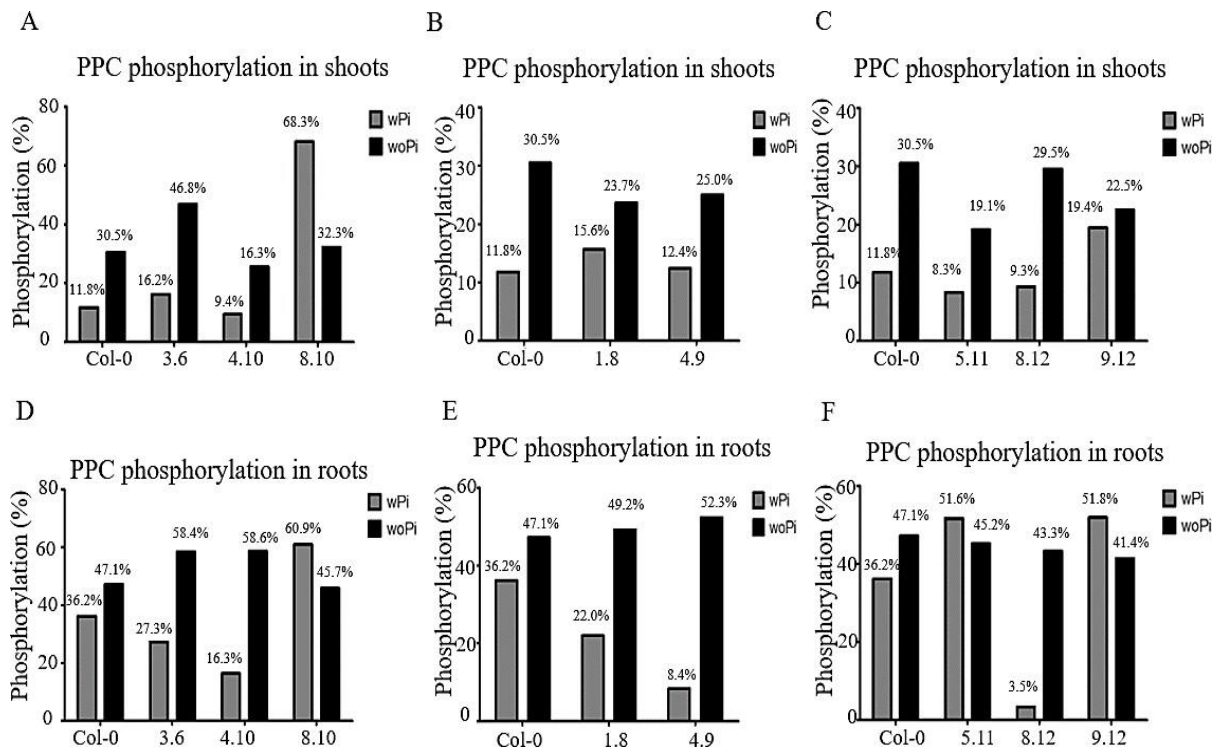


Figure 14: PPC phosphorylation levels in shoots and roots of *PPC* overexpression lines.

Percentage of shoot PPC phosphorylation in **A-*PPC1*** overexpression lines, **B-*PPC2*** overexpression lines and **C-*PPC3*** overexpression lines. The percentage of root PPC phosphorylation in **D-*PPC1*** overexpression lines, **E-*PPC2*** overexpression lines and **F-*PPC3*** overexpression lines. Seedlings were grown for six days on sufficient Pi before transfer to either sufficient or deficient Pi conditions for an additional five days before harvest. Data shown were collected from one biological replicate.

On Pi sufficient condition, PPC phosphorylation in shoots of *PPC1* overexpressing lines was about 16% and 68% in lines 3.6 and 8.10 while line 4.10 had about 9% the PPCs phosphorylated compared to wild type 12% (Figure 14A). In *PPC2* overexpression lines, the percentage of PPC phosphorylation was between 12-16% (Figure 14B) while *PPC3* overexpression lines had lower phosphorylation compared to wild type except line 9.12 which had more phosphorylation at about 19% (Figure 14C). Upon transfer to insufficient Pi conditions, PPC phosphorylation increased to about 31% in wild type and between 16-48% in *PPC1* overexpression lines (Figure 14A) while in *PPC2* overexpression lines, PPC phosphorylation was lower than in wild type at about 25% (Figure 14B). In a similar manner to phosphorylation in *PPC2* overexpression lines, though increased, PPC phosphorylation in *PPC3* overexpression lines was lower than in wild type and ranged between 19%-30% (Figure 14C).

PPC phosphorylation in roots under sufficient Pi condition was lower in *PPC1* overexpression line at about 16-27% except in line 8.10 which had 61% of its PPCs phosphorylated (Figure 14D). Similarly, PPCs phosphorylation in *PPC2* overexpression lines was lower at about 8-22% compared to wild types 36% (Figure 14E). In contrast, *PPC3* overexpression lines recorded higher PPCs phosphorylation at about 52% except in line 8.12 which had about 4% of its PPCs phosphorylated compared to wild type (Figure 14F). Upon transfer to insufficient Pi conditions, PPC phosphorylation increased to about 60% in *PPC1* overexpression lines except in line 8.10 which had about 45% phosphorylated PPCs (Figure 14D). In *PPC2* overexpression lines, PPC phosphorylation was higher than wild type at about 50% (Figure 14E) but was lower compared to wild type in *PPC3* overexpression lines at about 45% (Figure 14F).

In summary, Pi-starvation increased the percentage PPC phosphorylation in shoots and roots of wild type and *PPC* overexpression lines. However, since the overexpression lines had higher PPC protein levels than wild type (Col-0), the absolute number of phosphorylated PPCs in the *PPC* overexpression lines were higher than those of wild type.

2.5 Determination of malate and citrate content in tissues of *PPC* overexpression lines

2.5.1 Overexpression of *PPCs* increases root but not shoot malate

In shoots, only *PPC1* overexpression line 3.6 (Figure 15A) and *PPC3* overexpression line 5.11 (Figure 15C) showed significantly higher and lower malate levels, compared to wild type under insufficient and sufficient Pi conditions respectively. However, induction of shoot malate by Pi starvation in the overexpression lines was comparable to wild type levels except for *PPC1* overexpression lines 3.6 and 4.10 which accumulated more shoot malate than wild type (Two-way ANOVA: $p \leq 0.05$).

Similar to shoots, Pi starvation induced root malate accumulation in all overexpression lines and wild type (Figure 15). In sufficient Pi conditions, *PPC1* overexpression line 3.6 accumulated up to 20% more malate (Figure 15D) while *PPC2* overexpression lines 1.8 and 4.9 accumulated up to 70% and 86% more root malate compared to wild type respectively (Figure 15E). In contrast, root malate content in *PPC3* overexpression lines under sufficient Pi was comparable to the wild type (Figure 15F). Upon transfer to insufficient Pi conditions, increase in root malate content in *PPC1* overexpression lines ranged between 13-45% (Figure 15D) while in both *PPC2* overexpression lines malate content was about 1.7-fold higher compared to the wild type grown under similar conditions (Figure 15E). However, in *PPC3* overexpression lines Pi starvation-induced malate levels were by about 30% higher compared to wild type (Figure 15F).

Generally, Pi-induced changes in root malate content were comparable to wild type except in *PPC1* overexpression line 3.6 (Two-way ANOVA: $p = 0.01$) and lines 5.11 and 9.12 overexpressing *PPC3* (Two-way ANOVA: $p \leq 0.05$).

The effect of Pi starvation on tissue malate accumulation was clear as evidenced by the increased concentration in malate content in both wild type and overexpression lines under insufficient Pi condition (Figure 15). Fewer changes were observed in shoots between wild type and the overexpression lines, while more malate content was accumulated in roots of *PPC* overexpression lines compared to wild type upon Pi-starvation.

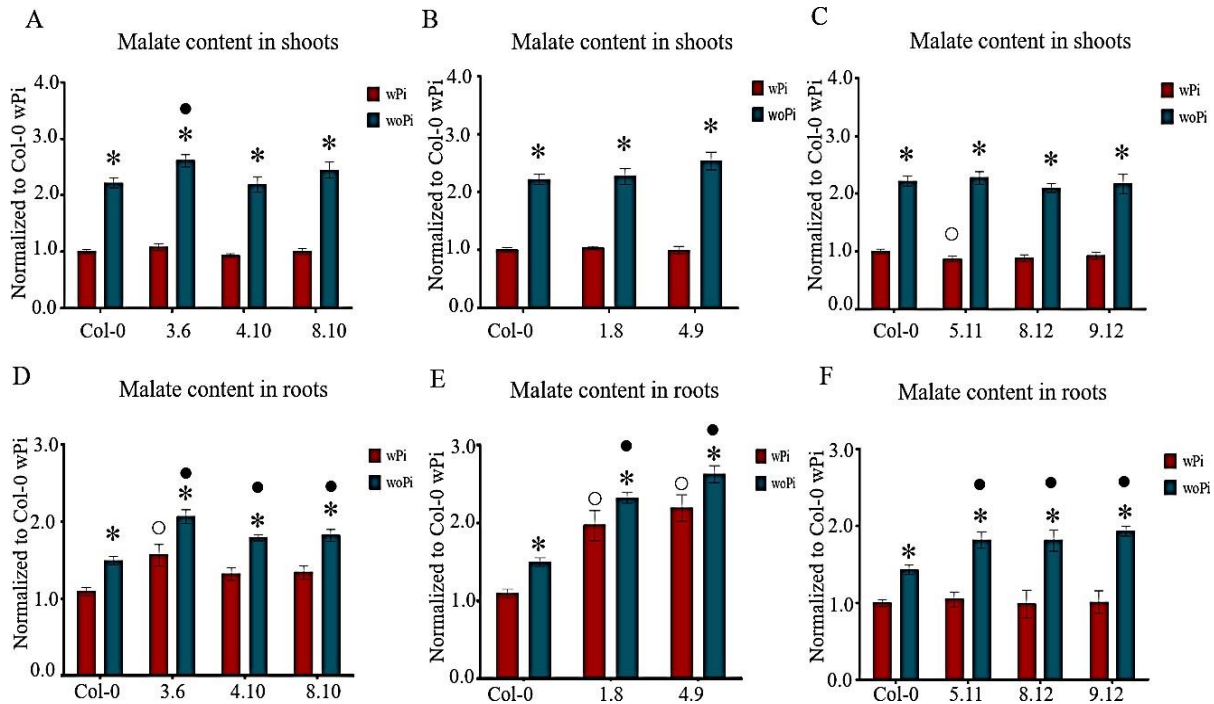


Figure 15: Tissue malate content in *PPC* overexpression lines.

Normalized (to wild type wPi) malate content in shoots of **A-*PPC1*** overexpression lines, **B-*PPC2*** overexpression lines and **C-*PPC3*** overexpression lines. Normalized (to wild type wPi) malate content in roots of **D-*PPC1*** overexpression lines, **E-*PPC2*** overexpression lines and **F-*PPC3*** overexpression lines. Seedlings were grown for six days on sufficient Pi before transfer to either sufficient or deficient Pi conditions for an additional five days before harvest. Error bars denote \pm SE (n=12). Significance analyses were performed by Student's t-test (two-tailed, equal variances): *p \leq 0.05, o p \leq 0.05 and • p \leq 0.05 compared to wPi, Col-0 wPi and Col-0 woPi, respectively.

2.5.2 Overexpression of *PPCs* increases shoot and root citrate content

As was observed for malate, shoot citrate content was induced by Pi starvation in wild type and all the overexpression lines (Figure 16). However, contrary to what had been observed for malate, the citrate content in the overexpression lines showed more alterations compared to wild type. On sufficient Pi condition, *PPC1* overexpression lines accumulated about 30% more shoot citrate compared to wild type (Figure 16A) while increase in shoot citrate for *PPC3* overexpression lines ranged between 19-32 % (Figure 16C). In contrast, *PPC2* overexpression lines showed about a 40% decrease in shoot citrate levels compared to wild type (Figure 16B). On insufficient Pi condition, *PPC1* overexpression lines

accumulated between 23-60% more shoot citrate (Figure 16A) while *PPC3* overexpression lines accumulated 59%, 50% and 17% more citrate compared to wild type for lines 5.11, 8.12 and 9.12 ($p=0.2$) respectively (Figure 16C). In a similar manner to what had been observed on sufficient Pi, *PPC2* overexpression lines showed a reduction by about 27% compared to wild type upon Pi starvation (Figure 16B). The Pi starvation response in the overexpression lines was however indistinguishable from wild type except for line 4.10 overexpressing *PPC1* (Two-way ANOVA: $p=0.002$) and lines 5.11 and 8.12 overexpressing *PPC3* (Two-way ANOVA: $p\leq 0.05$), which exhibited a stronger response.

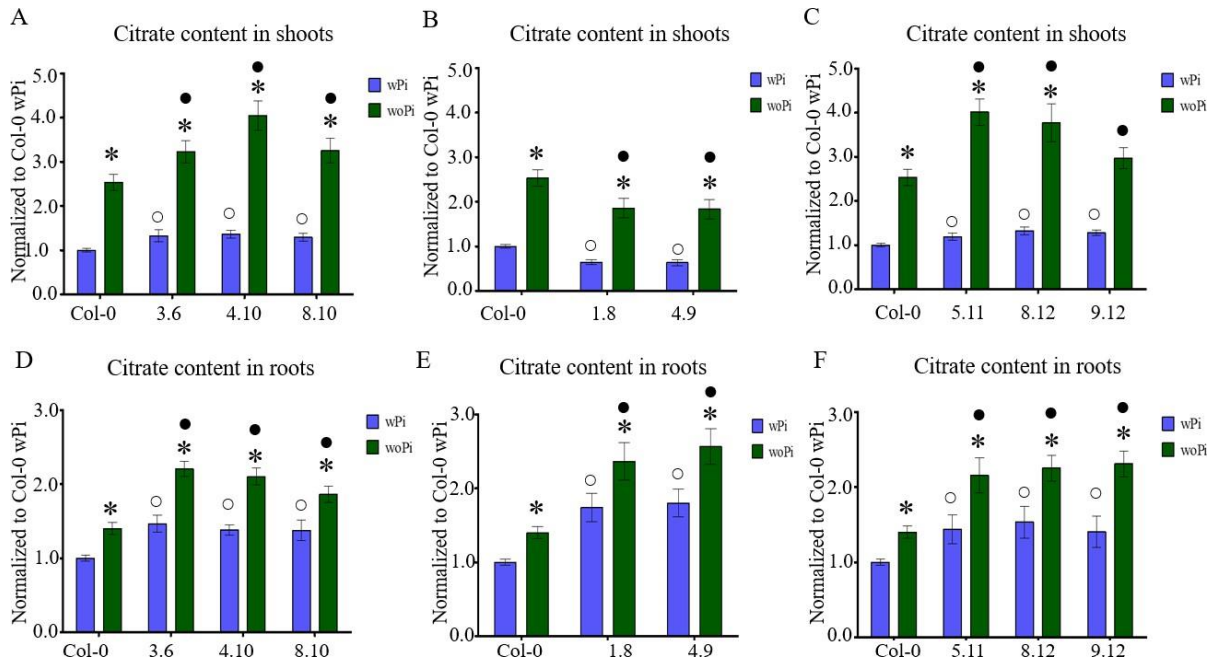


Figure 16: Tissue citrate content in *PPC* overexpression lines.

Normalized citrate content in shoots of **A-*PPC1*** overexpression lines, **B-*PPC2*** overexpression lines and **C-*PPC3*** overexpression lines. Normalized citrate content in roots of **D-*PPC1*** overexpression lines, **E-*PPC2*** overexpression lines and **F-*PPC3*** overexpression lines. Seedlings were grown for six days on sufficient Pi before transfer to either sufficient or deficient Pi conditions for an additional five days before harvest. Error bars denote \pm SE (n=12). Significance analyses were performed by Student's t-test (two-tailed, equal variances): * $p\leq 0.05$, o $p\leq 0.05$ and • $p\leq 0.05$ compared to wPi, Col-0 wPi and Col-0 woPi, respectively.

Like malate, citrate content in roots increased upon Pi starvation in wild type and in the overexpression lines (Figure 16). *PPC1* and *PPC3* overexpression lines accumulated about 40% more citrate compared to wild type on sufficient Pi (Figure 16A and Figure 16C). However, unlike shoots, roots of *PPC2* overexpression lines accumulated up to 80% more citrate in compared to wild type on sufficient Pi (Figure 16B).

Upon Pi starvation root citrate levels were higher in all overexpression lines compared to wild type being between 33-57% higher in *PPC1* overexpression lines (Figure 16D), between 68-83% higher in

PPC2 overexpression lines (Figure 16E), and between 54-65% higher in the *PPC3* overexpression lines (Figure 16F). However, the Pi deficiency-induced response was only significant for line 3.6 overexpressing *PPC1* (Two-way ANOVA: $p=0.01$) and line 9.12 overexpressing *PPC3* (Two-way ANOVA: $p=0.04$).

Overall, *PPC* overexpression lines accumulated more citrate in shoots on both sufficient and insufficient Pi compared to wild type except for both *PPC2* overexpression lines whose citrate levels were lower. However, in roots all *PPC* overexpression lines accumulated more citrate compared to wild type on both sufficient and insufficient Pi conditions.

2.5.3 Overexpression of *PPC2* enhances malate and citrate exudation

Phosphate starvation enhances exudation of OAs for increased solubilization of Pi bound to complexes. Having determined enhanced accumulation of malate and citrate content in root and shoot tissues of the overexpression lines, we were curious to find out whether the overexpression lines would also exude more malate and citrate than wild type. Pi starvation enhanced malate and citrate exudation for both wild type and the overexpression lines (Figure 17). In sufficient Pi condition, malate exuded by the *PPC1* and *PPC3* overexpression lines was comparable to the wild type levels except for line 8.10 and 8.12 overexpressing *PPC1* and *PPC3*, which exuded about 35% less malate than wild type under sufficient Pi (Figure 17A and Figure 17C). Unlike the other overexpression lines, *PPC2* overexpression lines showed increased malate exudation compared to wild type by about 40% on sufficient Pi and 34% on Pi starvation conditions respectively (Figure 17B). However, the Pi deficiency-induced malate exudation response in the overexpression lines was comparable to wild type (Two-way ANOVA: $p \geq 0.05$).

Like malate exudation, citrate exudation was elevated upon Pi starvation for wild type and the overexpression lines (Figure 17). Exuded citrate in *PPC1* (Figure 17D) and *PPC3* overexpression lines was comparable to wild type levels on both sufficient and insufficient Pi media except for line 9.12 overexpressing *PPC3* which exuded 39% more citrate than wild type on sufficient Pi (Figure 17F). As was observed for malate, both *PPC2* overexpression lines exuded about 40% and 35% more citrate compared to the wild type on sufficient and insufficient Pi conditions (Figure 17E). Like malate exudation, Pi deficiency-induced changes in citrate exudation in the overexpression lines were also indistinguishable from wild type response (Two-way ANOVA: $p \geq 0.05$).

While Pi starvation enhanced levels of exuded malate and citrate in wild type and *PPC* overexpression lines, only *PPC2* overexpression lines exuded more malate and citrate compared to wild type on sufficient and insufficient Pi conditions.

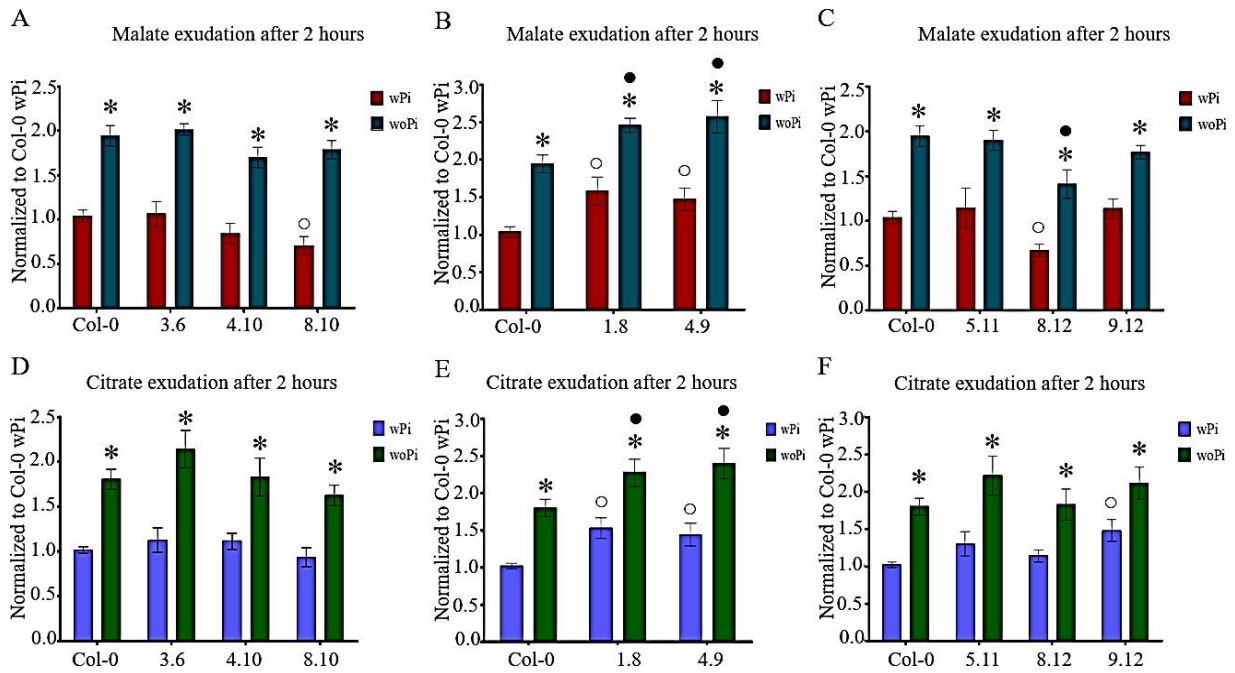


Figure 17: Root malate and citrate exudation in *PPC* overexpression lines.

Normalized (wild type wPi) malate exudation in **A**-Roots of *PPC1* overexpression lines, **B**-Roots of *PPC2* overexpression lines and **C**-Roots of *PPC3* overexpression lines. Normalized citrate exudation in **D**-Roots of *PPC1* overexpression lines, **E**-Roots of *PPC2* overexpression lines and **F**-Roots of *PPC3* overexpression lines. Seedlings were grown for six days on sufficient Pi before transfer to either sufficient or deficient Pi conditions for an additional five days before root were incubated in water for 2 hours. Error bars denote \pm SE (n=12). Significance analyses were performed by Student's t-test (two-tailed, equal variances): * $p \leq 0.05$, $\circ p \leq 0.05$ and $\bullet p \leq 0.05$ compared to wPi, Col-0 wPi and Col-0 woPi, respectively.

2.6 Other metabolite changes in *PPC* overexpression lines

2.6.1 Overexpression of *PPCs* enhances amino acid content under sufficient Pi

Since *PPCs* are at a core branch point of metabolism, it was interesting to see what other metabolic changes might occur. Failure to detect increased malate and citrate in shoots, roots or exudates in various overexpression lines might be due to further channeling of metabolites to other compounds. To investigate this, we analyzed tissue amino acid content in the overexpression lines in comparison to the wild type profile.

Changes in shoot amino acid were apparently much more on sufficient Pi compared to insufficient Pi condition (Figure 18A). Amino acid changes in *PPC1* overexpression lines were fewer compared to changes in *PPC2* and *PPC3* overexpression lines but they accumulated significantly high aspartate, histidine, and lysine levels compared to the wild type. Both *PPC2* overexpression lines also accumulated significantly higher histidine, and lysine levels in addition to leucine, iso-leucine, ornithine

and taurin compared to the wild type (Figure 18A). However, in contrast to *PPC1* overexpression lines, aspartate levels remained unaltered in the *PPC2* overexpression lines. More inconsistencies were observed in *PPC2* overexpression lines compared to *PPC1* and *PPC3* overexpression lines, with *PPC2* overexpression line 1.8 showing more amino acid changes than line 4.9. *PPC3* overexpression lines were in contrast more consistent across individual lines and were more similar to *PPC2* overexpression lines showing increases in histidine, iso-leucine, lysine, leucine, phenylalanine, arginine and tyrosine levels (Figure 18A). Additionally, two out of three lines overexpressing *PPC3* showed increased asparagine but decreased serine levels compared to wild type. Upon Pi starvation, amino acid changes in the overexpression were more comparable to amino acid changes in wild type when grown in similar growth conditions except for lysine and proline. Pi starvation enhanced higher accumulation of lysine levels in both *PPC2* overexpression lines compared to wild type, similar to proline levels which were accumulated in higher levels in *PPC2* and *PPC3* overexpression lines compared to wild type (Figure 18A).

As was observed in shoots, changes in root amino acid content were more pronounced in the overexpression lines on sufficient Pi compared to insufficient Pi, where no significant changes in amino acid content compared to wild type could be detected (Figure 18B). In *PPC1* overexpression lines aspartate, iso-leucine and valine were higher compared to wild type in all individual lines, while two out of three lines also accumulated higher leucine, threonine, tryptophan and tyrosine (Figure 18B). Amino acid changes in *PPC2* overexpression lines were higher and consistent for almost all amino acids compared to wild type except for methionine, citrulline and *O*-acetylserine which were highly accumulated in one of the two lines overexpressing *PPC2* (Figure 18B). Although inconsistent, the trend for *PPC3* overexpression lines resembled that observed for *PPC1* overexpression lines, but if showing changes, they were higher compared to wild type. Notably, all individual *PPC3* overexpression lines accumulated higher levels of methionine while higher levels of phenylalanine, histidine, iso-leucine, glutamine and tyrosine were accumulated in two of the three independent lines (Figure 18B). Notably, all overexpression lines accumulated higher valine content compared to wild type. Additionally, in comparison to wild type, all the overexpression lines accumulated higher arginine and isoleucine content in roots except in line 9.12 overexpressing *PPC3*. Furthermore, all overexpression lines accumulated higher lysine content except in *PPC1* overexpression line 3.6 (Figure 18B).

Shoot and root amino acid profiles for the *PPC* overexpression lines when grown on sufficient Pi closely resembled the profile for wild type when grown on insufficient Pi media (Figure 18). In cases where overexpression lines accumulated certain amino acids at higher levels on sufficient Pi, changes for the same were higher in roots compared to shoots while in wild type more amino acid level changes were observed for shoots compared to roots on insufficient Pi (Figure 18).

In summary, more significant amino acid changes were observed in shoots and roots of the *PPC* overexpression lines on sufficient Pi compared to wild type while upon Pi starvation, changes were more comparable to those observed in wild type.

2.6.2 Changes in TCA intermediates in *PPC* overexpression lines

We also investigated what happened to some of the TCA cycle intermediates. In sufficient Pi condition, shoot fumarate levels in *PPC1* overexpression lines were comparable to wild type levels except in line 4.10 which had lower levels while in *PPC2* overexpression lines, only line 1.8 accumulated higher fumarate levels while line 4.9 had levels comparable to wild type (Figure 18A). In contrast, all the three *PPC3* overexpression lines accumulated lower fumarate content compared to wild type on sufficient Pi condition (Figure 18A).

Shoot aconitate levels were more inconsistent among the overexpression lines. *PPC1* overexpression lines 4.10 and 8.10 and line 8.12 overexpressing *PPC3* accumulated more aconitate levels while all the other lines accumulated levels comparable to wild type on sufficient Pi conditions (Figure 18A). In contrast, shoot α -ketoglutarate in all the overexpression lines was comparable to wild type on sufficient Pi except for line 1.8 overexpressing *PPC2* while only the three lines overexpressing *PPC1* accumulated more succinate on sufficient Pi compared to wild type (Figure 18A).

As was observed in sufficient Pi condition, fumarate levels were also inconsistent among the overexpression lines upon transfer to Pi starvation condition and only lines 4.10 and 5.11 accumulated higher fumarate levels compared to wild type for lines overexpressing *PPC1* and *PPC3*, respectively (Figure 18A). In contrast, both lines overexpressing *PPC2* accumulated higher fumarate levels compared to wild type upon Pi starvation. Shoot aconitate levels upon Pi starvation were only higher in *PPC1* overexpression lines compared to wild type while in *PPC2* and *PPC3* overexpression lines shoot aconitate levels were comparable to wild type (Figure 18).

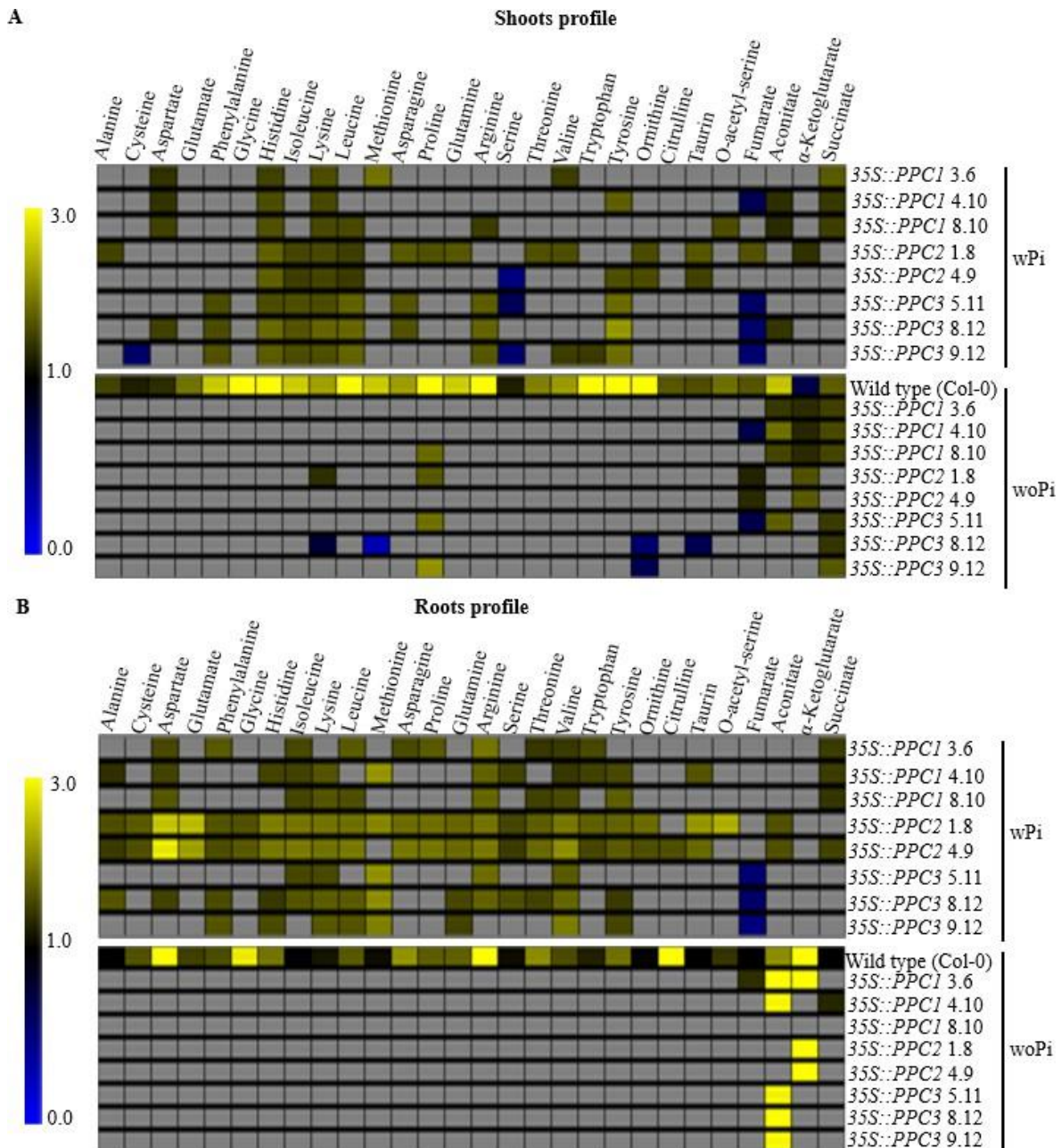


Figure 18: Heatmap showing metabolite changes in tissues of *PPC* overexpression lines.

Normalized (wild type wPi) amino acids profiles of **A-Shoots** of *PPC* overexpression lines and **B- Roots** of *PPC* overexpression lines. Seedlings were grown for six days on sufficient Pi before transfer to either sufficient or deficient Pi conditions for an additional five days before harvest. n=12. Grey boxes indicate non significance compared to the wild type, blue (significant but lower levels) and yellow (significant and high levels) to wild type (Col-0) wPi ($p < 0.05$, student t-test, two tailed).

More diverse and consistent changes were observed for α -ketoglutarate across the overexpression lines compared to wild type upon Pi deficiency. All three lines overexpressing *PPC1* accumulated lower levels of α -ketoglutarate while both *PPC2* overexpression lines accumulated higher levels compared to wild type (Figure 18A). However, α -ketoglutarate levels in *PPC3* overexpression lines were indistinguishable from those of wild type (Figure 18A). Upon Pi starvation, succinate levels were

higher in all the overexpression lines except for both lines overexpressing *PPC2* whose levels were comparable to wild (Figure 18A).

Changes in TCA intermediates for roots on sufficient Pi condition were more consistent across the overexpression lines compared to shoots. Similar to shoots fumarate levels were significantly lower in all the three *PPC3* overexpression lines but were comparable to wild type levels in *PPC1* and *PPC2* overexpression lines (Figure 18B). However, unlike in shoots, roots accumulated significantly higher aconitate levels in both *PPC2* overexpression lines on sufficient Pi, while all the other overexpression lines accumulated similar levels to wild type (Figure 18B). A similar trend for α -ketoglutarate levels in shoots was also observed for roots but unlike in shoots, α -ketoglutarate levels in all the overexpression lines were similar levels to those for wild type. Similar to shoot succinate levels, root succinate levels were comparable to wild type in the overexpression lines except in all the three lines overexpressing *PPC1* and line 4.9 overexpressing *PPC2* (Figure 18B).

Upon Pi starvation, fumarate and succinate levels in the overexpression lines were comparable to wild type except in lines 3.6 and 4.10, respectively both overexpressing *PPC1* (Figure 18B). Root aconitate levels were higher compared to wild type all overexpression lines except in line 8.10 overexpressing *PPC1* and in both *PPC2* overexpression lines (Figure 18B) while α -ketoglutarate levels upon Pi starvation were only higher in both *PPC2* overexpression lines and line 3.6 overexpressing *PPC1* (Figure 18B).

Generally, more changes in TCA intermediates were observed in shoots of overexpression lines compared to wild type upon Pi starvation. In roots fewer changes were observed for TCA intermediates and when present the levels were higher than wild type. Notably, fumarate levels were consistently lower in shoots and roots of *PPC3* overexpression lines grown on sufficient Pi condition.

2.7 Phenotypic characteristics of *PPC* overexpression lines

Previous studies on overexpression of C4 *PPCs* in C3 plants had reported negative effects such as reduced growth and yield (Kogami et al., 1994; Rademacher et al., 2002). We investigated whether overexpressing C3 *PPC* in C3 plants would have any effects on seedling growth in nutrient sufficient and nutrient deficient conditions as well as on plant development when grown in soil until seed set.

2.7.1 *PPC* overexpression increases tissue fresh weight

Shoot fresh weight was generally higher on sufficient Pi compared to Pi starvation for wild type and the overexpression lines. When grown on Pi sufficient conditions, shoot fresh weight was higher by about 11-22% in *PPC1* (Figure 19A) and *PPC3* (Figure 19C) overexpression, respectively, while overexpressing *PPC2* did not impact shoot fresh weight compared to wild type (Figure 19B). On transfer to Pi starvation condition, all the overexpression lines had increased shoot fresh weight compared to wild type. Similar to Pi sufficient condition, *PPC1* overexpression lines recorded an

increase of between 16-20% in shoot fresh weight on insufficient Pi while *PPC3* overexpression lines shoot fresh weight was 20-34% higher than wild type. In contrast to sufficient Pi, shoot fresh weight on insufficient Pi for *PPC2* overexpression lines increased by about 31-47%, compared to wild type (Figure 19B). Changes in shoot weight induced by Pi starvation in the overexpression lines were however comparable to wild type except in *PPC1* and *PPC2* overexpression lines 3.6 (Two-way ANOVA: $p \leq 0.001$) and 4.9 (Two-way ANOVA: $p \leq 0.05$) respectively.

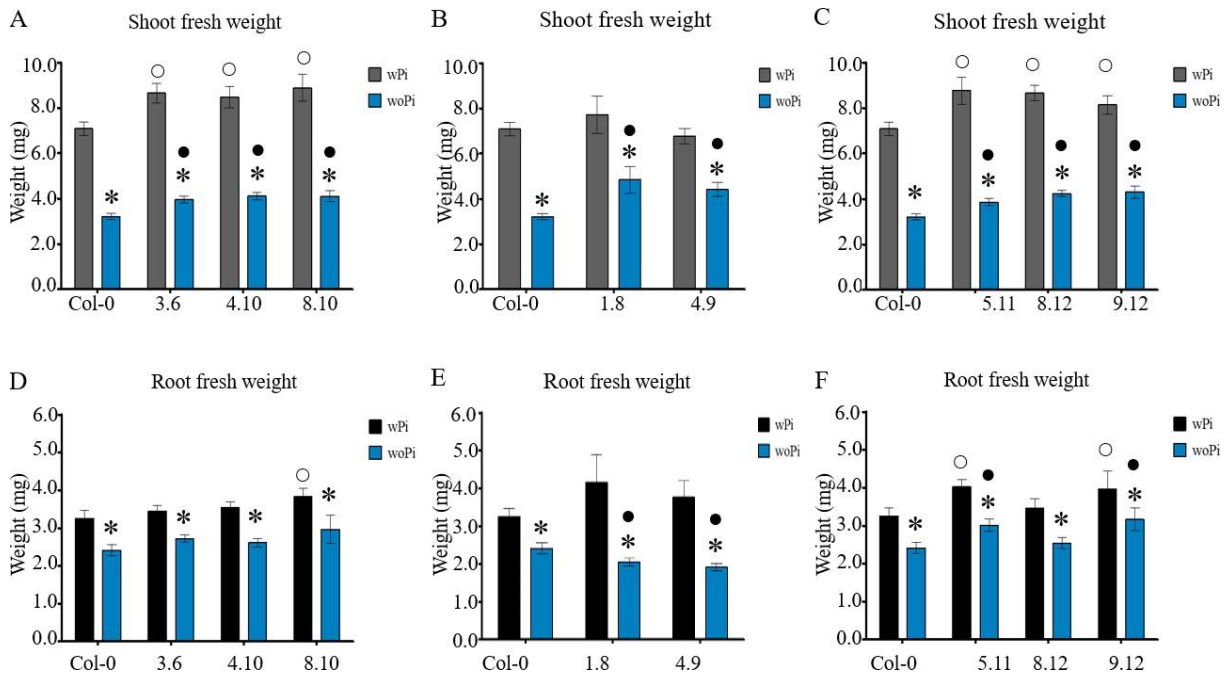


Figure 19: Tissue fresh weights of *PPC* overexpression lines.

Shoot fresh weight of **A-*PPC1*** overexpression lines, **B-*PPC2*** overexpression lines and **C-*PPC3*** overexpression lines. Root fresh weight of **D-*PPC1*** overexpression lines, **E-*PPC2*** overexpression lines and **F-*PPC3*** overexpression lines. Seedlings were grown for six days on sufficient Pi before transfer to either sufficient or deficient Pi conditions for an additional five days before harvest. Error bars denote \pm SE (n=12). Significance analyses were performed by Student's t-test (two-tailed, equal variances): * $p \leq 0.05$, o $p \leq 0.05$ and • $p \leq 0.05$ compared to wPi, Col-0 wPi and Col-0 woPi, respectively.

Root fresh weight was higher in wild type and overexpression lines on sufficient Pi compared to Pi starvation condition. On sufficient Pi, root fresh weight for the overexpression lines was comparable to wild type except for *PPC1* overexpression line 8.10 and *PPC3* overexpression lines 5.11 and 9.12, which had 25%, 31%, and 39% higher root fresh weight than wild type, respectively. (Figure 19D and Figure 19F). On transfer to insufficient Pi condition, higher root weight was observed for *PPC3* overexpression lines 5.11 and 9.12, which had 25% and 31% more root fresh weight while line 8.12 was comparable to wild type (Figure 19F). In contrast, *PPC2* overexpression lines had reduced root fresh weight by about 20% compared to wild type while *PPC1* overexpression lines root fresh weight was indistinguishable from wild type levels (Figure 19D). However, Pi- deficiency induced root fresh

weight changes in the overexpression lines were comparable to wild type changes as revealed by two-way ANOVA ($p \geq 0.05$).

Shoot fresh weight in the *PPC* overexpression lines was higher on insufficient Pi conditions compared to wild type, while on sufficient Pi only *PPC1* and *PPC3* overexpression had higher shoot fresh weight. Root fresh weight for the *PPC* overexpression lines was comparable to wild type except for *PPC3* overexpression lines which had higher root fresh weights. Upon Pi starvation, root fresh weight was comparable to wild type for *PPC1* overexpression lines but was lower and higher for *PPC2* and *PPC3* overexpression lines, respectively.

2.7.2 *PPC* overexpression increases gain of root length

One of the major indicators of low Pi in Arabidopsis is the shortening of the primary root. To investigate the effect of *PPC* overexpression on gain of root length after transfer to either Pi sufficient or Pi starvation conditions, measurements were done five days after transfer from sufficient phosphate to insufficient Pi media. As expected, gain of root length for wild type and the overexpression lines was lower in insufficient Pi compared to sufficient Pi (Figure 20). On sufficient Pi, gain of root length for *PPC1* and *PPC3* overexpression lines was higher by about 9-41% (Figure 20A) and 11-33% (Figure 20C) respectively compared to wild type. However, gain of root length in *PPC2* overexpression lines on sufficient Pi was comparable to wild type (Figure 20B).

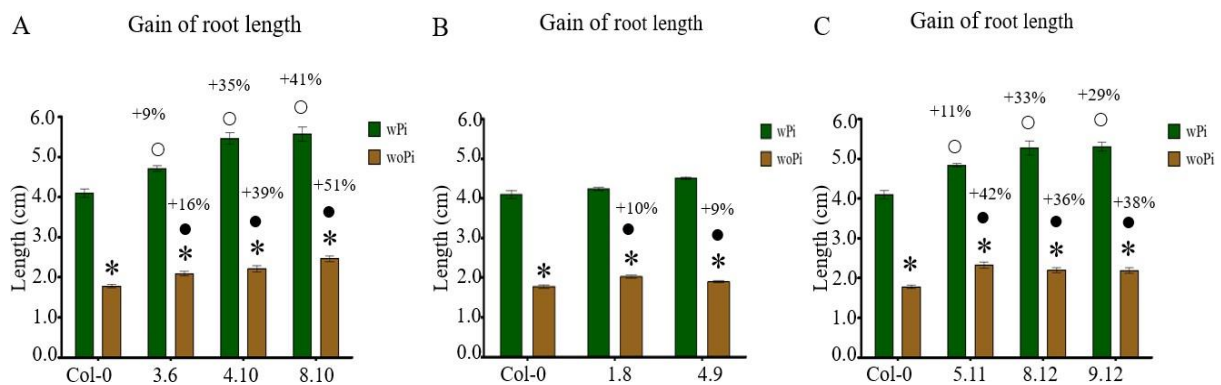


Figure 20: Gain of root length of *PPC* overexpression lines.

Gain of root length measurement of **A-*PPC1*** overexpression lines, **B-*PPC2*** overexpression lines and **C-*PPC3*** overexpression lines. Seedlings were grown for six days on sufficient Pi before transfer to either sufficient or deficient Pi conditions for an additional five days before harvest. Error bars denote \pm SE ($n=36$). Significance analyses were performed by Student's t-test (two-tailed, equal variances): * $p \leq 0.05$, $\circ p \leq 0.05$ and $\bullet p \leq 0.05$ compared to wPi, Col-0 wPi and Col-0 woPi, respectively. +denotes percentage increase compared to wild type wPi or woPi.

In contrast, on transfer to insufficient Pi condition, all overexpression lines had a higher gain of root length compared to wild type. As was observed on sufficient Pi growth condition, gain of root length for *PPC1* and *PPC3* overexpression lines was higher by between 16-51% (Figure 20A) and about 40%

(Figure 20C) compared to wild type, respectively. Unlike on sufficient Pi condition, *PPC2* overexpression lines had a 10% increase in gain of root length compared to wild type upon transfer to Pi starvation condition (Figure 20B). Notably, the gain of root length response upon Pi starvation was significantly different in the *PPC1* overexpression lines (Two-way ANOVA: $p \leq 0.05$) as well as lines 8.12 and 9.12 overexpressing *PPC3* (Two-way ANOVA: $p \leq 0.05$). In contrast, the Pi starvation response with respect to gain of root length in both lines overexpressing *PPC2* was comparable to that of wild type (Two-way ANOVA: $p \geq 0.25$).

Gain of root length was higher in almost all *PPC* overexpression lines on sufficient and insufficient Pi conditions compared to wild type except for both *PPC2* overexpression lines, which gain of root length comparable to wild type only on sufficient Pi condition.

2.7.3 *PPC* overexpression reduces seed weight and seed number

Transgenic C3 plants overexpressing C4 or bacterial *PPCs* had in the past resulted in contradictory phenotypes, with some studies reporting stunted growth and reduced yield, while other studies reported no difference between the transgenic lines and wild type plants (Kogami et al., 1994; Rademacher et al., 2002). We were also curious to investigate whether our adult transgenic lines overexpressing C3 *PPCs* would show any phenotypic difference compared to wild type. Seeds for individual lines overexpressing *AtPPCs* were planted in soil pots, stratified in the dark for two days before transfer to the green house where their flowering time, seed number and seed weight were determined. On soil, flowering time of *PPC* overexpression lines was different among the transgenic lines compared to wild type while growth of *PPC2* overexpression appeared to be stunted (Figure 21).

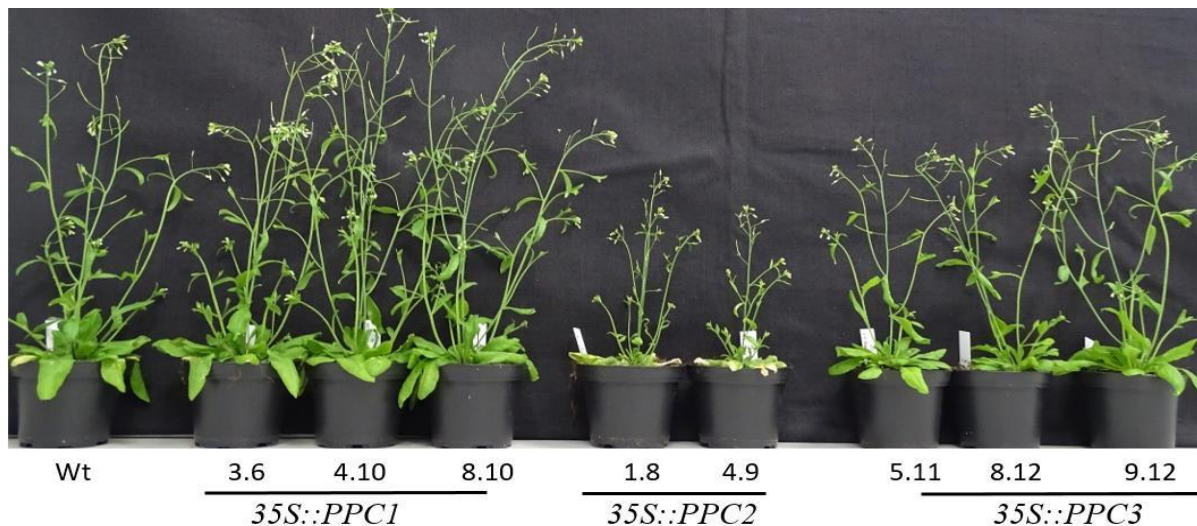


Figure 21: Growth of *PPC* overexpression lines on soil.

PPC2 overexpression lines show delayed growth and time to flowering. Adult wild type plants and *PPC* overexpression lines six weeks after sowing on soil.

Additionally, *PPC1* and *PPC3* overexpression lines flowered earlier (32 DAS) while wild type flowered later (34DAS) while *PPC2* overexpression lines showed delayed flowering at 36 DAS (Figure 22A). Analysis of seed weight per plant revealed lower seed weight for all the overexpression lines compared to wild type.

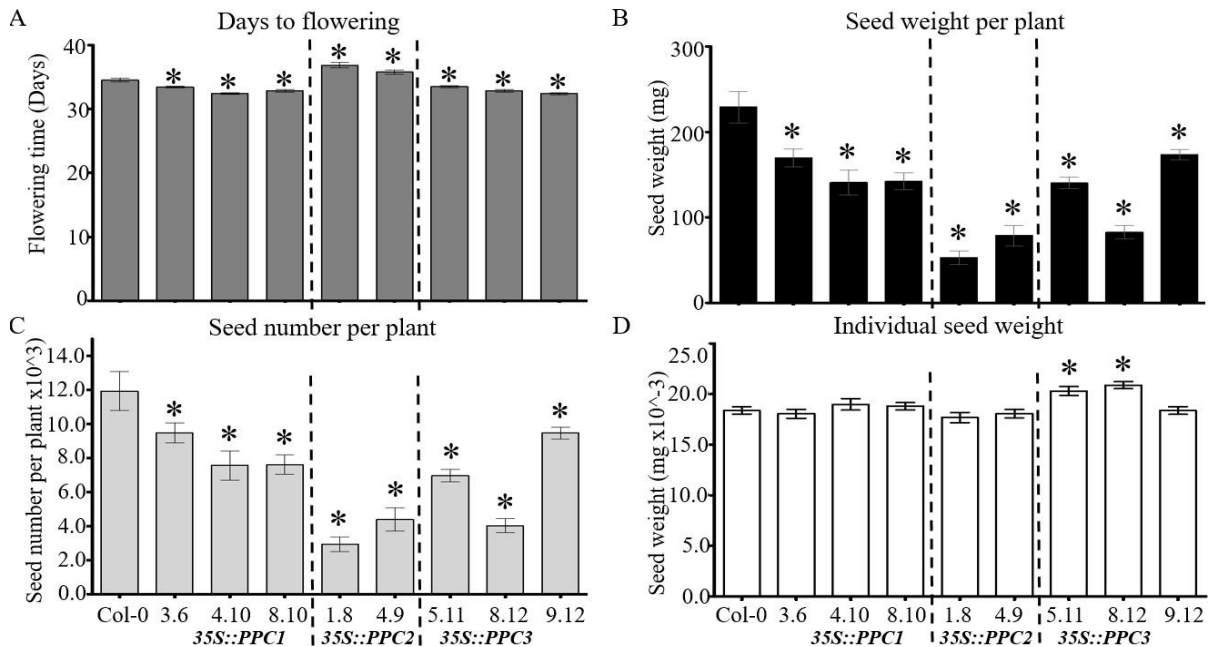


Figure 22: Phenotypic characteristics of *PPC* overexpression lines grown on soil.

Seeds were stratified in the dark for two days before transferring to greenhouse where **A-Flowering** **B-Seed weight** per plant, **C-Seed number** per plant and **D-Individual seed weight** for the overexpression lines were determined. Error bars indicate SE (n=15). Significance test was by student t-test (two tailed), * $p \leq 0.05$ compared to Col-0 (Wild type).

Seed weight for *PPC1* and *PPC3* overexpression lines was 24-39 % lower compared to wild type except in line 8.12 overexpressing *PPC3* whose seed weight was 64% lower than wild type. In *PPC2* overexpression lines, seed weight was severely reduced by 77 and 66% in lines 1.8 and 4.9 respectively compared to wild type (Figure 22B). Like seed weight per plant, total seed number per plant was lower in all the overexpression lines compared to wild type whereby *PPC1* and *PPC3* overexpression lines had between 21-66% lower seed number than wild type (Figure 22C). Similar to what was observed in seed weight per plant, seed number for *PPC2* overexpression lines was also severely lower by between 63-75% compared to wild type (Figure 22C). In contrast, individual seed weight for the overexpression lines was indistinguishable from wild type and only lines 5.11 and 8.12 overexpressing *PPC3* had approximately 10% heavier seed weight compared to wild type (Figure 22D).

After investigating the effects of overexpressing *AtPPCs* in Arabidopsis, we were also interested in studying the effects of PPCKs, the only known protein kinases (to date) that positively regulate PPC activity by reducing the affinity of negative allosteric inhibitors such as malate and aspartate. Since a

previous study in our group (Chutia, 2019) had extensively worked on overexpressing Arabidopsis *PPCKs* (*AtPPCK1* and *AtPPCK2*) and on the characterization of Arabidopsis *ppck1* knockout line, we decided to analyze Arabidopsis *ppck2* single and *ppck1ppck2* double loss of function mutants.

2.8 *PPCK1* is predominantly expressed in Arabidopsis shoots and roots

From previous analysis of the two Arabidopsis *PPCKs* transcripts in wild type shoots and roots in our group, basal transcript levels revealed higher *PPCK1* transcript levels in shoots and roots compared to *PPCK2* transcript levels under sufficient and insufficient Pi and differential induction on Pi starvation (Chutia, 2019). This was further validated by our transcript analysis of *PPCK* mRNAs in shoots and roots (Figure 23) using gene specific primers (Supplementary table 1). On sufficient Pi, shoot *PPCK1* transcripts were about 45-fold those of *PPCK2* and were induced 25-fold upon Pi starvation (Figure 23A) while *PPCK2* transcripts were strongly induced by about 750-fold but *PPCK1* transcript levels were still higher than those of *PPCK2* (Figure 23A).

In roots, *PPCK1* transcripts were about 7-fold higher than *PPCK2* transcripts on sufficient Pi and were induced about 5-fold upon Pi starvation. Induction of *PPCK2* was stronger in roots upon Pi starvation by about 13-fold (Figure 23B). Two-way ANOVA analysis revealed significant induction of *PPCKs* upon Pi starvation in both shoots ($p=0.02$) and roots ($p=6.6e^{-6}$).

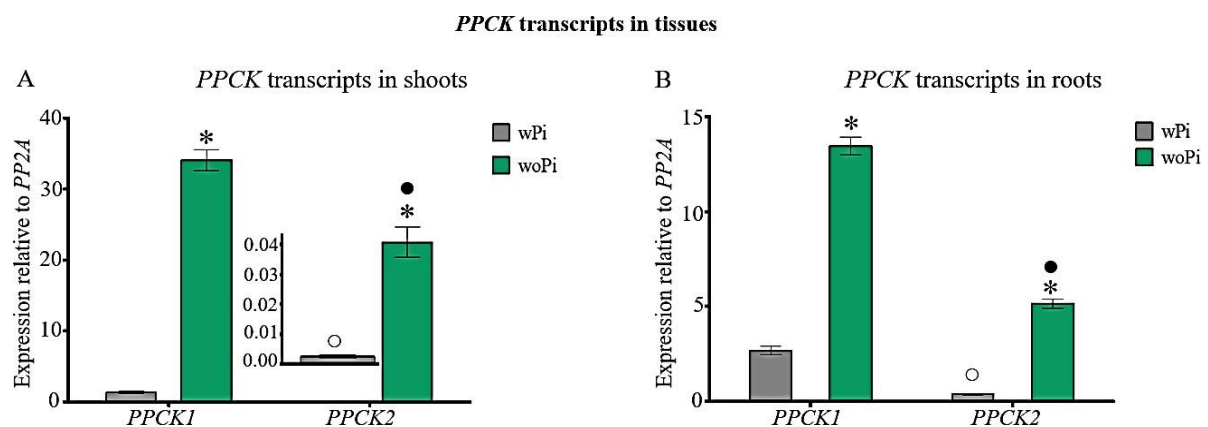


Figure 23: *PPCK* transcript levels in wild type shoots and roots.

Transcript levels in wild type **A-Shoots** and **B-Roots**. Seedlings were grown for six days on sufficient Pi before transfer to either sufficient or deficient Pi conditions for an additional five days before harvest. Error bars denote \pm SE ($n=3$). Significance analyses were performed by Student's t-test (two-tailed, equal variances): * $p \leq 0.05$ compared to wPi, ^o $p \leq 0.05$ compared to *PPCK1* wPi, [•] $p \leq 0.05$ compared to *PPCK1* woPi.

Differential induction of *PPCKs* in shoots and roots suggests possible different roles, which are still unknown. Previous studies from our group mainly focused on the effects of overexpressing *PPCKs* on OAs content and exudation in Arabidopsis (Chutia, 2019). Using a T-DNA knockout mutant, *ppck1-4* (Figure 24A), effects on OAs exudation and accumulation were additionally studied. Unfortunately, a *ppck2* loss of function mutant was not available because the *ppck2* T-DNA insertion lines analyzed had

considerable levels of *PPCK2* transcripts (Figure 24B). Furthermore, due to time constraints during the previous study (Chutia, 2019), the *ppck1-4* T-DNA insertion mutant could not be complemented. Since the *ppck1-4* mutant showed altered levels of OAs content, we therefore set out to first complement the *ppck1-4* knockout line and to generate additional *ppck2* knockout lines.

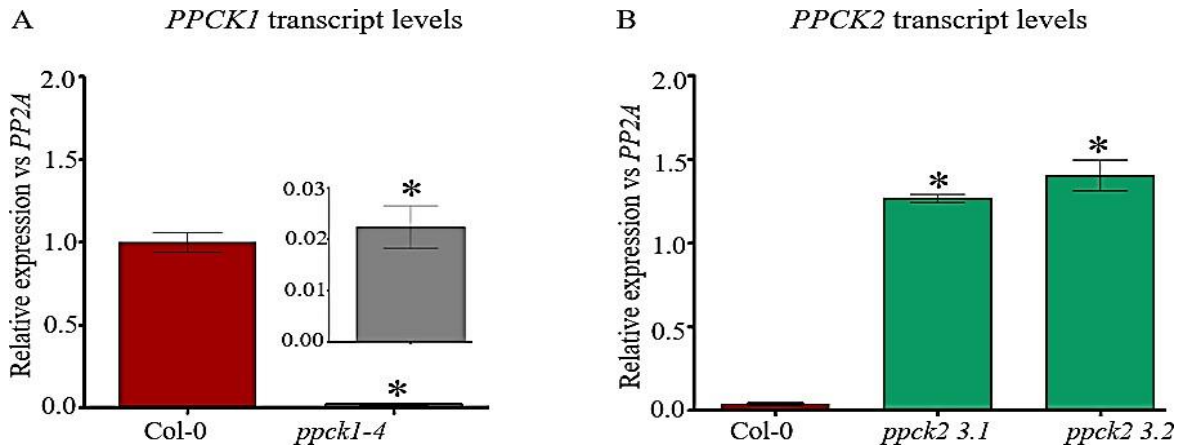


Figure 24: *PPCK* transcript levels in wild type and *ppck* mutants.

A-*PPCK1* transcript levels in wild type and *ppck1-4* mutant and **B-*PPCK2*** transcript levels in wild type and *ppck2* mutant lines 3.1 and 3.2. Seedlings were grown for six days on sufficient Pi condition before harvest. Error bars denote \pm SE (n=3). Significance analyses were performed by Student's t-test (two-tailed, equal variances): * $p \leq 0.05$ compared to Col-0. Results shown are unpublished data adapted from Chutia, (2019).

2.9 Complementation of *ppck1-4* mutant reverts *PPCK1* transcripts to wild type level

To confirm the effects of OAs production in the T-DNA insertion *ppck1-4* line, we complemented this mutant with a construct harboring the *PPCK1* ORF (1029bp) under control of its native *PPCK1* promoter (2468 bp). Two independent complementation lines were identified (lines 9.10 and 11.8) and their *PPCK1* transcripts analyzed using specific primers (Supplementary table 1). The *PPCK1* transcript levels in the *ppck1-4* knockout were successfully reverted to either slightly higher or wild type levels in the complementation lines on sufficient or insufficient Pi, respectively (Figure 25).

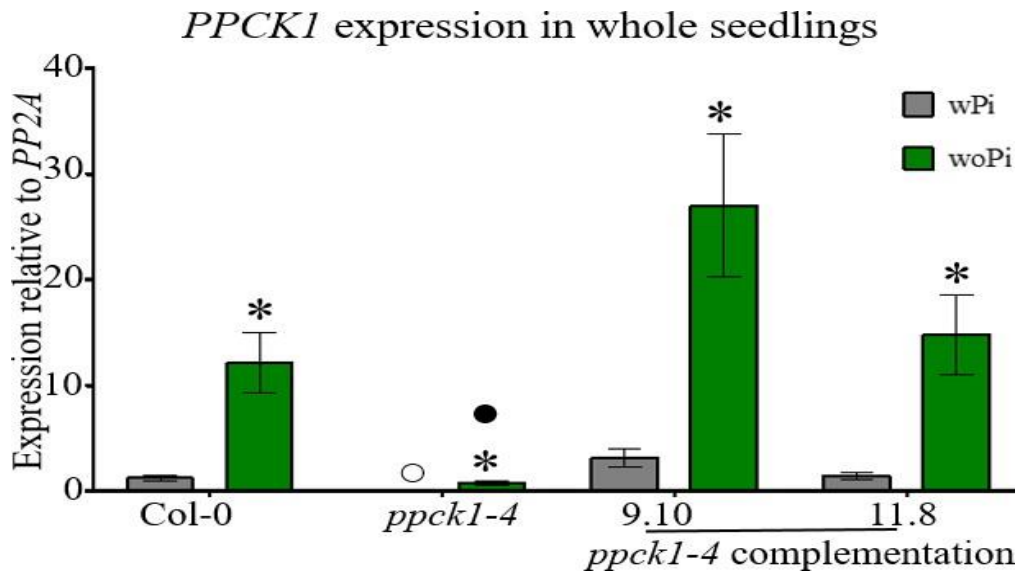


Figure 25: *PPCK1* transcript levels in *ppck1-4* mutant and *ppck1-4* complementation lines.

Seedlings were grown for six days on sufficient Pi before transfer to sufficient and insufficient Pi for addition five days before analysis. Error bars denote \pm SE (n=3). Significance analyses were performed by Student's t-test (two tailed, equal variances): * $p \leq 0.05$, ○ $p \leq 0.05$, ● $p \leq 0.05$ compared to wPi, Col-0 wPi and Col-0 woPi, respectively.

2.10 Generation of *ppck2* knockout lines by CRISPR/Cas 9 technology

Since the available *ppck2* T-DNA insertion lines had considerable transcript levels of *PPCK2*, we generated a *ppck2* CRISPR/Cas9 knockout mutant (Figure 26) using a two guide RNA (gRNA) approach (Ordon et al., 2017). The two gRNAs specific for the *PPCK2* gene were selected, based on their high editing efficiency (>70%), zero off target sites and zero chances of self-complementarity using CHOPCHOP (<https://chopchop.cbu.uib.no>), a freely available online tool. The two identified gRNAs were modified to contain BpII cloning sites, which would allow cloning into the shuttle vector containing all elements required for silencing. The complete cassette was then cloned into the destination vector containing a BASTA herbicide resistance gene through a cut-ligation reaction. The destination vector was transformed into *Agrobacterium* before transformation into wild type *Arabidopsis* plants by floral dipping.

Generation of *ppck2* mutant using CRISPR Cas 9 technology

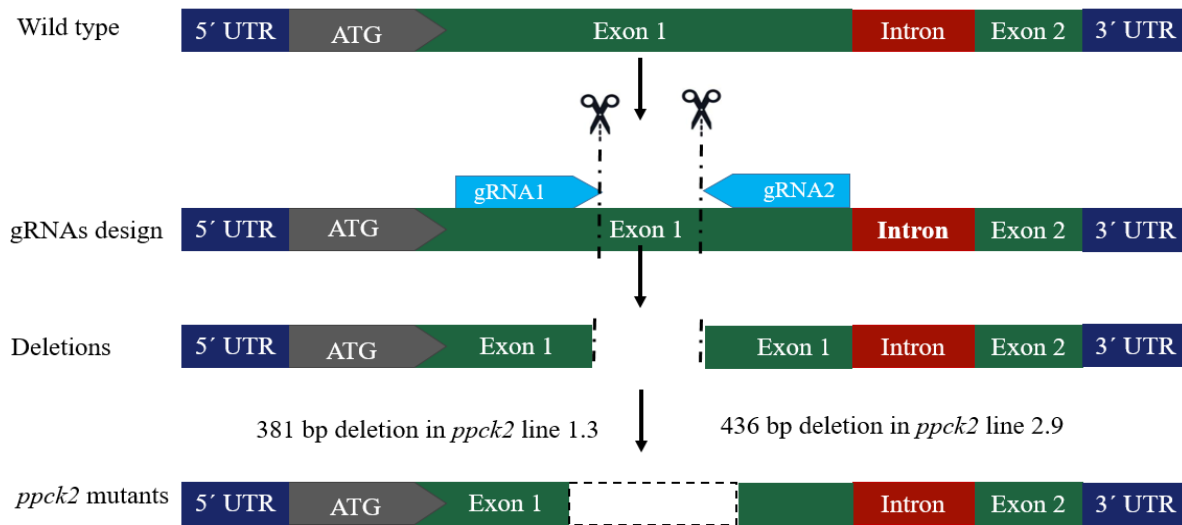


Figure 26: Generation of *ppck2* mutants using CRISPR/Cas 9 technology

The gRNAs targeting *PPCK2* exon 1 were identified from an online website: <https://chopchop.cbu.uib.no/> and led to deletion of either 381 base pairs or 436 base pairs for *ppck2* CRISPR/Cas 9 independent lines 1.3 and 2.9.

2.10.1 Identification and genotyping of *ppck2* CRISPR/Cas 9 mutant lines

Successful transformants were identified by spraying with BASTA and survivors were further genotyped using gene specific primers (Supplementary table 1) designed just slightly away from the deletion zone and generating approximately 650bp PCR product. While the wild type sample showed a band of about 650 bp, some of the transgenic plants showed a band of about 250 bp indicating possible deletion (Figure 27A). This was further confirmed by sequencing (Supplementary figure 5).

The successful transformants were then advanced to T2 and T3 generation until homozygous plants were obtained (Figure 27B). *PPCK2* transcripts in the *ppck2* were determined by RT qPCR using primers designed inside the deletion zone (Supplementary table 9). The RT-qPCR result revealed, heavily downregulated/absent *PPCK2* transcripts in the *ppck2* mutant lines compared to wild type levels (Figure 27C). The mutant lines were then used to study effects of *ppck2* knockout on tissue malate, citrate content, and exudates in relation to Pi starvation.

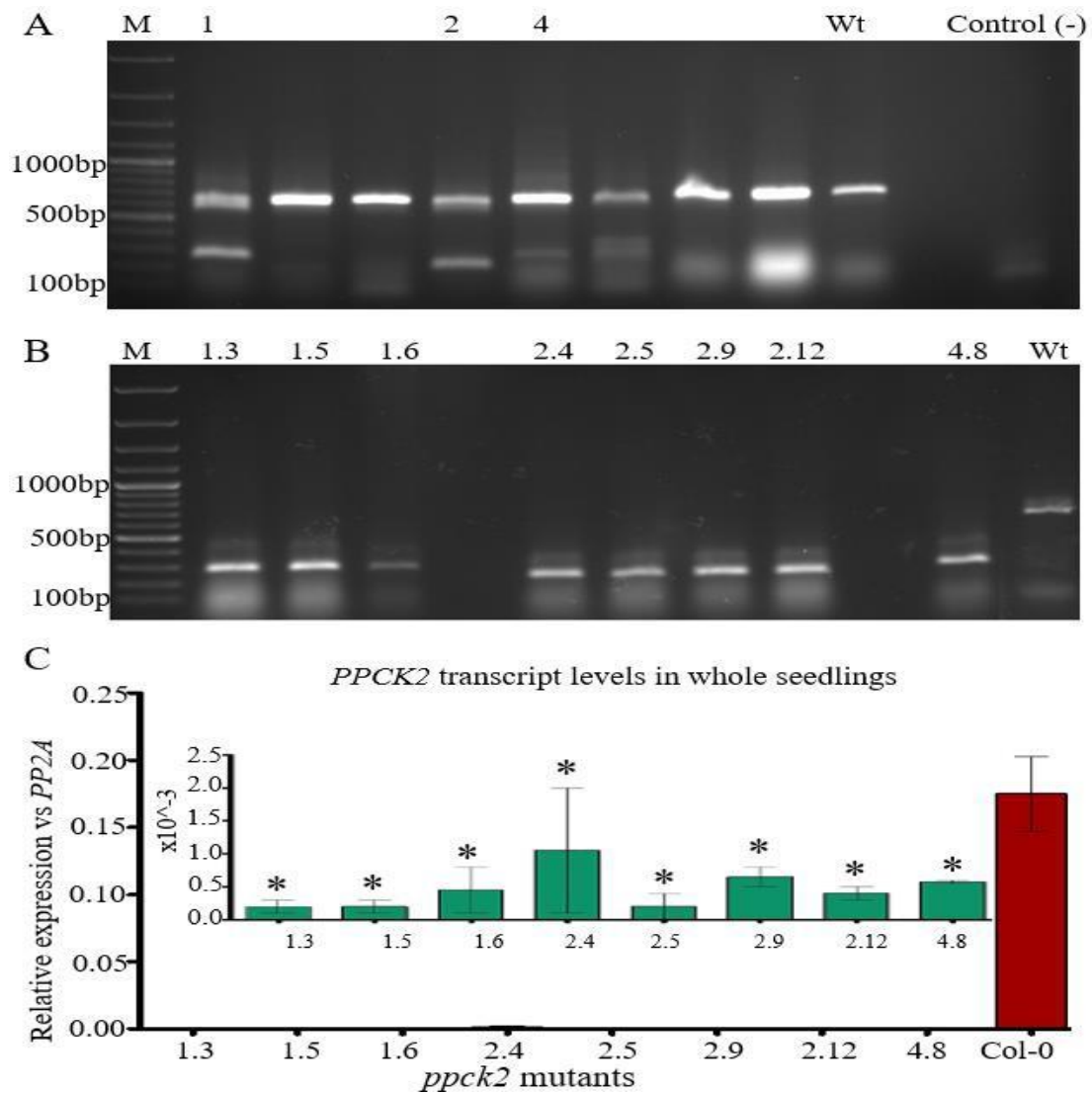


Figure 27: Selection of *ppck2* mutant lines generated using CRISPR/Cas 9 technology.

A-Genotyping of *ppck2* knockout lines in the T1 generation after BASTA selection, **B**-Genotyping of *ppck2* CRISPR/Cas9 homozygous knockout lines in the T3 generation and **C**-*PPCK2* transcript analysis in the homozygous *ppck2* knockout lines. Seedlings were grown on sufficient Pi before harvest and analysis. Error bars denote \pm SE (n=3). Significance analyses were performed by Student's t-test (two-tailed, equal variances): *p \leq 0.05 compared to Col-0.

2.10.2 Generation of a *ppck1ppck2* double knockout mutant

Since we were also interested in studying the effects of losing both *PPCK* genes, we crossed the *ppck1-4* T-DNA insertion line with either the *ppck2* CRISPR/Cas9 line 1.3 or 2.9 and generated double knockout lines *ppck1ppck2* 7.11 and *ppck1ppck2* 9.3. Since the *ppck2* knockout progeny still possessed the BASTA resistant gene, the crosses were selected by spraying them with BASTA and thereafter the survivors were then genotyped with gene-specific primers for *PPCK1* and *PPCK2* (Supplementary table 9).

Two independent lines i.e. 7.11 and 9.3 with loss of both *PPCK1* and *PPCK2* were identified after genotyping and were confirmed to be double knockouts by analyzing the transcript levels and comparing them to wild type levels (Supplementary figure 6).

2.11 Determination of malate and citrate content in tissues of *ppck* mutant lines

2.11.1 Loss of *PPCK1* and *PPCK2* reduces shoot and root malate content

Malate accumulation was strongly induced in shoots and roots after Pi starvation in wild type and all mutants and complementation lines analyzed (Figure 28). However, unlike previous results obtained (Chutia, 2019) where low malate levels were detected in shoots of *ppck1-4* mutant compared to wild type, malate levels in our study were comparable to wild type levels on sufficient Pi. Malate levels were additionally higher in the complementation lines by about 27% in line 9.10 and 14% in line 11.8 compared to wild type (Figure 28A). Similarly, *ppck2* CRISPR/Cas9 mutant lines 1.3 and 2.9 accumulated about 10% and 20 % more shoot malate than wild type respectively (Figure 28 B). In contrast, shoot malate levels were lower in *ppck1ppck2* lines with line 7.11 accumulating 9% less malate compared to wild type (Figure 28C).

On transfer to Pi starvation condition, shoot malate in *ppck1-4* mutant reduced by about 25% compared to wild type but was reverted to wild type levels in both complementation lines (Figure 28A). In *ppck2* knockout mutants shoot malate upon Pi starvation was comparable to wild type levels (Figure 28B), but was however reduced by upto 30% in both the *ppck1ppck2* knockout lines (Figure 28C). The Pi-starvation induced malate accumulation in shoots was significantly different compared to wild type (Two-way ANOVA: $p \leq 0.05$) in all the knockout mutants and only one *ppck1-4* complementation line 9.10 (Two-way ANOVA: $p \leq 0.01$).

Root malate content followed a similar trend as observed for shoots. Similar to previous observations (Chutia, 2019) of low malate level in *ppck1-4* mutant compared to wild type on sufficient Pi condition, in our study, we observed a 25% decrease in root malate levels in *ppck1-4* mutant compared to wild type. However, complementation of the *ppck1-4* mutant with a functional *PPCK1* gene restored root malate levels back to wild type levels and were even higher in complementation line 11.8 by about 35% compared to wild type (Figure 28D). Similar to shoots, root malate levels in *ppck2* mutants were higher by upto 20% compared to wild type on sufficient Pi condition (Figure 28E) but were lower in the *ppck1ppck2* double mutants by about 25% compared to wild type (Figure 28F). Upon transfer to insufficient Pi, root malate levels in the *ppck1-4* strongly reduced by about 40% but reverted to wild type levels in the complementation lines (Figure 28D). Root malate level was however indistinguishable from wild type levels for *ppck2* CRISPR/Cas9 mutants but were reduced by upto 50% in the *ppck1ppck2* double mutants upon Pi starvation (Figure 28F). Pi-starvation induced root malate accumulation was significantly different in *ppck1-4* and *ppck1ppck2* double knockout lines compared to wild type (Two-way ANOVA: $p \leq 0.01$) but was comparable to wild type for the *ppck2* knockout lines and the

ppck1-4 complementation (Two-way ANOVA: $p \geq 0.05$).

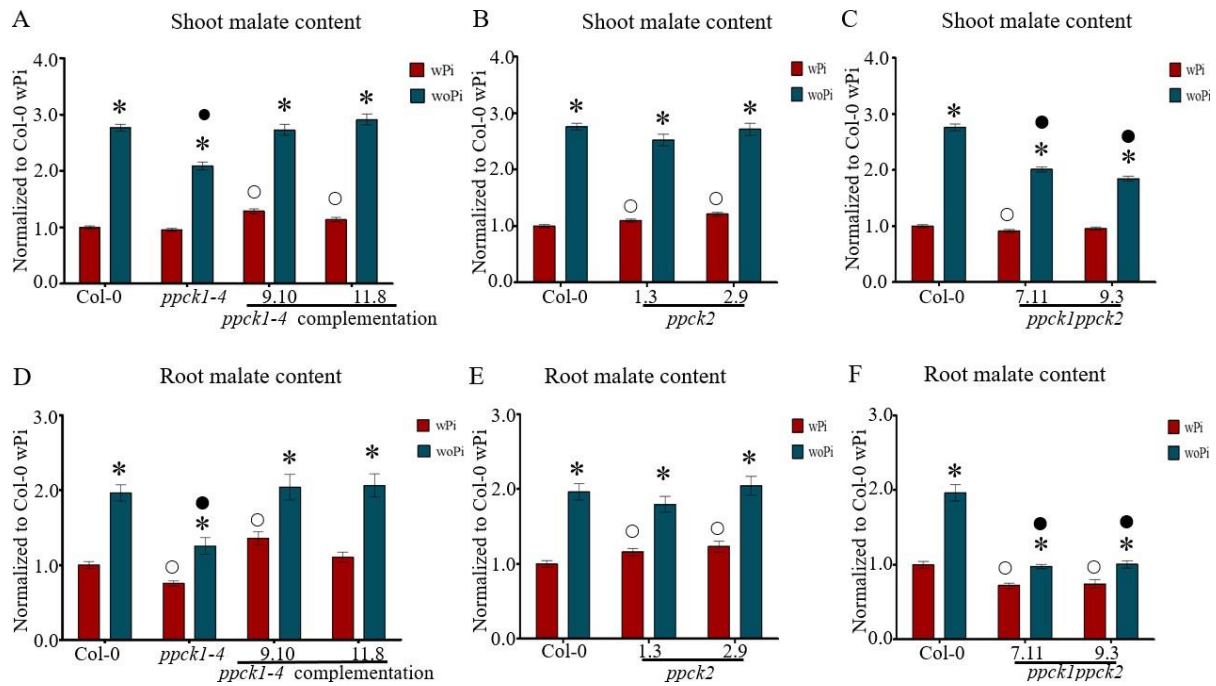


Figure 28: Tissue malate content in *ppck* mutants and *ppck1-4* complementation lines.

Normalized (to wild type wPi) shoot malate content in **A-*ppck1-4*** mutant and *ppck1-4* complementation lines and **B-*ppck2*** CRISPR/Cas9 and **C-*ppck1ppck2*** double knockout lines. Normalized root malate content in **D-*ppck1-4*** mutant and *ppck1-4* complementation lines, **E-*ppck2*** CRISPR/Cas9 and **F-*ppck1ppck2*** double knockout lines. Seedlings were grown for six days on sufficient Pi before transfer to either sufficient or deficient Pi conditions for an additional five days before harvest. Error bars denote \pm SE (n=12). Significance analyses were performed by Student's t-test (two-tailed, equal variances): * $p \leq 0.05$, o $p \leq 0.05$ and • $p \leq 0.05$ compared to wPi, Col-0 wPi and Col-0 woPi, respectively.

2.11.2 Loss of *PPCK1* increases shoot and root citrate content

Shoot citrate was higher in all mutants and one complementation lines compared to wild type. In sufficient Pi condition, shoot citrate increased by about 18% in *ppck1-4* knockout line but was reverted to wild type levels in *ppck1-4* complementation line 11.8 while line 9.10 accumulated 35% more citrate compared to wild type (Figure 29A). In *ppck2* CRISPR/Cas9 knockout lines, shoot citrate was higher by about 29-55% (Figure 29B) while *ppck1ppck2* double knockout lines 7.11 and 9.3 accumulated 10% and 44% more shoot citrate than wild type on sufficient Pi condition (Figure 29C).

Upon Pi starvation, *ppck1-4* mutant accumulated about 31% more citrate compared to wild type but similar to shoots, malate was reverted back to wild type levels in both complementation lines (Figure 29A). However, citrate levels in both *ppck2* CRISPR/Cas9 knockout lines was similar to wild type (Figure 29B). In contrast to shoot malate, shoot citrate in both *ppck1ppck2* double knockout lines

increased by about 35% and 50% in lines 7.11 and 9.3 respectively compared to wild type upon Pi starvation (Figure 29C). Two-way ANOVA analysis revealed significant difference for Pi-starvation induced citrate accumulation in shoots of *ppck1-4*, *ppck2* line 2.9 and the *ppck1ppck2* double knockout lines (Two-way ANOVA: $p \leq 0.05$) but no difference for the other transgenic lines (Two-way ANOVA: $p \geq 0.05$).

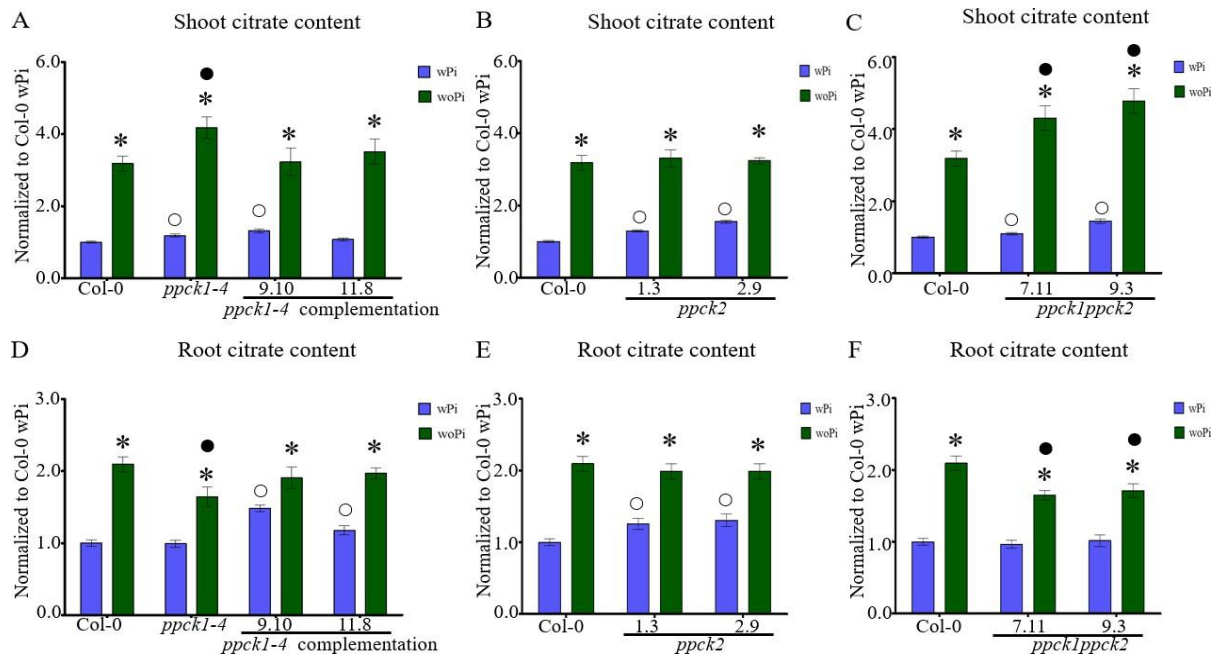


Figure 29: Tissue citrate content in *ppck* mutants and *ppck1-4* complementation lines.

Normalized (to wild type wPi) shoot citrate content in **A**-*ppck1-4* mutant and *ppck1-4* complementation lines, **B**-*ppck2* CRISPR/Cas9 and **C**-*ppck1ppck2* double knockout lines. Normalized root citrate content in **D**-*ppck1-4* mutant and *ppck1-4* complementation lines, **E**-*ppck2* CRISPR/Cas9 and **F**-*ppck1ppck2* double knockout lines. Seedlings were grown for six days on sufficient Pi before transfer to either sufficient or deficient Pi conditions for an additional five days before harvest. Error bars denote \pm SE (n=12). Significance analyses were performed by Student's t-test (two-tailed, equal variances): * $p \leq 0.05$, o $p \leq 0.05$ and • $p \leq 0.05$ compared to wPi, Col-0 wPi and Col-0 woPi, respectively.

Pi starvation induced citrate accumulation in roots of wild type, all mutants and complementation lines analyzed with some deviations compared to wild type for *ppck1-4* and the *ppck1ppck2* double knockout lines (Figure 29). Under sufficient Pi condition, root citrate was comparable to wild type levels in *ppck1-4* (Figure 29D) and both *ppck1ppck2* double knockout lines (Figure 29F). In contrast, root citrate in *ppck1-4* complementation lines 9.10 and 11.8 was higher by about 50% and 20% respectively, compared to wild type (Figure 29D) while *ppck2* CRISPR/Cas9 knockout mutants accumulated about 30% more citrate compared to wild type (Figure 29E). Upon Pi starvation, root citrate reduced by about 20% in *ppck1-4* (Figure 29D) and *ppck1ppck2* double knockout lines (Figure 29F) compared to the wild type but were similar to wild type levels in the *ppck1-4* complementation lines (Figure 29D) and *ppck2* CRISPR/Cas9 knockout lines (Figure 29E). Notably, Pi-starvation induced root citrate accumulation.

was significantly different compared to wild type for all mutants (Two-way ANOVA: $p \leq 0.05$) except in *ppck2* CRISPR/Cas9 line 2.9 (Two-way ANOVA: $p = 0.13$).

2.11.3 The *ppck1ppck2* double knockout mutant has reduced malate and citrate exudation

Malate and citrate exudation were more enhanced under Pi starvation for wild type and all transgenic lines analyzed (Figure 30). Under sufficient Pi condition, *ppck1-4* mutant exuded about 35% less malate than wild type but this was reverted to wild type levels in the *ppck1-4* complementation lines, with line 9.10 additionally exuding 40% more malate compared to wild type (Figure 30A). Similarly, both *ppck2* CRISPR/Cas9 knockout lines exuded about 30% less malate than wild type under sufficient Pi (Figure 30B) which was further reduced to about 33% and 47% in *ppck1ppck2* double knockout out lines 7.11 and 9.3 respectively (Figure 30C).

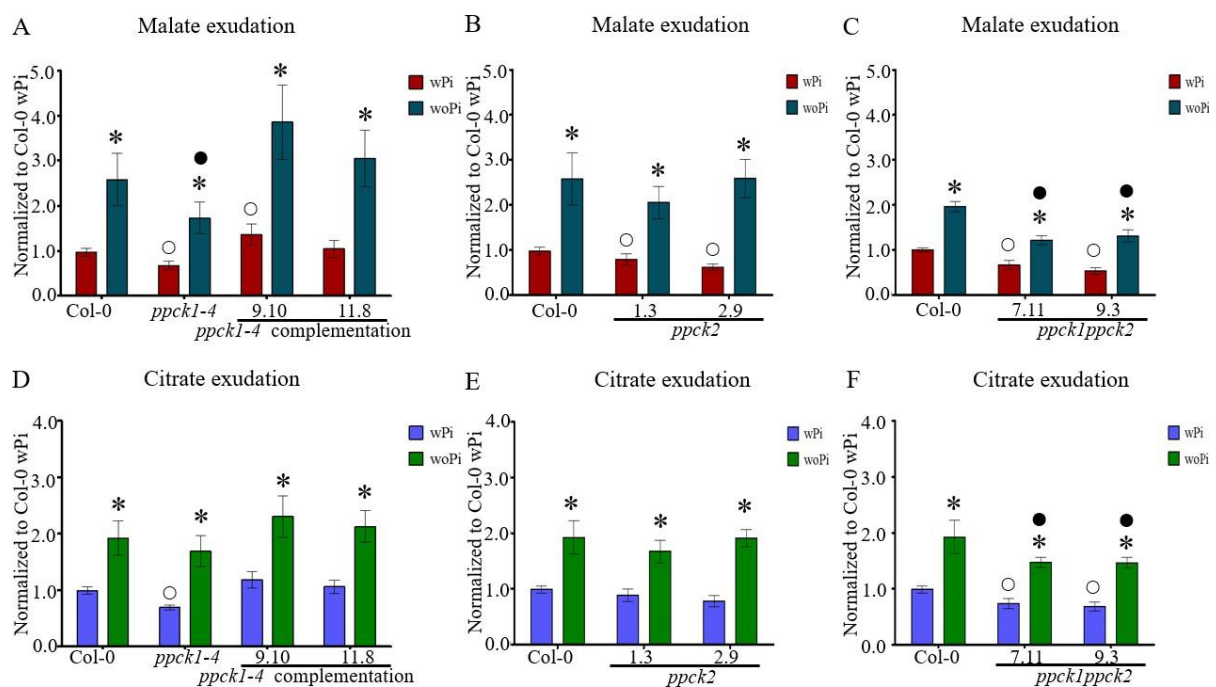


Figure 30: Root OAs exudation profiles of *ppck* mutants and *ppck1-4* complementation lines.

Normalized root malate exudation in **A**-*ppck1-4* mutant and *ppck1-4* complementation lines, **B**-*ppck2* CRISPR/Cas9 and **C**-*ppck1ppck2* double knockout lines. Normalized root citrate exudation in **D**-*ppck1-4* mutant and *ppck1-4* complementation lines, **E**-*ppck2* CRISPR/Cas9 and **F**-*ppck1ppck2* double knockout lines mutants. Seedlings were grown for six days on sufficient Pi before transfer to either sufficient or deficient Pi conditions for an additional five days before harvest. Error bars denote \pm SE (n=12). Significance analyses were performed by Student's t-test (two-tailed, equal variances): * $p \leq 0.05$, o $p \leq 0.05$ and ● $p \leq 0.05$ compared to wPi, Col-0 wPi and Col-0 woPi, respectively.

Upon Pi starvation, exuded malate in the *ppck1-4* mutant was reduced by 40% compared to wild type, which was reverted in the complementation lines 11.8 and was even higher by about 43% in complementation line 9.10 compared to wild type (Figure 30A). Malate exudation in *ppck2* CRISPR/Cas9 mutant lines was comparable to wild type but was severely reduced by about 55% in the

ppck1ppck2 double knockout lines upon Pi starvation (Figure 30B). Pi-induced malate exudation was only significantly different for double knockout lines compared to wild type (Two-way ANOVA: $p \leq 0.01$).

On sufficient Pi, citrate exudation was less by about 20% in *ppck1-4* mutant (Figure 30D) and both *ppck1ppck2* double knockout lines (Figure 30F) but was comparable to wild type for *ppck2* CRISPR/Cas9 mutant lines (Figure 30E). In contrast, exuded citrate in *ppck1-4* complementation lines was reverted to wild type levels with both lines exuding about 10% more citrate than wild type (Figure 30D). Upon Pi starvation, exuded citrate in *ppck1-4* mutant, both complementation lines (Figure 30D) and in *ppck2* CRISPR/Cas9 mutant lines (Figure 30E) was comparable to wild type. In contrast, citrate exudation in both *ppck1ppck2* double knockout lines was about 30% less compared to wild type (Figure 30F). However, Two-way ANOVA analysis for Pi-deficiency induced citrate exudation revealed no significant difference between transgenic lines and wild type (Two-way ANOVA: $p \geq 0.05$).

2.12 Other metabolites changes in the *ppck* mutants and *ppck1-4* complementation lines

2.12.1 Loss of *PPCK1* and *PPCK2* enhances accumulation of amino acids in tissues

Changes in amino acid levels for the *ppck* knockout mutants and the *ppck1-4* complementation lines grown on sufficient Pi resemble amino acid changes observed in wild type when grown on Pi insufficient media (Figure 31). Additionally, more distinct changes were observed in shoots compared to roots especially under insufficient Pi (Figure 31).

On sufficient Pi, *ppck1-4* mutant accumulated more shoot amino acids in higher levels compared to wild type except for cysteine, glutamate, glycine, taurin and *O*-acetylserine (Figure 31A). Likewise, more and consistent amino acid changes were observed for both *ppck1-4* complementation lines with the average increase being about 1.5-fold more compared to wild type (Figure 31A). More changes in amino acids levels were observed for *ppck2* CRISPR/Cas9 mutants compared to wild type although some changes were inconsistent. Similar to the *ppck1-4* complementation lines, both *ppck2* CRISPR/Cas9 mutant lines accumulated higher levels of all amino acids at average of about 1.4-fold higher except for glycine which was comparable to levels in wild type (Figure 31A). Similarly, both *ppck1ppck2* double knockout lines accumulated all amino acids in higher levels at an average of about 1.6-fold higher than wild type except for taurin and *O*-acetylserine levels which were comparable to wild type levels (Figure 31A).

Changes in amino acid were fewer for all mutants and the *ppck1-4* complementation lines on insufficient Pi as compared to when grown on sufficient Pi condition. In *ppck1-4* mutant changes in amino acid levels were comparable to wild type except for alanine, histidine, leucine, serine and *O*-acetylserine which were higher (Figure 31A). In contrast, more and more consistent changes in amino acid levels were observed in *ppck1-4* complementation lines. All amino acids levels in the complementation lines were higher except for cysteine, aspartate, glycine, histidine, methionine, serine, taurin and *O*-

acetylserine (Figure 31A).

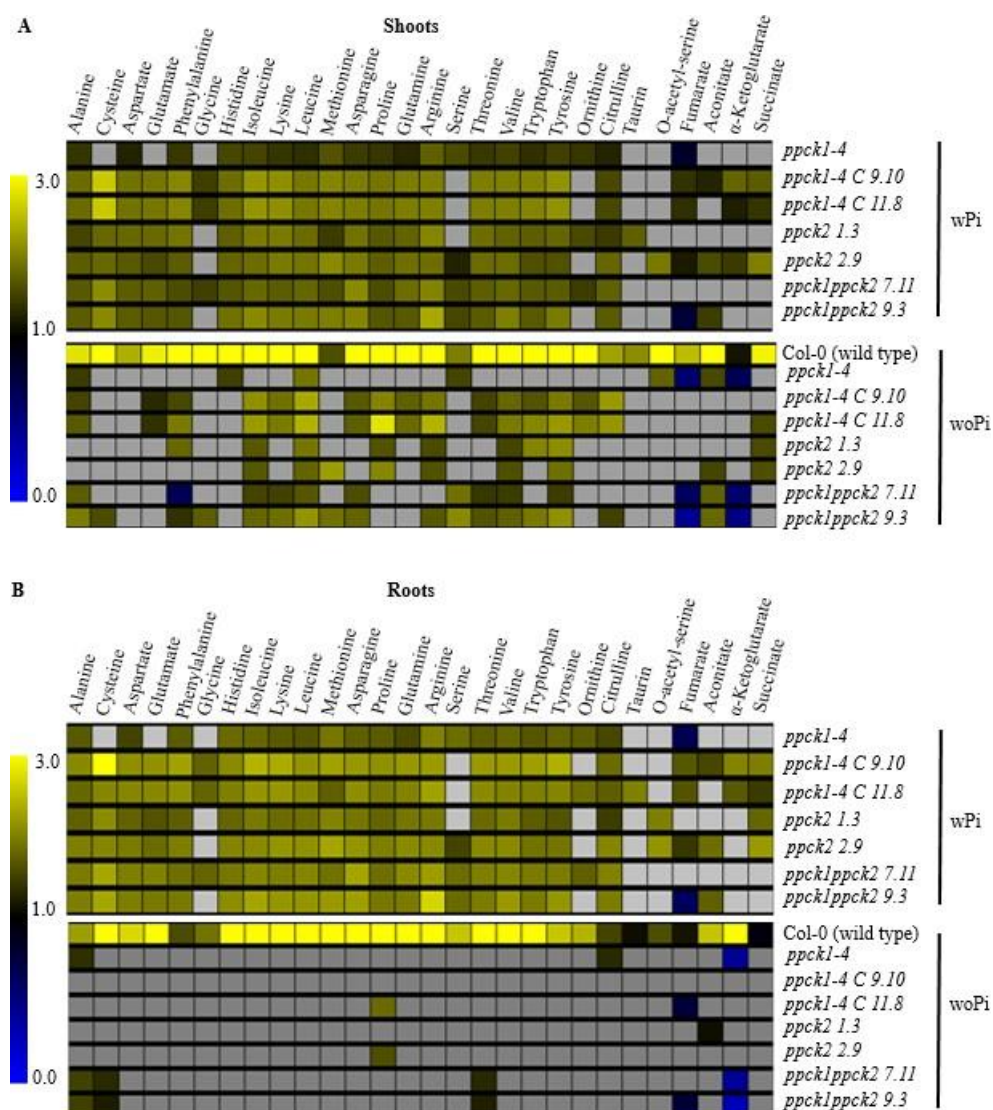


Figure 31: Heatmap showing metabolite changes in *ppck* knockouts and *ppck1-4* complementation lines.

Normalized (to wild type wPi) **A**-Shoot amino acid levels and **B**-Root amino acid levels. Seedlings were grown for six days on sufficient Pi before transfer to either sufficient or deficient Pi conditions for an additional five days before harvest. Grey boxes indicate non-significant, blue (significant but lower levels) and yellow (significantly and high levels) to wild type (Col-0) wPi ($p < 0.05$, student t-test, two tailed $n = 12$).

Upon Pi starvation, amino acid levels in both *ppck2* CRISPR/Cas 9 mutants lines were comparable to wild type levels, except for iso-leucine, leucine, proline, arginine, valine and tyrosine with phenylalanine and tryptophan being higher in *ppck2* CRISPR/Cas9 mutant line 1.3 while methionine was higher in *ppck2* CRISPR/Cas9 mutant line 2.9 (Figure 31A). More amino acid changes were observed also in *ppck1ppck2* double knockout lines although some were inconsistent. All amino acids

on Pi deficient condition were higher in the double knockout lines except for aspartate, glutamate, histidine, proline, glutamine, ornithine, taurin and *O*-acetylserine which were comparable to wild type levels and phenylalanine levels which were lower (Figure 31A). Additionally, *ppck1ppck2* double knockout line 9.3 accumulated higher levels of cysteine, glycine, methionine, arginine, tryptophan and citrulline while in line 7.11, these amino acids were comparable to wild type (Figure 31A)

Just like in shoots, changes in root amino acids under sufficient Pi closely resembled changes observed in wild type upon Pi starvation (Figure 31B). Unlike in shoots, changes were also more consistent in roots especially under sufficient Pi conditions (Figure 31B). The *ppck1-4* mutant accumulated slightly higher levels of all amino acids apart from aspartate, glutamate and proline compared to wild type while in the complementation lines, almost all amino acids were more abundant except for glycine and glutamate (Figure 31B). In *ppck2* CRISPR/Cas 9 mutant lines, all amino acid exhibited higher abundance compared to wild type. On average amino acid content was increased by about 1.7-fold with the highest change observed for aspartate (Figure 31B). However, the amino acid profile content of the double knockout lines resembled more that of *ppck1-4* mutant line (Figure 31B).

A lower number of changes were observed for root amino acid levels upon transfer to Pi starvation conditions. Alanine and citrulline in *ppck1-4* mutant line were more abundant compared to wild type while in *ppck1ppck2* double knockout lines, alanine, cysteine and threonine were higher with the rest comparable to wild type levels (Figure 31B). Notably, proline levels in all the transgenic lines were comparable to wild type levels except in *ppck1-4* complementation line 11.8 and in *ppck2* CRISPR/Cas 9 mutant line 2.9 which accumulated more proline in roots (Figure 31B).

2.12.2 TCA intermediates in *ppck* knockouts and *ppck1-4* complementation lines

On sufficient Pi condition, shoot fumarate levels were about 10% lower in *ppck1-4* mutant line while aconitate, α -ketoglutarate and succinate were comparable to wild type levels. Upon Pi, starvation, fumarate and α -ketoglutarate abundances in *ppck1-4* mutant were 30% and 22% lower while succinate levels remained comparable to wild type. In contrast, aconitate levels upon Pi starvation were 35% higher in the mutant compared to wild type (Figure 31A). The *ppck1-4* complementation lines accumulated higher fumarate, aconitate, α -ketoglutarate and succinate compared to wild type on sufficient Pi but upon Pi starvation, these organic acids abundance was reverted to wild type levels except for succinate in line 11.8 (Figure 31A). Changes of these four TCA intermediates in shoots were inconsistent in *ppck2* CRISPR/Cas 9 mutant lines whereby only line 2.9 accumulated higher levels while the abundance of these organic acids in *ppck2* CRISPR/Cas 9 mutant line 1.3 was comparable to wild type levels (Figure 31A). Upon Pi starvation, the abundance of fumarate, aconitate and α -ketoglutarate remained comparable to wild type while that of succinate was about 35% higher in both *ppck2* CRISPR/Cas 9 mutant lines (Figure 31A). Changes for these four organic acids on sufficient Pi condition were inconsistent among the two *ppck1ppck2* double knockout lines and if present were only

in line 9.3. In *ppck1ppck2* double knockout line 9.3 fumarate and aconitate levels were 45% lower and higher compared to wild type, respectively (Figure 31A). In contrast, upon Pi starvation, more changes were observed in the *ppck1ppck2* double knockout lines whereby fumarate and α -ketoglutarate were 25-45% and 30-40% lower compared to wild type, respectively (Figure 31A). In contrast shoot aconitate levels were about 50% higher while succinate levels were comparable to wild type levels (Figure 31A).

In roots more and consistent changes were observed for these four TCA intermediates on sufficient Pi compared to Pi starvation condition. In *ppck1-4* mutant α -ketoglutarate and succinate levels were 15% lower while fumarate and aconitate abundance were comparable to wild type. Upon transfer to Pi starvation condition, α -ketoglutarate levels were strongly reduced by about 60% while fumarate, succinate and aconitate abundance remained comparable to wild type levels (Figure 31B). On sufficient Pi changes in the *ppck1-4* complementation lines were few more and when present were only in line 9.10 and higher for α -ketoglutarate and succinate. In *ppck2* CRISPR/Cas 9 mutant lines growing on sufficient Pi, fumarate, α -ketoglutarate and succinate abundance was higher compared to wild type while aconitate levels were comparable to wild type. In contrast, upon Pi starvation, these four TCA intermediates were reverted to wild type levels except for aconitate in *ppck2* CRISPR/Cas 9 mutant line 1.3 which was about 13% higher than wild type levels (Figure 31B). on sufficient Pi condition in the *ppck1ppck2* double knockout lines, these four organic acids were consistently lower compared to wild type and upon transfer to Pi deficient condition, only α -ketoglutarate was consistently lower in both double knockout lines (Figure 31B).

2.13 Phenotypic characteristics of *ppck* mutant lines

In a recent study by (Feria et al., 2022) focusing on importance of *PPCKs* in Arabidopsis seed filling and quality, *ppck1* mutants had reduced seed yield and seed dry weight while *ppck2* CRISPR/Cas 9 mutants were not severely affected. In their study, parameters such as root length, shoot and root weight were not investigated neither was the effect of *PPCK* loss of function in responses to various abiotic stresses. To address this gap, we analyzed the effect of loss of *PPCK* isoforms on seedling tissue weight and root length especially during sufficient Pi and Pi starvation.

2.13.1 Loss of *PPCK1* reduces root and shoot weight

Shoot fresh weight was lower in the *ppck1-4* mutant by about 8% compared to wild type but was reverted to wild type weight in both the complementation line (Figure 32A). In contrast to *ppck1-4*, shoot fresh weight in both *ppck2* CRISPR/Cas 9 mutants was elevated by about 9% on sufficient Pi (Figure 32B), whereas it was comparable to wild type in the *ppck1ppck2* double knockout lines (Figure 32C). Upon Pi starvation, shoot fresh weight was comparable to wild type in the *ppck1-4* mutant, the complementation lines (Figure 32A) and in the *ppck1ppck2* double knockout lines (Figure 32C). However, similar to sufficient Pi condition, *ppck2* CRISPR/Cas 9 mutants had higher shoot fresh weight

compared to wild type by about 12% and 14 % in lines 1.3 and 2.9 respectively (Figure 32B). Notably, Pi-deficiency shoot changes in shoot weight were significantly different in all mutants and complementation lines compared to wild type as revealed by two-way ANOVA ($p \leq 0.05$).

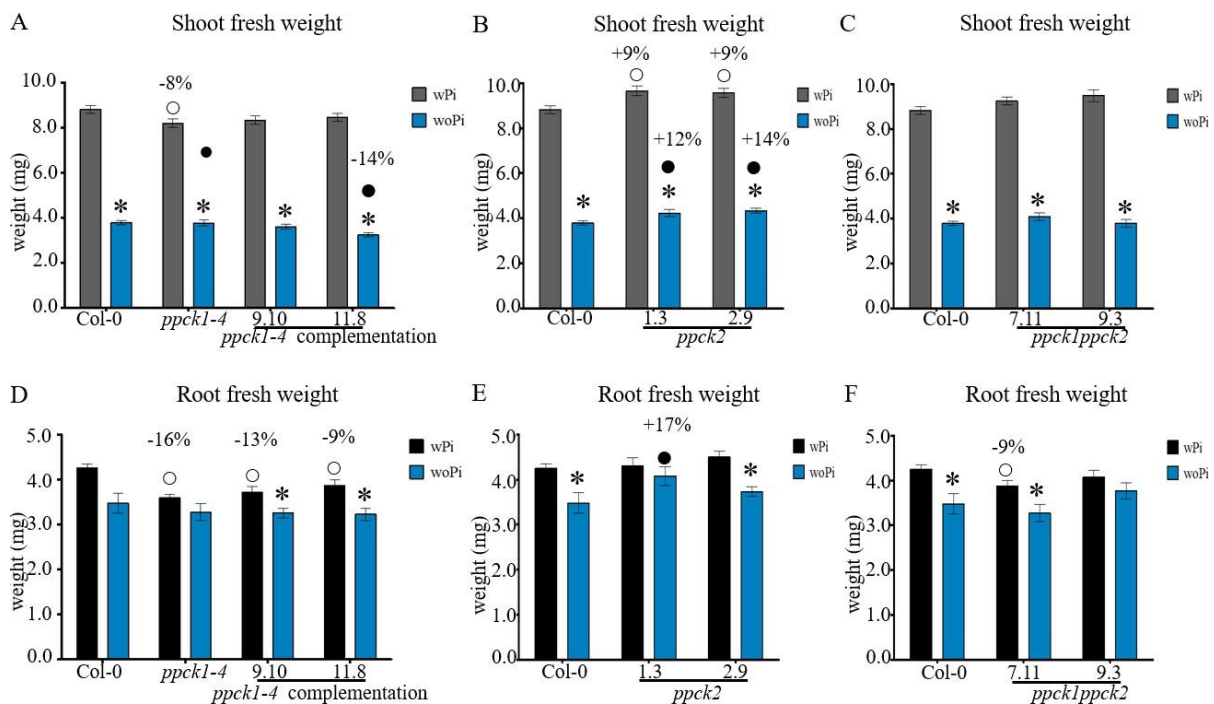


Figure 32: Seedling tissue fresh weights in wild type, *ppck* mutants and *ppck1-4* complementation lines.

Shoot weight for **A-*ppck1-4*** mutant and *ppck1-4* complementation lines and **B-*ppck2*** CRISPR/Cas 9 and **C-*ppck1ppck2*** double knockout lines mutants. Root fresh weight for **D-*ppck1-4*** mutant and *ppck1-4* complementation lines, **E-*ppck2*** CRISPR/Cas 9 and **F-*ppck1ppck2*** double knockout lines mutants. Seedlings were grown for six days on sufficient Pi before transfer to either sufficient or deficient Pi conditions for an additional five days before harvest. Error bars denote \pm SE (n=12). Significance analyses were performed by Student's t-test (two-tailed, equal variances): * $p \leq 0.05$, $\circ p \leq 0.05$ and $\bullet p \leq 0.05$ compared to wPi, Col-0 wPi and Col-0 woPi, respectively.

As was observed for shoots fresh weight on sufficient Pi, root fresh weight for *ppck1-4* mutant was reduced by up to 16% compared to wild type. However, unlike in shoots, reduced root fresh weight could not be restored in both complementation lines, which had about 13% and 9% lower root fresh weight in lines 9.10 and 11.8 respectively compared to wild type on sufficient Pi condition (Figure 32D). Root fresh weight in *ppck2* CRISPR/Cas 9 mutant lines (Figure 32E) and *ppck1ppck2* double knockout mutants (Figure 32F) was comparable to wild type except for *ppck1ppck2* double knockout line 7.11 which had a 7% reduction on sufficient Pi.

In contrast to sufficient Pi condition, root fresh weight for *ppck1-4* mutant and for the complementation lines was comparable to wild type upon Pi starvation (Figure 32D). Furthermore, root fresh weight in *ppck2* CRISPR/Cas 9 line 2.9 was similar to wild type but *ppck2* CRISPR/Cas 9 knockout line 1.3

which had 17% more root weight compared to wild type on insufficient Pi condition (Figure 32E). However, unlike shoot fresh weight response to Pi starvation, root fresh weight response was indistinguishable from wild type for all the mutants and complementation lines except for *ppck1-4* complementation line 11.8 and *ppck2* CRISPR/Cas 9 mutant line 2.9 (Two-way ANOVA: $p \leq 0.05$).

2.13.2 The *ppck1* mutant has higher gain of root length upon Pi starvation

On sufficient Pi, gain of root length for *ppck1-4* mutant was comparable to wild type but was longer by about 17% compared to wild type on Pi deficient media while in both *ppck1-4* complementation lines, gain of root length was comparable to wild type (Figure 33A). In contrast, on sufficient Pi condition, both *ppck2* CRISPR/Cas 9 mutant lines had about 8% longer gain of root length compared to wild type but upon Pi starvation only line 1.3 had about 17% longer gain of root length while gain of root length for line 2.9 was comparable to wild type (Figure 33B). Gain of root length for the *ppck1ppck2* double knockouts on sufficient and Pi deficient conditions were both comparable to wild type levels (Figure 33C). Notably, two-way ANOVA analysis revealed a similar gain of root length response to Pi starvation between the knockout lines, *ppck1-4* complementation lines and wild type (Two-way ANOVA: $p \geq 0.05$).

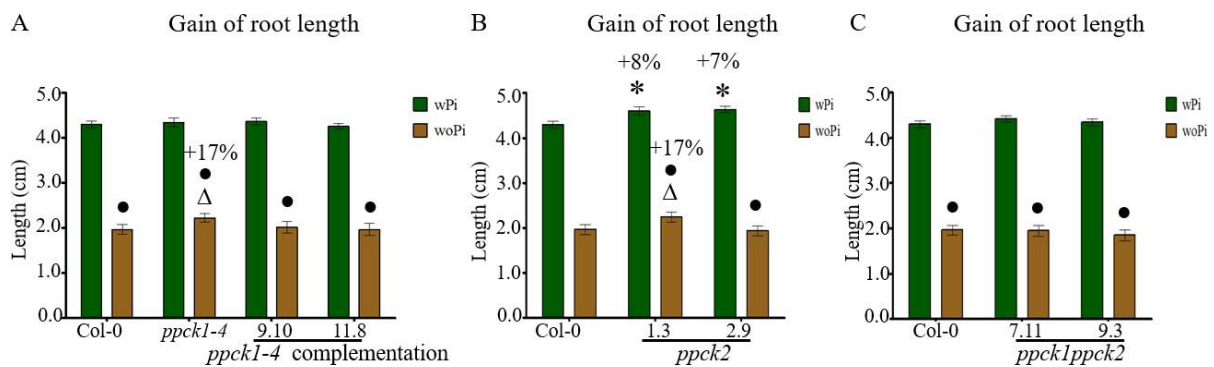


Figure 33: Gain of root length in wild type, *ppck* mutants and *ppck1-4* complementation lines.

Gain of root length in **A**-*ppck1-4* and *ppck1-4* complementation lines, **B**-*ppck2* CRISPR/Cas 9 and **C**-*ppck1ppck2* double knockout lines. Seedlings were grown for six days on sufficient Pi before transfer to either sufficient or deficient Pi conditions for an additional five days before harvest. Error bars denote \pm SE (n=36). Significance analyses were performed by Student's t-test (two-tailed, equal variances): * $p \leq 0.05$, Δ $p \leq 0.05$ and \bullet $p \leq 0.05$ compared to wPi, Col-0 wPi and Col-0 woPi, respectively.

3.0 DISCUSSION

3.1 The different Arabidopsis PPC isoforms have different functions

Most plant genomes contain several *PPCs* genes which are categorized as either photosynthetic in C4 and CAM plants or non-photosynthetic in C3 plants (Sánchez et al., 2006; Wang et al., 2016; Zhao Y et al., 2019). Additionally, most C3 *PPCs* enzymes are cytosolic except for a chloroplastic *PPC* isoenzyme described in rice (Masumoto et al., 2010). *PPC* genes are differentially expressed with the transcript levels being affected by the developmental stage (Caburatan & Park, 2021). The differential shoot and root expression of plant-type *PPC* genes in various species strongly points to the possibility of tissue-specific functions for each isoenzyme. The induction of different *PPC* genes is also influenced by varying biotic and abiotic stresses, further suggesting that the different *PPC* enzymes may have specific roles which assist the plants to withstand otherwise unfavorable growth conditions.

3.1.1 Differential induction of *PPC* genes during Pi starvation points to different roles

PPC genes are differentially induced in different tissues and in response to various stresses (Feria et al., 2016; Sánchez et al., 2006; Shi et al., 2015). Shi et al., (2015) working with *ppc1* and *ppc2* knockout mutants earlier demonstrated the crucial role of *PPCs* in carbon and nitrogen metabolism. The heterozygous *ppc1ppc2* double knockout showed severe growth phenotype and disturbed ammonium assimilation. This further demonstrated an important role of *PPCs* in leaves. Additionally, Feria et al., (2016) reported strong induction of *PPC3* transcript levels which was accompanied by primary root growth inhibition in salt stressed Arabidopsis wild type plant. However, these responses were alleviated in the *ppc3* knockout mutants indicating the specific role of *PPC3* during salt stress.

In our study, basal transcript analysis revealed *PPC2* as the major plant type *PPC* gene in shoots followed by *PPC1* while *PPC3* was the least abundant. Pi starvation induced expression of all the plant-type *PPCs* although at differing magnitudes (Figure 5). *PPC1* and *PPC2* transcripts were strongly induced almost to the same magnitude while *PPC3* was the least induced. These results are in agreement with already published results (Chutia, 2019; Feria et al., 2022; Shi et al., 2015). In roots, *PPC1* was the most predominant followed by *PPC3* while *PPC2* was the least abundant at basal level. Upon Pi starvation, *PPC1* was strongly induced while *PPC2* and *PPC3* were induced by almost the same magnitude further confirming what had earlier been observed by Chutia, (2019). However, the data slightly differs from results by Feria et al., (2016) in which *PPC3* was more strongly induced *PPC* isoform in roots. From their Pi starvation experimental set up, plants were grown for seven days on sufficient Pi before transfer to Pi starvation conditions for an additional four weeks before harvest and subsequent analysis while in our study and in Chutia, (2019) plants were grown for a total six days on sufficient Pi and additional five days on insufficient Pi. Based on the transcript induction of *PPCs*, we suggest that the role of *PPC2* may be more specific in shoots while *PPC3* functions in roots. The strong

presence and induction of *PPC1* in both shoots and roots may suggest a supportive role in these tissues. Our results and those already published (Chutia, 2019; Feria et al., 2022; Shi et al., 2015), strongly suggest that plant-type *PPCs* may have different roles which maybe stress specific. However, tissue specific expression of *PPCs* might not be enough to infer their roles or specificity and further information on their cell expression domains will be necessary. The information on cell-specific expression domains would further provide insights into the possible functions of plant type *PPCs*.

3.1.2 Cell-specific expression domains of *PPC* genes support different role for *PPCs*

In a further attempt to explore the possible different roles of *PPCs* genes, we mapped the expression domains of *PPCs* during sufficient and insufficient Pi conditions. The GFP fluorescent signals in the three *PPC* reporter lines revealed that in shoots *PPC2* promoter was more active, followed by *PPC1* while *PPC3* was the least active (Figure 8). These novel *PPC* shoot expression domains and intensities strongly corroborates the transcript data presented in this study, as well as already published transcript data (Feria et al., 2016; Sánchez et al., 2006; Shi et al., 2015). The strong promoter activity observed in shoots especially for *PPC2* reporter lines strongly suggest that it may be the plant type *PPC* isoform mainly involved in generation of malate and citrate in shoots whose fate may be translocation to roots, where it is exuded into the rhizosphere. This corroborates the exudation profiles of *PPC* overexpression lines whereby only *PPC2* overexpression lines exuded more malate and citrate than wild type. Furthermore, *PPC2* may be responsible for the anaplerotic function in shoots due to the high transcript levels and strong induction upon Pi starvation.

In roots, we detected differential GFP fluorescent signals between the three Arabidopsis *PPCs*, suggesting different promoter strength. *PPC1* reporter lines had more GFP signal followed by *PPC3* reporter lines while *PPC2* reporter lines had no visible GFP signals. Upon Pi starvation, more visible and intense GFP signals were detectable for all *PPC* reporter lines compared to sufficient Pi condition (Figure 7). Our microscopic expression domain results largely correlate with our *PPCs* transcript data and already published data (Chutia, 2019; Feria et al., 2016; Sánchez et al., 2006, 2006; Shi et al., 2015), in which *PPC3* and *PPC1* transcript levels were more abundant in roots compared to *PPC2*. We attributed the almost complete absence of a fluorescent signal in *PPC2* expression reporter line to the root section studied. While we mainly focused on the root tip for our microscopic analysis of the *PPC* expression domains, most transcript analysis were carried out using whole root tissues.

The GFP signal was present in the root stele, epidermis and root cap even though the intensity of the signal was different among the three *PPCs* in both sufficient and insufficient Pi conditions. The presence of GFP fluorescent signals at the root cap for all the three expression reporter lines indicates role of *PPCs* in local Pi sensing, which takes place at the root tip and for which malate exudation is crucial. It also coincides with the root section, i.e. root cap which accounts for up to 20% of total Pi uptake in plants (Kanno et al., 2016). Once taken up in the roots, Pi is loaded into the xylem and surrounding

phloem cells and translocated to shoots and other aerial parts of the plant (López- Arredondo et al., 2014). We propose that based on the GFP signals at the root cap and epidermis of *PPC3* reporter lines and its strong induction upon Pi starvation, OAs resulting from the activity of *PPC2* and *PPC3* may be involved in solubilizing bound Pi in the rhizosphere, at the apoplast and root cap. However, before reaching the xylem and its surrounding cells, Pi must pass through other cell layers where it may encounter positively charged ions such as Fe^{2+} , which may bind to it preventing its reach to the xylem vessels. To avoid this scenario and based on the diffused GFP signal (Figure 7), OAs originating from *PPC1* activity might be involved in binding iron in these cells allowing passage of Pi up to the xylem tissues. The GFP signals observed in the root stele additionally indicate that all the plant type PPCs contribute to a collective role in allowing loading and transport of Pi to the aerial part of the plant. It is proposed that iron translocation from roots to shoots happens in the vascular tissues, and iron additionally antagonizes Pi availability. Therefore, it is highly likely that OAs more so citrate resulting from all plant-type PPCs may be involved in binding iron and in the process allowing loading and transport of Pi to the aerial parts of the plant. From our results, we were able to map the expression domains of plant-type PPCs to the root stele, epidermis and root cap cells. These cells coincide with the regions involved in Pi uptake and iron translocation which suggests a possible additional role of organic acids generated by *PPCs* in iron translocation. While we focused on the root tip for our microscopic expression studies, our results correlate to the already published results for the plant PPCs and provides us with more visible evidence why we see a strong induction in roots for *PPC1* and *PPC3* but a weaker induction of *PPC2* upon Pi starvation.

3.1.3 *PPC* overexpression lines have different malate and citrate exudation profiles

Stronger consequences on metabolism as indicated by more amino acid changes were observed in shoots and roots of *PPC2* overexpression lines on sufficient Pi compared to overexpression lines of the other two *PPC* isoforms. *PPC2* transcript levels in shoots are high at basal levels compared to *PPC1* and *PPC3* levels (Chutia, 2019; Feria et al., 2022; Shi et al., 2015), which implies its dominant role in shoots. Upon overexpression under the strong constitutive 35S promoter, additional accumulation of *PPC2* transcripts could then lead to more amino acid changes, which we observed in shoots of lines overexpressing *PPC2*. It is also possible that in shoots, *PPC2* is part of special metabolons, which channels products to different pathways. Therefore, in *PPC2* overexpression lines more of these metabolons are formed which results in higher metabolite changes. These metabolons could additionally be specific for channeling shoot malate and citrate to roots for exudation. However, *PPC1* and *PPC3* may be part of other metabolons whose proteins are limited hence the reason we do not see many changes in shoots. Additionally, the metabolons for *PPC1* and *PPC3* may be specific for other processes and not exudation.

In roots, all *PPC* overexpression lines showed higher malate and citrate levels compared to wild type (Figure 15). It could then be expected that all three overexpression lines also exuded more of these two OAs than wild type. This was not the case and only *PPC2* overexpression lines exuded more malate and citrate. Microscopic images, which corroborated the transcript data, show that *PPC2* levels in roots are extremely low. However, *PPC2* overexpression under the constitutive 35S promoter leads to distribution throughout the plant and especially in roots. This would ultimately lead to increased *PPC2* activity in roots resulting to the observed increased accumulation and exudation of malate and citrate. Since *PPC2* expression in roots is weaker, it is likely that accumulation of products arising from its overexpression necessitate their exudation. *PPC3* is more root specific, and its overexpression should expectedly result in high exudation of malate and citrate. This was not the case, and we suggest that possibly, it performs the anaplerotic function in roots or its product was converted into other metabolites which escaped our analysis. These results strongly hint that overexpression of genes in tissues where they are normally weakly expressed might lead to desired outcomes as was the case with increased malate and citrate exudation due to *PPC2* overexpression.

3.1.4 Overexpression of C3 *PPCs* results in specific phenotypes

PPC1 and *PPC3* overexpression lines had longer root compared to *PPC2* overexpression lines under both sufficient and insufficient Pi conditions (Figure 20). Pi starvation inhibits primary root growth in an iron dependent manner. This inhibition is subject to the available external Pi levels (Thibaud et al., 2010). Furthermore, upon Pi starvation, malate exudation into the apoplast leads to Fe³⁺-malate/citrate complexes which by action of LPR1 multi copper ferroxidase activity leads to cell wall stiffening and root shortening (Balzergue et al., 2017). We hypothesized that overexpression lines exuding more malate or citrate should have shorter roots compared to wild type. Indeed, while all *PPC* overexpression lines accumulated more malate and citrate in roots, only *PPC2* overexpression lines exuded more compared to wild type. This shortening of primary root would enable them to scavenge for the bound Pi which is abundant at the upper root surface.

Next, we determined shoot fresh weight in the overexpression lines and wild type under sufficient and insufficient Pi conditions. Our results revealed higher shoot fresh weight in the overexpression lines compared to the wild type on sufficient Pi except for *PPC2* overexpression lines while on insufficient Pi media all overexpression lines recorded elevated fresh shoot weight. Root fresh weight was significantly higher on sufficient Pi for all overexpression lines while only *PPC1* overexpression lines recorded higher root weight during Pi starvation. We postulated that the higher shoot fresh weight was because of improved iron translocation from roots to shoots of *PPC* overexpression lines which improved the vegetative growth. This hypothesis is supported by results from (Wu et al., 2018) where they observed higher shoot weight in rice plants overexpressing a citrate transporter. However, this would need to be confirmed further with iron staining in shoots and roots to confirm whether there is more accumulation of iron in the transgenic lines compared to wild type. Comparison of fresh weights

for PPCs transgenic remains inconclusive. Shi et al., (2015) observed no differences in whole seedling weight of *ppc1* or *ppc2* single mutants but only in *ppc1ppc2* double knockout mutant while Feria et al., (2016) detected reduced rosette weight in all *ppc* mutants. However, no data on root weight was provided and all these analyses were not done in relation to Pi starvation making it even more difficult to compare the results. While in the present study, we can correlate increased tissue weight to enhanced accumulation or exudation of malate and citrate, no comparisons can be made between shoots and roots since the results for roots were inconsistent further suggesting overexpressing a single *PPC* isoform may not be enough to effect dramatic changes in tissue fresh weight.

To determine whether overexpressing *PPCs* impact plant development or performance on soil, we focused on flowering time, seed number, individual seed weight and total seed weight per plant. *PPC1* and *PPC3* overexpression lines flowered earlier than the wild type while The *PPC2* overexpression lines were the last to flower. Flowering is a vital plant process that depends on both biotic and abiotic factors (Mallik et al., 2017). Early flowering is induced in plants with limited access to nutrients (Wada and Takeno, 2010). Since the soil used for greenhouse experiments was sourced from the same place, we assumed that it contained similar nutrition parameters and alluded to the difference in flowering times to nutrition acquisition. *PPC2* overexpression lines exuded more malate and citrate compared to wild type and *PPC1* and *PPC3* overexpression lines suggesting they could have an efficient Pi uptake from the soil, which could avert the early flowering observed in the other transgenic lines.

To determine the effects of *PPC* overexpression on seed quality we focused on seed number, individual seed weight and total seed weight per plant. Seed quality is described by size, weight, nitrogen concentration among others and is dependent on the resources available for the maternal plant. These available resources impact on quantity and quality of the offspring (Obeso, 2002). We hypothesized that seeds from transgenic lines showing increased malate and citrate exudation should have high quality seeds. Seed number and total seed weight were significantly lower in *PPC2* overexpression lines but were comparable to the wild type for *PPC1* and *PPC3* overexpression lines. Since *PPC2* overexpression lines exuded more malate and citrate, we suggest this would lead to enhanced Pi solubilization and uptake ultimately resulting in improved growth, which would be reflected by high quality seeds. In Feria et al., (2022), *ppc* mutants showed reduced seed weight and seed yield by up to 33% and 38%, respectively further suggesting the important role of *PPCs* during plant development and seed quality. However, the morphological results obtained so far in this study are indispensable and further implicate a more specific role for *PPC2* in plant stress response and in growth and seed development.

3.2 Effects of overexpressing C3 PPCs in Arabidopsis

3.2.1 Effects of PPC overexpression on PPC crude activity and protein amount

Based on the complex regulation of *PPCs*, it was necessary to see whether increased transcript levels of *PPCs* in the overexpression lines resulted in higher protein levels, enzyme activity, and whether the resulting *PPCs* were still subject to phosphorylation. Already published studies have reported that high transcript levels may not directly correlate with high protein levels (Fukao, 2015; Kanobe et al., 2013; Koussounadis et al., 2015). In this study, transgenic lines overexpressing C3 *PPCs* had increased total *PPC* amounts and higher *PPC* enzyme activity in crude extracts compared to the wild type. These results corroborate results from a study using *Brassica napus* suspension cells, where increased *PPC* activity in suspension cells was due to the increased accumulation *PPC* protein upon Pi deficiency (Moraes & Plaxton, 2000).

However, although transcript changes for some of the overexpression lines in our study were sometimes higher by more than 10-fold compared to wild type levels (Figure 10), *PPC* protein levels (Figure 12) and crude enzyme activity (Figure 13) were at most 2-fold higher than in wild type. In contrast, in transgenic potato plants overexpressing (3-fold higher than wild type) a modified potato *PPC*, enzyme activity increased by up to 5-fold while (Rademacher et al., 2002). In their study, replacing serine 11 with aspartate in the transgenic lines reduced sensitivity to malate, which increased enzyme activity. This would then suggest that the posttranslational modification of the *PPC* protein might have a stronger impact on its activity than its abundance as has been reported for other proteins. Excess proteins are degraded to maintain cellular homeostasis (Guimaraes et al., 2014; Maier et al., 2009). We suggest the degradation of *PPCs* in the overexpression lines to be a possible reason we observed slight differences in *PPC* protein levels and enzyme activity despite their different transcript abundance.

In other studies, working with *ppc* mutants, reduced *PPC* enzyme activity and protein levels were observed for shoots and roots in *ppc2* and *ppc3* mutants respectively (Feria et al., 2016) while Shi et al., (2015) working on whole seedlings, reported reduced enzyme activity in *ppc2* and *ppc1* knockout mutants. However, in both these two studies, effects of reduced activity and protein levels on metabolites associated with this *PPC* enzymatic reaction were not investigated and when so did not reveal any differences compared to wild type. We postulated that, if modulation of this reaction is to be considered successful then increased enzyme activity should lead to increased metabolite changes in the overexpression lines compared to those in wild type. This was confirmed in the overexpression lines where more malate and citrate accumulated in roots compared to wild type especially upon Pi starvation. Additionally, changes in amino acid were more abundant in the overexpression lines on sufficient Pi compared to wild types in both shoots and roots. Lastly, the thorough investigation of our transgenic lines confirms specificity of observed metabolite changes to *PPC* overexpression.

3.2.2 Phosphate starvation enhances PPC phosphorylation in the transgenic lines

PPC activity depends on phosphorylation by PPCKs since unphosphorylated PPCs are subject to allosteric negative feedback inhibition by malate and aspartate (Chollet et al., 1996; Duff & Chollet, 1995). Having observed increased PPC protein levels and metabolic changes in our transgenic lines, we investigated whether this was also a result of increased phosphorylation upon Pi starvation. We hypothesized that the observed metabolite changes arose from increased PPC levels as well as from increased PPC phosphorylation, resulting in higher PPC activity because of lower feedback inhibition by malate. Indeed, results obtained confirmed increased shoot and root phosphorylation levels of PPCs in the transgenic lines upon Pi starvation (Figure 14). This agrees with a study by Willick et al., (2019) where they showed increased PPC phosphorylation in shoots and roots of transgenic plants in response to cadmium stress. However, in their study Willick et al., (2019) observed more phosphorylation of PPCs in shoots than in roots of transgenic lines. In contrast, we observed more PPC phosphorylation in roots compared to shoots suggesting that the level of PPC phosphorylation in plant tissue may be more tissue specific in enhancing plant resilience to different abiotic factors. Additionally, in their study, increased phosphorylation in shoots was not accompanied by increased PPC enzyme activity while more activity was detected in roots. Effects of increased PPC phosphorylation in reducing the negative allosteric inhibition are truly reflected through malate inhibition binding assays (Moody et al., 2020; Paulus et al., 2013; Schlieper et al., 2014). While our PPC activity assay in whole seedlings does not allow the direct correlation with increased phosphorylation, we were still able to correlate increased phosphorylation levels in our overexpression lines to the increased accumulation citrate and malate, which suggest that the observed increases in PPC phosphorylation might have increased in vivo PPC activity.

Although the percentage phosphorylation of PPCs in the overexpression lines was similar to wild type (Figure 14), the higher number of PPC proteins in the overexpression lines implies that we had more phosphorylated PPCs in our transgenic lines. This suggests that the available PPCKs in our *PPC* overexpression lines have the capacity to phosphorylate additional PPCs. However, the PPCKs may not be enough to realize the full potential of overexpressed PPCs, which should be at 100%. From previous studies, PPC phosphorylation which is solely the action of PPCKs, and phosphorylation status increased with prolonged light illumination (Hartwell. et al., 1999; Zhang et al., 1995). Since in this study we only focused on overexpressing *C3 PPCs* while maintaining *PPCKs* at basal level, we speculate that PPCKs might be the major limiting factor in influencing the PPC phosphorylation status. Therefore, regardless of how much we expressed *PPCs*, with limited PPCKs, the phosphorylation status of PPCs cannot exceed certain levels. To answer this, we generated transgenic lines overexpressing PPCKs and PPCs both under control of the constitutive CaMV 35S promoter with preliminary results showing enhanced accumulation of organic acids in shoots and roots (data not shown). However, due

to time constraints we were unable to check the phosphorylation levels or malate binding efficiency in these lines.

3.2.3 Pi starvation increases root malate levels in *PPC* overexpression lines

Modulation of PPCs previously focused on expressing either C4 or bacterial PPCs in C3 plants with the aim of improving plant performance. However, these studies reported conflicting results. For instance, transformation of potato with a C4 PPC (Rademacher et al., 2002) or bacterial PPC led to diminished plant growth and accelerated stomatal opening (Gehlen et al., 1996) while expression of maize C4 *PPC* led to improved plant performance (Kandoi et al., 2016). Additionally, while some studies reported increased malate levels correlated with increased PPC activity (Agarie et al., 2002; Begum et al., 2005; Fukayama et al., 2003), in a few instances, increased malate content was also detected in transgenic plants having low PPC activities (Begum et al., 2005). We related these adverse effects observed to regulation incompatibility between the C3 PPCs and the introduced C4 or bacterial PPC. We thus presumed that overexpressing C3 PPCs in a C3 plant would minimize the incompatibility problems. We successfully overexpressed C3 *PPCs*, which led to increased *PPC* transcripts, PPC protein levels and enzyme activity and increased phosphorylation and lastly studied their effect on malate and citrate accumulation and exudation.

However, we observed no significant differences in shoot malate levels in the overexpression lines compared to the wild type under sufficient or insufficient Pi conditions. This could imply that the high shoots *PPC* transcript levels in the overexpression lines were not accompanied by increased PPC protein levels and increased PPC activity. This was excluded since from our protein level measurements and enzyme activity assays, all overexpression lines accumulated high PPC protein levels and showed higher PPC enzyme activity than wild type. This would then suggest that probably the generated malate in shoots inhibited PPCs and negatively affected the activity of PPCs and resulted in unaltered malate levels. This would imply that phosphorylation levels in shoots of the overexpression lines were lower compared to wild type. Our results on PPC phosphorylation alleviated this malate feedback inhibition possibility, since we observed more phosphorylation in these transgenic lines compared to wild type based on number of phosphorylated PPCs. In a study by Moraes & Plaxton, (2000), upregulation of PPC activity was attributed largely to the increased accumulation of more PPCs under deficient Pi condition. Astoundingly, our data for PPC quantification showed transgenic lines had more total PPCs compared to the wild type. It would then be expected that the transgenic lines would accumulate more malate also in shoots. Since this was not the case, we thought that either: (i) it was rapidly converted to amino acids or malate esters such as sinapoyl malate or (ii) malate accumulated in shoots was quickly translocated to roots. Shoot amino acid profile revealed more changes in the overexpression lines compared to wild type on sufficient Pi while changes upon Pi starvation were largely comparable to wild type. While tissue amino acids profiles partially support the first assumption, it was still unclear what happened upon Pi starvation. We then looked at the second assumption by determining malate

levels in roots.

In sufficient Pi conditions, roots malate levels were up to 90% higher in *PPC2* overexpression lines but were largely comparable to wild type in *PPC1* and *PPC3* overexpression lines compared to the wild type. However, upon Pi starvation, root malate levels increased by up to 45%, 84% and 35% for *PPC1*, *PPC2*, and *PPC3*, respectively. These results confirmed the possible additional effects of malate translocation from shoots to roots. We correlated the increase in root malate with increased PPCs protein amount and increased activity. Additionally, our root PPC phosphorylation results revealed higher phosphorylation levels of PPCs in the overexpression lines compared to the wild type indicating that malate inhibition in roots was reduced which might have also led to increased malate accumulation.

3.2.4 *PPC* overexpression increases shoot and root citrate levels in *Arabidopsis*

Citrate is mainly synthesized in the TCA cycle through the condensation of acetyl CoA and oxaloacetate by the action of citrate synthase (Akram, 2014). In addition to the TCA cycle, the anaplerotic cytosolic PPC reaction provides carbon intermediates which can be imported into the mitochondria and utilized to generate citrate (Fan et al., 2013; O'leary et al., 2011). Oxaloacetate produced from HCO₃⁻ reaction with PEP can undergo different fates that can lead to increased citrate levels in the plants. It could:

- (i) be imported directly to the mitochondria where it is converted to citrate,
- (ii) be converted to malate by the action of cytosolic MDH and the generated malate is then imported to mitochondria where it is reconverted back to oxaloacetate by action of mitochondria MDH and further condensed with acetyl CoA to citrate
- (iii) be decarboxylated by cytosolic NADP-ME to pyruvate and further condensed with acetyl-CoA to citrate in the cytosol (Wheeler et al., 2008) or
- (iv) be converted into aspartate and later reverted by mitochondrial aspartate transamination to oxaloacetate which is then used for citrate synthesis (Dornfeld et al., 2015).

PPC1 and *PPC3* overexpression lines showed higher citrate content in shoots while intriguingly, *PPC2* overexpression lines showed significantly reduced shoot citrate levels.

Since only *PPC2* overexpression lines showed reduced citrate levels in shoots, we postulated that it might have been translocated to the roots where it might complex iron, load it to the xylem and translocate it to distal tissues (López-Millán et al., 2000; Rellán-Álvarez et al., 2010; Roschztardt et al., 2011). Since iron is required for most biological process and our media contained considerable levels of iron (25µM), if the *PPC2* overexpression lines also accumulated increased citrate levels in roots, it could then be that shoot citrate was translocated from shoots to roots. Citrate levels detected in roots of *PPC2* overexpression lines was 75% and 80% higher than wild type under sufficient and insufficient Pi, respectively. This confirmed our earlier postulation of the high possibility that citrate accumulated in *PPC2* overexpression lines was translocated from shoots.

Since Pi is negatively charged, it binds to the positively charged iron. However, during Pi starvation, more iron is free for absorption by plants through the roots where it could accumulate to toxic levels. The increased iron uptake would then provide substrate for generation of free radicals which would ultimately damage the cells (Hell & Stephan, 2003). To overcome this obstacle, plants accumulate citrate in the roots, which binds the soluble Fe²⁺ ions, which can then be transported to other distal plant tissues. To confirm this, iron staining experiments need to be carried out in the future with the *PPC* overexpression lines and if this is true, the overexpression lines should accumulate more iron than the wild type in the roots. In other studies, increased citrate accumulation and exudation was detected in mutants over accumulating iron in the root (Durrett et al., 2007). In contrast, citrate levels decreased by up to 50% in *ppc* knockout mutants exposed to high levels of cadmium (Willick et al., 2019) which implicated the role of PPCs during metal toxicity. Notably in this study, accumulation of citrate in addition to malate in roots of transgenic lines might enhance the resilience to other abiotic stresses such as iron in addition to Pi limitation.

3.2.5 *PPC2* overexpression induces malate and citrate exudation during Pi starvation

Plants exude OAs in response to various nutritional limitations. During Pi starvation, low molecular weight organic acids are released into the rhizosphere (Krishnapriya & Pandey, 2016; Wang et al., 2015; Wen et al., 2017). In our study, only *PPC2* overexpression lines exuded more malate and citrate under both sufficient and insufficient Pi conditions. This was quite astounding since all overexpression lines accumulated significantly higher levels compared to wild type of both malate and citrate especially during phosphate starvation. Considering that among all *PPCs*, *PPC2* was the least induced while *PPC1* and *PPC3* were strongly induced in roots of wild type (Chutia, 2019; Fera et al., 2016), it would then be expected that rather either *PPC1* or *PPC3* overexpression lines would exude more malate or citrate. As this was not the case, we were intrigued and thought this had a lot to do with either (i) minimizing the carbon loss for the plant (ii) translocation of citrate from the shoots or (iii) stability of PPC proteins.

While exudation is condition specific and assists in enhancing nutrient availability from the soil, it has been estimated that plants lose up to 40% of carbon in this essential process (Lynch & Whipps, 1990). Furthermore, while investigating role of PPCs in exudation during Pi starvation, (Johnson et al., 1996) estimated that the PPCK-PPC module accounted up to 25% and 34% of carbon exuded in form of citrate and malate, respectively. This massive carbon loss during exudation occurs at the cost of other metabolites and shifts carbon resources from other processes. To avert excessive carbon loss from plants, it would then be rational that exudation of metabolites generated and associated with this pathway would be carried out by proteins whose induction is not so high in roots. Of all the plant-type *PPCs*, *PPC2* would be the most suitable candidate due to its high transcript levels and strong induction in shoots and low transcript levels in roots. The other two PPCs would then fulfill their anaplerotic function in cells while *PPC2* would be majorly involved in exudation. This would ultimately reduce the rate of carbon loss while at the same time ensuring continuity of plant response to stresses.

Shoot photosynthates are partitioned and translocated to roots where they are exuded into the rhizosphere. In partially defoliated wheat plants, the proportion of new photosynthates subsequently partitioned to and exuded from the roots was substantially reduced (Dilkes et al., 2004). In shoots of *PPC* overexpression lines, malate levels were indistinguishable from wild type while citrate levels were significantly higher in *PPC1*, *PPC3* but lower in *PPC2* overexpression lines. If shoot malate and citrate were translocated to roots, it would imply that root malate and citrate content should be higher than in wild type. Indeed, root malate and citrate were higher. These transgenic lines would then expectedly exude more malate and citrate compared to wild type. However, this was only true for *PPC2* overexpression lines, which led us to hypothesize that perhaps exudations for the *PPC1* and *PPC3* overexpression lines happened at earlier or later time points. Earlier reports on root exudates in wheat showed that they peaked after three hours after incubation, and declined thereafter (Dilkes et al., 2004). Since in our experimental setup, exudation was carried out four days after transfer to Pi insufficient condition preceded by growth on Pi sufficient media for six days, we thought that possibly *PPC1* and *PPC3* overexpression lines could have also exuded more malate and citrate but either at earlier or later time points that may have escaped our experimental setup. To confirm whether true or not, time course exudation experiments should be done.

Different OAs are exuded by different plants in response to different stimuli (Aoki et al., 2012). In white lupin, citrate exudation increased with reduced shoot Pi levels (Shen et al., 2005). In maize response to low Pi, changes in root architecture are more prominent than organic acid exudation although both malate and citrate are exuded (Wen et al., 2017). In *Brassica napus*, Pi starvation reduced plant growth but did not induce organic acid exudation (Ligaba et al., 2003). However, presence of aluminum strongly induced accumulation and exudation of both malate and citrate. Interestingly, we detected increased exudation of both malate and citrate in *PPC2* overexpression lines, which points to the fact that exudation of organic acids also occurs in response to combined nutritional status in our case Pi starvation and increased iron availability in the growth media. Although the solubilizing ability of exuded organic acids by *PPC2* overexpression lines was not analyzed, exuded malate and citrate is thought to improve plant growth by solubilizing the metal phosphate complexes and releasing Pi which can then be easily taken up by plants.

Lastly, we successfully managed to overexpress C3 *PPCs* in *Arabidopsis*, which resulted in increased malate, and citrate levels in either shoots, roots or both. We also showed that these changes positively correlated to increased transcript levels, *PPC* protein level and activity and increased *PPC* phosphorylation status. Additionally, these changes did not have adverse effects on the plant morphology as shown from our phenotypic characterization. Furthermore, we showed that overexpression of one *PPC* did not affect the transcript levels of the others which suggests that the observed changes in the overexpression lines were specific. Altogether, results from malate and citrate

levels give us a more informed choice of which PPCs are easy to exploit and would result in more desirable changes such increased tissue malate and citrate levels and exudates.

3.3 Role of *PPCKs* during plant development and Pi starvation

Most plants express *PPCK* isoenzymes encoded by small gene families with *Arabidopsis* having two *PPCK* genes (Fontaine et al., 2002; Fukayama et al., 2006; Nimmo, 2003; Shenton et al., 2006). However, it is still unclear whether these isoenzymes have the same physiological function or if they are different. We used *ppck* knockout lines to investigate whether the two *Arabidopsis* isoforms have redundant physiological functions or not. Effects of *ppck1* knockout on plant development and response to stress have already been investigated in several studies (Chutia, 2019; Meimoun et al., 2009). However, *PPCK2* transcripts in the *ppck2* T-DNA insertion mutant lines (SALK_102132.37.95.x) were more abundant compared to wild type, which rendered them unsuitable for further studies. We therefore embarked and successfully generated *ppck2* knockout lines using CRISPR/Cas 9 technology (Figure 26). We additionally crossed the *ppck1-4* lines from Chutia, (2019) with the *ppck2* CRISPR/Cas 9 knockout lines and generated *ppck1ppck2* double knockout lines. To draw meaningful conclusions from these knockout lines, it was also imperative to check whether the transcription of these two kinases influenced each other or not.

From our transcript analysis, *PPCK1* abundance in wild type was higher in shoots and roots compared to *PPCK2* transcripts in both sufficient and insufficient Pi conditions. Due to its low abundance in shoots and roots, Pi starvation strongly induced *PPCK2* transcripts by up to 750-fold in shoots and about 13-fold in roots. The transcript results by Chutia, (2019) also showed higher *PPCK1* transcript levels in shoots and roots indicating its predominance compared to *PPCK2* in the same tissues. To further investigate the influence of these two *Arabidopsis* isoforms on each other, we checked for transcript abundance of each *PPCKs* in the *ppck1-4*, *ppck2* CRISPR/Cas 9 and *ppck1ppck2* double knockout mutant lines. Transcript profiles in the single mutant lines revealed that loss of one *PPCK* isoform did not influence the transcript levels of the other, as they remained comparable to wild type levels (Supplementary figure 6). More so, both *PPCK* isoforms transcript levels were severely reduced in the *ppck1ppck2* double knockout lines. Complementation of the *ppck1-4* mutant with a construct harboring the *PPCK1* ORF under the control of its native promoter reverted the *PPCK1* transcript levels to wild type levels (Figure 25). Additionally, the abundance of *PPCK2* transcript levels in these complementation lines was not affected (Supplementary figure 6), which implied that effects observed after loss of *PPCK1* would not be reverted by the presence of *PPCK2* and the effects observed would be specific for *PPCK1*.

3.3.1 Effects of *ppck* knockouts on tissue fresh weight

Tissue fresh weights are a good indicator to monitor plant performance especially during response to stress. Phosphate starvation results in reduced shoot growth but increased root weight due to increase

in number and length of lateral roots (Lynch and Brown, 2001). Since, loss of one *PPCK* isoform did not affect the abundance of the other isoform and *PPCK1* transcript levels were more abundant in both shoots and roots compared to those of *PPCK2*, we hypothesized that its loss would negatively affect the shoot and root fresh weight. *Ppck1-4* knockout mutant had reduced shoot fresh weight under both nutrient sufficient and deficient conditions while root fresh weight was only lower on sufficient Pi compared to wild type (Figure 32). Astoundingly, *ppck2* CRISPR/Cas 9 knockout lines had elevated shoot fresh weight while root fresh weight was comparable to wild type. Tissue fresh weight in the double knockout was also comparable to wild type either in nutrient sufficient or nutrient deprived plants.

Our results slightly differ from those by Chutia, (2019) where no differences were observed neither in shoot nor root fresh weights between *ppck1-4* mutant and wild type. Decreased shoot weight is an indicator of perturbed developmental process happening in the plants, which suggests that in the *ppck1* mutant, the machinery for remobilizing internal Pi stores may be operating suboptimally which would lead to reduced shoot growth resulting in low shoot fresh weight. In contrast, presence of *PPCK1* transcripts in shoots of *ppck2* CRISPR/Cas 9 mutants would then imply that the Pi remobilization machinery would be on and responsible for the observed increase in shoot fresh weight. Since *PPCKs* are responsible for phosphorylating PPCs and with the assumption that *PPCK1* phosphorylates more PPCs compared to *PPCK2* based on their transcript levels, it would further imply that the levels of phosphorylated PPCs could have an influence on shoot growth in these mutants. However, to confirm this more experiments on phosphorylated PPCs need to be done to ascertain whether this school of thought holds true or not.

3.3.2 Effects of *ppck* mutants on root length upon Pi starvation

Low Pi causes inhibition of the primary root growth in Arabidopsis and to combat this, plants exude more organic acids to liberate the residual in complexes. *PPCK* positively influences malate and citrate exudation during Pi starvation by increasing PPC phosphorylation. Phosphorylated PPCs are more active and result in more exudation of malate and citrate, which liberates Pi from complexes. We hypothesized that in mutants with low exudation of malate and citrate, we should expect longer roots, since the Pi sensing mechanism is compromised. The gain of root length measurements revealed no distinct differences between wild type, *ppck1-4* and its complementation lines under sufficient Pi. However, in the loss of function *ppck1-4* and *ppck2* CRISPR/Cas 9 mutant line 1.3 knockout mutants a 17% increase in primary root length was observed under insufficient Pi indicating a compromised low Pi sensing mechanism (Figure 33). Root length in the *ppck1ppck2* double knockout mutants were however comparable to wild type. Our results are in agreement with those by Chutia, (2019) where the *ppck1-4* mutant had a longer gain of root length only on nutrient deprived condition. Additionally, primary root growth for *ppck* mutants in Ferial et al., (2016) was comparable to that of wild type. With the assumption of less phosphorylated PPCs in the double knockout mutant lines and having observed similar primary

root growth in the *ppck1ppck2* double knockout lines as in wild type, it then implies that gain of root length is not influenced by the levels of phosphorylated PPCs but rather by other processes. Inhibition of root growth in Arabidopsis upon Pi starvation has been reported to be iron dependent (Dong et al., 2017). Since upon Pi starvation we have more freely available iron, which is known to inhibit primary root growth, it would be expected that wild type plants with a functional Pi sensing mechanism should exude more OAs. This exuded OAs should then chelate the excess iron, liberate and allow uptake of available residual Pi. In contrast, mutants with a compromised Pi sensing mechanism and exuding low amounts of OAs should show some insensitivity to low Pi, which should result in longer primary root. While we detected low levels of OAs in the *ppck1-4* and *ppck1ppck2* double mutant lines only *ppck1-4* mutant, had a longer root compared to wild type indicating slight insensitivity to low Pi. However, primary root growth in *ppck1ppck2* double knockout lines was comparable to wild type. While these results underpin the important role of exuded OAs in influencing primary root growth, they also reveal the intricacy associated with root growth. While inhibition of primary root growth is not a one-process affair, we were still able to show how loss of *PPCK1* affects root growth upon Pi starvation further implying the unique role of OAs exudation in root development during abiotic stresses such as Pi starvation.

3.4 Effects of *PPCK* loss affects tissue metabolites during Pi starvation

Phosphorylation of PPCs by PPCKs reduces their allosteric inhibition by inhibitors such as malate and aspartate and additionally increases their activation by activators such as glucose-6-phosphate and acetyl CoA. Arabidopsis has two *PPCK* isoforms i.e. *PPCK1* and *PPCK2* (Chutia, 2019; Meimoun et al., 2009). Since it was unclear whether they were redundant or not, we worked with mutants to comprehend this. If PPC phosphorylation levels decreased in *ppck* mutants, this would result in changes in metabolites especially of malate and citrate. Additionally, if PPCK roles were physiologically redundant, loss of either one of them would have no adverse effect on the endogenous levels of either malate or citrate and additive changes should only occur in the *ppck1ppck2* double knockout lines. In contrast, if they are not redundant as suggested by tissue transcript levels, then loss of either one of them should result in different metabolite changes. Previous studies on *ppck* mutants have focused on their effect on seed development (Feria et al., 2022) or on endogenous OAs (Chutia, 2019; Feria et al., 2016; Meimoun et al., 2009). However, in all these studies, they either did not investigate exudates and if they did *ppck2* and *ppck1ppck2* double knockout mutant lines were missing. We therefore carried out these experiments using all these mutants.

3.4.1 Effects of *ppck* mutants on shoot malate and citrate content during Pi starvation

Reduced malate levels were observed in shoots of *ppck1-4* and *ppck1ppck2* double knockout mutant lines, while shoot malate levels in *ppck2* CRISPR/Cas 9 mutant lines were comparable to wild type upon Pi starvation (Figure 28). These results indicated that loss of *PPCK1* resulted in more adverse

malate chemotype compared to the loss of *PPCK2*. Contrary to malate, shoot citrate in *ppck1-4* and *ppck1ppck2* double knockout mutant lines was higher than wild type but was comparable to wild type in *ppck2* CRISPR/Cas 9 mutant lines upon Pi starvation (Figure 29). To confirm whether these changes in malate and citrate levels were specific to loss of *PPCK1*, we determined malate and citrate levels in the *ppck1-4* complementation lines and indeed, they were reverted to wild type levels. Furthermore, malate and citrate changes observed in *ppck1ppck2* double knockout lines were very similar to those observed in *ppck1-4* mutant lines further supporting the hypothesis of *PPCK1* dominance especially upon Pi starvation.

Our results for *ppck1-4* mutant are in agreement with those from Chutia, (2019) and Meimoun et al., (2009), where significant low malate and high citrate levels were reported for *ppck1-4* mutant and the *dln1* and *csi8* lines (*ppck1* mutant lines). By knocking out the shoot predominant *PPCK1*, PPC phosphorylation would be reduced. This would result in reduced PPC activity due to increased feedback inhibition by malate or aspartate. This would then lead to diminished levels of oxaloacetate and ultimately low levels of shoot malate as was observed in *ppck1-4* and *ppck1ppck2* double knockout lines. However, the increased shoot citrate in these mutant lines is puzzling, as it might be expected that they should also be lower. Keeping in mind that the substrate for the PPC reaction i.e. PEP is also a substrate for the TCA cycle, we speculate that in the *ppck1-4* mutant and *ppck1ppck2* double knockout lines, more PEP is channeled to the TCA cycle which leads to increased citrate generation. When this happens, it would diminish the oxaloacetate pools in the cytoplasm, depriving cMDH its much-needed substrate for the generation of malate. This would ultimately result in low levels of malate as was observed in the same mutants. In contrast, in *ppck2* CRISPR/Cas9 mutant lines shoot malate and citrate remained comparable to wild type. Bearing in mind that we have a functional *PPCK1* in the *ppck2* CRISPR/Cas9 mutants whose transcript levels remained comparable to those in wild type, we propose that its phosphorylation capacity of PPCs was sufficient to allow generation of enough oxaloacetate pools that could be to malate in the cytosol. These results imply that PPC phosphorylation may be an indirect determinant on whether to channel the oxaloacetate to malate or citrate generation. Moreover, from these it is evident that *PPCK1* maybe more involved in generation of malate and citrate destined for exudation during Pi starvation while *PPCK2* may have a supportive role, or it could be involved during other stress responses which are still unknown.

3.4.2 Effects of *ppck* knockouts on root malate and citrate content during Pi starvation

In roots, malate and citrate levels were significantly lower in *ppck1-4* and *ppck1ppck2* double knockout lines but like shoots, malate and citrate levels were comparable to wild type levels in *ppck2* CRISPR/Cas 9 mutant lines upon Pi starvation. Complementation of the *ppck1-4* mutant reverted both citrate and malate to wild type levels further confirming the changes were *PPCK1* specific. Our results are in full agreement with those of Chutia, (2019) in which *ppck1-4* mutant had reduced root malate and citrate levels. In another

study working on *ppck1* mutant lines i.e. *dln1* and *csi8*, lower malate levels were reported for both mutant lines while citrate levels in line *dln1* were slightly higher than in wild type but lower in the *csi8* mutant line (Meimoun et al., 2009). The *dln1* and *csi8* had reduced PPC phosphorylation, which was the reason for metabolite changes. However, these two mutant lines were not complemented which made it difficult to conclude whether the malate and citrate changes were specific to the loss of *PPCK1*. Roots are the major and initial site of contact with nutrient deficient soils and play an integral role in nutrient absorption. Growing in Pi starved condition would require the plant to rearrange its metabolic requirements and prioritize the process that would allow for its continued survival by exudation. This would then imply that the anaplerotic role of the PPC pathway would be lowered, while generation of malate and citrate for exudation would be prioritized and boosted. All this with the aim of taking up more Pi and reducing effects associated with the now freely available iron. However, due to loss of *PPCK1* in *ppck1-4* mutant or both *PPCK* isoforms in the *ppck1ppck2* double knockout lines, PPCs would be less active due to inhibition reducing their activity. The reduced activity would result in limited pools of oxaloacetate, with less of it converted to malate thus the low levels in these mutants. From the shoot and root malate and citrate levels, it is evident that loss of *PPCK1* is more devastating compared to loss of *PPCK2*. The malate and citrate profiles for *ppck1ppck2* double knockout mutants are like those of *ppck1-4* mutant albeit stronger which indicates that *PPCK2* plays a minor role during Pi starvation which nicely correlates to the detected transcript levels.

3.4.3 Effects of *ppck* knockout on exuded malate and citrate during Pi starvation

Exuded malate and citrate in *ppck1-4* and *ppck1ppck2* knockout mutants was decreased under both sufficient and insufficient Pi but was reverted to wild type levels in the *ppck1-4* complementation lines. In contrast, exuded malate and citrate in *ppck2* CRISPR/Cas 9 knockout lines was comparable to wild type levels. Our results agree with those of Chutia, (2019) where reduced malate and citrate were detected in the *ppck1-4* mutant. However, in that study (Chutia, 2019), high *PPCK2* transcript levels in *ppck2* T-DNA insertion lines meant they could not be used in the study. Hence, the reason for generating *ppck2* CRISPR/Cas 9 mutant lines. It is suggested that upon loss of one of the *PPCKs*, the remaining *PPCK* takes over the phosphorylation roles. In seeds of *ppck* mutants, PPC phosphorylation levels and even PPC activity were indistinguishable between the *ppck1* or *ppck2* mutants (Feria et al., 2022). If this then applies to other plant tissues and organs, then malate and citrate levels in the single mutants should also be indistinguishable. However, from data obtained from this study, loss of *PPCK1* led to significant reduction in root malate and citrate exudation while loss of *PPCK2* barely influenced endogenous and exuded malate and citrate. Low levels of exuded malate and citrate indirectly imply low PPC activity, which arises from allosteric inhibition. This further implies differential PPC phosphorylation in roots of *ppck1-4*, *ppck2* CRISPR/Cas 9 and *ppck1ppck2* double knockout lines. Compared to results by Feria et al., (2022) on *ppck* mutant seeds, our data suggest *PPCKs* roles might additionally be tissue specific.

Higher levels of exuded malate and citrate have been reported in other plants such as white lupin where they increased Pi uptake (Tiziani et al., 2021). As such, mutants with reduced exudation of malate and citrate should absorb less amount of Pi. This experiment needs to be performed to confirm whether this also holds true for Arabidopsis or not. Additionally, reduced malate and citrate exudation should expectedly lead to reduced metabolites closely associated with PPC pathway such as aspartate. This was however unchanged in the shoots and roots of *ppck1-4* mutant line but was surprisingly elevated in *ppck2* CRISPR/Cas 9 and *ppck1ppck2* double knockout lines under sufficient Pi compared to wild type. In contrast, on Pi deprived conditions, only *ppck1-4* and *ppck1ppck2* had reduced malate exudation. The aspartate levels in both shoots and roots were comparable to those of wild type but malate levels were lower. Although these mutants have lower malate levels in roots, it appears as if the levels are still enough to cause feedback inhibition. However, when all endogenous and exudation profiles from our *ppck* single and *ppck1ppck2* double knockout lines are considered, we propose that the phosphorylation role of PPCK1 during Pi starvation is more is more dominant and its loss results in reduced endogenous and exuded malate.

4.0 SUMMARY

The quest to understand phosphate sensing in plants continues to draw more attention due to its irreplaceable role in most biological functions but also due to its limited availability in nature. This has led to the exploration and modulation of various processes aimed at improving remobilization and enhanced Pi uptake by plants. This study was designed to investigate the effects of manipulating the PPCK-PPC module by (i) overexpressing C3 PPCs and (ii) knocking out PPCKs and (iii) mapping the cell expression domains of plant type PPCs in the root tip.

This study revealed that PPCs are expressed at the root cap, epidermis and root stele, which coincide with regions of either Pi uptake and translocation and sites for OA exudation. Additionally, we were able to follow the differential induction of plant type PPCs upon Pi starvation microscopically. Furthermore, the restriction of PPC2 and PPC3 to the epidermal or stele cells provides us with a better understanding why we observe their slight induction in roots as compared to PPC1, which diffused to all cell layers and had the highest induction upon Pi starvation.

By successfully overexpressing C3 PPCs in Arabidopsis, we were able to elevate the endogenous malate and citrate levels and increase exudation in PPC2 transgenic lines. This data shows the potential of how C3 PPCs can be attuned to bioengineer crops, with desired properties such as improved stress resilience such as low Pi. Furthermore, the PPCs percentage phosphorylation results obtained point out to PPCKs being a possible bottleneck in modulating this pathway, which could limit its success. Additionally, phenotypic data obtained from seeds and flowering times indicate that modulation of this pathway by overexpressing PPCs would have minimal or no adverse effects on plant growth and maturation.

Lastly, results obtained from *ppck* mutants in this study, further confirmed the important role of PPCKs during Pi starvation. Moreover our data provides evidence showing that PPCK isoforms are not redundant as has been previously assumed. While it was clear from our data the role of PPCK2 in this pathway cannot be overlooked, it was evident that PPCK1 has a much more dominant role since its loss had more adverse effects on the plant chemotype regarding malate and citrate during Pi starvation.

5.0 OUTLOOK

Although significant strides about the PPCK-PPC module were made in this study, some questions remain unanswered. However, the transgenic lines generated during our study provide invaluable tools that can be exploited to perform future experiments, which will enlighten us more about this pathway such as:

To elucidate the effect of exuded malate and citrate on Pi-solubilization from complexes

- Overexpression lines displaying elevated malate and citrate exudation or knockout lines displaying reduced malate and citrate exudation could be grown on soils or media supplemented with insoluble Pi-complexes such as calcium, aluminum, and iron phosphate at different pH and their growth and performance monitored and compared to wild type.

To elucidate the role of *PPCs* in iron translocation from roots to shoots

- Since we observed elevated levels of root citrate in *PPC* overexpression lines, and citrate plays a role in iron homeostasis, iron accumulation in shoots and roots of the *PPC* overexpression lines should be investigated, followed by transcript analysis of genes involved in iron transport such as *IRT1* and iron storage such as ferritin. If true, overexpression lines accumulating more citrate in shoots and roots should stain heavily for iron and vice versa. Additionally, some genes involved in iron transport and storage should be induced in these lines.

To determine the metabolic flux in *PPC* overexpression lines

- Since we observed increased malate only in roots and shoots of the overexpression lines, it begs the question what happened to the malate in shoots. It could either be translocated to roots or converted to other compounds such as malate esters. Therefore, nontargeted metabolic analysis needs to be carried out in shoots and roots to check which other metabolites changes occurred in these overexpression lines.

To elucidate the phosphorylating ability of *PPCK1* and *PPCK2*

- With *ppck1*, *ppck2* and *ppck1ppck2* mutants at hand, it would be prudent to investigate whether they both phosphorylate PPCs to the same extent in shoot and root tissues or not. This would be a further confirmation of which PPCK is more dominant.

To elucidate the role of *PPCK2* in other stresses

- While we observed strong induction of *PPCK2* during Pi starvation, metabolite and phenotypic results during phosphate indicate a minor role of *PPCK2* during Pi starvation. This leads to a strong possibility that *PPCK2* may have different roles in plants. Therefore, its role during different stresses such ammonium toxicity, water, salt, heat and metal stresses, should be investigated.

6.0 MATERIAL AND METHODS

6.1 Chemicals and reagents

All chemicals, media constituents, and solvents used were of reagent or HPLC grade and were obtained from the following suppliers: Carl Roth (Karlsruhe, Germany), Merck (Darmstadt, Germany), Macherey-Nagel (Düren, Germany), Sigma-Aldrich (St Louis, MO, USA), J.T. Baker (Deventer, The Netherlands), Duchefa Biochemie (Haarlem, The Netherlands), CDN isotopes (Point Claire, QC, Canada), and Caissons Laboratories (East Smithfield, USA). Molecular Biology supplies and kits were obtained from Life Technologies and Thermo Fischer Scientific (California, USA), and New England Biolabs (Massachusetts, USA). Sequencing and primer synthesis was performed by Eurofins Genomics (Ebersberg, Germany).

6.2 Plant growth and bacterial culture media

Bacteria (*E. coli* and *A. tumefaciens*) used for transformation during cloning were cultured in either LB or SOC media. Antibiotics for selection of the positively transformed cells were initially filter sterilized before addition to the autoclaved growth media.

For growing Arabidopsis media was constituted as listed in Table 1. However, to remove residual phosphate, which is important for performing Pi starvation experiments, agar (Duchefa, Haarlem, The Netherlands) was repeatedly washed in deionized water and subsequent dialyzed using Dowex 1X8 anion exchanger (Sigma-Aldrich, St Louis, MO, USA) before drying on plastic crucibles at 60° C for 2-3 days (Ward et al., 2008). Basta supplement for selection of positively transformed seeds was added to the liquid autoclaved media after filter sterilization. All media were sterilized at 121° C and 2 bars for 20 min.

Table 1: Plant growth and bacterial culture media composition

Medium	Composition	Reference
LB	10 g/L Bacto tryptone, 10 g/L NaCl, 5 g/L Yeast extract, pH 7.5. For solid agar, 15 g/L agar was added	(Bertani, 1951)
SOC	20 g/L Tryptone, 5 g/L Yeast Extract, 10 mM NaCl, 2.5 mM KCl, 10 mM MgCl ₂ , 10 mM MgSO ₄ , 20 mM Glucose	(Hanahan, 1983)
Modified ATS	2.5 mM (+Pi) or 0 mM (-Pi) KH ₂ PO ₄ , 0.5% D-Sucrose, 5 mM KNO ₃ , 0.025 mM Fe ³⁺ -EDTA, 2 mM Ca(NO ₃) ₂ , 2 mM MgSO ₄ , 2.5 mM MES-KOH, 0.005 mM CuSO ₄ , 0.001 mM ZnSO ₄ , 0.07 mM H ₃ BO ₃ , 0.014 mM MnCl ₂ , 0.0002 mM Na ₂ MoO ₄ , 0.010 mM CoCl ₂ , pH 5.6 For solid medium, 1% Washed Agar was added	(Müller et al., 2015)

LB-Luria Bertani medium

SOC- Super Optimal Broth with Catabolite repression

6.3 Bacterial strains, plasmid vectors, culture and transformation

6.3.1 Bacterial strains and plasmid vectors

The bacterial strain *Escherichia coli* One Shot® TOP10 chemically competent cells provided with the pENTR™ Directional TOPO® Cloning kit from Invitrogen was used for propagation of the Gateway entry cassette. Whereas self-made chemically competent cells of bacterial strain *Escherichia coli* TOP10 was used for propagation of the Gateway expression cassette. The *Agrobacterium tumefaciens* strain *GV3101::pMP90RK* (Koncz & Schell, 1986) was used for plant transformation via the floral dip method (Clough & Bent, 1998). The plasmid vectors used during this work for molecular cloning and recombinant expression are listed below.

Table 2: Plasmid vectors used in generation of PPCs overexpression lines and features

Plasmid	Purpose	Feature	Reference
pENTR/D-TOPO	Entry vector for Gateway cloning	<i>rrnB</i> T1 and T2, M13 forward and reverse priming site, <i>attL1</i> and <i>attL2</i> , TOPO cloning site (directional), T7 promoter/priming site, Kan ^r , pUC ori	Thermo Fischer Scientific
pB7WG	Binary plant expression vector	<i>attR1</i> and <i>attR2</i> , <i>ccdB</i> , LB and RB site, Sm/SpR, T35S, Bar	
pB7WG2	Binary plant expression vector	<i>attR1</i> and <i>attR2</i> , p35S, T35S, CmR, <i>ccdB</i> , Sm/SpR, Bar	
pB7FWG2	Binary plant expression vector	<i>attR1</i> , <i>attR2</i> , p35S, T35S, <i>ccdB</i> , Sm/SpR, Bar, <i>Egfp</i>	(Karimi et al., 2002; Karimi et al., 2005)
pB7WGF2	Binary plant expression vector	<i>attR1</i> , <i>attR2</i> , p35S, T35S, <i>ccdB</i> , Sm/SpR, Bar, <i>Egfp</i>	
pUB-C-GFP-Dest	Binary plant expression vector	pUBQ10, <i>attR1</i> , Bar, LB, RB, SmR, pBR322, pVS1 <i>attR2</i> , CmR, <i>ccdB</i> , T35S	
pUB-N-GFP-Dest	Binary plant expression vector	pUBQ10, <i>attR1</i> , Bar, LB, RB, SmR, pBR322, VS1 <i>attR2</i> , CmR, <i>ccdB</i> , T35S	

6.3.2 *Escherichia coli* and *Agrobacterium tumefaciens* cultivation

E. coli cells were cultured in LB liquid medium or on LB plates containing appropriate antibiotics for 24 h at 37° C. The *Agrobacteria* were also cultured in LB liquid or solid medium with appropriate antibiotics and cultivated for 48 h at 28° C. The liquid cultures were incubated on a rotary shaker which was set at 150 rpm. For long-term storage of bacterial clones, glycerol stocks were prepared by mixing bacterial cultures with glycerol to reach a final glycerol concentration of 20% (v/v). Stocks were then flash-frozen in liquid nitrogen and stored at -80° C until used.

6.3.3 *Escherichia coli* and *Agrobacterium tumefaciens* transformation

Chemically competent *E. coli* Top10 and One-Shot cells were transformed through the heat shock method as described in the Invitrogen pENTR™ Directional TOPO® Cloning Kit. Transformed cells were cultivated overnight (16 h) at 37° C on LB plates containing appropriate antibiotics for selection of the transformed plasmid. For transformation of *A. tumefaciens* strain *GV3101::pMP90RK*, 100 ng of purified plasmids were carefully mixed with 50 µl of competent cells and incubated on ice for 30 min. The cells were then frozen in liquid nitrogen for 5 min, followed by incubation at 37° C for 5 min. 250 µl of SOC medium was added to this mixture and incubated horizontally at 28° C in a shaker at 150 rpm for 2 h. For the selection of transformed plasmids, the cells were plated on an LB plate with the respective antibiotics and cultured for 48 h at 30° C.

6.4 Generation of stably transformed lines and plant growth conditions

Transgenic lines used in this study were generated either using the Gateway cloning system from Thermo Fisher Scientific or the golden gate cloning system for *ppck2* CRISPR/Cas 9 knockout mutant and *PPC* expression reporter lines. The complete list of all transgenic lines generated together with their intended purpose is listed in Table 3.

Table 3: Transgenic lines and knockout mutants used in this study

Transgenic lines	Purpose
<i>Pro PPC1-NLS-GFP</i>	Cell specific expression domains
<i>Pro PPC2-NLS-GFP</i>	Cell specific expression domains
<i>Pro PPC3-NLS-GFP</i>	Cell specific expression domains
<i>35S::PPC1</i>	Overexpression of <i>PPC1</i>
<i>35S::PPC2</i>	Overexpression of <i>PPC2</i>
<i>35S::PPC3</i>	Overexpression of <i>PPC3</i>
<i>Ppck1-4</i> mutant	Knockout for <i>PPCK1</i>
<i>ppck2</i> -mutant	Knockout for <i>PPCK2</i>
<i>ppck1ppck2</i> -mutant	<i>ppck1ppck2</i> double knockout mutant

6.4.1 Generation of *PPC* expression reporter lines

For the cellular localization of *PPC* expression domains, native promoters were cloned and fused to a GFP and NLS using a modified golden gate method based as described by Binder et al., (2014). Internal type IIS (BsaI and BpiI) restriction sites that could interfere with the assembly of the construct were removed by site-directed mutagenesis. Genomic DNA was used to amplify the corresponding *PPC* promoter using specific primers with additional sequences for BsaI enzyme and the 4 bp overhang (Supplementary table 2). Promoter sequences were then cloned into a level 0 vector before advancing into a level 1 vector. For the assembly into level II constructs, the level I promoter sequences were ligated with N-terminal GFP, a NLS, a hygromycin selection marker and a nopaline synthase terminator

before assembly into the final level III expression vector harboring the mCherry seed coat selection marker. After each cloning step, positive clones were confirmed by restriction digestion using different restriction enzymes (Supplementary table 3) before being sent for sequencing using either universal or specific primers (Supplementary table 4). The expression vector was then transformed into *Agrobacterium tumefaciens* GV3101 competent cells before transformation to *Arabidopsis* using floral dip method.

6.4.2 Generation of *PPC* overexpression lines

PPCs overexpression lines under the control of the strong and constitutive 35S promoter were generated using the gateway cloning system using the plasmids listed in table 5-2. Entry clones were generated via the topoisomerase-assisted pENTR/D-TOPO vector system (pENTR™ Directional TOPO® Cloning Kit, Thermo Fisher Scientific). To meet the requirements of cloning into pENTR/D-TOPO vector, CACC extensions were added at the 5' end of the forward primers. The coding sequences for *PPC1*, *PPC2* and *PPC3* were then amplified from wild type cDNA using gene specific primers (Supplementary table 5). After extracting the amplified product from the gel, the TOPO cloning reaction was performed according to the manufacturer's protocol. Plasmids from positive colonies were then extracted using plasmid purification kit (Thermo Fischer Scientific) and confirmed by restriction digestion using different restriction enzymes (Supplementary table 6) before additional confirmation by sequencing (Supplementary table 7). The positively identified entry clones, were then introduced into the expression vectors and transformed into *Agrobacterium tumefaciens* GV3101 competent cells. Lastly, the positive expression vectors were transformed into the respective overexpression construct through floral dipping.

6.4.3 Generation of *ppck2* CRISPR/Cas 9 knockout line

Since available T-DNA insertion lines did not show decreased *PPCK2* transcript levels, *Arabidopsis thaliana* lines with lowered or absent expression of *PPCK2* were generated through CRISPR/Cas 9 technology (Ordon *et al.*, 2017). A two-gRNA system was adopted for this task. Briefly, appropriate sequences for the two guide RNAs (Table 4) were identified using the online tool CHOP CHOP, a freely available online tool (<https://chopchop.cbu.uib.no>) and the best *PPCK2* sequences stretches were selected based on the percentage of silencing efficiency (>70%) with zero number of off target sites and zero probability of self-complementarity.

Table 4: Sequences for guide RNA used to generate *ppck2* through CRISPR/Cas 9

gRNA	Forward primer	Reverse primer
1	ATTGATCGGTTAATCTCCGCCGGG	AAACCCGGCGGAGATTAACCGAT
2	ATTGACAGACCCAAACTTCTTCGG	AAACCCGAAGAAGTTTGGGTCTGT

Both gRNAs were modified by addition of BpI cleavage sites, i.e. **TTGAAGACAA** and **TTGAAGACAA** in forward and reverse primers, respectively.

The guide RNAs were designed to contain recognition sequences for type II restriction enzymes and 4 base pair overhang which would facilitate ligation into the respective shuttle vector i.e. pDGE332 and pDGE334. These shuttle vectors contain all required elements for efficient silencing using CRISPR/Cas 9 technology, i.e. the U6 promoter sequence, the two guide RNA sequences, and the guide RNA scaffold. 5 µl of the forward and reverse (100 µM) primers were diluted in 40 µl H₂O and denatured by heating at a 98 °C for 5 min. The mixture was cooled and hybridized at room temperature for 30 minutes, before dilution in a 1:200 ratio (50 fmol / µl). 5 µl of the hybridized primers was then incubated with respective shuttle vector in a cut-ligate reaction and later introduced into an expression vector containing all the cassettes for CRISPR/Cas 9 editing. Lastly, the expression vector was introduced into a destination vector pDGE347 containing a Basta selection marker gene, the right and left boarder regions essential for integration into the Agrobacterium which would mediate transformation into Arabidopsis. After every cloning step, positive clones were identified by restriction digestion (Supplementary table 8) Once expressed in the plant, the CRISPR associated protein 9 (Cas 9) would be directed by the two gRNA sequences to the specific target sequence where it should then cleave the DNA sequence of gene of interest (*PPCK2*) leading to a double stranded break. In an attempt to repair the double stranded break, the cell would introduce errors leading to insertions or deletions (INDEL) in the coding sequence which would then lead to a frameshift in the coding sequence of the *PPCK2* resulting in a *ppck2* CRISPR/Cas 9 mutant.

6.4.4 Generation of *ppck1ppck2* double knockout line

To generate a *ppck1ppck2* double knockout line, *ppck1-4* T-DNA insertion line (Chutia, 2019) was crossed with the generated *ppck2* CRISPR/Cas 9 knockout line and crosses left to grow until they set seeds (F1). The obtained seeds were sown on soil, allowed to germinate before spraying with Basta selective chemical as the *ppck2* CRISPR/Cas 9 knockout line contained BASTA resistance gene. Since we used *ppck1-4* as the mother plant, only crosses harboring *ppck2* CRISPR/Cas 9 crosses would survive upon spraying with BASTA since CRISPR/Cas 9 mutants since they had the herbicide resistant marker gene while *ppck1-4* mutant was selected using kanamycin. After setting seeds (F2), the surviving crosses were further selected on Basta plates for a 3:1 ratio. From the crosses showing a 3:1 ration (F3), 12 plants per cross were selected and grown on soil until seed were obtained after which they were then further selected on Basta plates for homozygosity (F4). Only crosses that showed 100% survival on Basta plates were homozygous for *ppck2* and were used for further analysis. At F3 generation, seedlings were further genotyped for the presence of the T-DNA insertion of the *ppck1-4* mutant and the INDEL of *ppck2* CRISPR/Cas 9 mutant using gene specific primers (Supplementary table 9). Low transcripts levels for both *PPCK1* and *PPCK2* were further confirmed by qPCR and only lines that showed low levels of both transcripts were used for further studies.

6.5 Transformation and selection of Arabidopsis transgenic lines

Arabidopsis plants were transformed by *A. tumefaciens* mediated transfection using the floral deep method as described by Clough and Bent, 1998. Before transformation, colony PCR were performed to confirm presence of gene of interest using primers listed in (Supplementary table 10). Agrobacteria harboring the gene of interest in a binary vector were cultivated on LB plates with appropriate antibiotics for 2 days at 28° C. The cells were re-suspended in liquid LB medium and diluted to an OD₆₀₀ of 2.0. A freshly prepared 5% (w/v) sucrose solution was added to the bacterial suspension in a 4:1 ratio. Before dipping, Silwet-L77 at a concentration of 0.03% (v/v) was added to the suspension. Arabidopsis plants, which had begun flowering were dipped upside down into the suspension solution and gently agitated for nearly 30-60 seconds. The plants were then placed in a horizontal manner on a tray and kept moist by covering the tray with plastic foil. After two days, the plastic foil was removed, and the plants moved to a vertical position and cultivated in the greenhouse until they set seeds.

6.6 Plant growth conditions

Before sowing on plates, seeds were surface sterilized with chlorine gas and sown on sterile agar plates containing modified ATS medium. Plates were incubated for two days at 4° C in the dark to synchronize seed germination and thereafter the plates were kept vertically in a growth chamber at 22° C under illumination for 16 h daily (170 μmol s⁻¹ m⁻²; Osram LumiluxDeLuxe Cool Daylight L58W/965, Osram, Augsburg, Germany). After 6 days of growth, seedlings were transferred to fresh plates containing +Pi (2.5 mM KH₂PO₄) or -Pi (0 mM KH₂PO₄) modified ATS media and allowed to grow for five more days. Seedling were photographed for root length measurements and thereafter roots and shoots separated, their fresh weights recorded, and the samples frozen in liquid nitrogen until further processing. One biological replicate consisted of roots or shoots from three seedlings. Plants for propagation, transformation, selection and phenotyping purposes were grown in the greenhouse under long-day conditions at 18-20°C and 55-65% relative humidity. The soil substrate used was 'Einheitserde Typ GS 90' mixed with vermiculite (1-2 mm) in a 4:3 ratio.

6.7 Analysis of PPC protein from whole seedlings, shoot and root tissues

6.7.1 Protein extraction and quantification

Around 100 mg of Arabidopsis seedlings were harvested from agar plates and frozen in liquid nitrogen. The samples were ground using a 5 mm glass beads in a Tissue Lyser II (QIAGEN) bead mill at 25 s⁻¹ for 60 s and total protein was extracted by adding 300 ul of protein extraction buffer. The protein extraction buffer consisted of Tris-Cl (25 mM, pH-7.6), MgCl₂ (15 mM), NaCl (85 mM), NaF (2.5 mM), EGTA (15 mM), DTT (5 mM), PMSF (1 mM), nonidet P40 (0.1% v/v), tween 20 (0.1% v/v), disodium nitrophenyl phosphate (15 mM), and disodium-β-glycerophosphate (60 mM). After vortexing the samples for 60 s, the samples were kept on a heat block 95° C for 10 minutes and then shaken

vigorously at room temperature for another 20 min. The samples were centrifuged two times at 10,000 rpm for 10 min at 4° C and the supernatant was collected in a 1.5 ml eppendorf tube before storage at -80° C until further processing. To quantify the protein concentration, a standard curve was prepared using known quantities of Bovine Serum albumin (BSA) protein and the Bradford reagent. The absorbance of each sample and standard was then read at 595 nm using water as a reference with the Tecan Nanoquant Infinite M1000 (Männedorf, Switzerland).

6.7.2 Sodium dodecyl sulfate polyacrylamide gel electrophoresis (SDS-PAGE)

30 µg of protein for each sample were separated by SDS-PAGE gel (Laemmli, 1970). The stacking gel and separating gel consisted of 4% and 10 % polyacrylamide, respectively. The samples were mixed with 3x loading buffer (200 mM Tris-HCl, pH 6.8 (w/v), 8% SDS, 0.4% (w/v) Bromophenol blue, 50% glycerol (v/v), and 20% β-Mercaptoethanol (v/v) before loading on the gels. SDS-PAGE was performed at 100 V in a running buffer (25 mM Tris, pH 8.3, 192 mM glycine, and 0.1% (w/v) SDS) until the dye front had reached the lower rim of the gel. The components of stacking and separating gel are listed in Table 5.

Table 5: Composition of SDS-PAGE Gel

Components	Separating gel (10%)	Stacking gel (4%)
Millipore water	4.07 ml	6.07 ml
0.5 M Tris pH 6.8	-	2.5ml
1.5 M Tris pH 8.8	2.5mlm	-
30% Acrylamide (w/v)	3.33 ml	1.33 ml
10% SDS (w/v)	0.1 ml	0.1 ml
10% Ammonium persulphate (w/v)	0.04ml	0.04 ml
TEMED	0.02 ml	0.02 ml
Total Volume	10.06 ml	10.06 ml

6.7.3 Immunoblotting (Western Blot)

Proteins electrophoretically separated on SDS-PAGE gel were transferred to a nitrocellulose membrane (Amersham Protran 0.45 µm) via wet transfer at 120 V and 150 Watt for 2 h. After transfer, the membranes were blocked in 3% (w/v) milk powder in TBS buffer for one hour with gently shaking before being separated into two parts (Upper part for PPC, lower part for actin). Each part was then incubated for two hours with specific primary antibody i.e. PPC antibody raised in rabbit at 1:2,000 dilution and actin antibody raised in mouse at 1:20,000 dilution in blocking buffer (3% milk powder in TBS buffer). The membrane was then washed three times for 20 minutes with TBS-T (TBS buffer with 0.1% tween) at room temperature before incubation for two hours with the specific secondary antibody i.e. Anti-mouse coupled to HRP for actin and anti-rabbit coupled to HRP for PPC both at 1:5,000 dilution in 3 % (w/v) milk powder before washing three times for 20 minutes each with 1x

TBS-T before detection. For detection, Pico chemiluminescent substrate from Thermo Fischer scientific company was added to the membranes in the dark before the x-ray film was carefully laid over and then incubated for five minutes before detection using Amersham ECL Prime Western Blotting Detection

6.7.4 PPC enzyme activity

Approximately 100 mg of seedlings of 6 days-old wild-type and *PPC* overexpression lines were harvested into 2ml Eppendorf tubes containing glass beads and snap frozen in liquid nitrogen and later ground to fine powder using a bead crusher. 300µl of the extraction buffer containing (200 mM HEPES-NaOH pH 7, 10 mM MgCl₂, 5 mM dithiothreitol, and 2% [w/v] polyvinylpyrrolidone Li *et al.*, (2010) was added and the samples shaken for 30 minutes in the cold room. The crude extracts were centrifuged at 14,000 RPM for 5 min before transferring the supernatant to pre-cooled Eppendorf tubes. The extracts were then used immediately for the PPC activity assay as described by Gregory *et al.*, 2009. Reaction conditions were as follows: 50 mM HEPES-KOH (pH 8) containing 15% (v/v) glycerol, 2 mM PEP, 2 mM KHCO₃, 5 mM MgCl₂, 2 mM dithiothreitol, 0.15 mM NADH, and 2 units/ml malate dehydrogenase in a volume of 200µL. The consumption of NADH was then monitored at 340 nm for 500 seconds, recorded and used later to determine the PPC enzyme activity. In case of high enzyme activity, the PPC present in the crude extract should quickly convert the PEP substrate to oxaloacetate, which would be converted to malate by the supplied malate dehydrogenase enzyme resulting in an increased consumption of NADH.

6.7.5 PPC phosphorylation status

Wild type and *PPC* overexpression lines were grown for six days on phosphate sufficient media before transfer to sufficient and low phosphate media for an additional five days. The seedlings were separated into shoots and roots before protein extraction under denaturing conditions as described (Bassal *et al.*, 2020). To quantify the phosphorylation level of PPCs, 25 µg of protein were separated on 10% SDS-PAGE before the gel bands between the molecular size markers for 100 kDa and 130 kDa for PPC and 40-50kDa for the loading control actin were excised after staining with ethylene blue. The gel pieces were then processed as described by Bassal *et al.*, 2020. Briefly, the gel pieces were destained by several rounds of washing with water and acetonitrile until the blue color of the staining solution disappeared. This was followed by reduction with dithiothreitol at 50°C for 30 minutes and subsequent alkylation with iodoacetamide at 22°C for 15 minutes and overnight in-gel digestion of proteins with trypsin at 37°C. The trypsin digested proteins/peptides were then desalted, dried and dissolved in 10 µl of 5% (v/v) ACN, 0.1% (v/v) TFA and injected into an EASY-nLC 1200 liquid chromatography system (Thermo Fisher Scientific). Peptides were then separated using liquid chromatography C18 reverse phase chemistry employing a 120 min gradient increasing from 4% to 40% acetonitrile in 0.1% FA, and a flow rate of 250 nL/min.

6.8 Molecular Biology methods

6.8.1 Isolation of genomic DNA

Plant material was collected into 2ml Eppendorf tubes with a 5mm stainless-steel grinding bead and snap frozen in liquid nitrogen before being pulverized to fine powder using a Tissue Lyser II instrument from Qiagen. 350 μ l of DNA extraction buffer composed of 200 mM Tris-HCl (pH 7.5), 25 mM EDTA (pH 8), 250 mM NaCl, 0.5% w/v SDS was then added to the milled samples, followed by five minutes of vigorous shaking. Samples were then centrifuged for five minutes at 14 000 rpm and 300 μ l of the supernatant was transferred to fresh Eppendorf tube and mixed with an equal volume of ice-cold isopropanol, followed by centrifugation at the same conditions. Supernatant was removed and the DNA pellets were washed two times with 70% ethanol. After centrifugation for five minutes at 14 000 rpm, the ethanol was discarded, and the pellets left to air-dry for 30 minutes. The DNA pellet was then re-suspended in 30 μ l Milli-Q water and stored at -20°C until used for reactions.

6.8.2 Isolation of plasmid DNA from E. coli

Plasmid DNA was extracted with the GeneJET Plasmid Mini Prep Kit (Thermo Fisher Scientific) according to manufacturer's guidelines and instructions. The concentration of isolated plasmid DNA was determined using a spectrophotometer model Infinite[®] 200 NanoQuant (Tecan) device.

6.8.3 Standard polymerase chain reaction (PCR)

Standard colony PCRs and PCRs for genotyping were performed using 10x DreamTaq Polymerase Green buffer and DreamTaq polymerase (Thermo Fischer Scientific). A reaction volume of 20 μ l was generally used and the concentration of other components included is mentioned below (Table 6).

Table 6: Components of standard PCR and colony PCR reaction

Components	Stock concentration	Final concentration	Volume
Dream Taq green buffer	10 x	1x	2 μ l
DNTPs	10 mM	500 μ M	1 μ l
Forward primer	10 μ M	0.5 μ M	1 μ l
Reverse primer	10 μ M	0.5 μ M	1 μ l
Template	-	50 ng	2 μ l
DreamTaq polymerase	5U/ μ l	0.0625 U/ μ l	0.5 μ l
Millipore water	-	-	12.5 μ l

All PCR reactions were carried out in a Veriti™ 96-Well Thermal Cycler (Applied Biosystems) with the recycling profile listed in Table 7.

Table 7: Thermal profile for DreamTaq PCR

Phase	Temperature	Duration	No. of cycles
Initial denaturation	94° C	1 min	1
Denaturation	94° C	1 min	35
Annealing	~T _m ° C	1 min	
Extension	72° C	1 min/kb	
Final extension	72° C	7 min	1

6.8.4 High fidelity PCR for molecular cloning

For the generation of entry clones either for gateway or golden gate cloning, PCR products were amplified from either wild type (Col-0) genomic or cDNA using gene-specific primers in a 50 µl reaction (Table 8)

Table 8: Components of high-fidelity PCR

Components	Stock concentration	Final concentration	Volume
5x Phusion Green HF buffer	5x	1x	10 µl
dNTPs	10 Mm	300 µM	1.5 µl
Forward primer	10 µM	0.4 µM	2 µl
Reverse primer	10 µM	0.4 µM	2 µl
Template	-	~200 ng DNA or cDNA	2 µl
Phusion polymerase	2U/ µl	0.02 U/µl	0.5 µl
Millipore water	-	-	32 µl

The primers were designed such that their annealing temperature was between 55-60°C. The recycling profile is listed below (Table 9)

Table 9: Thermal profile Phusion High-Fidelity PCR

Phase	Temperature	Duration	No. of cycles
Initial denaturation	98° C	1 min	1
Denaturation	98° C	1 min	35
Annealing	55-60° C	1 min	
Extension	72° C	2 min	
Final extension	72° C	7 min	1

6.8.5 Agarose gel electrophoresis and purification of gel products

To visualize the presence of PCR products, separation was carried out on a 1% Agarose Gel in TAE buffer stained with Serva DNA stain G at 0.003% (v/v). Separation was performed at 120 V for 60 min depending on the size of the product followed by immediate visualization of the PCR products using a Gene Genius UV transilluminator (Syngene).

If needed for further downstream cloning procedures, PCR products purified using the GeneJET Gel Extraction Kit (Thermo Fisher Scientific) adhering to the manufacturer's instructions. The concentration

of the extracted PCR product was then determined and used for the different cloning systems used in this study.

6.8.6 Isolation of RNA with on column dNASE digestion

To determine the transcript levels in *PPC* overexpression or *ppck* knockout lines, 50 mg of seedling or tissue was collected in 2 ml Eppendorf tubes with glass beads and frozen in liquid nitrogen before grinding into fine powder. Total RNA was extracted with the RNeasy Plant Mini Kit (Qiagen) following the manufacturer's protocol with on column genomic DNA digestion using RNase-Free DNase Set (Qiagen). An endonuclease, dsDNase (Qiagen) showing high specific activity towards double-stranded DNA was used for genomic DNA elimination. A total reaction volume of 80 μ l consisting of 70 μ l 10x dsDNase buffer and 10 μ l dsDNase was added on to the column containing RNA and incubated at room temperature for 15 minutes. The sample was then rinsed with a washing buffer containing absolute ethanol before being eluted with nucleic acid free water. The concentration of RNA was determined spectrophotometrically using Infinite[®] 200 NanoQuant (Tecan) device and the isolated RNA used for cDNA synthesis as described below.

6.8.7 cDNA synthesis

1 μ g dsDNase digested RNA was used to synthesize cDNA in a total reaction volume of 20 μ l using RevertAid Reverse Transcriptase (Thermo Fisher Scientific). A volume of dsDNase digested RNA containing 1 μ g RNA was adjusted to 12 μ l with nucleic acid free water and mixed with 1 μ l of 100 μ M oligodT18VN (5'-TTTTTTTTTTTTTTTTTTTTVN-3') and 2 μ l of 40 mM dNTPs (10 mM each). This was then incubated at 65° C for 5 min followed by 2 min incubation on ice after which 4 μ l of 5x Reaction buffer (final concentration: 1x), 0.5 μ l of 40 U/ μ l RiboLock RNase Inhibitor (final concentration: 1 U/ μ l), and 0.5 μ l of 200 U/ μ l Reverse Transcriptase (final concentration: 5 U/ μ l) were added. The mixture was then vortexed spun down and incubated at 42° C for 1 hour, followed by the termination of the reaction by heating at 70° C for 15 min. The samples were stored at -20° C until further use.

6.6.8 Quantitative Real-Time-PCR (RT-qPCR)

A 10 μ l reaction was used for all the RT-qPCR experiments using components listed in table 10. The cDNA obtained above was diluted in a 1:10 ratio and of this dilution 3 μ l were used as the template in RT-qPCR assay. For relative quantification of transcripts in each sample, the constitutively expressed *PROTEIN PHOSPHATASE 2A (PP2A)* gene was used as the reference gene in all RT-qPCR experiments. The experiments were performed on a QuantStudio 5 Real-Time PCR System (Applied Biosystems) using the PowerUp[™] SYBR[®] Green Master Mix (Thermo Fisher Scientific). For the negative control, dsDNase digested RNA preparations were used as control template. Gene specific

primers for RT-qPCR were designed manually to generate PCR products sizes of 60-100bp. The quality of the primers was checked through primer efficiency tests and only those primers with an efficiency of 100% were used. RT-qPCR primers used during this work are listed in Supplementary table 1. Components for RT-qPCR are listed below.

Table 10: Components of RT-qPCR reaction

Components	Final concentration	Volume (10 μ l/well)
PowerUp™ SYBR Green Master Mix(2x)	1x	5 μ l
Forward primer (10 μ M)	0.4 μ M	0.4 μ l
Reverse primer (10 μ M)	0.4 μ M	0.4 μ l
Template	-	3.0 μ l (1:10 dilution)
Millipore water	-	1.2 μ l

6.9 Analysis of metabolites from plant tissues and exudates

6.9.1 Preparation of tissue extracts for targeted metabolite profiling

Three tissues per replicate weighing between 3-15 mg were ground using glass beads in a Tissue Lyser II (QIAGEN) bead mill at 25 s⁻¹ for 60 s. The resulting powder was extracted by vigorous shaking for 20 min with 200 μ l of 70 % (v/v) methanol containing 2 nmol L-norvaline as internal standard for quantification of amino acids as well as 5 nmol each of [2,2,4,4-²H] citric acid, [2,3,3-²H] malic acid, and [2,2,3,3-²H] succinic acid as internal standards for quantification of organic acids. After two centrifugations at 10000 \times g for 10 min each, the resulting supernatant was stored at -80° C until further processing.

6.9.2 Analysis of amino acids

Amino acids were analyzed as described by Ziegler et al., (2019). To record the calibration curve, the standard stock solution containing 500 pmol of each amino acid was diluted. For derivatization, 50 μ l of 0.5 M sodium borate buffer pH 7.9 and 100 μ l of a 3 mM Fmoc-Cl solution in acetone was added to 25 μ l of samples. After 5 minutes of incubation, the reaction was extracted three times with 0.5 ml of n-pentane and the organic phase discarded. After removing the organic phase in the last extraction step, remaining organic acid was allowed to evaporate for 10 min. 500 μ l of 5% (v/v) acetonitrile was added to the aqueous phase before loading into the SPE resin. HR-X-resin (50mg/well) was distributed into the 96-well filtration plate. After this, the resin was conditioned by adding 1 ml of methanol followed by 1 ml of water. All the centrifugation steps to pass the liquid through the resin were performed in a JS5.3 swingout rotor in an Avanti J-26XP centrifuge (Beckman Coulter, Fullerton, CA, USA) at 250 \times g for 5 min. The resin was washed with 1 ml of water after loading the samples, followed by eluting with 1 ml of methanol into a 96-deep well plate (Roth, Karlsruhe, Germany). After transferring the eluates to 2 ml Eppendorf tubes, the solvent was evaporated in an Eppendorf Concentrator 5301 at 45° C (Eppendorf, Hamburg, Germany) under vacuum until 150-200 μ l of eluate was left in the tubes. After centrifugation at 10000 \times g for 10 minutes, the samples were transferred to auto sampler vials for LC-MS/MS analysis.

A Zorbax Eclipse Plus C18 Rapid Resolution HD column (50 × 2.1mm, particle size 8 μm; Agilent, Waldbronn, Germany) at 30° C was used to perform the separation using an Agilent 1900 Infinity series HPLC system (Agilent Waldbronn, Germany). Eluents A and B were composed of 0.2 % acetic acid in either water or acetonitrile respectively. The percentage of B was increased from 25% to 50% over the first 6 min, further to 98% in 0.5 min, followed by an isocratic period of 0.5 min at 98% B. Within the next 0.5 min, the starting conditions were restored, followed by column re-equilibration at 25% B for 5 min. The flow rate was set to 0.7 ml/min. The analytes were detected on-line by ESI-MS/MS using an API 3200 triple-quadrupole LC-MS/MS system equipped with an ESI Turbo Ion Spray interface, operated in the negative ion mode (AB Sciex, Darmstadt, Germany). The ion source parameters were set as follows: curtain gas: 30 psi, ion spray voltage: -4500 V, ion source temperature: 350°C, nebulizing and drying gas: 50 psi. Triple-quadrupole scans were acquired in the MRM mode with Q1 and Q3 set at 'unit' resolution. Scheduled MRM was performed with a window of 90 s and a target scan time of 0.5 s. The MRMs for each amino acid are used as mentioned in (Ziegler et al., 2019). The IntelliQuant algorithm of the Analyst 1.6 software (AB Sciex, Darmstadt, Germany) was used to calculate the peak areas automatically and adjusted manually if necessary. Microsoft Excel was used to perform subsequent calculations.

6.9.3 Analysis of organic acids

OAs were analyzed as described by Ziegler et al., (2016). 20μl of root or shoot extracts were evaporated to dryness, methoxylated with 20 μl of 20 mg/ml of methoxyamine in pyridine for one hour at room temperature, and silylated with 35 μl of Silyl 991 for one hour at room temperature. Gas chromatography (GC)-MS/MS analysis was performed using an Agilent 7890 GC system equipped with an Agilent 7000B triple quadrupole mass spectrometer operated in the positive chemical ionization mode (reagent gas: methane, gas flow: 20%, ion source temperature: 230°C). One microliter was injected [pulsed (25 psi) splitless injection, 220°C and separations were performed on a OPTIMA 5 column (10 m×0.25 mm, 0.25 μm, Macherey-Nagel, Düren, Germany) using Helium as a carrier gas (2.39 ml/minute).

The initial temperature of 70° C was held for one minute, followed by increases at 9° C/minute to 150° C and 30° C/minute to 300° C. The final temperature of 300° C was held for 5 minutes. The transfer line was set to a temperature of 250° C, and N₂ and He were used as collision and quench gases, respectively (1.5 and 2.25 ml/minute). Data were acquired by multiple reaction monitoring using compound-specific parameters with Q1 and Q3 set to unit resolution. Peak areas were automatically integrated using the Agile algorithm of the MassHunter Quantitative Analysis software (version B.06.00) and manually adjusted if necessary. All subsequent calculations were performed with Excel,

using the peak areas of the respective internal standards for quantification. MS parameters for MRM-transitions are mentioned in Supplementary table 11.

6.9.4 Organic acid exudation experiments

Seedlings were grown aseptically on agar plates as described in section 6.3.3. Root exudates were collected after 3 days of transfer of seedlings to sufficient (wPi) or insufficient (woPi) conditions. For each genotype, four technical replicates were measured in each treatment. Three seedlings for each biological replicate were carefully lifted with forceps from agar plates and washed with deionized water for 3-5 seconds. The seedlings were then incubated in 300 μ l of deionized water which was filled in each well of 96 well microplate (Greiner Bio-one, Kremsmünster, Germany) ensuring only the roots were dipped in water. After 2 hours of incubation seedlings were harvested by separating roots from shoots and fresh root weights recorded. Exudates from each well were then collected into a 2 ml Eppendorf tube and frozen in liquid nitrogen and stored at -80° C until further processing. For exudate measurements, 150 μ l of root exudate was mixed with 100 pmol each of [2,2,4,4- 2 H] citric acid, [2,3,3- 2 H] malic acid, and [2,2,3,3- 2 H] succinic acid as internal standards and the samples evaporated to dryness. The subsequent steps of derivatization and Gas chromatography (GC)-MS/MS analysis were performed as described before in section 6.9.3.

6.10 Confocal Laser microscopy

Imaging for confocal microscopy was performed with a Zeiss LSM 900 inverted microscope using 20x water immersion objective. The excitation wavelength for Green Fluorescent Protein (GFP) was 488 nm, and emission was detected between 493 and 550 nm. For propidium iodide, excitation wavelength used was 561nm and emission was detected between 578 and 651nm. Zen Software (Zeiss, Jena, Germany) was used to operate the microscope while image processing was performed using the same software and Microsoft PowerPoint. The images shown are representative of one out of three biological experiments. In each biological experiment, at least 6 individual plants for every genotype and condition were imaged.

6.11 Root elongation assay

Seeds were sown on modified ATS medium and stratified for 2 days at 4° C in the dark and the plates placed vertically in a growth chamber at 22° C under illumination for 16 hours daily ($170 \mu\text{mol s}^{-1} \text{m}^{-2}$; Osram LumiluxDeLuxe Cool Daylight L58W/965, Osram, Augsburg, Germany). After six days of growth, seedlings were transferred to fresh plates containing either 2.5 mM KH_2PO_4 (wPi) or 0 μM KH_2PO_4 (woPi) and allowed to grow for additional five days before the images of seedlings growing on the plates were taken. Images were taken using a Nikon camera and primary root elongation was analysed with the ImageJ software (Schneider et al., 2012) with the NeuronJ plugin (Meijering et al., 2004).

6.12 Statistical analysis and data visualization

Three biological replicates were performed, and, in each analyte, data was normalized to wild type values. Significance analyses were performed by Student's *t*-test (two-tailed, equal variances) in GraphPad Prism version 5.04. Bar graphs and students *t*-test (two-tailed, equal variances) were done using GraphPad Prism version 5.04 while generation of heat maps for amino acids visualization and two-way ANOVA analysis were done using the MultiExperiment Viewer (MEV) software (Saeed et al., 2003).

7.0 REFERENCES

- Abel, S. (2011). Phosphate sensing in root development. *Current Opinion in Plant Biology*, 14 (3), 303-309.
- Abel, S. (2017). Phosphate scouting by root tips. *Current Opinion in Plant Biology*, 39, 168-177.
- Aerts, R. (1999). Interspecific competition in natural plant communities: mechanisms, trade-offs and plant-soil feedbacks. *Journal of Experimental Botany*, 50 (330), 29-37.
- Agarie, S., Miura, A., Sumikura, R., Tsukamoto, S., Nose, A., Arima, S., Matsuoka, M., & Miyao-Tokutomi, M. (2002). Overexpression of C4 PEPC caused O₂-insensitive photosynthesis in transgenic rice plants. *Plant Science*, 162 (2), 257-265.
- Akram, M. (2014). Citric acid cycle and role of its intermediates in metabolism. *Cell Biochemistry and Biophysics*, 68 (3), 475-478.
- Aoki, M., Fujii, K., & Kitayama, K. (2012). Environmental control of root exudation of low-molecular weight organic acids in tropical rainforests. *Ecosystems*, 15, 1194-1203.
- Bakrim, N., Brulfert, J., Vidal, J., & Chollet, R. (2001). Phosphoenolpyruvate carboxylase kinase is controlled by a similar signaling cascade in CAM and C (4) plants. *Biochemical and Biophysical Research Communications*, 286 (5), 1158-1162. <https://doi.org/10.1006/bbrc.2001.5527>.
- Balzerque, C., Darteville, T., Godon, C., Laugier, E., Meisrimler, C., Teulon, J.M., Creff, A., Bissler, M., Bouchoud, C., & Hagège, A. (2017). Low phosphate activates STOP1-ALMT1 to rapidly inhibit root cell elongation. *Nature Communications*, 8 (1), 15300.
- Bates, T.R., & Lynch, J.P (1996). Stimulation of root hair elongation in *Arabidopsis thaliana* by low phosphorus availability. *Plant, Cell & Environment*, 19 (5), 529-538.
- Beaujean, A., Issakidis-Bourguet, E., Catterou, M., Dubois, F., Sangwan, R.S, & Sangwan-Norreel, B.S. (2001). Integration and expression of Sorghum C (4) phosphoenolpyruvate carboxylase and chloroplastic NADP (+) malate dehydrogenase separately or together in C (3) potato plants (1). *Plant Science*, 160 (6), 1199-1210.
- Bechtaoui, N., Rabiou, M.K., Raklami, A., Oufdou, K., Hafidi, M., & Jemo, M. (2021). Phosphate-dependent regulation of growth and stresses management in plants. *Frontiers in Plant Science*, 12, 679916.
- Begum, H.H., Osaki, M., Shinano, T., Miyatake, H., Wasaki, J., Yamamura, T., & Watanabe T., (2005). The function of a maize-derived phosphoenolpyruvate carboxylase (PEPC) in phosphorus-deficient transgenic rice. *Soil Science and Plant Nutrition*, 51 (4), 497-506. <https://doi.org/10.1111/j.1747-0765.2005.tb00058.x>.

- Begum, H.H., Osaki, M., Watanabe, T., & Shinano, T. (2009). Mechanisms of aluminum tolerance in phosphoenolpyruvate carboxylase transgenic rice. *Journal of Plant Nutrition*, 32 (1), 84-96. <https://doi.org/10.1080/01904160802531035>.
- Benitez-Alfonso, Y., Cilia, M., Roman, A. S., Thomas, C., Maule, A., Hearn, S., & Jackson, D. (2009). Control of Arabidopsis meristem development by thioredoxin-dependent regulation of intercellular transport. *Proceedings of the National Academy of Sciences*, 106 (9), 3615-3620.
- Blonde, J.D., & Plaxton, W.C. (2003). Structural and kinetic properties of high and low molecular mass phosphoenolpyruvate carboxylase isoforms from the endosperm of developing castor oilseeds. *The Journal of Biological Chemistry*, 278 (14), 11867-11873.
- Borland A.M., Hartwell, J., Jenkins, G.I., Wilkins, M.B., & Nimmo, H.G. (1999). Metabolite control overrides circadian regulation of phosphoenolpyruvate carboxylase kinase and CO₂ fixation in crassulacean acid metabolism. *Plant Physiology*, 121 (3), 889-896.
- Buchanan-Bollig, I.C., & Smith, J.A. (1984). Circadian rhythms in crassulacean acid metabolism: Phase relationships between gas exchange, leaf water relations and malate metabolism in *Kalanchoë daigremontiana*. *Planta*, 161 (4), 314-319. <https://doi.org/10.1007/BF00398721>.
- Bustos, R., Castrillo, G., Linhares, F., Puga, M.I., Rubio, V., Pérez-Pérez, J., Solano, R., Leyva, A., & Paz-Ares, J. (2010). A central regulatory system largely controls transcriptional activation and repression responses to phosphate starvation in Arabidopsis. *PLoS Genetics*, 6 (9), e1001102. <https://doi.org/10.1371/journal.pgen.1001102>.
- Caburatan, L., & Park, J. (2021). Differential expression, tissue-specific distribution, and posttranslational controls of phosphoenolpyruvate carboxylase. *Plants*, 10 (9), 1887.
- Carter, P.J., Nimmo, H.G., Fewson, C.A., & Wilkins, M.B. (1991). Circadian rhythms in the activity of a plant protein kinase. *The EMBO Journal*, 10 (8), 2063-2068. <https://doi.org/10.1002/j.1460-2075.1991.tb07737.x>.
- Carvalhais, L.C., Dennis, P.G., Fedoseyenko, D., Hajirezaei, M.R., Borriss, R., & Wirén, N. (2011). Root exudation of sugars, amino acids, and organic acids by maize as affected by nitrogen, phosphorus, potassium, and iron deficiency. *Journal of Plant Nutrition and Soil Science*, 174 (1), 3-11. <https://doi.org/10.1002/jpln.201000085>.
- Cheffings, C.M., Pantoja, O., Ashcroft, F.M., & Smith, J. (1997). Malate transport and vacuolar ion channels in CAM plants. *Journal of Experimental Botany*, 48, 623-631. <https://doi.org/10.1093/jxb/48>.

- Chen, Z.H., Nimmo, G.A., Jenkins, G.I., & Nimmo, H.G. (2007). Bhlh32 modulates several biochemical and morphological processes that respond to Pi starvation in Arabidopsis. *The Biochemical Journal*, 405 (1), 191-198. <https://doi.org/10.1042/BJ20070102>.
- Choi, J.M., Latigui, A., & Lee, C.W. (2013). Visual symptom and tissue nutrient contents in dry matter and petiole sap for diagnostic criteria of phosphorus nutrition for 'Seolhyang' strawberry cultivation. *Horticulture, Environment, and Biotechnology*, 54, 52-57.
- Chollet, R., Vidal, J., & O'Leary, M.H. (1996). Phosphoenolpyruvate carboxylase: A ubiquitous, highly regulated enzyme in plants. *Annual Review of Plant Physiology and Plant Molecular Biology*, 47, 273-298. <https://doi.org/10.1146/annurev.arplant.47.1.273>.
- Chutia, R. (2019). Manipulation of malate biosynthesis and exudation in Arabidopsis thaliana.
- Clough, S.J., & Bent, A.F. (1998). Floral dip: A simplified method for Agrobacterium-mediated transformation of Arabidopsis thaliana. *The Plant Journal*, 16 (6), 735-743.
- Cordell, D. (2010). The Story of Phosphorus: Sustainability implications of global phosphorus scarcity for food security. EndNote Tagged Import Format.
- Correll, D.L. (1998). The Role of Phosphorus in the Eutrophication of Receiving Waters: A Review. *Journal of Environmental Quality*, 27 (2), 261-266.
- Cruz-Ramírez, A., Oropeza-Aburto, A., Razo-Hernández, F., Ramírez-Chávez, E., & Herrera-Estrella, L. (2006). Phospholipase DZ2 plays an important role in extraplastidic galactolipid biosynthesis and phosphate recycling in Arabidopsis roots. *Proceedings of the National Academy of Sciences*, 103 (17), 6765-6770.
- Dalziel, K.J., O'Leary B., Brikis C., Rao, S.K., She, Y.M., Terry Cyr T., & Plaxton, W. (2012). The bacterial-type phosphoenolpyruvate carboxylase isozyme from developing castor oil seeds is subject to in vivo regulatory phosphorylation at serine 451. *FEBS Letters*, 586 (7), 1049-1054.
- Delgado, M., Zúñiga-Feest, A., Alvear, M., & Borie, F. (2013). The effect of phosphorus on cluster-root formation and functioning of *Embothrium coccineum*. *Plant and Soil*, 373, 765-773.
- Delhaize, E., Ryan, P.R., Hebb, D.M., Yamamoto, Y., Sasaki, T., & Matsumoto, H. (2004). Engineering high-level aluminum tolerance in barley with the *ALMT1* gene. *Proceedings of the National Academy of Sciences*, 101 (42), 15249-15254.
- Dilkes, N.B., Jones, D.L., & Farrar, J. (2004). Temporal dynamics of carbon partitioning and rhizodeposition in wheat. *Plant Physiology*, 134 (2), 706-715.

- Dinkelaker, B., Hengeler, C., & Marschner, H. (1995). Distribution and function of proteoid roots and other root clusters. *Botanica Acta*, *108* (3), 183-200. <https://doi.org/10.1111/j.1438-8677.1995.tb00850.x>
- Dong, D., Peng X., & Yan, X. (2004). Organic acid exudation induced by phosphorus deficiency and/or aluminum toxicity in two contrasting soybean genotypes. *Physiologia Plantarum*, *122* (2), 190-199.
- Dong, P., Li, X., Yang, H., Liu, Y., Murphy, A.S., Kochian, L.V., & Liu, D. (2017). An Arabidopsis ABC transporter mediates phosphate deficiency-induced remodeling of root architecture by modulating iron homeostasis in roots. *Molecular Plant*, *10* (2), 244-259.
- Dong, J., Ma, G., Sui, L., Wei, M., Satheesh, V., Zhang, R., Ge, S., Li, J., Zhang, T.E., & Wittwer, C. (2019). Inositol pyrophosphate InsP8 acts as an intracellular phosphate signal in Arabidopsis. *Molecular Plant*, *12* (11), 1463-1473.
- Dong, L., Ermolova, N.V., & Chollet, R. (2001). Partial purification and biochemical characterization of a heteromeric protein phosphatase 2A holoenzyme from maize (*Zea mays L.*) leaves that dephosphorylates C4 phosphoenolpyruvate carboxylase. *Planta*, *213* (3), 379-389. <https://doi.org/10.1007/s004250100604>.
- Dornfeld, K., Madden, M., Skildum, A., & Wallace, K.B. (2015). Aspartate facilitates mitochondrial function, growth arrest and survival during doxorubicin exposure. *Cell Cycle*, *14* (20), 3282-3291. <https://doi.org/10.1080/15384101.2015.1087619>.
- Doubnerová, V.H., Miedzińska, L., Dobrá, J., Vankova, R., & Ryšlavá H. (2014). Phosphoenolpyruvate carboxylase, NADP-malic enzyme, and pyruvate, phosphate dikinase are involved in the acclimation of *Nicotiana tabacum L.* to drought stress. *Journal of Plant Physiology*, *171* (5), 19-25. <https://doi.org/10.1016/j.jplph.2013.10.017>
- Driscoll, B.T., & Finan, T.M. (1993). NAD⁺ dependent malic enzyme of *Rhizobium meliloti* is required for symbiotic nitrogen fixation. *Molecular Microbiology*, *7* (6), 865-873.
- Duff, S., & Chollet, R. (1995). In Vivo regulation of wheat-leaf phosphoenolpyruvate carboxylase by reversible phosphorylation. *Plant Physiology*, *107*(3), 775-782.
- Durall, C., & Lindblad, P. (2015). Mechanisms of carbon fixation and engineering for increased carbon fixation in cyanobacteria. *Algal Research*, *11*, 263-270.
- Durrett, T.P., Gassmann, W., & Rogers, E.E. (2007). The FRD3-mediated efflux of citrate into the root vasculature is necessary for efficient iron translocation. *Plant Physiology*, *144*(1), 197-205. <https://doi.org/10.1104/pp.107.097162>.

- Engelmann, S., Bläsing, O.E., Gowik, U., Svensson, P., & Westhoff, P. (2003). Molecular evolution of C4 phosphoenolpyruvate carboxylase in the genus *Flaveria*. A gradual increase from C3 to C4 characteristics. *Planta*, *217* (5), 717-725. <https://doi.org/10.1007/s00425-003-1045-0>.
- Etienne, A., Génard, M., Lobit, P., Mbeguié-A.D., & Bugaud, C. (2013). What controls fleshy fruit acidity? A review of malate and citrate accumulation in fruit cells. *Journal of Experimental Botany*, *64* (6), 1451-1469. <https://doi.org/10.1093/jxb/ert035>.
- Fan, Z., Li, J., Lu, M., Li, X., & Yin, H. (2013). Overexpression of phosphoenolpyruvate carboxylase from *Jatropha curcas* increases fatty acid accumulation in *Nicotiana tabacum*. *Acta Physiologiae Plantarum*, *35*, 2269-2279.
- Feria, A.B., Bosch, N., Sánchez, A., Nieto-Ingelmo, A.I., La Osa, C., Echevarría, C., García-Mauriño, S., & Monreal, J.A. (2016). Phosphoenolpyruvate carboxylase (PEPC) and PEPC-kinase (PEPC-k) isoenzymes in *Arabidopsis thaliana*: Role in control and abiotic stress conditions. *Planta*, *244* (4), 901-913. <https://doi.org/10.1007/s00425-016-2556-9>
- Feria, A.B., Ruíz-Ballesta, I., Baena, G., Ruíz-López, N., Echevarría, C., & Vidal, J. (2022). Phosphoenolpyruvate carboxylase and phosphoenolpyruvate carboxylase kinase isoenzymes play an important role in the filling and quality of *Arabidopsis thaliana* seed. *Plant Physiology and Biochemistry*, *190*, 70-80. <https://doi.org/10.1016/j.plaphy.2022.08.012>.
- Fernie, A.R., Carrari, F., & Sweetlove L.J. (2004). Respiratory metabolism: glycolysis, the TCA cycle and mitochondrial electron transport. *Current Opinion in Plant Biology*, *7* (3), 254-261. <https://doi.org/10.1016/j.pbi.2004.03.007>.
- Fonseca, H.M., & Berbara, R.L. (2008). Does *Lunularia cruciata* form symbiotic relationships with either *Glomus proliferum* or *G. intraradices*? *Mycological Research*, *112* (9), 1063-1068.
- Fontaine, V., Hartwell, J., Jenkins, G.I., & Nimmo, H.G. (2002). *Arabidopsis thaliana* contains two phosphoenolpyruvate carboxylase kinase genes with different expression patterns. *Plant, Cell & Environment*, *25* (1), 115-122. <https://doi.org/10.1046/j.0016-8025.2001.00805.x>.
- Fontecha, G., Silva-Navas, J., Benito, C., Mestres, M.A., Espino, F.J., Hernández-Riquer, M.V., & Gallego, F.J. (2007). Candidate gene identification of an aluminum-activated organic acid transporter gene at the Alt4 locus for aluminum tolerance in rye (*Secale cereale* L.). *TAG. Theoretical and Applied Genetics. Theoretische Und Angewandte Genetik*, *114* (2), 249-260. <https://doi.org/10.1007/s00122-006-0427-7>.
- Fukao, Y. (2015). Discordance between protein and transcript levels detected by selected reaction monitoring. *Plant Signaling & Behavior*, *10* (5), e1017697.

- Fukayama, H., Hatch, M.D., Tamai, T., Tsuchida, H., Sudoh, S., Furbank, R.T., & Miyao, M. (2003). Activity regulation and physiological impacts of maize C4-specific phosphoenolpyruvate carboxylase overproduced in transgenic rice plants. *Photosynthesis Research*, 77 (2), 227-239. <https://doi.org/10.1023/A:1025861431886>.
- Fukayama, H., Tamai, T., Taniguchi, Y., Sullivan, S., Miyao, M., & Nimmo, H.G. (2006). Characterization and functional analysis of phosphoenolpyruvate carboxylase kinase genes in rice. *The Plant Journal*, 47 (2), 258-268. <https://doi.org/10.1111/j.1365-313X.2006.02779.x>.
- Furukawa, J., Yamaji, N., Wang, H., Mitani, N., Murata, Y., Sato, K., Katsuhara, M., Takeda, K., & Ma, J.F. (2007). An aluminum-activated citrate transporter in barley. *Plant & Cell Physiology*, 48 (8), 1081-1091. <https://doi.org/10.1093/pcp/pcm091>.
- Furumoto, T., Izui, K., Quinn, V., Furbank, R.T., & Caemmerer, S. (2007). Phosphorylation of phosphoenolpyruvate carboxylase is not essential for high photosynthetic rates in the C4 species *Flaveria bidentis*. *Plant Physiology*, 144 (4), 1936-1945.
- Gardner, W.K., Barber D., & Parbery, D.G. (1983). The acquisition of phosphorus by *Lupinus albus* L. III. The probable mechanism by which phosphorus movement in the soil/root interface is enhanced. *Plant and Soil*, 70, 107-124.
- Gardner, W.K., Parbery, D.G., & Barber D. (1981). Proteoid root morphology and function in *Lupinus albus*. *Plant and Soil*, 60, 143-147.
- Gehlen, J., Panstruga, R., Smets, H., Merkelbach, S., Kleines, M., Porsch, P., Fladung, M., Becker, I., Rademacher, T., Häusler, R.E., & Hirsch, H.J. (1996). Effects of altered phosphoenolpyruvate carboxylase activities on transgenic C3 plant *Solanum tuberosum*. *Plant Molecular Biology*, 32 (5), 831-848. <https://doi.org/10.1007/BF00020481>.
- Geigenberger, P., & Fernie, A.R. (2014). Metabolic control of redox and redox control of metabolism in plants. *Antioxidants & Redox Signaling*, 21 (9), 1389-1421.
- Gennidakis, S., Rao, S., Greenham, K., Uhrig, R.G., O'Leary, B., Snedden, W.A., Lu, C., & Plaxton, W.C. (2007). Bacterial and plant-type phosphoenolpyruvate carboxylase polypeptides interact in the hetero-oligomeric Class-2 PEPC complex of developing castor oil seeds. *The Plant Journal*, 52 (5), 839-849. <https://doi.org/10.1111/j.1365-313X.2007.03274.x>.
- Gregory, A.L., Hurley, B.A., Tran, H.T., Valentine, A.J., She, Y.M., Knowles, V.L., & Plaxton, W.C. (2009). In vivo regulatory phosphorylation of the phosphoenolpyruvate carboxylase AtPPC1 in phosphate-starved *Arabidopsis thaliana*. *The Biochemical Journal*, 420 (1), 57-65. <https://doi.org/10.1042/BJ20082397>.

- Guimaraes, J.C., Rocha, M., & Arkin, A.P. (2014). Transcript level and sequence determinants of protein abundance and noise in *Escherichia coli*. *Nucleic Acids Research*, 42 (8), 4791-4799. <https://doi.org/10.1093/nar/gku126>.
- Haes, H.U. de, Jansen, J., van der Weijden, & Smit, W. (2009). Phosphate from surplus to shortage. Policy Memorandum of the Steering Committee for Technology Assessment. Utrecht: Ministry of Agriculture, Nature and Food Quality.
- Härtel, H., Dörmann, P., & Benning, C. (2000). DGD1-independent biosynthesis of extraplasmidic galactolipids after phosphate deprivation in *Arabidopsis*. *Proceedings of the National Academy of Sciences*, 97 (19), 10649-10654.
- Hartwell, J., Nimmo, G.A., Wilkins, M.B., Jenkins, G.I., & Nimmo, H.G. (2002). Probing the circadian control of phosphoenolpyruvate carboxylase kinase expression in *Kalanchoë fedtschenkoi*. *Functional Plant Biology: FPB*, 29 (6), 663-668.
- Hartwell, J., Gill, A., Nimmo, G.A., Wilkins, M.B., Jenkins, G.I., & Nimmo, H.G. (1999). Phosphoenolpyruvate carboxylase kinase is a novel protein kinase regulated at the level of expression. *The Plant Journal*, 20 (3), 333-342. <https://doi.org/10.1046/j.1365-3113x.1999.t01-1-00609.x>.
- Hatch, M. (1987). C4 photosynthesis: A unique blend of modified biochemistry, anatomy and ultrastructure. *Biochimica Et Biophysica Acta (BBA) - Reviews on Bioenergetics*, 895 (2), 81-106. [https://doi.org/10.1016/S0304-4173\(87\)80009-5](https://doi.org/10.1016/S0304-4173(87)80009-5).
- Häusler, R.E., Hirsch, H.J., Kreuzaler, F., & Peterhänsel, C. (2002). Overexpression of C4-cycle enzymes in transgenic C3 plants: a biotechnological approach to improve C3-photosynthesis. *Journal of Experimental Botany*, 53 (369), 591-607.
- Helariutta, Y., Fukaki, H., Wysocka-Diller, J., Nakajima, K., Jung, J., Sena, G., Hauser, M.T., & Benfey, P.N. (2000). The SHORT-ROOT gene controls radial patterning of the *Arabidopsis* root through radial signaling. *Cell*, 101 (5), 555-567.
- Hell, R., & Stephan, U.W. (2003). Iron uptake, trafficking and homeostasis in plants. *Planta*, 216 (4), 541-551. <https://doi.org/10.1007/s00425-002-0920-4>.
- Hinsinger, P. (2001). Bioavailability of soil inorganic P in the rhizosphere as affected by root-induced chemical changes: a review. *Plant and Soil*, 237 (2), 173-195.
- Hochholdinger, F., Woll, K., Sauer, M., & Dembinsky, D. (2004). Genetic dissection of root formation in maize (*Zea mays*) reveals root-type specific developmental programmes. *Annals of Botany*, 93 (4), 359-368. <https://doi.org/10.1093/aob/mch056>.

- Hoehenwarter, W., Mönchgesang, S., Neumann, S., Majovsky, P., Abel, S., & Müller, J. (2016). Comparative expression profiling reveals a role of the root apoplast in local phosphate response. *BMC Plant Biology*, *16*, 1-21.
- Hoekenga, O.A., Maron, L.G., Piñeros, M.A., Cançado, G.M.A., Shaff, J., Kobayashi, Y., Ryan, P.R., Dong, B., Delhaize, E., Sasaki, T., Matsumoto, H., Yamamoto, Y., Koyama, H., & Kochian, L.V. (2006). AtALMT1, which encodes a malate transporter, is identified as one of several genes critical for aluminum tolerance in Arabidopsis. *Proceedings of the National Academy of Sciences*, *103* (25), 9738-9743. <https://doi.org/10.1073/pnas.0602868103>.
- Hudspeth, R.L., Grula, J.W., Dai, Z., Edwards, G.E., & Ku, M.S. (1992). Expression of maize phosphoenolpyruvate carboxylase in transgenic tobacco: Effects on biochemistry and physiology. *Plant Physiology*, *98* (2), 458-464. <https://doi.org/10.1104/pp.98.2.458>.
- Igamberdiev, A.U., & Eprintsev, A.T. (2016). Organic acids: the pools of fixed carbon involved in redox regulation and energy balance in higher plants. *Frontiers in Plant Science*, *7*, 1042.
- Izui, K., Matsumura, H., Furumoto, T., & Kai, Y. (2004). Phosphoenolpyruvate carboxylase: A new era of structural biology. *Annual Review of Plant Biology*, *55*, 69-84.
- Jain, A., Vasconcelos, M.J., Raghothama, K.G., & Sahi, S.V. (2007). Molecular mechanisms of plant adaptation to phosphate deficiency. *Plant Breeding Reviews*, *29*, 359.
- Jiao, J.A., & Chollet, R. (1991). Posttranslational regulation of phosphoenolpyruvate carboxylase in C (4) and crassulacean acid metabolism plants. *Plant Physiology*, *95* (4), 981-985. <https://doi.org/10.1104/pp.95.4.981>
- Johnson, J.F., Vance, C.P., & Allan, D.L. (1996). Phosphorus Deficiency in *Lupinus albus*. Altered lateral root development and enhanced expression of phosphoenolpyruvate carboxylase. *Plant Physiology*, *112* (1), 31-41. <https://doi.org/10.1104/pp.112.1.31>.
- Johnson, J.F., Allan, D.L., & Vance, C.P. (1994). Phosphorus stress-induced proteoid roots show altered metabolism in *Lupinus albus*. *Plant Physiology*, *104* (2), 657-665.
- Jones, D.L., & Brassington, D.S. (1998). Sorption of organic acids in acid soils and its implications in the rhizosphere. *European Journal of Soil Science*, *49* (3), 447-455.
- Kai, Y., Matsumura, H., Inoue, T., Terada, K., Nagara, Y., Yoshinaga, T., Kihara, A., Tsumura, K., & Izui, K. (1999). Three-dimensional structure of phosphoenolpyruvate carboxylase: A proposed mechanism for allosteric inhibition. *Proceedings of the National Academy of Sciences*, *96* (3), 823-828. <https://doi.org/10.1073/pnas.96.3.823>.

- Kandoi, D., Mohanty, S., Govindjee, & Tripathy, B. C. (2016). Towards efficient photosynthesis: overexpression of *Zea mays* phosphoenolpyruvate carboxylase in *Arabidopsis thaliana*. *Photosynthesis Research*, 130 (1), 47-72. <https://doi.org/10.1007/s11120-016-0224-3>.
- Kanno, S., Arrighi, J.F., Chiarenza, S., Bayle, V., Berthomé, R., Péret, B., Javot, H., Delannoy, E., Marin, E., Nakanishi, T.M., Thibaud, M.C., & Nussaume, L. (2016). A novel role for the root cap in phosphate uptake and homeostasis. *ELife*, 5, e14577.
- Kanobe, M.N., Rodermel, S.R., Bailey, T., & Scott, M.P. (2013). Changes in endogenous gene transcript and protein levels in maize plants expressing the soybean ferritin transgene. *Frontiers in Plant Science*, 4, 196. <https://doi.org/10.3389/fpls.2013.00196>.
- Karimi, M., Inzé, D., & Depicker, A. (2002). Gateway vectors for Agrobacterium-mediated plant transformation. *Trends in Plant Science*, 7 (5), 193-195. [https://doi.org/10.1016/s1360-1385\(02\)02251-3](https://doi.org/10.1016/s1360-1385(02)02251-3).
- Karimi, M., Meyer, B., & Hilson, P. (2005). Modular cloning in plant cells. *Trends in Plant Science*, 10 (3), 103-105. <https://doi.org/10.1016/j.tplants.2005.01.008>
- Kochian, L.V., Hoekenga, O.A., & Pineros, M.A. (2004). How do crop plants tolerate acid soils? Mechanisms of aluminum tolerance and phosphorous efficiency. *Annual Review of Plant Biology*, 55, 459-493.
- Kogami, H., Shono, M., Koike, T., Yanagisawa, S., Izui, K., Sentoku, N., Tanifuji, S., Uchimiya, H., & Toki, S. (1994). Molecular and physiological evaluation of transgenic tobacco plants expressing a maize phosphoenolpyruvate carboxylase gene under the control of the cauliflower mosaic virus 35S promoter. *Transgenic Research*, 3 (5), 287-296.
- Koncz, C., & Schell, J. (1986). The promoter of TL-DNA gene 5 controls the tissue-specific expression of chimeric genes carried by a novel type of Agrobacterium binary vector. *Molecular and General Genetics MGG*, 204 (3), 383-396. <https://doi.org/10.1007/BF00331014>.
- Kopriva, S., & Chu, C. (2018). Are we ready to improve phosphorus homeostasis in rice? *Journal of Experimental Botany*, 69 (15), 3515-3522. <https://doi.org/10.1093/jxb/ery163>.
- Koussounadis, A., Langdon, S.P., Um, I.H., Harrison, D.J., & Smith, V.A. (2015). Relationship between differentially expressed mRNA and mRNA-protein correlations in a xenograft model system. *Scientific Reports*, 5 (1), 10775. <https://doi.org/10.1038/srep10775>.
- Koyama, H., Okawara, R., Ojima, K., & Yamaya, T. (1988). Re-evaluation of characteristics of a carrot cell line previously selected as aluminum tolerant cells. *Physiologia Plantarum*, 74 (4), 683-687.

- Krishnapriya, V., & Pandey, R. (2016). Root exudation index: screening organic acid exudation and phosphorus acquisition efficiency in soybean genotypes. *Crop and Pasture Science*, *67* (10), 1096-1109.
- Kuroda, T., & Tsuchiya, T. (2009). Multidrug efflux transporters in the MATE family. *Biochimica Et Biophysica Acta*, *1794* (5), 763-768. <https://doi.org/10.1016/j.bbapap.2008.11.012>.
- Lambers, H., & Plaxton, W.C. (2018). Phosphorus: back to the roots. *Annu Plant Rev*, *48*: 3-22.
- Lambers, H, Shane, M.W., Cramer, M.D., Pearse, S.J., & Veneklaas, E.J. (2006). Root structure and functioning for efficient acquisition of phosphorus: matching morphological and physiological traits. *Annals of Botany*, *98* (4), 693-713.
- Larsen, S., & Gunary, D. (1961). Phosphate requirement of lupins grown as a pioneer crop on Culm measure soil with impeded drainage. *Nature*, *189* (4765), 691.
- Lepiniec, L., Keryer, E., Philippe, H., Gadal, P., & Crépin, C. (1993). Sorghum phosphoenolpyruvate carboxylase gene family: Structure, function and molecular evolution. *Plant Molecular Biology*, *21* (3), 487-502. <https://doi.org/10.1007/BF00028806>.
- Li, B. & Chollet, R. (1993). Resolution and identification of C4 phosphoenolpyruvate carboxylase protein kinase polypeptides and their reversible light activation in maize leaves. *Archives of Biochemistry and Biophysics*, *307* (2), 416-419. <https://doi.org/10.1006/abbi.1993.1609>.
- Li, B. & Chollet, R. (1994). Salt induction and the partial purification/characterization of phosphoenolpyruvate carboxylase protein-serine kinase from an inducible crassulacean-acid-metabolism (cam) plant, *Mesembryanthemum crystallinum* L. *Archives of Biochemistry and Biophysics*, *314* (1), 247-254. <https://doi.org/10.1006/abbi.1994.1437>.
- Li, Z., & Chollet, R. (1996). Phosphoenolpyruvate carboxylase kinase in tobacco leaves is activated by light in a similar but not identical way as in maize. *Plant Physiology*, *111* (2), 497-505. <https://doi.org/10.1104/pp.111.2.497>.
- Li, M., Qin, C., Welti, R., & Wang, X. (2006). Double knockouts of phospholipases D ζ 1 and D ζ 2 in Arabidopsis affect root elongation during phosphate-limited growth but do not affect root hair patterning. *Plant Physiology*, *140* (2), 761-770.
- Li, M., Welti, R., & Wang, X. (2006). Quantitative profiling of Arabidopsis polar glycerolipids in response to phosphorus starvation. Roles of phospholipases D ζ 1 and D ζ 2 in phosphatidylcholine hydrolysis and digalactosyldiacylglycerol accumulation in phosphorus-starved plants. *Plant Physiology*, *142* (2), 750-761.

- Lian, L., Wang, X., Zhu, Y., He, W., Cai, Q., Xie, H., Zhang, M., & Zhang, J. (2014). Physiological and photosynthetic characteristics of indica Hang2 expressing the sugarcane PEPC gene. *Molecular Biology Reports*, *41* (4), 2189-2197. <https://doi.org/10.1007/s11033-014-3070-4>.
- Ligaba, A., Katsuhara, M., Ryan, P.R., Shibasaki, M., & Matsumoto, H. (2006). The BnALMT1 and BnALMT2 genes from rape encode aluminum-activated malate transporters that enhance the aluminum resistance of plant cells. *Plant Physiology*, *142* (3), 1294-1303. <https://doi.org/10.1104/pp.106.085233>.
- Lin, W.Y., Huang, T.K., Leong, S.J., & Chiou, T.J. (2014). Long-distance call from phosphate: systemic regulation of phosphate starvation responses. *Journal of Experimental Botany*, *65* (7), 1817-1827.
- Liu, J., Magalhaes, J.V., Shaff, J., & Kochian, L.V. (2009). Aluminum-activated citrate and malate transporters from the MATE and ALMT families function independently to confer Arabidopsis aluminum tolerance. *The Plant Journal*, *57* (3), 389-399. <https://doi.org/10.1111/j.1365-313X.2008.03696.x>.
- Liu, D., Hu, R., Zhang, J., Guo, H.B., Cheng, H., Li, L., Borland, A.M., Qin, H., Chen, J.G., Muchero, W., Tuskan, G.A., & Yang, X. (2021). Overexpression of Agave phosphoenolpyruvate carboxylase improves plant growth and stress tolerance. *Cells*, *10* (3). <https://doi.org/10.3390/cells10030582>.
- Liu, Y., Villalba, G., Ayres, R.U., & Schroder, H. (2008). Global Phosphorus flows and environmental impacts from a consumption perspective. *Journal of Industrial Ecology*, *12* (2), 229-247. <https://doi.org/10.1111/j.1530-9290.2008.00025.x>.
- López-Arredondo, D.L., Leyva-González, M.A., González-Morales, S.I., López-Bucio, J., & Herrera-Estrella, L. (2014). Phosphate nutrition: improving low-phosphate tolerance in crops. *Annual Review of Plant Biology*, *65*, 95-123.
- López-Bucio, J., Nieto-Jacobo, M.F., Ramírez-Rodríguez, V.V., & Herrera-Estrella, L. (2000). Organic acid metabolism in plants: From adaptive physiology to transgenic varieties for cultivation in extreme soils. *Plant Science*, *160* (1), 1-13. [https://doi.org/10.1016/s0168-9452\(00\)00347-2](https://doi.org/10.1016/s0168-9452(00)00347-2).
- López-Millán, A.F., Morales, F., Abadía, A., & Abadía, J. (2000). Effects of iron deficiency on the composition of the leaf apoplastic fluid and xylem sap in sugar beet. Implications for iron and carbon transport. *Plant Physiology*, *124* (2), 873-884.
- Lynch, J.P. (1995). Root architecture and plant productivity. *Plant Physiology*, *109* (1), 7-13.

- Lynch, J.P., & Whipps, J.M. (1990). Substrate flow in the rhizosphere. *Plant and Soil*, 129 (1), 1-10. <https://doi.org/10.1007/BF00011685>
- Lynch, J.P., & Brown, K.M. (2008). Root strategies for phosphorus acquisition. In *The ecophysiology of plant-phosphorus interactions* pp. 83-116. Springer.
- Macias-Benitez, S., Garcia-Martinez, A.M., Caballero Jimenez, P., Gonzalez, J.M., Tejada Moral, M., & Parrado Rubio, J. (2020). Rhizospheric organic acids as biostimulants: Monitoring feedback on soil microorganisms and biochemical properties. *Frontiers in Plant Science*, 11. <https://doi.org/10.3389/fpls.2020.00633>.
- Magalhaes, J.V., Liu, J., Guimarães, C.T., Lana, U.G.P., Alves, V.M.C., Wang, Y.H., Schaffert, R. E., Hoekenga, O.A., Piñeros, M.A., Shaff, J.E., Klein, P.E., Carneiro, N.P., Coelho, C.M., Trick, H.N., & Kochian, L.V. (2007). A gene in the multidrug and toxic compound extrusion (MATE) family confers aluminum tolerance in sorghum. *Nature Genetics*, 39 (9), 1156-1161. <https://doi.org/10.1038/ng2074>.
- Maier, T., Güell, M., & Serrano, L. (2009). Correlation of mRNA and protein in complex biological samples. *FEBS Letters*, 583 (24), 3966-3973.
- Malhotra, H., Vandana, Sharma, S., & Pandey, R. (2018). Phosphorus nutrition: Plant growth in response to deficiency and excess. *Plant Nutrients and Abiotic Stress Tolerance* pp. 171-190. Springer Singapore. https://doi.org/10.1007/978-981-10-9044-8_7.
- Mallhi, Z.I., Rizwan, M., Mansha, A., Ali, Q., Asim, S., Ali, S., Hussain, A., Alrokayan, S.H., Khan, H.A., Alam, P., & Ahmad, P. (2019). Citric acid enhances plant growth, photosynthesis, and phytoextraction of lead by alleviating the oxidative stress in castor beans. *Plants*, 8 (11). <https://doi.org/10.3390/plants8110525>.
- Mamedov, T.G., Moellering, E.R., & Chollet, R. (2005). Identification and expression analysis of two inorganic C and N responsive genes encoding novel and distinct molecular forms of eukaryotic phosphoenolpyruvate carboxylase in the green microalga *Chlamydomonas reinhardtii*. *The Plant Journal*, 42 (6), 832-843. <https://doi.org/10.1111/j.1365-313X.2005.02416.x>.
- Maron, L.G., Piñeros, M.A., Guimarães, C.T., Magalhaes, J.V., Pleiman, J.K., Mao, C., Shaff, J., Belicuas, S.N.J., & Kochian, L.V. (2010). Two functionally distinct members of the MATE (multi-drug and toxic compound extrusion) family of transporters potentially underlie two major aluminum tolerance QTLs in maize. *The Plant Journal*, 61 (5), 728-740. <https://doi.org/10.1111/j.1365-313X.2009.04103.x>.
- Marsh, J.T., Sullivan, S., Hartwell, J., & Nimmo, H.G. (2003). Structure and expression of phosphoenolpyruvate carboxylase kinase genes in solanaceae. A novel gene exhibits alternative splicing. *Plant Physiology*, 133 (4), 2021-2028. <https://doi.org/10.1104/pp.103.030775>.

- Martínez-Cuenca, M.R., Iglesias, D. J., Talón, M., Abadía, J., López-Millán, A.F., Primo-Millo, E., & Legaz, F. (2013). Metabolic responses to iron deficiency in roots of Carrizo citrange [*Citrus sinensis* (L.) Osbeck. × *Poncirus trifoliata* (L.) Raf.]. *Tree Physiology*, 33 (3), 320-329. <https://doi.org/10.1093/treephys/tpt011>.
- Maruyama, H., Sasaki, T., Yamamoto, Y., & Wasaki, J. (2019). AtALMT3 is involved in malate efflux induced by phosphorus deficiency in *Arabidopsis thaliana* root hairs. *Plant & Cell Physiology*, 60 (1), 107-115.
- Masumoto, C., Miyazawa, S., Ohkawa, H., Fukuda, T., Taniguchi, Y., Murayama, S., Kusano, M., Saito, K., Fukayama, H., & Miyao, M. (2010). Phosphoenolpyruvate carboxylase intrinsically located in the chloroplast of rice plays a crucial role in ammonium assimilation. *Proceedings of the National Academy of Sciences*, 107 (11), 5226-5231
- Matsumura, H., Xie, Y., Shirakata, S., Inoue, T., Yoshinaga, T., Ueno, Y., Izui, K., & Kai, Y. (2002). Crystal structures of C4 form maize and quaternary complex of *E. Coli* phosphoenolpyruvate carboxylases. *Structure*, 10 (12), 1721–1730. [https://doi.org/10.1016/s0969-2126\(02\)00913-9](https://doi.org/10.1016/s0969-2126(02)00913-9).
- Maurino, V. G., & Engqvist, M. K. M. (2015). 2-Hydroxy Acids in Plant Metabolism. *The Arabidopsis Book*, 13, e0182. <https://doi.org/10.1199/tab.0182>
- Meimoun, P., Gousset-Dupont, A., Lebouteiller, B., Ambard-Bretteville, F., Besin, E., Lelarge, C., Mauve, C., Hodges, M., & Vidal, J. (2009). The impact of PEPC phosphorylation on growth and development of *Arabidopsis thaliana*: Molecular and physiological characterization of PEPC kinase mutants. *FEBS Letters*, 583 (10), 1649-1652.
- Meijering E., Jacob M., Sarria J.C.F., Steiner P., Hirling H. & Unser M. (2004). Design and validation of a tool for neurite tracing and analysis in fluorescence microscopy images. *Cytometry*, 58A: 167-176. <https://doi.org/10.1002/cyto.a.20022>.
- Meyer, S., Angeli, A., Fernie, A. R., & Martinoia, E. (2010). Intra and extra-cellular excretion of carboxylates. *Trends in Plant Science*, 15 (1), 40-47.
- Moellering, E.R., Ouyang, Y., Mamedov, T.G., & Chollet, R. (2007). The two divergent PEP-carboxylase catalytic subunits in the green microalga *Chlamydomonas reinhardtii* respond reversibly to inorganic N supply and co-exist in the high molecular mass, hetero-oligomeric Class-2 PEPC complex. *FEBS Letters*, 581 (25), 4871-4876.
- Monreal, J.A., López-Baena, F.J., Vidal, J., Echevarría, C., & García-Mauriño, S. (2007). Effect of LiCl on phosphoenolpyruvate carboxylase kinase and the phosphorylation of phosphoenolpyruvate carboxylase in leaf disks and leaves of *Sorghum vulgare*. *Planta*, 225 (4), 801-812.
- Monreal, J.A., McLoughlin, F., Echevarria, C., Garcia-Maurino, S., & Testerink, C. (2010).

- Phosphoenolpyruvate carboxylase from C4 leaves is selectively targeted for inhibition by anionic phospholipids. *Plant Physiology*, 152 (2), 634-638.
- Moody, N.R., Christin, P.A., & Reid, J.D. (2020). Kinetic modifications of C (4) PEPC are qualitatively convergent, but larger in panicum than in Flaveria. *Frontiers in Plant Science*, 11, 1014. <https://doi.org/10.3389/fpls.2020.01014>.
- Moraes, T.F., & Plaxton, W.C. (2000). Purification and characterization of phosphoenolpyruvate carboxylase from *Brassica napus* (rapeseed) suspension cell cultures. *European Journal of Biochemistry*, 267 (14), 4465-4476. <https://doi.org/10.1046/j.1432-1327.2000.01495.x>.
- Mora-Macías, J., Ojeda-Rivera, J.O., Gutiérrez-Alanís, D., Yong-Villalobos, L., Oropeza-Aburto, A., Raya-González, J., Jiménez-Domínguez, G., Chávez-Calvillo, G., Rellán-Álvarez, R., & Herrera-Estrella, L. (2017). Malate-dependent Fe accumulation is a critical checkpoint in the root developmental response to low phosphate. *Proceedings of the National Academy of Sciences*, 114 (17), E3563-E3572.
- Müller, T., Heisters, M., Teller, J., Moore, K.L., Hause, G., Dinesh, D.C., Bürstenbinder, K., & Abel, S. (2015). Iron-dependent callose deposition adjusts root meristem maintenance to phosphate availability. *Developmental Cell*, 33 (2), 216-230.
- Müller, K., Doubnerová, V., Synková, H., Cerovská, N., & Ryslavá, H. (2009). Regulation of phosphoenolpyruvate carboxylase in PVY(NTN) infected tobacco plants. *Biological Chemistry*, 390 (3), 245-251. <https://doi.org/10.1515/BC.2009.029>.
- Muñoz-Clares, R.A., González-Segura, L., Juárez-Díaz, J.A., & Mújica-Jiménez, C. (2020). Structural and biochemical evidence of the glucose 6-phosphate-allosteric site of maize C4 phosphoenolpyruvate carboxylase: its importance in the overall enzyme kinetics. *The Biochemical Journal*, 477 (11), 2095-2114. <https://doi.org/10.1042/BCJ20200304>.
- Nakagawa, T., Izumi, T., Banba, M., Umehara, Y., Kouchi, H., Izui, K., & Hata, S. (2003). Characterization and expression analysis of genes encoding phosphoenolpyruvate carboxylase and phosphoenolpyruvate carboxylase kinase of *Lotus japonicus*, a model legume. *Molecular Plant-Microbe Interactions*, 16 (4), 281-288. <https://doi.org/10.1094/MPMI.2003.16.4.281>.
- Naumann, C., Heisters, M., Brandt, W., Janitza, P., Alfs, C., Tang, N., Nienguesso, A. T., Ziegler, J., Imre, R., & Mechtler, K. (2022). Bacterial-type ferroxidase tunes iron-dependent phosphate sensing during Arabidopsis root development. *Current Biology*, 32 (10), 2189-2205.
- Naumann, C., Müller, J., Sakhonwasee, S., Wieghaus, A., Hause, G., Heisters, M., Bürstenbinder, K., & Abel, S. (2019). The local phosphate deficiency response activates endoplasmic reticulum stress-dependent autophagy. *Plant Physiology*, 179 (2), 460-476.

- Neumann, G., Massonneau, A., Martinoia, E., & Römheld, V. (1999). Physiological adaptations to phosphorus deficiency during proteoid root development in white lupin. *Planta*, *208*, 373-382.
- Nimmo, H.G. (2003). Control of the phosphorylation of phosphoenolpyruvate carboxylase in higher plants. *Archives of Biochemistry and Biophysics*, *414* (2), 189-196.
- Nimmo, G.A., Nimmo, H.G., Fewson, C.A., & Wilkins, M.B. (1984). Diurnal changes in the properties of phosphoenolpyruvate carboxylase in Bryophyllum leaves: a possible covalent modification. *FEBS Letters*, *178* (2), 199-203. [https://doi.org/10.1016/0014-5793\(84\)80600-6](https://doi.org/10.1016/0014-5793(84)80600-6).
- Nimmo, G.A., Wilkins, M.B., & Nimmo, H.G. (2001). Partial purification and characterization of a protein inhibitor of phosphoenolpyruvate carboxylase kinase. *Planta*, *213* (2), 250-257. <https://doi.org/10.1007/s004250000501>.
- Nimmo, H.G. (2000). The regulation of phosphoenolpyruvate carboxylase in CAM plants. *Trends in Plant Science*, *5* (2), 75-80. [https://doi.org/10.1016/s1360-1385\(99\)01543-5](https://doi.org/10.1016/s1360-1385(99)01543-5).
- O'leary, B., Park, J., & Plaxton, W.C. (2011). The remarkable diversity of plant PEPC (phosphoenolpyruvate carboxylase): Recent insights into the physiological functions and post-translational controls of non-photosynthetic PEPCs. *The Biochemical Journal*, *436* (1), 15-34. <https://doi.org/10.1042/BJ20110078>.
- Obeso, J.R. (2002). The costs of reproduction in plants. *New Phytologist*, *155* (3), 321-348.
- O'Leary, B., Rao, S.K., Kim, J., & Plaxton, W.C. (2009). Bacterial-type phosphoenolpyruvate carboxylase (PEPC) functions as a catalytic and regulatory subunit of the novel class-2 PEPC complex of vascular plants. *The Journal of Biological Chemistry*, *284* (37), 24797-24805. <https://doi.org/10.1074/jbc.M109.022863>.
- Osbourne, S.L., Schepers, J., Francis D., & Schlemmer, M.R. (2002). Detection of phosphorus and nitrogen deficiencies in corn using spectral radiance measurements, *7*.
- Osmont, K.S., Sibout, R., & Hardtke, C.S. (2007). Hidden branches: Developments in root system architecture. *Annual Review of Plant Biology*, *58*, 93-113.
- Panchal, P., Miller, A.J., & Giri, J. (2021). Organic acids: Versatile stress-response roles in plants. *Journal of Experimental Botany*, *72* (11), 4038-4052.
- Paulus, J.K., Schlieper, D., & Groth, G. (2013). Greater efficiency of photosynthetic carbon fixation due to single amino-acid substitution. *Nature Communications*, *4*, 1518. <https://doi.org/10.1038/ncomms2504>.
- Peng, Hu, L., Li, Y., Qi, X., Wang, H., Hua, X., & Zhao, M. (2018). Effects of the maize C4 phosphoenolpyruvate carboxylase (ZmPEPC) gene on nitrogen assimilation in transgenic wheat. *Plant Growth Regulation*, *84* (1), 191-205. <https://doi.org/10.1007/s10725-017-0332-x>.

- Peng, W., Wu, W., Peng, J., Li, J., Lin, Y., Wang, Y., Tian, J., Sun, L., Liang, C., & Liao, H. (2018). Characterization of the soybean GmALMT family genes and the function of GmALMT5 in response to phosphate starvation. *Journal of Integrative Plant Biology*, *60* (3), 216-231. <https://doi.org/10.1111/jipb.12604>.
- Peng C, Xu, W., Hu, L., Li, Y., Qi, X., Wang, H., Hua, X., & Zhao, M. (2018). Effects of the maize C4 phosphoenolpyruvate carboxylase (ZmPEPC) gene on nitrogen assimilation in transgenic wheat. *Plant Growth Regulation*, *84*, 191-205.
- Perrot-Rechenmann, C., Vidal, J., Brulfert, J., Burlet, A., & Gadal, P. (1982). A comparative immunocytochemical localization study of phosphoenolpyruvate carboxylase in leaves of higher plants. *Planta*, *155* (1), 24-30. <https://doi.org/10.1007/BF00402927>.
- Petricka, J., Winter, C.M., & Benfey, P.N. (2012). Control of Arabidopsis root development. *Annual Review of Plant Biology*, *63*, 563-590.
- Icard, P., Poulain, L., & Lincet, H. (2012). Understanding the central role of citrate in the metabolism of cancer cells. *Biochimica Et Biophysica Acta (BBA). Reviews on Cancer*, *1825* (1), 111-116. <https://doi.org/10.1016/j.bbcan.2011.10.007>.
- Podestá, F.E., & Plaxton, W.C. (1994). Regulation of cytosolic carbon metabolism in germinating *Ricinus communis* cotyledons. *Planta*, *194* (3), 374-380. <https://doi.org/10.1007/BF00197538>.
- Popova, T.N., & Pinheiro de Carvalho, M. (1998). Citrate and isocitrate in plant metabolism. *Biochimica Et Biophysica Acta (BBA). Bioenergetics*, *1364* (3), 307-325. [https://doi.org/10.1016/S0005-2728\(98\)00008-5](https://doi.org/10.1016/S0005-2728(98)00008-5).
- Pracharoenwattana, I., Cornah, J.E., & Smith, S.M. (2005). Arabidopsis peroxisomal citrate synthase is required for fatty acid respiration and seed germination. *The Plant Cell*, *17* (7), 2037-2048. <https://doi.org/10.1105/tpc.105.031856>.
- Puga, M.I., Mateos, I., Charukesi, R., Wang, Z, Franco-Zorrilla, J.M., Lorenzo, L. de, Irigoyen, M. L., Masiero, S., Bustos, R., & Rodríguez, J. (2014). SPX1 is a phosphate- dependent inhibitor of Phosphate Starvation Response 1 in Arabidopsis. *Proceedings of the National Academy of Sciences*, *111* (41), 14947-14952.
- Qin, K., Qiu, P., Wen, J., Zhu, Y., Li, N., & Li, S. (2016). High throughput transformation of a Sorghum cDNA library for rice improvement. *Plant Cell, Tissue and Organ Culture (PCTOC)*, *125* (3), 471-478. <https://doi.org/10.1007/s11240-016-0962-0>.
- Rademacher, T., Häusler, R.E., Hirsch, H.J., Zhang, L., Lipka, V., Weier, D., Kreuzaler, F., & Peterhänsel, C. (2002). An engineered phosphoenolpyruvate carboxylase redirects carbon and

- nitrogen flow in transgenic potato plants. *The Plant Journal*, 32 (1), 25-39. <https://doi.org/10.1046/j.1365-313x.2002.01397.x>.
- Raghothama, K.G. (1999). Phosphate acquisition. *Annual Review of Plant Physiology and Plant Molecular Biology*, 50 (1), 665-693. <https://doi.org/10.1146/annurev.arplant.50.1.665>.
- Razaq, M., Zhang, P., Shen, H., & Salahuddin (2017). Influence of nitrogen and phosphorous on the growth and root morphology of acer mono. *PLOS ONE*, 12 (2), 1-13.
- Rellán-Álvarez, R., Giner-Martínez-Sierra, J., Orduna, J., Orera, I., Rodríguez-Castrillón, J.Á., García-Alonso, J.I., Abadía, J., & Álvarez-Fernández, A. (2010). Identification of a tri-iron (III), tri-citrate complex in the xylem sap of iron-deficient tomato resupplied with iron: new insights into plant iron long-distance transport. *Plant and Cell Physiology*, 51 (1), 91-102.
- Ried, M.K., Wild, R., Zhu, J., Pipercevic, J., Sturm, K., Broger, L., Harmel, R.K., Abriata, L.A., Hothorn, L.A., Fiedler, D., Hiller, S., & Hothorn, M. (2021). Inositol pyrophosphates promote the interaction of SPX domains with the coiled-coil motif of PHR transcription factors to regulate plant phosphate homeostasis. *Nature Communications*, 12 (1), 384. <https://doi.org/10.1038/s41467-020-20681-4>.
- Roch, V.G., Maharajan, T., Ceasar, S.A., & Ignacimuthu, S. (2019). The role of PHT1 family transporters in the acquisition and redistribution of phosphorus in plants. *Critical Reviews in Plant Sciences*, 38 (3), 171-198.
- Roschttardt, H., Séguéla-Arnaud, M., Briat, J.F., Vert, G., & Curie, C. (2011). The FRD3 citrate effluxer promotes iron nutrition between symplastically disconnected tissues throughout Arabidopsis development. *The Plant Cell*, 23 (7), 2725-2737.
- Rosendahl, S., Rosendahl, C.N., & Söchting, U. (1990). Distribution of VA mycorrhizal endophytes amongst plants from a Danish grassland community. *Agriculture, Ecosystems & Environment*, 29 (1-4), 329-335.
- Rustin, P., Meyer, C.R., & Wedding, R.T. (1988). Identification of substrate and effector binding sites of phosphoenolpyruvate carboxylase from *Crassula argentea*. A possible role of phosphoenolpyruvate as substrate and activator. *The Journal of Biological Chemistry*, 263 (33), 17611-17614.
- Ryan, P.R., Raman, H., Gupta, S., Horst, W.J., & Delhaize, E. (2009). A second mechanism for aluminum resistance in wheat relies on the constitutive efflux of citrate from roots. *Plant Physiology*, 149 (1), 340-351. <https://doi.org/10.1104/pp.108.129155>.
- Ryan, P.R., Tyerman, S.D., Sasaki, T., Furuichi, T., Yamamoto, Y, Zhang, W.H., & Delhaize, E (2011). The identification of aluminum-resistance genes provides opportunities for enhancing

- crop production on acid soils. *Journal of Experimental Botany*, 62 (1), 9-20. <https://doi.org/10.1093/jxb/erq272>.
- Sánchez, R., & Cejudo, F.J. (2003). Identification and expression analysis of a gene encoding a bacterial-type phosphoenolpyruvate carboxylase from Arabidopsis and rice. *Plant Physiology*, 132 (2), 949-957. <https://doi.org/10.1104/pp.102.019653>.
- Sánchez, R., Flores, A., & Cejudo, F.J. (2006). Arabidopsis phosphoenolpyruvate carboxylase genes encode immunologically unrelated polypeptides and are differentially expressed in response to drought and salt stress. *Planta*, 223 (5), 901-909. <https://doi.org/10.1007/s00425-005-0144-5>.
- Sangwan, R.S., Singh, N., & Plaxton, W.C. (1992). Phosphoenolpyruvate carboxylase activity and concentration in the endosperm of developing and germinating castor oil seeds. *Plant Physiology*, 99 (2), 445-449. <https://doi.org/10.1104/pp.99.2.445>.
- Sasaki, T., Yamamoto, Y., Ezaki, B., Katsuhara, M., Ahn, S.J., Ryan, P.R., Delhaize, E., & Matsumoto, H. (2004). A wheat gene encoding an aluminum-activated malate transporter. *The Plant Journal*, 37 (5), 645-653. <https://doi.org/10.1111/j.1365-313x.2003.01991.x>.
- Sawaki, Y., Iuchi, S., Kobayashi, Y., Kobayashi, Y., Ikka, T., Sakurai, N., Fujita, M., Shinozaki, K., Shibata, D., & Kobayashi, M. (2009). STOP1 regulates multiple genes that protect Arabidopsis from proton and aluminum toxicities. *Plant Physiology*, 150 (1), 281-294.
- Schlieper, D., Förster, K., Paulus, J.K., & Groth, G. (2014). Resolving the activation site of positive regulators in plant phosphoenolpyruvate carboxylase. *Molecular Plant*, 7 (2), 437-440. <https://doi.org/10.1093/mp/sst130>.
- Schmidt, G., & Laskowski Sr, M. (1961). Phosphate ester cleavage (Survey). *The Enzymes*, 2nd Edn. Academic Press, New York, 3-35.
- Schneider, C., Rasband, W. & Eliceiri, K. (2012). NIH Image to ImageJ: 25 years of image analysis. *Nat Methods* 9, 671–675. <https://doi.org/10.1038/nmeth.208>.
- Schneiderei, J., Häusler, R.E., Fiene, G., Kaiser, W.M., & Weber, A.P. (2006). Antisense repression reveals a crucial role of the plastidic 2-oxoglutarate/malate translocator DiT1 at the interface between carbon and nitrogen metabolism. *The Plant Journal*, 45 (2), 206-224. <https://doi.org/10.1111/j.1365-313X.2005.02594.x>.
- Schulz, M., Klockenbring, T., Hunte, C., & Schnabl, H. (1993). Involvement of ubiquitin in phosphoenolpyruvate carboxylase degradation. *Botanica Acta*, 106 (2), 143-145. <https://doi.org/10.1111/j.1438-8677.1993.tb00350.x>.
- Schulze, J., Tesfaye, M., Litjens, R., Bucciarelli, B., Trepp, G., Miller, S., Samac, D., Allan, D., & Vance, C. P. (2002). Malate plays a central role in plant nutrition. *Plant and Soil*, 247, 133-139.

- Shahbaz, A.M., Oki, Y., Adachi, T., Murata, Y., & Khan, M.H.R. (2006). Phosphorus starvation induced root-mediated pH changes in solubilization and acquisition of sparingly soluble P sources and organic acids exudation by Brassica cultivars. *Soil Science and Plant Nutrition*, 52 (5), 623-633. <https://doi.org/10.1111/j.1747-0765.2006.00082.x>.
- Shen, J., Li, H., Neumann, G., & Zhang, F. (2005). Nutrient uptake, cluster root formation and exudation of protons and citrate in *Lupinus albus* as affected by localized supply of phosphorus in a split-root system. *Plant Science*, 168 (3), 837-845.
- Shen, J., Yuan, L., Zhang, J., Li, H., Bai, Z., Chen, X., Zhang, W., & Zhang, F. (2011). Phosphorus dynamics: From soil to plant. *Plant Physiology*, 156 (3), 997-1005.
- Shenton, M., Fontaine, V., Hartwell, J., Marsh, J.T., Jenkins, G.I., & Nimmo, H.G. (2006). Distinct patterns of control and expression amongst members of the PEP carboxylase kinase gene family in C4 plants. *The Plant Journal*, 48 (1), 45-53.
- Shi, J., Yi, K., Liu, Y., Xie, L., Zhou, Z., Chen, Y., Hu, Z., Zheng, T., Liu, R., Chen, Y., & Chen, J. (2015). Phosphoenolpyruvate carboxylase in *Arabidopsis* leaves plays a crucial role in carbon and nitrogen metabolism. *Plant Physiology*, 167 (3), 671-681.
- Skene, K.R. (2001). Cluster roots: Model experimental tools for key biological problems. *Journal of Experimental Botany*, 52, 479-485. https://doi.org/10.1093/jexbot/52.suppl_1.479.
- Smit, A.L., Bindraban, P.S., Schröder, J.J., Conijn, J.G., & van der Meer, H.G. (2009). Phosphorus in agriculture: global resources, trends and developments: report to the Steering Committee Technology Assessment of the Ministry of Agriculture, Nature and Food Quality, The Netherlands, and in collaboration with the Nutrient Flow Task Group (NFTG), supported by DPRN (Development Policy review Network). Plant Research International.
- Smith, L., & Monaghan, R.M. (2003). Nitrogen and phosphorus losses in overland flow from cattle-grazed pasture in Southland. *New Zealand Journal of Agricultural Research*, 46 (3), 225-237. <https://doi.org/10.1080/00288233.2003.9513549>
- Smith, S., & Smith, F. (2011). Roles of arbuscular mycorrhizas in plant nutrition and growth: New paradigms from cellular to ecosystem scales. *Annual Review of Plant Biology*, 62, 227-250.
- Sørensen, D.M., Holen, H.W., Holemans, T., Vangheluwe, P., & Palmgren, M.G. (2015). Towards defining the substrate of orphan P5A-ATPases. *Biochimica Et Biophysica Acta (BBA)-General Subjects*, 1850 (3), 524-535.
- Stigter, K.A., & Plaxton, W.C. (2015). Molecular mechanisms of phosphorus metabolism and transport during leaf senescence. *Plants*, 4 (4), 773-798. <https://doi.org/10.3390/plants4040773>.
- Sullivan, S., Jenkins, G.I., & Nimmo, H.G. (2004). Roots, cycles and leaves. Expression of the phosphoenolpyruvate carboxylase kinase gene family in soybean. *Plant Physiology*, 135 (4),

2078-2087. <https://doi.org/10.1104/pp.104.042762>.

- Sun, M., Sun, X., Zhao, Y., Zhao, C., DuanMu, H., Yu, Y., Ji, W., & Zhu, Y. (2014). Ectopic expression of *GsPPCK3* and *SCMRP* in *Medicago sativa* enhances plant alkaline stress tolerance and methionine content. *PLOS ONE*, *9*(2), e89578.
- Svistoonoff, S., Creff, A., Reymond, M., Sigoillot-Claude, C., Ricaud, L., Blanchet, A., Nussaume, L., & Desnos, T. (2007). Root tip contact with low-phosphate media reprograms plant root architecture. *Nature Genetics*, *39* (6), 792-796.
- Taybi, T., Nimmo, H.G., & Borland, A.M. (2004). Expression of phosphoenolpyruvate carboxylase and phosphoenolpyruvate carboxylase kinase genes. Implications for genotypic capacity and phenotypic plasticity in the expression of crassulacean acid metabolism. *Plant Physiology*, *135* (1), 587-598. <https://doi.org/10.1104/pp.103.036962>.
- Taybi, T., Patil, S., Chollet, R., & Cushman, J.C. (2000). A minimal serine/threonine protein kinase circadianly regulates phosphoenolpyruvate carboxylase activity in crassulacean acid metabolism-induced leaves of the common ice plant. *Plant Physiology*, *123* (4), 1471-1482. <https://doi.org/10.1104/pp.123.4.1471>.
- Tesfaye, M., Dufault, N.S., Dornbusch, M.R., Allan, D.L., Vance, C.P., & Samac D.A. (2003). Influence of enhanced malate dehydrogenase expression by alfalfa on diversity of rhizobacteria and soil nutrient availability. *Soil Biology and Biochemistry*, *35* (8), 1103-1113. [https://doi.org/10.1016/S0038-0717\(03\)00162-7](https://doi.org/10.1016/S0038-0717(03)00162-7).
- Tesfaye, M., Temple, S.J., Allan, D.L., Vance, C.P., & Samac, D.A. (2001). Overexpression of malate dehydrogenase in transgenic alfalfa enhances organic acid synthesis and confers tolerance to aluminum. *Plant Physiology*, *127* (4), 1836-1844.
- Mimura, T. (1999). Regulation of phosphate transport and homeostasis in plant cells. *International Review of Cytology*, *191*, 149-200. [https://doi.org/10.1016/S0074-7696\(08\)60159-X](https://doi.org/10.1016/S0074-7696(08)60159-X).
- Theng, V., Agarie S., & Nose A. (2007). Regulatory properties of phosphoenolpyruvate carboxylase in crassulacean acid metabolism plants: diurnal changes in phosphorylation state and regulation of gene expression. *Plant Production Science*, *10* (2), 171-181.
- Thibaud, M.C., Arrighi, J.F., Bayle, V., Chiarenza, S., Creff, A., Bustos, R., Paz-Ares, J., Poirier, Y., & Nussaume, L. (2010). Dissection of local and systemic transcriptional responses to phosphate starvation in Arabidopsis. *The Plant Journal*, *64* (5), 775-789.
- Ticconi, C.A., & Abel, S. (2004). Short on phosphate: plant surveillance and countermeasures. *Trends in Plant Science*, *9* (11), 548-555.
- Tiziani, R., Mimmo, T., Valentinuzzi, F., Pii, Y., Celletti, S., & Cesco, S. (2021). Root handling affects carboxylates exudation and phosphate uptake of white lupin roots. *Frontiers in Plant Science*,

12, 681263. <https://doi.org/10.3389/fpls.2021.681263>.

- Tiziani, R., Puschenreiter, M., Smolders, E., Mimmo, T., Herrera, J.C., Cesco, S., & Santner, J. (2020). Quantifying and mapping citrate exudation in soil-grown root systems. In *EGU General Assembly Conference Abstracts*.
- Tran, H.T., Hurley, B.A., & Plaxton, W.C. (2010). Feeding hungry plants: the role of purple acid phosphatases in phosphate nutrition. *Plant Science*, *179* (1-2), 14-27.
- Tsuchida, Y., Furumoto, T., Izumida, A., Hata, S., & Izui, K. (2001). Phosphoenolpyruvate carboxylase kinase involved in C₄ photosynthesis in *Flaveria trinervia*. *FEBS Letters*, *507* (3), 318-322. [https://doi.org/10.1016/S0014-5793\(01\)02994-5](https://doi.org/10.1016/S0014-5793(01)02994-5).
- Udvardi, M.K., & Day, D.A. (1997). Metabolite transport across symbiotic membranes of legume nodules. *Annual Review of Plant Physiology and Plant Molecular Biology*, *48*, 493-523.
- Uhrig, R.G., She, Y.M., Leach, C.A., & Plaxton, W.C. (2008). Regulatory monoubiquitination of phosphoenolpyruvate carboxylase in germinating castor oil seeds. *The Journal of Biological Chemistry*, *283* (44), 29650-29657. <https://doi.org/10.1074/jbc.M806102200>.
- Vaccari, D.A. (2009). Phosphorus: A Looming Crisis. *Scientific American*, *300* (6), 54-59. <http://www.jstor.org/stable/26001380>.
- van de Wiel, C.C. M., van der Linden, C.G., & Scholten, O.E. (2016). Improving phosphorus use efficiency in agriculture: opportunities for breeding. *Euphytica*, *207* (1), 1-22.
- van der Merwe, M.J., Osorio, S., Moritz, T., Nunes-Nesi, A., & Fernie, A.R. (2008). Decreased mitochondrial activities of malate dehydrogenase and fumarase in tomato lead to altered root growth and architecture via diverse mechanisms. *Plant Physiology*, *149* (2), 653-669.
- Vance, C.P. (2008). Plants without arbuscular mycorrhizae. In *The ecophysiology of plant-phosphorus interactions* 117–142.
- Vance, C.P., Uhde-Stone, C., & Allan, D.L. (2003). Phosphorus acquisition and use: Critical adaptations by plants for securing a nonrenewable resource. *New Phytologist*, *157* (3), 423-447.
- Vatén, A., Dettmer, J., Wu, S., Stierhof, Y.D., Miyashima, S., Yadav, S.R., Roberts, C.J., Campilho, A., Bulone, V., & Lichtenberger, R. (2011). Callose biosynthesis regulates symplastic trafficking during root development. *Developmental Cell*, *21* (6), 1144-1155.
- Vidal, J., & Chollet, R. (1997). Regulatory phosphorylation of C₄ PEP carboxylase. *Trends in Plant Science*, *2* (6), 230-237. [https://doi.org/10.1016/S1360-1385\(97\)89548-9](https://doi.org/10.1016/S1360-1385(97)89548-9).
- Viégas, I., Cordeiro, R.A.M., Almeida, G.M. de, Silva, D.A.S., Da Silva, B.C., Okumura, R.S., Da Silva Júnior, M.L., Da Silva, S.P., & Freitas, J.M.N. (2018). Growth and visual symptoms of nutrients

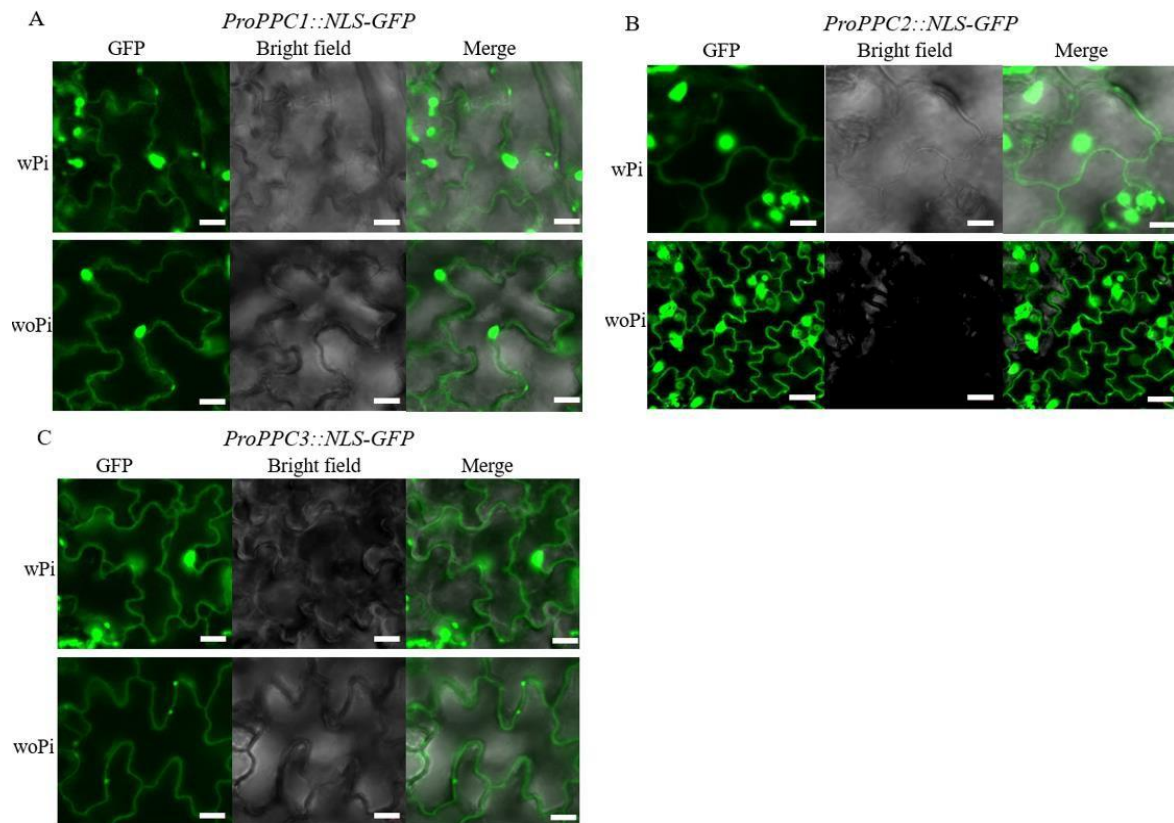
- deficiency in mangosteens (*Garcinia mangostana* L.). *American Journal of Plant Sciences*, 9 (5), 1014-1028.
- Wang, B.L., Shen, J.B., Zhang, W.H., Zhang, F.S., & Neumann, G. (2007). Citrate exudation from white lupin induced by phosphorus deficiency differs from that induced by aluminum. *New Phytologist*, 176 (3), 581-589.
- Wang, N., Zhong, X., Cong, Y., Wang, T., Yang, S., Li, Y., & Gai, J. (2016). Genome wide analysis of phosphoenolpyruvate carboxylase gene family and their response to abiotic stresses in soybean. *Scientific Reports*, 6, 38448. <https://doi.org/10.1038/srep38448>
- Wang, D., Lv, S., Jiang, P., & Li, Y. (2017). Roles, regulation, and agricultural application of plant phosphate transporters. *Frontiers in Plant Science*, 8, 817.
- Wang, Y.L., Almvik, M., Clarke, N., Eich-Greatorex, S., Øgaard, A.F., Krogstad, T., Lambers, H., & Clarke, J.L. (2015). Contrasting responses of root morphology and root-exuded organic acids to low phosphorus availability in three important food crops with divergent root traits. *AoB Plants*, 7, plv097.
- Ward, J.T., Lahner, B., Yakubova, E., Salt, D.E., & Raghothama, K.G. (2008). The effect of iron on the primary root elongation of *Arabidopsis* during phosphate deficiency. *Plant Physiology*, 147 (3), 1181-1191.
- Waseem, M., & Ahmad, F. (2019). The phosphoenolpyruvate carboxylase gene family identification and expression analysis under abiotic and phytohormone stresses in *Solanum lycopersicum* L. *Gene*, 690, 11-20. <https://doi.org/10.1016/j.gene.2018.12.033>
- Wei, Z., Zhu, Y., Hua, Y., Cai, H., Ji, W., Bai, X., Wang, Z., & Wen, Y. (2013). Transgenic alfalfa with GsPPCK1 and its alkaline tolerance analysis. *Acta Agronomica Sinica*, 39 (1), 68-75.
- Weil, R., & Brady, N. (2017). Soil Phosphorus and Potassium. In pp. 643–695.
- Wen, Z., Li, H., Shen, J., & Rengel, Z. (2017). Maize responds to low shoot P concentration by altering root morphology rather than increasing root exudation. *Plant and Soil*, 416, 377- 389.
- Wheeler, G., Mariel C., Arias, C.L., Tronconi, M.A., Maurino, V.G., Andreo, C.S., & Drincovich, M.F. (2008). *Arabidopsis thaliana* NADP malic enzyme isoforms: high degree of identity but clearly distinct properties. *Plant Molecular Biology*, 67, 231-242.
- Williamson, L.C., Ribrioux, S.P., Fitter, A.H., & Leyser, H.O. (2001). Phosphate availability regulates root system architecture in *Arabidopsis*. *Plant Physiology*, 126 (2), 875-882.
- Willick, I.R., Plaxton, W., Lolle, S.J., & Macfie S.M. (2019). Transcriptional and post- translational upregulation of phosphoenolpyruvate carboxylase in *Arabidopsis thaliana* (L. Heynh) under

- cadmium stress. *Environmental and Experimental Botany*, 164, 29-39.
- Winter, K. (1982). Properties of phosphoenolpyruvate carboxylase in rapidly prepared, desalted leaf extracts of the crassulacean acid metabolism plant *Mesembryanthemum crystallinum* L. *Planta*, 154 (4), 298-308. <https://doi.org/10.1007/BF00393907>.
- Wong, K.F., & Davies, D.D. (1973). Regulation of phosphoenolpyruvate carboxylase of *Zea mays* by metabolites. *The Biochemical Journal*, 131 (3), 451-458. <https://doi.org/10.1042/bj1310451>.
- Wu, X., Li, R., Shi, J., Wang, J., Sun, Q., Zhang, H., Xing, Y., Qi, Y., Zhang, N., & Guo, Y.D. (2014). *Brassica oleracea* MATE encodes a citrate transporter and enhances aluminum tolerance in *Arabidopsis thaliana*. *Plant & Cell Physiology*, 55 (8), 1426-1436.
- Wu, P., Ma, X., Tigabu, M., Wang, C., Liu, A., & Oden, P.C. (2011). Root morphological plasticity and biomass production of two Chinese fir clones with high phosphorus efficiency under low phosphorus stress. *Canadian Journal of Forest Research*, 41 (2), 228-234.
- Wu, T.Y., Gruissem, W., & Bhullar, N.K. (2018). Facilitated citrate-dependent iron translocation increases rice endosperm iron and zinc concentrations. *Plant Science*, 270, 13-22.
- Wu, W.L., Hsiao, Y.Y., Lu, H.C., Liang, C.K., Fu, C.H., Huang, T.H., Chuang, M.H., Chen, L.J., Liu, Z.J., & Tsai, W.C. (2020). Expression regulation of malate synthase involved in glyoxylate cycle during protocorm development in *Phalaenopsis aphrodite* (Orchidaceae). *Scientific Reports*, 10 (1), 10123. <https://doi.org/10.1038/s41598-020-66932-8>.
- Xiang, G., Ma, W., Gao, S., Jin, Z., Yue, Q., & Yao, Y. (2019). Transcriptomic and phosphoproteomic profiling and metabolite analyses reveal the mechanism of NaHCO₃ induced organic acid secretion in grapevine roots. *BMC Plant Biology*, 19 (1), 383. <https://doi.org/10.1186/s12870-019-1990-9>.
- Xu, W., Ahmed, S., Moriyama, H., & Chollet, R. (2006). The importance of the strictly conserved, c-terminal glycine residue in phosphoenolpyruvate carboxylase for overall catalysis: Mutagenesis and truncation of gly-961 in the sorghum c4 leaf isoform. *The Journal of Biological Chemistry*, 281 (25), 17238-17245. <https://doi.org/10.1074/jbc.M602299200>.
- Xu, W., Zhou, Y., & Chollet, R. (2003). Identification and expression of a soybean nodule-enhanced PEP-carboxylase kinase gene (NE-PPCK) that shows striking up-/down-regulation in vivo. *The Plant Journal*, 34 (4), 441-452. <https://doi.org/10.1046/j.1365-313X.2003.01740.x>.
- Yang, L.T., Qi, Y.P., Jiang, H.X., Chen, L.S., & Kessler, M.R. (2013). Roles of organic acid anion secretion in aluminum tolerance of higher plants. *BioMed Research International*, 173682. <https://doi.org/10.1155/2013/173682>.
- Yang, X., Hu, R., Yin, H., Jenkins, J., Shu, S., Tang, H., Liu, D., Weighill, D.A., Yim, C.W., Ha, J., Heyduk, K., Goodstein, D.M., Guo, H.B., Moseley, R.C., Fitzek, E., Jawdy, S., Zhang,

- Z., Xie, M., Hartwell, J., Tuskan, G.A. (2017). The *Kalanchoe* genome provides insights into convergent evolution and building blocks of crassulacean acid metabolism. *Nature Communications*, 8 (1), 1899. <https://doi.org/10.1038/s41467-017-01491-7>.
- Kai, Y., Matsumura, H., Inoue, T., Terada, K., Nagara, Y., Yoshinaga, T., Tsumura, K.K., & Izui, K. (1999). Three-dimensional structure of phosphoenolpyruvate carboxylase: A proposed mechanism for allosteric inhibition. *Proceedings of the National Academy of Sciences*, 96 (3), 823-828.
- Yu, B., Xu, C., & Benning, C. (2002). Arabidopsis disrupted in SQD2 encoding sulfolipid synthase is impaired in phosphate-limited growth. *Proceedings of the National Academy of Sciences*, 99 (8), 5732-5737.
- Zhang, Y., Chen, F.S., Wu, X.Q., Luan, F.G., Zhang, L.P., Fang, X.M., Wan, S.Z., Hu, X.F., & Ye, J.R. (2018). Isolation and characterization of two phosphate solubilizing fungi from rhizosphere soil of moso bamboo and their functional capacities when exposed to different phosphorus sources and pH environments. *PLOS ONE*, 13 (7), 1-14. <https://doi.org/10.1371/journal.pone.0199625>.
- Zhang, X.Q., & Chollet, R. (1997). Phosphoenolpyruvate carboxylase protein kinase from soybean root nodules: partial purification, characterization, and up/down-regulation by photosynthate supply from the shoots. *Archives of Biochemistry and Biophysics*, 343 (2), 260-268. <https://doi.org/10.1006/abbi.1997.0190>.
- Zhang, Y., Primavesi, L.F., Jhurreea, D., Andralojc, P.J., Mitchell, R.A., Powers, S.J., Schluempmann, H., Delatte, T., Wingler, A., & Paul, M.J. (2009). Inhibition of SNF1-related protein kinase1 activity and regulation of metabolic pathways by trehalose-6-phosphate. *Plant Physiology*, 149 (4), 1860-1871. <https://doi.org/10.1104/pp.108.133934>.
- Zhang, X.Q., Li, B., & Chollet, R. (1995). In vivo regulatory phosphorylation of soybean nodule phosphoenolpyruvate carboxylase. *Plant Physiology*, 108 (4), 1561-1568.
- Zhang, Y., Wang, X., Lu, S., & Liu, D. (2014). A major root-associated acid phosphatase in Arabidopsis, AtPAP10, is regulated by both local and systemic signals under phosphate starvation. *Journal of Experimental Botany*, 65 (22), 6577-6588.
- Zhao Y., Guo, A., Wang, Y., & Hua, J. (2019). Evolution of PEPC gene family in *Gossypium* reveals functional diversification and GhPEPC genes responding to abiotic stresses. *Gene*, 698, 61-71. <https://doi.org/10.1016/j.gene.2019.02.061>.
- Zhou, J., Jiao, F., Wu, Z., Li, Y., Wang, X., He, X., Zhong, W., & Wu, P. (2008). OsPHR2 is involved in phosphate-starvation signaling and excessive phosphate accumulation in shoots of plants. *Plant Physiology*, 146(4), 1673-1686.

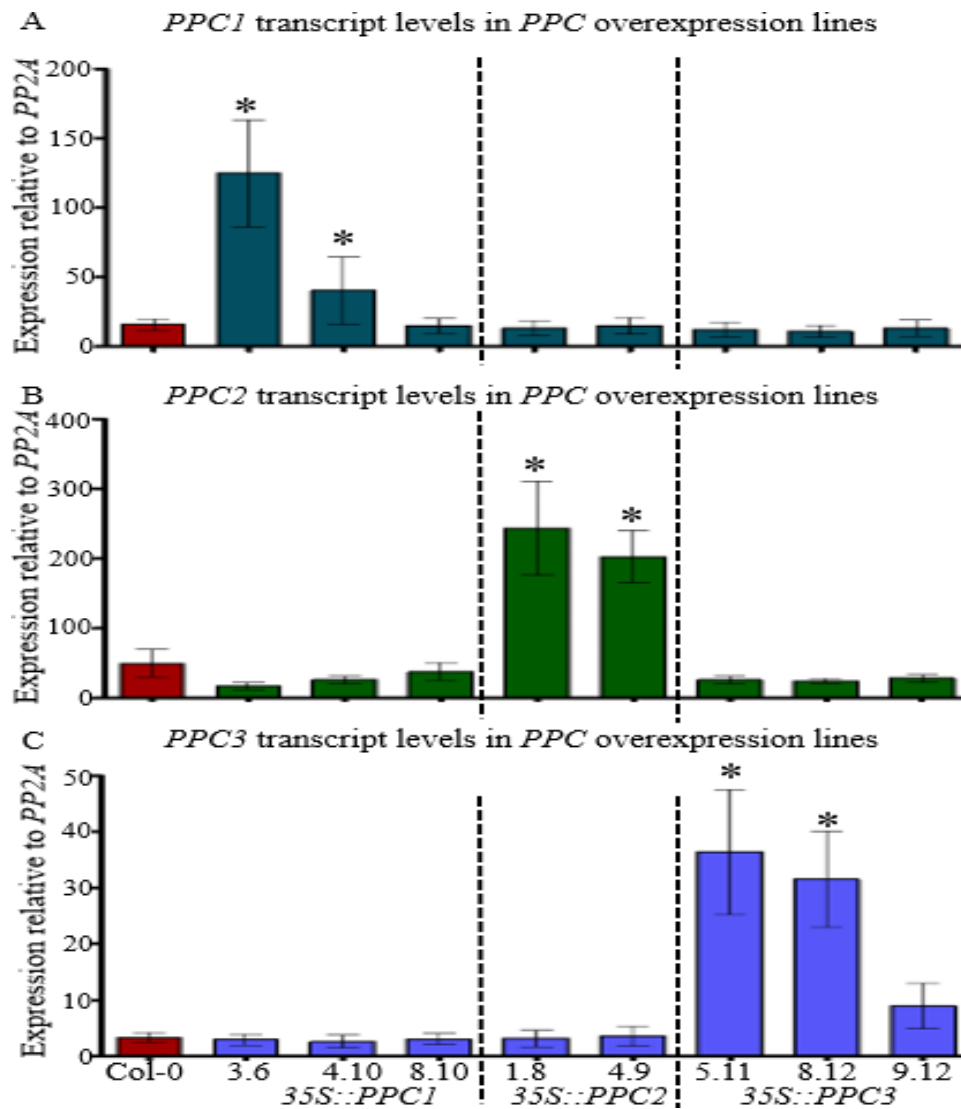
- Zhou, Z., Wang, Z., Lv, Q., Shi, J., Zhong, Y., Wu, P., & Mao, C. (2015). SPX proteins regulate Pi homeostasis and signaling in different subcellular level. *Plant Signaling & Behavior*, *10*(9), e1061163. <https://doi.org/10.1080/15592324.2015.1061163>.
- Ziegler, J., Hussain, H., Neubert, R.H.H., & Abel, S. (2019). Sensitive and selective amino acid profiling of minute tissue amounts by HPLC/electrospray negative tandem mass spectrometry using 9-fluorenylmethoxycarbonyl (Fmoc-Cl) derivatization. *Amino Acid Analysis: Methods and Protocols*, 365-379.
- Ziegler, J., Schmidt, S., Chutia, R., Müller, J., Böttcher, C., Strehmel, N., Scheel, D., & Abel, S. (2016). Non-targeted profiling of semi-polar metabolites in Arabidopsis root exudates uncovers a role for coumarin secretion and lignification during the local response to phosphate limitation. *Journal of Experimental Botany*, *67*(5), 1421-1432.

8.0 APPENDIX



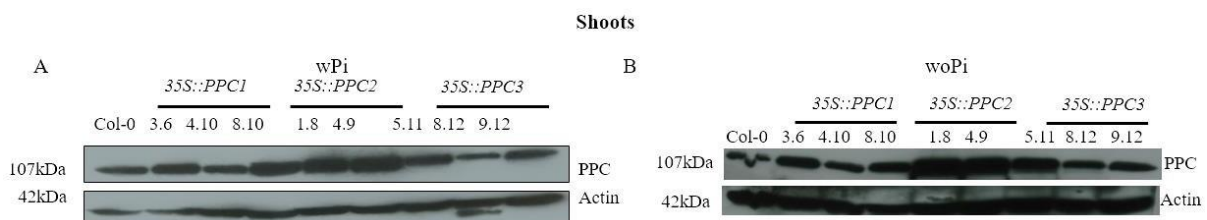
Supplementary figure 1: Cell-specific expression domains of *PPCs* in shoots of *Arabidopsis*.

Expression of GFP fused to NLS and plant type *PPCs* native promoters of **A-*PPC1***, **B-*PPC2*** and **C-*PPC3***. Representative images for shoots were captured in GFP channel (Left), bright field (Centre) and merged (Right). Seedlings were grown for six days on sufficient Pi before transfer to either sufficient or insufficient Pi for additional five days before imaging. Scale bars represent 20 μ m.



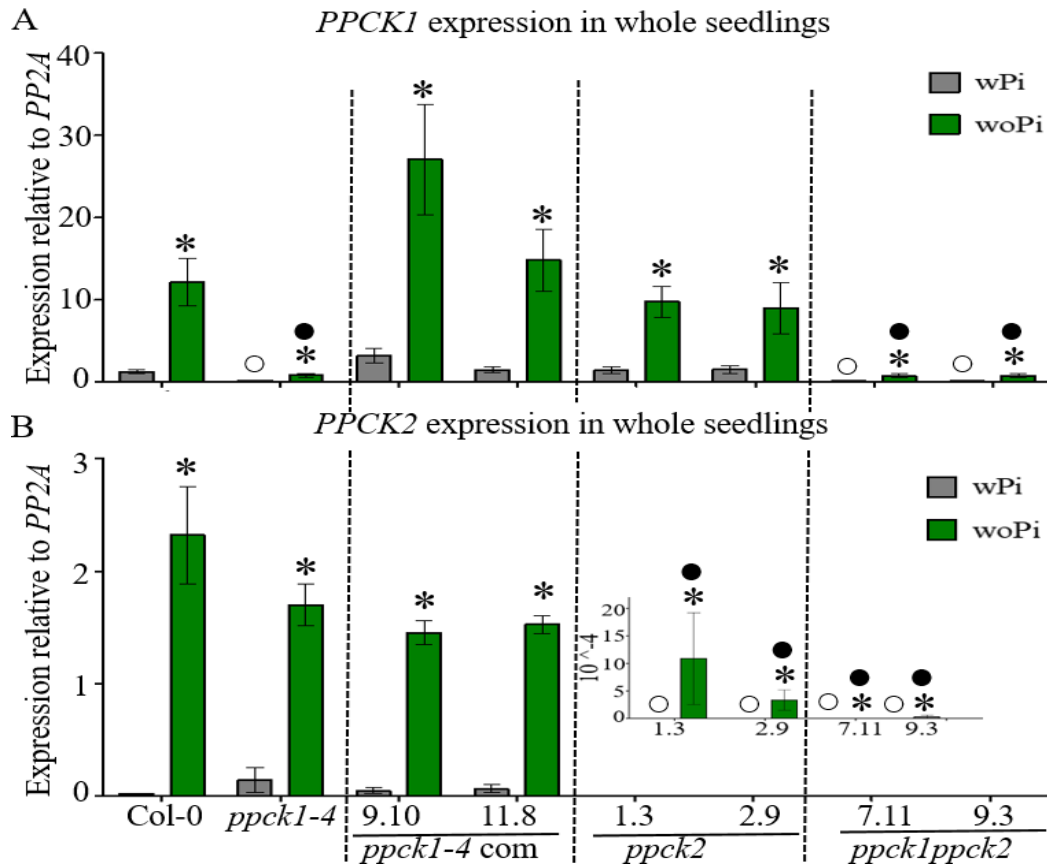
Supplementary figure 2: *PPC* transcript analysis in wild type and overexpression lines.

A-*PPC1*, B-*PPC2* and C-*PPC3* transcript levels in *PPC* overexpression. Seedlings were grown for six days on sufficient Pi before harvest and *PP2A* was used as the reference gene. Error bars denote \pm SE (n=3). Significance test was by Student's t-test (two tailed, equal variances), $p \leq 0.05$ compared to wild type (Col-0) wPi.



Supplementary figure 3: Detection of total PPCs in *PPC* overexpression lines by immunoblot analysis.

PPC quantification in **A-Shoots** grown in Pi sufficient conditions and **B-Shoots** grown in Pi deficient conditions. Seedlings were grown for six days on sufficient Pi before transfer to sufficient or insufficient Pi for an additional five days before harvest. 30 μ g of total protein extract was loaded on to the SDS-PAGE gel and probed with anti-PPC or anti-Actin antibody. Actin was used as a loading control.



Supplementary figure 6: *PPCK* transcript levels in whole seedlings of wild type, *ppck* mutants and *ppck1-4* complementation lines.

A-*PPCK1* transcript levels and **B-*PPCK2*** transcript levels. Seedlings were grown for six days on sufficient Pi before transfer to either sufficient or insufficient Pi for an additional five days after which they were harvested. Error bars denote \pm SE (n=3). Significance analyses were performed by Student's t-test (two tailed, equal variances).

* $p \leq 0.05$, $op \leq 0.05$ and $\bullet p \leq 0.05$ compared to wPi, Col-0 wPi and Col-0 woPi, respectively.

Supplementary table 1: List of primers used for RT qPCR analysis

Template	Locus	Primer	5'→3' sequence
<i>PPC1</i>	At1G53310	PPC1-FP	CCATGTGACTCTGCGACCACAC
		PPC1-RP	CCAGCAGCAATACCCTTCATCG
<i>PPC2</i>	At2G42600	PPC2-FP	GTCCGGCCACATCTCTCTAAGG
		PPC2-RP	GCATACCAGCAGCGATAACCCTT
<i>PPC3</i>	At3G14940	PPC3-FP	GCAATCAAGCAAATCAGCACA
		PPC3-RP	AGATAAGTGTGTCCTCAAGTCC
<i>PPCK1</i>	At1G08650	PPCK1-FP	GCTTATCATCTCTCTCGGTGGT
		PPCK1-RP	TTACATGCCCGACTCCTC
<i>PPCK2</i>	At3G04530	PPCK2-FP	CTAGCTGGAGAACCGCCGTTTAAC
		PPCK2-RP	CTAGCTGGAGAACCGCCGTTTAAC
<i>PP2A</i>	AT1G13320	PP2A-FP	AGCCAAGTAGGACGGATCTGGT
		PP2A-RP	GCTATCCGAAGTCTGCCTCATTA

FP and RP denote forward and reverse primer, respectively

Supplementary table 2: Primers used for amplification of Arabidopsis plant type *PPC* promoters.

Promoter	Size (bp)	Primer	5'→3' sequence
<i>PPC1</i>	2790	<i>PPC1</i> -FP	AAGGTCTCAGCGGAACTTGAGCCGGTTCGATGTC
		<i>PPC1</i> -RP	AAGGTCTCACAGATTTTTTCACCTGCTTCGCTCTG
<i>PPC2</i>	1139	PPC2-FP1	AAGAAGACAATACGGGTCTCAGCGGATATATTCCCCTAG CCACCAC
		PPC2-RP1	AAGAAGACAACGGTTTCTTATCATATAGTTTTTTTCT
	976	PPC2-FP2	AAGAAGACAAACCGTAATAGACGTGGTACGTTT
		PPC2-RP2	AAGAAGACAAAAACGATGGAAAGAGAAGCGAC
	353	PPC2-FP3	AAGAAGACAATTTTCTCGTGAACGAACTTCT
		PPC2-RP3	AAGAAGACAACAGAGGTCTCACAGAGGTTTGGTTGATGCT TTTTCTC
<i>PPC3</i>	561	PPC3-FP1	AAGAAGACAATACGGGTCTCAGCGGCCGCGTTATTGCGGT AACC
		PPC3-RP1	AAGAAGACAATGCCGTCCTCTTAATTTGAATTTTA
	1872	PPC3-FP2	AAGAAGACAAGGCATGATTTGTAAAACCATAAAG
		PPC3-RP2	AAGAAGACAACAGAGGTCTCACAGATATCGCCGATCAATC AAATCTTC

FP and RP denote forward and reverse primer, respectively.

Supplementary table 3: Restriction enzymes used to confirm *PPC* promoter positive clones

<i>PPC</i> promoter level 0 clones		
<i>PPC1</i> -promoter	Hind III	1797, 3459
<i>PPC2</i> -promoter	BsaBI and BstXI	928, 1656, 2304
<i>PPC3</i> -promoter	Hind III	2125, 2721
<i>PPC</i> promoter level I clones		
<i>PPC1</i> -promoter	XhoI	3668, 9713
<i>PPC2</i> -promoter	XhoI	3668, 9573
<i>PPC3</i> -promoter	HindIII	2125, 2725
<i>PPC</i> promoter level II clones		
<i>PPC1</i> -promoter	BbSI and NcoI	1830, 2055,2843, 6661
<i>PPC2</i> -promoter	BbSI and NcoI	1830, 2055,2703, 6661
<i>PPC3</i> -promoter	BbSI and NcoI	1830, 2055,2479, 6661
<i>PPC</i> promoter level III clones		
LIII- <i>PPC1</i> -promoter	XhoI and HindIII	1824, 3668, 9573
LIII- <i>PPC2</i> -promoter	XhoI and HindIII	195, 746, 3668, 10320
LIII- <i>PPC3</i> -promoter	XhoI and HindIII	2200, 3668, 8833

Supplementary table 4: List of sequencing primers used for confirmation of positive clones for PPC promoters.

Target	Primer	5'→3' sequence
<i>PPC1</i> promoter LI	M13uni -21	TGTAAAACGACGGCCAGT
	M13 RP -29	CAGGAAACAGCTATGACC
<i>PPC2</i> promoter LI	M13uni -21	TGTAAAACGACGGCCAGT
	M13 RP -29	CAGGAAACAGCTATGACC
<i>PPC3</i> promoter LI	M13uni -21	TGTAAAACGACGGCCAGT
	M13 RP -29	CAGGAAACAGCTATGACC
<i>PPC1</i> promoter L II and III	Primer-LB	ACGAGTCGGAATCGCAGAC
	Primer-RB	CGGATAAACCTTTTCACGC
<i>PPC2</i> promoter LII and III	Primer-LB	ACGAGTCGGAATCGCAGAC
	Primer-RB	CGGATAAACCTTTTCACGC
<i>PPC3</i> promoter L II and III	Primer-LB	ACGAGTCGGAATCGCAGAC
	Primer-RB	CGGATAAACCTTTTCACGC
mCherry	MCherry-FP	CCTTTGATTCAGTGGGAAC
	mCherry-RP	CTCTCTCTATTTTCTCCAG
GFP & Hygromycin segment	HygGfp-FP	GAGAGCTGCATCAGGTCCG
	HygGfp-RP	CAAGAAGGGAGGTGGAGG

Products were sent to Eurofins for sequencing. FP and RP denote forward and reverse primers while LB and RB denote left and right border primers, respectively.

Supplementary table 5: Primers used for amplification of open reading frames of PPCs for Directional TOPO cloning.

Target	Size (bp)	Primer	5'→3' sequence
<i>PPC1</i> -CDS+STOP	2904	PPC1-FP	CACCATGGCGAATCGGAAGTTAGAG
		PPC1-RP	TTAACCGGTGTTTTGTAGACCAGC
<i>PPC1</i> -CDS-STOP	2901	PPC1-FP	CACCATGGCGAATCGGAAGTTAGAG
		PPC1-RP	ACCGGTGTTTTGTAGACCAGC
<i>PPC2</i> -CDS+STOP	2892	PPC2-FP	CACCATGGCTGCGAGAAATTTGG
		PPC2-RP	TTAACCGGTGTTTTGCATAC
<i>PPC2</i> -CDS-STOP	2889	PPC2-FP	CACCATGGCTGCGAGAAATTTGG
		PPC2-RP	ACCGGTGTTTTGCATAC
<i>PPC3</i> -CDS+STOP	2907	PPC3-FP	CACCATGGCGGGTCGGAACATA
		PPC3-RP	TTAACCGGTGTTTTGCAATCCTG
<i>PPC3</i> -CDS-STOP	2904	PPC3-FP	CACCATGGCGGGTCGGAACATA
		PPC3-RP	ACCGGTGTTTTGCAATCCTG

FP and RP denote forward and reverse primers respectively.

Supplementary table 6: List of restriction enzymes used to confirm positive entry and destination clones for *PPC* overexpression lines.

Cloning cassette	Restriction enzymes	Product size (bp)
<i>PPC</i> overexpression entry clones		
<i>pENTR-PPC1-CDS+STOP</i>	SacII and XhoI	1535, 3949
<i>pENTR-PPC2-CDS+STOP</i>	ApaI and BstXI	674, 4798
<i>pENTR-PPC3-CDS+STOP</i>	ApaI and BsaB1	993, 4494
<i>PPC</i> overexpression destination clones		
<i>pEXP-pB7WG2-PPC1-CDS+STOP</i>	ApaI and BstXI	590, 12319
<i>pEXP-pB7WG2-PPC2-CDS+STOP</i>	ApaI and BstXI	2636, 9544
<i>pEXP-pB7WG2-PPC3-CDS+STOP</i>	ApaI and BcuI	3252, 8943

Supplementary table 7: Primers used for sequencing of *PPC* overexpression entry clones

Target	Primer	5'→3' sequence
<i>PPC1</i> CDS	M13 FP -20	GTAAAACGACGGCCAG
	M13 RP	CAGGAAACAGCTATGAC
<i>PPC2</i> CDS	M13 FP -20	GTAAAACGACGGCCAG
	M13 RP	CAGGAAACAGCTATGAC
<i>PPC3</i> CDS	M13 FP -20	GTAAAACGACGGCCAG
	M13 RP	CAGGAAACAGCTATGAC

FP and RP denote forward and reverse primers respectively.

Supplementary table 8: Restriction enzymes used in confirmation of *ppck2* CRISPR/Cas 9 mutant positive clones

Cloning cassette	Restriction enzymes	Product size (bp)
<i>ppck2</i> CRISPR/Cas 9 knockout entry clone		
<i>pDGE332</i>	BsaI	229, 2736
<i>pDGE334</i>	BsaI	212, 2736
<i>ppck2</i> CRISPR/Cas 9 knockout destination clone		
<i>pDGE347</i>	NcoI and HindIII	475, 1060, 7625, 9507

Supplementary table 9: List of primers used to genotype and sequence positive clones for *ppck2* CRISPR/Cas 9 and *ppck1ppck2* mutants.

Target	Primer	5'→3' sequence	Purpose
<i>PPCK1</i>	LBb1.3	ATTTTGCCGATTTCCGAAC	Genotyping <i>PPCK1</i>
	PPCK1- RP	TCCTTTTACTCACCCACATG	
<i>PPCK2</i>	PPCK2- FP	CGCCGCATCCGAATATCATC	Genotyping and sequencing <i>PPCK2</i>
	PPCK2- RP	CACCATTACAAATTGATGAGCAAATC	

FP and RP denote forward and reverse primers, respectively

Supplementary table 10: List of primers used for colony PCR in Agrobacterium.

Expression cassette	Primers	5'→ 3' sequence
<i>pUB-N-GFP-PPC1-CDS+STOP</i>	FP-PPC1-CDS RP-PPC1-CDS+S	CACCATGGCGAATCGGAAGTTAGAG TTAACCGGTGTTTTGTAGACCAGC
<i>pUB-C-GFP-PPC1-CDS-STOP</i>	FP-PPC1-CDS RP-PPC1-CDS-S	CACCATGGCGAATCGGAAGTTAGAG ACCGGTGTTTTGTAGACCAGC
<i>pUB-Dest-PPC1-CDS+STOP</i>	FP-PPC1-CDS RP-PPC1-CDS+S	CACCATGGCGAATCGGAAGTTAGAG TTAACCGGTGTTTTGTAGACCAGC
<i>pUB-N-GFP-PPC2-CDS+STOP</i>	FP-PPC2-CDS RP-PPC2-CDS+S	CACCATGGCTGCGAGAAATTTGG TTAACCGGTGTTTTGCATAC
<i>pUB-C-GFP-PPC2-CDS-STOP</i>	FP-PPC2-CDS RP-PPC2-CDS-S	CACCATGGCTGCGAGAAATTTGG ACCGGTGTTTTGCATAC
<i>pUB-Dest-PPC2-CDS+STOP</i>	FP-PPC2-CDS RP-PPC2-CDS+S	TTAACCGGTGTTTTGTAGACCAGC CACCATGGCTGCGAGAAATTTGG
<i>pUB-Dest-PPC3-CDS+STOP</i>	FP-PPC3-CDS RP-PPC3-CDS+S	CACCATGGCGGGTTCGGAACATA TTAACCGGTGTTTTGCAATCCTG
<i>pUB-C-GFP-PPC3-CDS-STOP</i>	FP-PPC3-CDS RP-PPC3-CDS-S	CACCATGGCGGGTTCGGAACATA ACCGGTGTTTTGCAATCCTG
<i>pUB-Dest-PPC3-CDS+STOP</i>	FP-PPC3-CDS RP-PPC3-CDS+S	CACCATGGCGGGTTCGGAACATA TTAACCGGTGTTTTGCAATCCTG
<i>pB7FWGF2-PPC1-CDS+STOP</i>	FP-PPC1-CDS RP-PPC1-CDS+S	CACCATGGCGAATCGGAAGTTAGAG TTAACCGGTGTTTTGTAGACCAGC
<i>pB7FWG2-PPC1-CDS-STOP</i>	FP-PPC1-CDS RP-PPC1-CDS-S	CACCATGGCGAATCGGAAGTTAGAG ACCGGTGTTTTGTAGACCAGC
<i>pB7WG2-PPC1-CDS-STOP</i>	FP-PPC1-CDS RP-PPC1-CDS+S	CACCATGGCGAATCGGAAGTTAGAG TTAACCGGTGTTTTGTAGACCAGC
<i>pB7FWGF2-PPC2-CDS+STOP</i>	FP-PPC2-CDS RP-PPC2-CDS+S	CACCATGGCTGCGAGAAATTTGG TTAACCGGTGTTTTGCATAC
<i>-pB7FWG2-PPC2-CDS-STOP</i>	FP-PPC2-CDS RP-PPC2-CDS-S	CACCATGGCTGCGAGAAATTTGG ACCGGTGTTTTGCATAC
<i>pB7WG2-PPC2-CDS-STOP</i>	FP-PPC2-CDS RP-PPC2-CDS+S	TTAACCGGTGTTTTGTAGACCAGC CACCATGGCTGCGAGAAATTTGG
<i>pB7FWGF2-PPC3-CDS+STOP</i>	FP-PPC3-CDS RP-PPC3-CDS+S	CACCATGGCGGGTTCGGAACATA TTAACCGGTGTTTTGCAATCCTG
<i>pB7FWG2-PPC3-CDS-STOP</i>	FP-PPC3-CDS RP-PPC3-CDS-S	CACCATGGCGGGTTCGGAACATA ACCGGTGTTTTGCAATCCTG
<i>pB7WG2-PP3-CDS-STOP</i>	FP-PPC3-CDS RP-PPC3-CDS+S	CACCATGGCGGGTTCGGAACATA TTAACCGGTGTTTTGCAATCCTG
<i>pLIIIβ BB52-pPPC1+STOP</i>	FP-pPPC1 RP-pPPC1	CTTGAGCCGGTTCGATGTC TTTCACCTGCTTCGCTCTG
<i>pLIIIβ BB52-pPPC2+STOP</i>	FP-pPPC2 RP-pPPC2	ATATTCCCACTAGCCACCAC TTTGGTTGATGCTTTTCCTC
<i>pLIIIβ BB52-pPPC3+STOP</i>	FP-pPPC3 RP-pPPC3	CGCGTTATTGCGGTAACC ATCGCCGATCAATCAAATCTTC

FP and RP denote forward and reverse primer respectively

Supplementary table 11: Mass spectrophotometry (MS) parameters for MRM-transitions of organic acids.

Organic acid	MRM transitions	Retention time (min)	Segment	Ionization energy, eV	Collision energy, eV				
Succinate-D4	267→177	5.01	1	-135	5				
	267→251				5				
Succinate	263→173	5.05			1	-135	5		
	263→247						5		
Fumarate	261→245	5.50					1	-135	5
	261→171								10
Malate	351→233	7.55	2	-135					5
	351→189								15
Malate-D3	354→236	7.53			2	-135			5
	351→192								15
α -ketoglutarate	320→244	8.65					3	-135	5
	320→230								10
Aconitate	391→211	10.55	3	-135					5
	391→301								15
Citrate-D4	485→276	11.03			4	-135			5
	485→367								15
Citrate	481→273	11.04					4	-135	5
	481→363								15

MRM denotes multiple reaction monitoring

Supplementary table 12: Comparison of metabolite in shoots of PPC overexpression lines compared to wild type on sufficient Pi.

Seedlings were germinated for 6 days on sufficient media before transfer to sufficient or insufficient media for an additional five days before harvest. Significance analyses were performed by Student's t-test (two-tailed, equal variances). Number in bold indicates significant difference between the overexpression lines and wild type with $p < 0.05$, $n = 12$. Dark and light grey cells highlight metabolites that were increased and decreased in the overexpression lines compared to wild type.

Shoot metabolites measurements in PPC overexpression lines grown on Pi sufficient conditions																
	35S::PPC1 3.6		35S::PPC1 4.10		35S::PPC1 8.10		35S::PPC2 1.8		35S::PPC2 4.9		35S::PPC3 5.11		35S::PPC3 8.12		35S::PPC3 9.12	
Metabolite	Fold	T-test	Fold	T-test	Fold	T-test	Fold	T-test	Fold	T-test	Fold	T-test	Fold	T-test	Fold	T-test
Alanine	1.21	0.074	1.18	0.221	1.18	0.228	1.30	0.011	1.09	0.429	1.06	0.637	1.08	0.570	1.05	0.685
Cysteine	0.78	0.156	0.74	0.087	0.71	0.051	0.98	0.924	0.68	0.080	0.68	0.061	0.68	0.055	0.66	0.021
Aspartate	1.20	0.019	1.20	0.031	1.29	0.018	1.47	0.111	1.06	0.729	1.15	0.399	1.28	0.029	0.99	0.959
Glutamate	0.97	0.738	0.95	0.569	1.03	0.817	1.41	0.076	1.05	0.755	0.97	0.839	0.97	0.768	0.84	0.308
Phenylalanine	1.20	0.055	1.22	0.080	1.18	0.100	1.15	0.226	1.15	0.316	1.37	0.021	1.38	0.019	1.43	0.003
Glycine	1.37	0.151	1.62	0.062	1.30	0.204	1.07	0.672	0.96	0.836	1.15	0.490	0.99	0.942	0.94	0.711
Histidine	1.30	0.025	1.38	0.038	1.41	0.009	1.58	0.002	1.55	0.005	1.37	0.023	1.67	5.6e5	1.53	0.001
Isoleucine	1.24	0.057	1.21	0.116	1.25	0.056	1.32	0.007	1.26	0.038	1.39	0.011	1.43	0.024	1.38	0.012
Lysine	1.40	0.001	1.34	0.006	1.34	3.0e4	1.34	0.011	1.31	0.007	1.38	0.020	1.61	0.001	1.40	3.2e5
Leucine	1.35	0.068	1.40	0.067	1.34	0.012	1.27	0.009	1.24	0.033	1.59	0.012	1.65	0.029	1.62	1.4e4
Methionine	1.82	0.029	1.56	0.152	1.36	0.263	1.10	0.777	1.72	0.150	1.43	0.457	1.86	0.094	1.18	0.665
Asparagine	1.14	0.290	1.33	0.096	1.32	0.061	1.50	0.004	1.27	0.060	1.46	0.013	1.42	0.012	1.30	0.065
Proline	1.19	0.157	1.07	0.602	1.11	0.389	1.41	0.022	1.28	0.129	1.06	0.725	1.02	0.870	1.08	0.668
Glutamine	1.17	0.133	1.05	0.663	1.18	0.295	1.47	0.002	1.20	0.092	1.07	0.616	0.97	0.826	0.99	0.940
Arginine	1.12	0.482	1.50	0.067	1.26	0.021	1.29	0.179	1.32	0.114	1.53	0.001	1.61	3.4e4	1.49	0.004
Serine	0.92	0.522	1.35	0.122	0.90	0.434	0.86	0.321	0.50	1.6e7	0.77	0.011	0.78	0.053	0.61	1.9e6
Threonine	1.14	0.222	1.09	0.445	1.15	0.278	1.41	0.003	1.13	0.199	1.13	0.333	1.08	0.547	1.06	0.619
Valine	1.28	0.044	1.26	0.073	1.27	0.056	1.40	0.003	1.22	0.063	1.27	0.074	1.29	0.075	1.27	0.043
Tryptophan	1.23	0.064	1.20	0.136	1.14	0.184	1.19	0.070	1.08	0.496	1.28	0.081	1.26	0.059	1.26	0.044
Tyrosine	1.50	0.091	1.56	0.029	1.62	0.061	1.31	0.066	1.39	0.020	1.72	0.004	2.29	0.012	1.74	0.003
Ornithine	1.09	0.395	1.24	0.058	1.09	0.347	1.37	0.015	1.37	0.046	1.08	0.510	1.03	0.817	1.07	0.440
Citrulline	1.07	0.583	1.15	0.282	0.97	0.826	1.16	0.316	0.88	0.292	0.94	0.689	0.84	0.200	0.81	0.178
Taurin	1.09	0.311	1.16	0.209	1.06	0.490	1.46	0.003	1.28	0.009	1.06	0.613	0.97	0.786	1.04	0.693
O-acetylserine	1.31	0.066	1.20	0.221	1.37	0.025	1.24	0.121	0.98	0.877	1.10	0.554	1.17	0.452	1.26	0.247
Fumarate	0.89	0.243	0.78	0.020	0.89	0.284	1.43	0.001	1.15	0.132	0.66	4.3e4	0.64	0.002	0.61	2.7e4
Aconitate	1.13	0.071	1.17	0.026	1.16	0.047	1.05	0.484	0.94	0.405	1.19	0.179	1.22	0.022	1.02	0.866
α -ketoglutarate	1.17	0.135	1.02	0.848	1.13	0.241	1.19	0.030	1.21	0.144	0.88	0.439	0.85	0.300	0.86	0.316
Succinate	1.52	3.8e4	1.23	0.006	1.27	0.003	1.26	0.277	0.95	0.577	1.03	0.740	1.04	0.642	1.10	0.194

Supplementary table 13: Comparison of metabolite in shoots of *PPC* overexpression lines compared to wild type upon Pi starvation.

Seedlings were germinated for 6 days on sufficient media before transfer to insufficient media for an additional five days before harvest. Significance analyses were performed by Student's t-test (two-tailed, equal variances). Number in bold indicates significant difference between the overexpression lines and wild type with $p < 0.05$, $n = 12$. Dark and light grey cells highlight metabolites that were increased and decreased in the overexpression lines compared to wild type.

Shoot metabolites measurements in <i>PPC</i> overexpression lines grown on Pi insufficient condition																
Metabolite	<i>35S::PPC1 3.6</i>		<i>35S::PPC1 4.10</i>		<i>35S::PPC1 8.10</i>		<i>35S::PPC2 1.8</i>		<i>35S::PPC2 4.9</i>		<i>35S::PPC3 5.11</i>		<i>35S::PPC3 8.12</i>		<i>35S::PPC3 9.12</i>	
	Fold	T-test	Fold	T-test	Fold	T-test	Fold	T-test	Fold	T-test	Fold	T-test	Fold	T-test	Fold	T-test
Alanine	1.08	0.759	1.35	0.293	1.19	0.469	1.19	0.432	1.04	0.886	1.47	0.221	1.10	0.716	1.09	0.730
Cysteine	1.00	0.990	1.01	0.919	1.16	0.337	1.21	0.268	0.91	0.576	0.99	0.960	1.01	0.941	0.93	0.709
Aspartate	1.00	0.994	0.94	0.785	1.07	0.752	1.16	0.512	1.05	0.812	0.99	0.949	0.95	0.813	0.97	0.905
Glutamate	0.94	0.499	0.96	0.687	1.05	0.638	1.15	0.059	1.10	0.273	0.93	0.472	0.88	0.147	0.90	0.323
Phenylalanine	1.18	0.496	1.09	0.729	1.26	0.355	1.21	0.441	1.15	0.600	1.16	0.552	1.00	0.989	1.21	0.466
Glycine	0.88	0.667	1.14	0.683	1.03	0.916	0.82	0.492	0.78	0.366	0.91	0.767	0.93	0.831	0.74	0.318
Histidine	1.17	0.583	1.10	0.725	1.18	0.528	1.44	0.219	1.11	0.693	1.24	0.475	0.86	0.553	1.31	0.326
Isoleucine	1.22	0.432	1.20	0.442	1.35	0.205	1.48	0.124	1.16	0.537	1.47	0.107	1.10	0.644	1.26	0.346
Lysine	1.11	0.379	1.07	0.459	1.12	0.155	1.37	0.005	1.07	0.487	1.07	0.525	0.79	0.023	0.96	0.714
Leucine	1.22	0.525	1.24	0.478	1.35	0.291	1.37	0.254	1.19	0.503	1.36	0.294	1.12	0.639	1.29	0.352
Methionine	0.82	0.672	1.24	0.667	0.83	0.747	1.22	0.681	0.45	0.129	1.13	0.811	0.32	0.042	0.53	0.180
Asparagine	1.01	0.959	1.10	0.735	1.14	0.603	1.13	0.617	1.03	0.913	1.21	0.486	0.94	0.767	1.07	0.800
Proline	1.52	0.154	1.38	0.215	1.83	0.043	1.68	0.046	1.47	0.132	1.87	0.014	1.56	0.082	2.14	0.006
Glutamine	1.03	0.902	0.96	0.889	1.10	0.673	1.18	0.442	1.09	0.710	1.03	0.915	0.78	0.249	0.96	0.859
Arginine	1.50	0.230	1.33	0.375	1.54	0.182	1.60	0.129	1.32	0.325	1.61	0.123	1.08	0.711	1.48	0.210
Serine	1.02	0.930	1.32	0.274	1.20	0.497	1.17	0.508	0.78	0.313	1.16	0.548	0.97	0.900	0.96	0.855
Threonine	1.06	0.763	1.00	0.983	1.18	0.413	1.12	0.564	1.00	0.983	1.13	0.533	0.97	0.876	1.10	0.638
Valine	1.18	0.499	1.21	0.407	1.25	0.332	1.46	0.106	1.18	0.465	1.35	0.199	1.09	0.681	1.22	0.405
Tryptophan	1.27	0.394	1.33	0.301	1.34	0.264	1.35	0.231	1.11	0.698	1.54	0.089	1.13	0.641	1.26	0.389
Y-Tyrosine	1.41	0.298	1.59	0.167	1.58	0.167	1.76	0.097	1.29	0.441	1.57	0.184	1.17	0.625	1.29	0.446
Ornithine	0.98	0.884	0.93	0.498	0.86	0.330	1.28	0.061	0.94	0.655	0.85	0.229	0.57	0.001	0.68	0.008
Citrulline	1.04	0.868	1.03	0.910	1.09	0.719	1.25	0.312	0.94	0.740	1.13	0.661	0.71	0.106	1.06	0.814
Taurin	0.90	0.435	0.88	0.356	0.86	0.285	1.19	0.322	0.94	0.637	0.75	0.086	0.67	0.018	0.76	0.071
O-acetylserine	1.05	0.662	1.13	0.404	1.17	0.369	1.05	0.606	1.11	0.418	1.18	0.289	1.05	0.751	1.16	0.336
Fumarate	1.04	0.735	0.70	0.018	0.94	0.589	1.28	0.024	1.33	0.008	0.71	0.026	0.78	0.106	0.82	0.151
Aconitate	1.44	0.011	1.87	1.5e4	1.55	0.003	0.98	0.902	0.94	0.720	1.74	0.003	1.22	0.200	1.15	0.403
α -ketoglutarate	1.35	0.028	1.31	0.037	1.33	0.048	1.63	0.001	1.70	0.004	0.90	0.496	0.80	0.201	0.87	0.504
Succinate	1.51	4.0e4	1.58	0.001	1.54	0.001	1.01	0.901	1.11	0.403	1.46	2.9e4	1.42	0.005	1.69	1.4e5

Supplementary table 14: Comparison of metabolite in roots of *PPC* overexpression lines compared to wild type grown on sufficient Pi condition.

Seedlings were germinated for 6 days on sufficient media before transfer to insufficient media for an additional five days before harvest. Significance analyses were performed by Student's t-test (two-tailed, equal variances). Number in bold indicates significant difference between the overexpression lines and wild type with $p < 0.05$, $n = 12$. Dark and light grey cells highlight metabolites that were increased and decreased in the overexpression lines compared to wild type.

Root metabolites measurements in <i>PPC</i> overexpression lines grown on sufficient Pi condition																
Metabolite	<i>35S::PPC1 3.6</i>		<i>35S::PPC1 4.10</i>		<i>35S::PPC1 8.10</i>		<i>35S::PPC2 1.8</i>		<i>35S::PPC2 4.9</i>		<i>35S::PPC3 5.11</i>		<i>35S::PPC3 8.12</i>		<i>35S::PPC3 9.12</i>	
	Fold	T-test	Fold	T-test	Fold	T-test	Fold	T-test	Fold	T-test	Fold	T-test	Fold	T-test	Fold	T-test
Alanine	1.11	0.286	1.18	0.045	1.21	0.055	1.40	0.023	1.25	0.038	1.17	0.155	1.46	0.024	1.08	0.515
Cysteine	1.22	0.089	1.03	0.748	1.21	0.063	1.50	0.007	1.40	0.001	1.07	0.558	1.08	0.495	1.29	0.073
Aspartate	1.35	0.008	1.30	2.7e4	1.46	0.001	2.75	0.005	2.93	2.1e4	1.21	0.115	1.30	0.014	1.34	0.065
Glutamate	0.77	0.068	0.92	0.522	0.88	0.325	2.69	0.006	2.42	0.003	0.88	0.307	1.00	0.987	0.90	0.420
Phenylalanine	1.52	0.031	1.29	0.068	1.31	0.055	1.44	0.030	1.38	0.001	1.14	0.314	1.37	0.039	1.46	0.011
Glycine	1.00	0.995	1.03	0.766	0.91	0.472	1.42	0.027	1.49	0.011	0.84	0.145	1.06	0.651	1.17	0.250
Histidine	1.23	0.088	1.31	0.007	1.12	0.180	1.97	0.001	1.86	5.2e7	1.19	0.163	1.23	0.023	1.37	0.035
Isoleucine	1.35	0.023	1.29	0.009	1.32	0.035	1.84	0.003	1.92	1.4e5	1.34	0.040	1.45	0.008	1.26	0.077
Lysine	1.35	0.056	1.45	4.8e4	1.45	0.008	1.81	0.001	1.79	1.8e5	1.35	0.020	1.53	2.6e4	1.49	0.003
Leucine	1.51	0.010	1.25	0.066	1.40	0.013	1.77	0.004	1.90	1.4e5	1.26	0.083	1.52	0.008	1.45	0.008
Methionine	1.60	0.072	2.28	0.005	1.92	0.051	2.08	0.017	1.70	0.083	2.23	0.014	2.18	0.023	2.01	0.034
Asparagine	1.36	0.023	1.18	0.148	1.22	0.088	1.73	0.007	1.87	1.4e5	1.17	0.184	1.27	0.056	1.25	0.142
Proline	1.51	0.006	1.13	0.245	1.20	0.091	1.76	2.4e4	1.83	7.8e5	1.03	0.839	1.17	0.189	1.04	0.786
Glutamine	1.22	0.053	1.03	0.732	1.18	0.117	1.64	6.7e5	1.69	1.2e6	1.18	0.172	1.33	0.028	1.31	0.040
Arginine	1.85	0.004	1.59	0.002	1.65	0.002	1.82	0.007	1.89	4.2e6	1.73	0.010	1.59	0.002	1.35	0.054
Serine	1.18	0.051	1.30	0.002	1.16	0.073	1.33	0.030	1.25	0.011	1.17	0.137	1.39	0.010	1.12	0.353
Threonine	1.24	0.024	1.10	0.209	1.28	0.008	1.54	0.001	1.68	1.7e7	1.15	0.217	1.30	0.014	1.19	0.179
Valine	1.25	0.040	1.22	0.022	1.35	0.010	1.89	0.004	2.19	0.001	1.50	0.017	1.62	0.004	1.95	0.003
Tryptophan	1.35	0.029	1.29	0.017	1.29	0.088	1.57	0.013	1.32	0.029	1.12	0.476	1.12	0.428	1.07	0.729
Tyrosine	1.27	0.130	1.35	0.024	1.54	0.014	1.62	0.003	1.51	8.0e6	1.13	0.218	1.25	0.042	1.33	0.047
Ornithine	0.87	0.426	1.18	0.204	0.93	0.606	1.71	0.034	1.40	0.045	1.08	0.604	1.17	0.211	1.05	0.718
Citrulline	1.13	0.399	1.11	0.324	1.16	0.369	1.36	0.097	1.41	0.037	1.02	0.866	1.13	0.414	1.55	0.094
Taurin	1.15	0.245	1.44	0.008	1.16	0.879	2.29	0.003	1.68	0.047	1.17	0.324	1.26	0.122	1.17	0.351
<i>O</i> -acetylserine	1.26	0.060	1.33	0.084	1.23	0.338	2.57	0.039	48.62	0.108	1.13	0.416	1.37	0.085	1.08	0.591
Fumarate	1.00	0.981	1.12	0.438	0.98	0.879	0.83	0.235	1.13	0.250	0.60	0.001	0.68	0.017	0.55	0.001
Aconitate	1.12	0.194	1.03	0.731	1.20	0.065	1.42	0.013	1.42	0.001	0.94	0.653	1.28	0.111	1.18	0.244
α -ketoglutarate	1.20	0.179	1.08	0.553	1.12	0.414	1.07	0.673	1.21	0.106	0.76	0.066	0.71	0.090	0.78	0.119
Succinate	1.27	0.001	1.26	0.001	1.21	0.027	1.13	0.261	1.30	0.015	0.97	0.708	1.03	0.862	0.92	0.613

Supplementary table 15: Comparison of metabolite in roots of *PPC* overexpression lines compared to wild type upon Pi starvation.

Seedlings were germinated for 6 days on sufficient media before transfer to insufficient media for an additional five days before harvest. Significance analyses were performed by Student's t-test (two-tailed, equal variances). Number in bold indicates significant difference between the overexpression lines and wild type with $p < 0.05$, $n = 12$. Dark and light grey cells highlight metabolites that were increased and decreased in the overexpression lines compared to wild type.

Root metabolites measurements in <i>PPC</i> overexpression lines grown on Pi insufficient condition																
	<i>35S::PPC1 3.6</i>		<i>35S::PPC1 4.10</i>		<i>35S::PPC1 8.10</i>		<i>35S::PPC2 1.8</i>		<i>35S::PPC2 4.9</i>		<i>35S::PPC3 5.11</i>		<i>35S::PPC3 8.12</i>		<i>35S::PPC3 9.12</i>	
Metabolite	Fold	T-test	Fold	T-test	Fold	T-test	Fold	T-test	Fold	T-test	Fold	T-test	Fold	T-test	Fold	T-test
Alanine	0.81	0.527	0.94	0.862	0.930	0.825	0.95	0.863	0.89	0.712	0.90	0.758	0.95	0.870	1.00	0.996
Cysteine	0.98	0.956	0.95	0.861	1.101	0.714	1.11	0.717	1.20	0.538	0.98	0.945	0.96	0.871	1.15	0.648
Aspartate	0.68	0.522	0.54	0.325	0.804	0.707	0.78	0.658	0.76	0.629	0.58	0.375	0.47	0.247	0.51	0.288
Glutamate	0.59	0.385	0.53	0.319	0.718	0.574	0.80	0.697	0.81	0.719	0.59	0.387	0.46	0.240	0.51	0.301
Phenylalanine	0.75	0.503	0.78	0.545	0.803	0.608	0.86	0.714	0.78	0.544	0.74	0.471	0.77	0.540	0.82	0.612
Glycine	0.53	0.138	0.52	0.127	0.602	0.227	0.62	0.236	0.64	0.270	0.48	0.096	0.49	0.100	0.53	0.130
Histidine	0.96	0.893	0.97	0.933	1.138	0.684	1.23	0.522	1.43	0.272	1.01	0.972	1.00	0.997	1.22	0.541
Isoleucine	1.07	0.865	1.16	0.710	1.270	0.526	1.38	0.394	1.43	0.347	1.45	0.335	1.54	0.235	1.59	0.214
Lysine	1.28	0.489	1.34	0.433	1.418	0.309	1.59	0.187	1.80	0.113	1.41	0.339	1.46	0.281	1.66	0.162
Leucine	0.97	0.931	0.99	0.978	0.970	0.922	1.12	0.722	1.23	0.513	1.07	0.838	1.01	0.968	1.16	0.640
Methionine	1.40	0.307	1.18	0.643	1.024	0.952	0.85	0.666	1.13	0.759	0.80	0.594	1.33	0.540	1.15	0.729
Asparagine	1.01	0.987	0.97	0.928	1.069	0.844	1.14	0.697	1.34	0.393	0.98	0.956	1.07	0.838	1.18	0.614
Proline	1.18	0.643	1.09	0.797	1.406	0.364	1.29	0.456	1.52	0.266	1.41	0.373	1.21	0.596	1.71	0.177
Glutamine	0.94	0.846	0.93	0.817	1.053	0.871	1.18	0.598	1.34	0.360	0.98	0.945	1.08	0.815	1.11	0.751
Arginine	1.20	0.595	1.26	0.494	1.231	0.532	1.30	0.436	1.46	0.294	1.24	0.575	1.22	0.571	1.33	0.452
Serine	0.93	0.839	1.02	0.964	1.028	0.933	1.08	0.829	1.09	0.796	0.97	0.940	1.00	0.992	1.13	0.720
Threonine	0.95	0.876	0.85	0.628	1.001	0.997	0.96	0.896	1.11	0.743	0.94	0.838	0.97	0.919	1.03	0.931
Valine	0.93	0.825	0.97	0.917	0.987	0.969	1.06	0.857	1.15	0.658	1.06	0.854	1.04	0.913	1.19	0.579
Tryptophan	0.82	0.577	0.91	0.788	0.961	0.907	0.95	0.880	0.88	0.718	1.04	0.924	1.02	0.956	1.06	0.874
Y-Tyrosine	0.76	0.093	0.88	0.477	1.176	0.492	1.12	0.581	0.94	0.703	0.91	0.595	1.06	0.763	1.03	0.879
Ornithine	0.77	0.562	0.86	0.728	1.122	0.789	1.07	0.875	1.15	0.727	0.79	0.591	0.82	0.653	0.92	0.856
Citrulline	0.55	0.318	0.47	0.223	0.671	0.484	0.73	0.571	0.61	0.389	0.60	0.384	0.53	0.283	0.65	0.450
Taurin	0.59	0.206	0.66	0.287	0.770	0.509	0.81	0.603	0.75	0.447	0.68	0.324	0.62	0.252	0.66	0.313
<i>O</i> -acetylserine	0.72	0.279	0.67	0.188	0.757	0.322	0.94	0.821	0.92	0.763	0.72	0.266	0.73	0.293	0.81	0.444
Fumarate	1.37	0.047	1.15	0.299	1.047	0.735	1.07	0.697	1.02	0.901	0.78	0.111	0.88	0.434	0.77	0.135
Aconitate	1.64	0.002	1.39	0.017	1.146	0.299	1.24	0.151	1.28	0.095	1.38	0.017	1.55	0.002	1.40	0.008
α -ketoglutarate	1.41	0.009	1.13	0.229	1.158	0.247	1.41	0.013	1.77	0.000	1.00	0.992	1.03	0.784	0.97	0.801
Succinate	1.16	0.271	1.31	0.033	1.167	0.255	1.12	0.537	1.00	0.982	1.09	0.544	1.22	0.090	1.04	0.785

Supplementary table 16: Comparison of metabolite in shoots of *ppck* mutants and *ppck1-4* complementation lines compared to wild type on sufficient Pi condition.

Seedlings were germinated for 6 days on sufficient media before transfer to insufficient media for an additional five days before harvest. Significance analyses were performed by Student's t-test (two-tailed, equal variances). Number in bold indicates significant difference between the overexpression lines and wild type with $p < 0.05$, $n = 12$. Dark and light grey cells highlight metabolites that were increased and decreased in the overexpression lines compared to wild type.

Shoot metabolites measurements in <i>ppck</i> mutants and <i>ppck1-4</i> complementation lines grown on sufficient Pi condition														
Metabolite	<i>ppck1-4</i>		<i>ppck1-4C 9.10</i>		<i>ppck1-4C 11.8</i>		<i>ppck2 1.3</i>		<i>ppck2 2.9</i>		<i>ppck1ppck2 7.11</i>		<i>ppck1ppck2 9.3</i>	
	Fold	T-test	Fold	T-test	Fold	T-test	Fold	T-test	Fold	T-test	Fold	T-test	Fold	T-test
Alanine	1.24	4.6e3	1.57	1.1e5	1.32	2.2e4	1.28	2.2e4	1.47	2.8e5	1.44	3.5e5	1.46	6.0e5
Cysteine	1.19	0.122	2.32	0.048	1.54	0.016	1.60	0.008	1.54	0.004	1.84	0.002	1.84	0.003
Aspartate	1.15	0.045	1.63	2.2e6	1.55	7.7e6	1.28	4.9e5	1.45	5.1e5	1.46	0.003	1.46	0.003
Glutamate	1.10	0.085	1.65	3.9e5	1.55	3.0e5	1.20	0.003	1.34	0.002	1.49	0.001	1.43	0.002
Phenylalanine	1.25	1.1e4	1.79	5.5e5	1.64	2.1e5	1.26	4.7e5	1.46	2.2e8	1.37	2.1e5	1.43	9.9e5
Glycine	1.14	0.099	1.28	0.044	1.29	0.043	1.10	0.371	1.11	0.280	1.29	0.012	1.14	0.194
Histidine	1.33	8.1e5	1.58	4.2e4	1.48	6.5e5	1.31	0.001	1.52	3.4e6	1.42	0.001	1.61	1.7e6
Isoleucine	1.31	1.5e6	1.94	2.9e9	1.69	1.5e9	1.43	1.5e7	1.58	3.2e10	1.53	2.3e7	1.83	2.3e8
Lysine	1.24	0.004	1.87	5.5e6	1.69	7.7e8	1.34	3.2e5	1.69	1.4e5	1.46	9.0e6	1.70	2.4e4
Leucine	1.21	0.001	1.67	1.2e6	1.57	2.0e6	1.37	5.0e5	1.64	1.3e7	1.53	0.001	1.68	7.6e5
Methionine	1.41	0.002	1.79	0.008	1.28	0.046	1.50	0.003	1.83	0.007	1.38	0.046	1.73	3.7e5
Asparagine	1.27	3.2e4	1.72	7.7e6	1.61	2.2e5	1.41	8.7e9	1.69	6.4e7	1.82	5.8e6	1.78	2.2e5
Proline	1.25	3.9e4	1.64	1.0e6	1.43	6.8e6	1.29	7.5e6	1.48	7.2e8	1.36	2.7e5	1.42	2.8e5
Glutamine	1.17	0.011	1.72	9.0e6	1.50	1.2e4	1.41	7.4e8	1.59	5.3e5	1.57	9.2e5	1.44	4.4e4
Arginine	1.49	0.001	1.74	0.001	1.79	2.5e4	1.43	1.2e4	1.58	3.2e5	1.76	2.6e4	2.10	1.4e4
Serine	1.35	9.5e7	1.03	0.708	0.92	0.235	1.09	0.117	1.15	0.005	1.35	0.001	1.33	0.004
Threonine	1.25	3.8e4	1.72	1.4e7	1.59	1.2e6	1.34	7.0e4	1.57	1.4e7	1.47	3.1e7	1.45	6.3e5
Valine	1.30	7.9e5	1.74	3.1e7	1.51	1.3e6	1.45	2.3e6	1.57	1.2e8	1.54	8.6e7	1.73	1.6e6
Tryptophan	1.22	0.006	1.78	0.002	1.48	0.001	1.25	0.004	1.39	3.2e4	1.45	1.3e4	1.44	2.8e5
Tyrosine	1.29	3.6e5	1.91	1.5e4	1.53	1.2e6	1.22	0.001	1.39	2.8e7	1.45	2.9e5	1.68	1.2e6
Ornithine	1.25	0.014	1.59	0.079	1.35	0.035	1.04	0.648	1.07	0.429	1.28	0.015	1.18	0.192
Citrulline	1.16	0.030	1.34	2.0e4	1.27	0.002	1.13	0.008	1.53	3.1e7	1.50	5.4e5	1.45	0.002
Taurin	1.13	0.069	1.82	0.085	1.49	0.013	0.98	0.819	1.06	0.309	1.30	0.089	1.11	0.144
O-acetylserine	1.19	0.249	1.11	0.475	1.31	0.139	1.47	0.007	1.68	0.002	1.04	0.778	0.96	0.693
Fumarate	0.90	0.047	1.23	0.001	1.21	0.033	0.98	0.742	1.12	0.014	0.99	0.912	0.87	0.015
Aconitate	1.00	0.991	1.16	0.049	1.07	0.525	1.11	0.153	1.36	1.2e4	1.00	0.947	1.28	0.014
α -ketoglutarate	0.98	0.755	1.53	4.5e4	1.24	0.014	1.15	0.088	1.22	0.056	0.89	0.230	1.02	0.869
Succinate	1.00	0.973	1.46	1.4e5	1.12	0.047	1.31	2.9e5	1.73	4.0e7	0.96	0.616	1.22	0.123

Supplementary table 17: Comparison of metabolite in shoots of *ppck* mutants and *ppck1-4* complementation lines compared to wild type upon Pi starvation.

Seedlings were germinated for 6 days on sufficient media before transfer to insufficient media for an additional five days before harvest. Significance analyses were performed by Student's t-test (two-tailed, equal variances). Number in bold indicates significant difference between the overexpression lines and wild type with $p < 0.05$, $n = 12$. Dark and light grey cells highlight metabolites that were increased and decreased in the overexpression lines compared to wild type.

Shoot metabolites measurements in <i>ppck</i> mutants and <i>ppck1-4</i> complementation lines grown on Pi insufficient condition														
Metabolite	<i>ppck1-4</i>		<i>ppck1-4C 9.10</i>		<i>ppck1-4C 11.8</i>		<i>ppck2 1.3</i>		<i>ppck2 2.9</i>		<i>ppck1ppck2 7.11</i>		<i>ppck1ppck2 9.3</i>	
	Fold	T-test	Fold	T-test	Fold	T-test	Fold	T-test	Fold	T-test	Fold	T-test	Fold	T-test
Alanine	1.27	0.014	1.32	5.0e4	1.44	2.0e4	1.15	0.097	1.12	0.161	1.46	0.001	1.70	5.1e9
Cysteine	1.02	0.867	1.09	0.491	1.19	0.081	1.14	0.241	1.09	0.453	1.31	0.055	1.37	0.022
Aspartate	0.90	0.299	1.12	0.189	1.16	0.121	1.14	0.150	1.11	0.298	1.03	0.752	1.15	0.286
Glutamate	0.96	0.651	1.18	0.050	1.22	0.020	1.11	0.294	1.02	0.872	0.97	0.701	1.15	0.134
Phenylalanine	1.12	0.340	1.34	0.006	1.70	2.3e4	1.55	0.001	1.23	0.051	0.79	0.014	1.23	0.013
Glycine	1.22	0.259	0.95	0.729	1.09	0.615	0.90	0.493	0.87	0.395	1.26	0.148	1.47	0.033
Histidine	1.03	0.890	1.16	0.479	1.53	0.068	1.20	0.416	1.45	0.159	0.99	0.960	1.16	0.537
Isoleucine	1.29	0.037	1.88	8.9e7	1.98	2.2e5	1.43	0.003	1.43	0.019	1.32	0.004	1.53	7.8e5
Lysine	1.15	0.294	1.61	0.002	1.70	2.1e5	1.29	0.065	1.35	0.059	1.30	0.031	1.60	1.1e4
Leucine	1.64	1.0e4	2.10	1.2e6	2.16	1.7e6	1.65	3.4e5	1.52	0.006	1.42	0.003	1.92	7.3e10
Methionine	1.31	0.212	2.45	0.077	1.23	0.285	1.23	0.337	1.99	0.013	1.20	0.280	1.61	0.047
Asparagine	1.14	0.362	1.44	0.006	1.48	0.001	1.19	0.180	1.35	0.069	1.36	0.019	1.51	0.002
Proline	1.10	0.477	1.78	1.5e5	2.47	4.4e9	1.41	0.003	1.80	0.001	1.16	0.202	1.13	0.366
Glutamine	0.90	0.466	1.50	0.029	1.56	1.9e4	1.10	0.441	1.10	0.483	1.03	0.815	1.13	0.255
Arginine	1.20	0.216	1.64	1.5e5	2.17	1.3e7	1.36	0.041	1.39	0.036	1.01	0.911	1.44	0.004
Serine	1.32	0.032	1.04	0.643	1.09	0.374	1.10	0.374	1.04	0.719	1.61	1.6e4	1.84	1.1e5
Threonine	1.08	0.573	1.32	0.006	1.32	0.008	1.21	0.117	1.20	0.116	1.25	0.039	1.41	0.002
Valine	1.18	0.233	1.54	0.002	1.69	2.6e4	1.33	0.029	1.38	0.040	1.28	0.042	1.49	0.003
Tryptophan	1.40	0.129	1.41	0.036	1.81	0.011	1.79	0.022	1.66	0.089	1.16	0.357	1.68	0.006
Tyrosine	1.50	0.011	1.69	6.7e5	1.97	0.001	1.85	0.001	1.60	0.035	1.28	0.032	1.89	3.8e6
Ornithine	0.83	0.250	1.44	0.008	1.73	0.003	0.79	0.116	0.82	0.110	0.83	0.127	0.97	0.776
Citrulline	1.11	0.385	1.97	4.3e6	1.94	1.4e5	1.03	0.747	1.04	0.719	1.21	0.078	1.30	0.013
Taurin	0.90	0.529	1.25	0.167	1.25	0.184	0.96	0.809	0.82	0.173	0.87	0.329	0.98	0.913
O-acetylserine	0.86	0.648	0.78	0.473	0.79	0.455	0.54	0.108	0.76	0.459	1.23	0.575	1.06	0.861
Fumarate	0.70	1.4e5	1.21	0.053	1.20	0.073	0.91	0.070	0.99	0.862	0.75	2.1e4	0.55	1.9e9
Aconitate	1.34	0.013	1.25	0.167	1.19	0.111	1.16	0.073	1.32	0.043	1.50	0.001	1.55	0.002
α -ketoglutarate	0.78	0.014	0.78	0.473	1.03	0.815	0.95	0.596	1.00	0.991	0.71	0.006	0.61	4.6e5
Succinate	1.05	0.636	1.21	0.053	1.35	0.012	1.35	0.001	1.38	2.8e4	1.02	0.868	0.98	0.765

Supplementary table 18: Comparison of metabolite in roots of *ppck* mutants and *ppck1-4* complementation lines compared to wild type on sufficient Pi condition.

Seedlings were germinated for 6 days on sufficient media before transfer to insufficient media for an additional five days before harvest. Significance analyses were performed by Student's t-test (two-tailed, equal variances). Number in bold indicates significant difference between the overexpression lines and wild type with $p < 0.05$, $n = 12$. Dark and light grey cells highlight metabolites that were increased and decreased in the overexpression lines compared to wild type.

Shoot metabolites measurements in <i>ppck</i> mutants and <i>ppck1-4</i> complementation lines grown on sufficient Pi														
Metabolite	<i>ppck1-4</i>		<i>ppck1-4C 9.10</i>		<i>ppck1-4C 11.8</i>		<i>ppck2 1.3</i>		<i>ppck2 2.9</i>		<i>ppck1ppck2 7.11</i>		<i>ppck1ppck2 9.3</i>	
	Fold	T-test	Fold	T-test	Fold	T-test	Fold	T-test	Fold	T-test	Fold	T-test	Fold	T-test
Alanine	1.46	2.7e5	1.61	6.6e9	1.50	1.9e8	1.54	1.9e5	1.83	8.2e7	1.60	1.6e9	1.83	7.8e8
Cysteine	1.15	0.039	1.65	1.4e5	1.51	4.6e6	1.39	1.2e5	1.58	1.9e8	1.36	7.8e5	1.48	6.3e8
Aspartate	1.09	0.213	1.82	3.9e4	1.53	0.035	2.35	0.014	2.65	0.015	1.57	4.8e4	1.87	0.001
Glutamate	1.10	0.192	1.51	0.001	1.28	0.108	1.76	0.027	1.73	0.040	1.33	3.3e4	1.35	0.001
Phenylalanine	1.28	0.003	1.36	1.5e4	1.51	0.001	1.36	2.4e4	1.53	1.2e4	1.22	0.001	1.56	2.2e5
Glycine	1.28	0.015	1.26	0.090	1.16	0.134	1.33	0.002	1.26	0.019	1.11	0.215	1.19	0.070
Histidine	1.37	0.002	1.73	8.5e5	1.67	0.001	1.56	1.5e4	1.91	3.3e7	1.49	4.1e4	1.73	2.9e4
Isoleucine	1.30	3.8e4	1.83	2.1e8	1.82	1.7e7	1.50	1.1e6	1.71	3.8e8	1.41	1.3e4	1.81	1.9e6
Lysine	1.46	0.002	2.16	1.5e7	2.10	7.9e6	1.81	1.2e5	1.96	1.3e6	1.64	9.9e6	1.97	5.7e8
Leucine	1.28	0.001	1.94	4.0e9	1.93	1.1e7	1.71	4.2e7	1.87	6.1e7	1.41	2.3e6	1.79	1.3e7
Methionine	1.34	0.026	1.55	5.0e4	2.01	0.002	1.92	6.9e6	2.10	4.2e6	1.54	1.5e4	2.10	1.1e5
Asparagine	1.18	0.061	1.59	3.0e4	1.52	3.9e5	1.57	2.3e5	1.84	9.7e6	1.41	2.8e4	1.54	6.7e5
Proline	1.02	0.791	1.74	3.2e6	1.45	8.1e5	1.37	2.5e5	2.13	1.5e11	1.30	0.001	1.54	4.0e4
Glutamine	1.19	0.02	1.51	8.0e7	1.37	3.5e4	1.42	0.001	1.61	2.1e4	1.32	5.1e5	1.37	3.8e5
Arginine	1.54	0.009	2.00	5.9e5	1.74	1.5e5	1.79	1.4e4	2.12	3.3e6	1.71	0.001	2.04	1.0e4
Serine	1.44	2.0e4	1.42	1.8e5	1.35	1.7e6	1.45	4.9e5	1.56	8.5e6	1.44	5.1e7	1.71	1.7e7
Threonine	1.20	0.005	1.62	3.6e5	1.54	8.9e7	1.48	1.2e7	1.64	4.5e9	1.39	5.4e6	1.58	1.1e8
Valine	1.29	0.012	1.41	0.002	1.38	0.001	1.54	4.2e6	1.59	1.0e6	1.26	0.005	1.61	4.9e5
Tryptophan	1.28	0.014	1.50	2.3e4	1.34	0.001	1.30	0.005	1.54	1.8e5	1.34	0.001	1.61	1.5e4
Tyrosine	1.39	0.001	1.61	1.4e5	1.74	0.001	1.46	4.3e5	1.52	1.3e5	1.46	1.1e4	1.87	1.2e4
Ornithine	1.55	0.007	1.82	3.3e6	2.01	5.6e5	1.53	0.001	1.74	0.001	1.41	0.001	1.54	1.9e4
Citrulline	1.30	0.006	1.30	0.003	1.20	0.02	1.43	0.002	1.57	0.001	1.37	0.004	1.39	0.010
Taurin	1.23	0.04	1.39	0.005	1.37	0.001	1.30	0.022	1.35	0.002	1.20	0.05	1.38	0.008
<i>O</i> -acetylserine	1.18	0.118	1.88	0.003	1.61	1.1e6	1.54	0.03	1.91	0.018	1.04	0.688	1.19	0.112
Fumarate	0.98	0.868	1.34	0.096	0.90	0.281	1.20	0.011	1.15	0.059	0.73	9.9e5	0.78	0.012
Aconitate	0.97	0.536	1.09	0.117	1.00	0.938	1.00	0.939	1.00	0.967	0.86	0.011	0.90	0.039
α -ketoglutarate	0.85	0.013	1.19	0.019	0.93	0.384	1.13	0.021	1.15	0.021	0.87	0.047	0.82	0.040
Succinate	0.85	0.049	1.30	0.001	1.04	0.667	1.31	0.019	1.40	0.003	0.84	0.017	0.90	0.194

Supplementary table 19: Comparison of metabolite in roots of *ppck* mutants and *ppck1-4* complementation lines compared to wild type upon Pi starvation.

Seedlings were germinated for 6 days on sufficient media before transfer to insufficient media for an additional five days before harvest. Significance analyses were performed by Student's t-test (two-tailed, equal variances). Number in bold indicates significant difference between the overexpression lines and wild type with $p < 0.05$, $n = 12$. Dark and light grey cells highlight metabolites that were increased and decreased in the overexpression lines compared to wild type.

Shoot metabolites measurements in <i>ppck</i> mutants and <i>ppck1-4</i> complementation lines grown on Pi insufficient condition														
Metabolite	<i>ppck1-4</i>		<i>ppck1-4C 9.10</i>		<i>ppck1-4C 11.8</i>		<i>ppck2 1.3</i>		<i>ppck2 2.9</i>		<i>ppck1ppck2 7.11</i>		<i>ppck1ppck2 9.3</i>	
	Fold	T-test	Fold	T-test	Fold	T-test	Fold	T-test	Fold	T-test	Fold	T-test	Fold	T-test
Alanine	1.38	0.036	0.88	0.318	0.93	0.560	1.22	0.228	1.17	0.321	1.52	0.011	1.51	0.024
Cysteine	1.07	0.550	0.97	0.782	0.98	0.853	1.18	0.145	1.05	0.649	1.34	0.003	1.23	0.041
Aspartate	0.96	0.864	0.84	0.456	0.86	0.517	1.17	0.483	1.09	0.667	0.86	0.492	0.81	0.346
Glutamate	0.96	0.827	0.78	0.229	0.80	0.280	1.07	0.731	1.04	0.811	0.86	0.471	0.75	0.160
Phenylalanine	0.98	0.891	1.11	0.424	1.08	0.462	1.09	0.443	1.09	0.490	1.16	0.185	1.20	0.209
Glycine	1.06	0.668	1.05	0.705	1.04	0.765	1.10	0.496	1.04	0.758	1.16	0.277	1.15	0.277
Histidine	0.86	0.409	0.94	0.726	1.07	0.703	1.13	0.495	1.22	0.294	1.10	0.580	1.05	0.829
Isoleucine	1.14	0.446	0.97	0.867	1.00	0.978	1.27	0.178	1.14	0.490	1.17	0.298	1.24	0.276
Lysine	1.07	0.641	1.00	0.998	1.13	0.398	1.21	0.280	1.09	0.599	1.14	0.439	1.03	0.867
Leucine	1.21	0.168	1.00	0.999	1.07	0.604	1.34	0.063	1.19	0.265	1.24	0.128	1.24	0.253
Methionine	1.15	0.415	0.94	0.763	1.01	0.931	1.33	0.084	1.10	0.574	1.10	0.561	1.19	0.369
Asparagine	1.11	0.255	0.93	0.423	1.09	0.248	1.27	0.060	1.19	0.088	1.11	0.267	1.09	0.368
Proline	0.91	0.475	1.27	0.057	1.84	3.1e5	1.26	0.108	1.64	0.013	1.15	0.230	0.92	0.643
Glutamine	0.96	0.680	0.92	0.360	1.11	0.153	1.12	0.399	1.03	0.786	1.00	0.990	0.94	0.525
Arginine	0.91	0.599	0.92	0.591	1.14	0.434	1.15	0.479	1.12	0.513	0.92	0.635	0.93	0.714
Serine	1.11	0.412	0.96	0.699	1.03	0.814	1.16	0.308	1.11	0.466	1.25	0.092	1.24	0.135
Threonine	1.12	0.170	1.00	0.972	1.01	0.854	1.19	0.098	1.09	0.360	1.34	0.002	1.26	0.005
Valine	1.11	0.671	0.82	0.368	0.94	0.773	1.21	0.451	1.16	0.537	1.11	0.654	1.15	0.618
Tryptophan	1.03	0.839	0.95	0.780	1.01	0.943	1.12	0.505	1.12	0.534	1.15	0.389	1.15	0.506
Tyrosine	1.02	0.905	1.01	0.968	1.03	0.890	1.11	0.616	1.07	0.717	1.13	0.505	1.24	0.366
Ornithine	1.13	0.484	1.06	0.755	1.47	0.083	1.14	0.480	1.21	0.312	1.17	0.430	1.21	0.332
Citrulline	1.34	0.011	1.10	0.487	1.19	0.138	1.05	0.761	1.02	0.877	1.25	0.192	1.18	0.239
Taurin	1.12	0.424	1.03	0.795	1.18	0.184	1.05	0.737	1.09	0.562	1.28	0.122	1.17	0.303
<i>O</i> -acetylserine	1.01	0.933	1.96	0.073	2.04	0.080	1.16	0.247	1.08	0.548	2.24	0.061	1.90	0.068
Fumarate	0.80	0.082	0.93	0.557	0.77	0.049	1.01	0.918	0.87	0.236	0.87	0.261	0.78	0.046
Aconitate	0.92	0.167	1.08	0.277	1.09	0.222	1.13	0.028	1.09	0.167	1.04	0.306	0.96	0.412
α -ketoglutarate	0.40	0.001	1.29	0.121	0.82	0.310	0.99	0.972	0.97	0.845	0.40	3.7e4	0.28	4.3e5
Succinate	0.97	0.820	0.99	0.964	0.94	0.644	1.23	0.215	1.12	0.413	1.01	0.958	0.98	0.848

ACKNOWLEDGEMENT

I would like to thank my supervisor **Prof. Dr. Steffen Abel** for hosting and giving me the chance to work in the Molecular Signal Processing Department and more so in his Nutrient Sensing Research Group. The freedom he gave me during my studies allowed what was initially a new topic for me to turn into a great adventure filled with memorable, unforgettable moments. Additionally, his trust, patience and advice gave me time to positively shape this study. I would also like to express my gratitude to **Prof. Dr. Edgar Peiter** and **Prof. Dr. Paul B. Larsen** for reviewing my thesis. Many thanks to **PD. Dr. Thomas Vogt** who as part of my thesis supervising committee gave invaluable advice and guidance throughout the study.

I am and will forever be indebted to my mentor **Dr. Joerg Ziegler** for his invaluable guidance and unwavering support. His patience committed supervision and constant encouragement were not in vain as they helped shape not only my research but also my critical thinking towards research and life. The uncountable discussions went a long way towards ensuring that our work bore fruits at the end.

I have great pleasure in acknowledging the insights given by **Dr. Christin Naumann** and **Dr. Martina Ried** on this project. My heartfelt thanks to for reading my thesis and giving me feedback which made it even better.

I greatly acknowledge the funding from the **Deutscher Akademischer Austauschdienst (DAAD)** for the initial funding and support of my research and the **Institute of Plant Biochemistry** for the PhD completion grant.

A big shout out to all my colleagues at the department and the Institute for the wonderful time spent together. To friends like Imran, Pradeep, Mukesh, Ranju, Mingdang, Pinelopi, Carolin, Thanos, David, Max, Kiran, Jonas and Birgit, your words of encouragement made this journey worthwhile. Special thanks to Kathrin and Mike, your family and friends, for the great times shared. Our friendship is more than words can describe.

I would also like to thank my best friend and partner in crime **Ruth**, for her patience and support during this study period. Your love and companionship kept me motivated and gave me the strength to keep pushing. To my nieces and nephews, and my in-laws I cannot forget your support and words of encouragement throughout this period. To my dearest Dad (**Paul Kariithi**), mum (**Margret Kariithi**) and my siblings **Peter, James, Nancy** and **Teresia**, you have always had my back and you hold a special place in my heart. Lastly, I would like to give thanks to God for preserving me throughout this study and making it possible to experience and see a part of the world that was beyond my imagination.

Curriculum Vitae

Name: Samuel Ngure Kariithi
Date of birth: 16/08/1988
Nationality: Kenyan
Place of birth: Nakuru, Kenya

Education

10/2019-11/2023 **Doctorate**
Faculty of Natural Sciences 1 - Biosciences, Martin Luther University Halle-Wittenberg
Dissertation: Contribution of the PPCK-PPC module to phosphate-dependent malate accumulation and exudation in *Arabidopsis thaliana*

Supervisor: Prof. Dr. Steffen Abel
Mentor: Dr. Joerg Ziegler
Leibniz Institute of Plant Biochemistry, Halle (Saale), Germany

01/2017-04/2019 **Graduate assistant**
University of Kabinga, Kericho Kenya

01/2018-04/2019 Egerton University, Nakuru Kenya

09/2013-12/2016 **Master of Science**
Egerton University, Nakuru Kenya
Biochemistry and Molecular Biology
Final mark: 68/100 (Good)
Master thesis: Effects of genotype and environmental effect on nutritional quality of stem rust resistant Kenyan bread wheat varieties
Supervisor: Dr. Stephen Indieka

08/2008-12/2012 **Bachelor of Science**
Moi University, Eldoret, Kenya
Department of Chemistry and Biochemistry
Final mark: 65/100 (Second Class Honors Upper Division)
Bachelor thesis: Investigating the antimicrobial activities of citrus fruits extracts
Supervisor: Prof. Paul Ndalut

01/2003-11/2006 **High School education**
Jomo Kenyatta High School
Nakuru, Kenya
Final mark: A- (78/84)

01/1995-11/2002 **Primary School education**
Njoro Township Primary School
Njoro, Kenya
Final mark: 404/500

Conferences

Plant Science Student Conference, 3-4 July 2023, IPK (Leibniz-Institut für Pflanzengenetik und Kulturpflanzenforschung) Gatersleben, Germany.

20th International Symposium on Iron Nutrition and Interactions in Plant Molecular responses of plants, 4-8 July 2022, Reims, France.

Plant Science Student Conference, 15-18 June 2021, IPB (Leibniz-Institute of Plant Biochemistry) Halle (Saale), Germany (online format)

Plant Science Student Conference, 16-19 June 2020, IPK (Leibniz-Institut für Pflanzengenetik und Kulturpflanzenforschung) Gatersleben, Germany (online format)

Datum

Unterschrift des Antragstellers

STATUTORY DECLARATION

Hiermit erkläre ich an Eides statt, dass ich mich mit der vorliegenden wissenschaftlichen Arbeit erstmals um die Erlangung des Doktorgrades bewerbe, die Arbeit selbständig und ohne fremde Hilfe verfasst, nur die angegebenen Quellen und Hilfsmittel genutzt und die den benutzten Werken wörtlich oder inhaltlich entnommenen Stellen als solche kenntlich gemacht habe.

Datum

Unterschrift des Antragstellers